



The University of
Nottingham

UNITED KINGDOM · CHINA · MALAYSIA

Interplay between quorum
sensing and metabolism in
Pseudomonas aeruginosa

Avika Ruparell, BSc

Submitted to The University of Nottingham
for the degree of Doctor of Philosophy

July 2012

Declaration

Unless otherwise acknowledged, the work presented in this thesis is my own. No part has been submitted for another degree at The University of Nottingham or any other institute of learning.

Avika Ruparell

September 2011

Abstract

The important human pathogen *Pseudomonas aeruginosa* causes a broad-spectrum of diseases including life threatening infections. A cell density-dependent regulatory network termed quorum sensing (QS) is pivotal in the control of *P. aeruginosa* pathogenicity, and the signal molecules employed are *N*-acyl-L-homoserine lactones (AHLs) and the *Pseudomonas* quinolone signal (PQS). Production of these QS signal molecules (QSSMs) requires precursors including fatty acids, *S*-adenosyl-L-methionine (SAM) and aromatic amino acids. SAM is derived from the activated methyl cycle (AMC) which is an important pathway dedicated to the degradation of the toxic metabolite *S*-adenosyl-L-homocysteine (SAH). Through removing the genes encoding the AHL synthases, RhlI and LasI from the complex hierarchical system of *P. aeruginosa* by expressing them in the heterologous host, *Escherichia coli*, this study has measured the influence of AHL production upon bacterial metabolism. AHL profiles were broader than previously reported, correlated with a reduction in the intracellular concentrations of several metabolites, and were more pronounced in the *E. coli* strain producing the LasI synthase than the RhlI enzyme. Production of foreign QSSM synthases had a knock-on effect on the native *E. coli* QSSM, autoinducer-2 (AI-2). We hypothesize that AI-2 production was significantly reduced since it also requires AMC metabolites for its synthesis. The influence that these metabolic perturbations had on cell fitness was manifest through reduced growth in minimal media. Complementation of growth by exogenously added metabolites confirmed our hypothesis that QSSM synthesis creates a drain on metabolite levels with consequences for cell fitness. Site-directed mutagenesis of key catalytic residues in the QSSM synthases was performed to directly prove that the effects observed were due to the function of the synthases, and not the production of a heterologous protein. Moreover, complete profiling of *P. aeruginosa* PA01 AHL synthase mutants is unravelling the interrelationship between metabolism and cell-to-cell communication in *P. aeruginosa*.

Acknowledgments

Apologies for the length of this, but there were just so many people to be thanked!

First and foremost I must thank my supervisors Kim Hardie and Dave Barrett who gave me this amazing opportunity to perform a PhD, provided invaluable guidance over the past four years and helped considerably with the writing of this thesis... MY THESIS!! Many thanks must also go to: Jean Dubern for his input and assistance with construction of the site-directed mutants; Nigel Halliday for his chemistry knowledge and assistance with the countless number of mass spectroscopy problems I experienced over the years, and Stéphanie Pommier and Jeni Luckett for their various assistances. Special thanks to Catherine Ortori for performing the LC-MS/MS detection of QSSMs and her assistance and patience with my training and constant queries regarding the QUAT'TRO. Also, Abigail Emtage and Charles Laughton who performed the predictive RhII modelling and gave invaluable advice regarding the mutagenesis strategies and last but not least the brilliant lab technicians Penny Howick and Irene Reynolds must not be forgotten.

On a personal note, I must thank my parents and brother who I think to this day do not understand what I have been doing for the past 4 years of my life, but have supported me nonetheless. A few very important people who aren't related by blood, but are even better than family for which I can say... Sometimes it's difficult talking to people who have the same pressures as you, even though you know they'll happily take the time out of their day for you; you don't want to burden them with your problems when you feel they have enough of their own. Saying that, there are no words out there for me to be able to thank Sharae, Christa and Mohamed for all their invaluable patience, love and support, especially through the tough times. Thank you for being... AMAZING! I don't know how I would have got through the past 4 years without you guys being a part of my life.

Now for the boys who made the past 4 years... THE BEST YEARS OF MY LIFE... Most importantly, I'd like to acknowledge Dave, Rob & Roman, the guys who I started with who have passed on their cigarette smoke to me during our countless coffee breaks and have created the best memories memories of my time in Nottingham. In addition, and in no particular order:

Stéphanie, mentioned again, who was important to both my time inside and outside of the lab and still very much so is! As well as being a great female scientist, she has been a great friend, the perfect Wagamama's dinner companion and bad shopping influence even after leaving Nottingham.

Owen for his "sarcastic" comments and amusing conversation which accompanied my time in the lab and made it all the more enjoyable. Surprisingly to him, he was a senior role model for me during his time in CBS, the PhD student's footsteps I had to follow and improve on, which let's be realistic, wasn't too difficult.!!! Sorry Dr. Darchy...!!!

Magda for the kindest compliments, constant optimism, comments of self value and worth towards me and last but not least love of Beyoncé! I'll treasure the memories of our trip to Poland for Nat's wedding forever. Her husband, Michal, must also be thanked for providing invaluable support, especially during my stays in Nottingham throughout the thesis writing period.

Fadilah for her genuine, kind and caring nature. You are one of the most down to earth people I have ever met and I'm so lucky to have had you there during my PhD. Thank you also for appreciating my daily outfits and general fashion sense!

Manisha for showing me an important principle that no matter what life throws at you it's possible to overcome anything and succeed.

Marco for attempting to convince me to appreciate Apple products!

Christian, Sonia and Sapna for illustrating another important principle: "the balance of business and pleasure"!! Thank you for your presence in my "nightlife" and creating many memories in Dogma, Tantra and Coco Tang!

Dina for making the perfect replacement for Owen as a lab bench neighbour.

Esteban and Hadi for making the final year of partying worth every second!

Chris P and Steve A for their smiles and witty conversation which have brightened up my each and every day.

...Any remaining past or current members of B-floor phase I which were there during my time there. Special thanks to the members of the Gram-negative group for putting up with my music over the years!

...And anyone else who has graced me with their presence during my time in Nottingham... THANK YOU, THANK YOU, THANK YOU...!!!

List of contents

Declaration	i
Abstract.....	ii
Acknowledgments	iii
List of contents.....	vi
Table of contents.....	vii
List of figures	xiii
List of tables	xvi
Abbreviations.....	xvii
Chapter 1: Introduction.....	1
Chapter 2: Materials and methods.....	34
Chapter 3: Analysis of the metabolic implications of the <i>P. aeruginosa</i> AHL synthase genes in <i>E. coli</i>.....	60
Chapter 4: Analysis of the metabolic implications of the <i>P. aeruginosa</i> AHL synthase genes by site directed mutagenesis .	84
Chapter 5: Analysis of the metabolic implications of the <i>lasI_{Pa}</i> and <i>rhlI_{Pa}</i> in <i>E. coli</i> MG1655Δ<i>luxS</i>, Δ<i>pfs</i>, Δ<i>sdiA</i> mutants.....	110
Chapter 6: Analysis of the metabolic implications of the AHL synthase genes in the native <i>P. aeruginosa</i> background.....	128
Chapter 7: General discussion	139
Bibliography	149
Appendix	175

Table of contents

Chapter 1: Introduction	1
1.1 Quorum sensing	2
1.1.1 Interspecies communication	6
1.1.2 Intraspecies communication	7
1.1.2.1 QS in Gram-positive bacteria.....	7
1.1.2.2 QS in Gram-negative bacteria.....	8
1.2 The genus <i>Pseudomonas</i>	9
1.2.1 <i>Pseudomonas aeruginosa</i>	9
1.2.1.1 Clinical significance of <i>P. aeruginosa</i>	10
1.2.1.2 Virulence determinants of <i>P. aeruginosa</i>	11
1.3 QS in <i>P. aeruginosa</i>	15
1.4 Global QS regulators in <i>P. aeruginosa</i>	20
1.5 Biosynthesis of AHLs in <i>P. aeruginosa</i>	20
1.6. AQ-dependent QS in <i>P. aeruginosa</i>	24
1.7 The activated methyl cycle (AMC).....	27
1.8 Fatty acid biosynthesis.....	30
1.9 Aims and objectives	32
Chapter 2: Materials and methods	34
2.1 Chemical reagents.....	35
2.1.1 General chemicals.....	35
2.1.2 Synthesis of QSSMs	35
2.2 Growth media and additives.....	35

2.2.1 Luria Bertani media	35
2.2.2 Chemically defined media (CDM).....	36
2.2.3 MOPS minimal media (MMM).....	36
2.2.4 Antibiotics/ X-Gal/ IPTG	36
2.3 Growth conditions	37
2.4 Bacterial strains	37
2.5 Plasmids	38
2.6 DNA preparation and manipulation	41
2.6.1 Preparation of plasmid DNA.....	41
2.6.2 Purification of chromosomal DNA.....	41
2.6.3 Precipitation of DNA.....	42
2.6.4 Quantifying DNA concentrations.....	42
2.6.5 Restriction enzymes.....	42
2.6.6 Analysis and purification of DNA by agarose gel electrophoresis	43
2.6.7 Molecular weight markers.....	43
2.6.8 DNA ligation.....	44
2.7 Polymerase chain reaction (PCR) amplification.....	44
2.7.1 Synthesis of oligonucleotide primers	44
2.7.2 PCR amplification.....	47
2.8 DNA sequencing.....	47
2.8.1 Obtaining DNA sequence data	47
2.8.2 DNA sequence analysis	48
2.9 Transformation.....	48
2.9.1 Preparation of electro-competent <i>E. coli</i> cells.....	48
2.9.2 Electroporation of electro-competent <i>E. coli</i> cells	48
2.9.3 Preparation of electro-competent <i>P. aeruginosa</i> cells	49
2.9.4 Electroporation of electro-competent <i>P. aeruginosa</i> cells.....	49

2.10 Recombinant protein production, purification and analysis	49
2.10.1 Whole cell protein preparation	49
2.10.2 Sodium dodecyl sulphate-polyacrylamide gel electrophoresis (SDS-PAGE) analysis.....	50
2.10.3 Western blotting	50
2.11 Extraction, detection and quantification of QSSMs	52
2.11.1 Extraction of QSSMs.....	52
2.11.2 Analysis of AHLs by TLC-biosensor overlay plates	52
2.11.3 AHL detection by biosensor strain overlay plates.....	53
2.11.4 LC-MS/MS analysis of QSSMs.....	53
2.12 Extraction, detection and quantification of AMC metabolites	54
2.12.1 Sample collection and storage.....	54
2.12.2 Extraction of AMC metabolites	54
2.12.3 Chemical derivatization of AMC metabolites	55
2.12.4 LC-MS/MS analysis of AMC metabolites	56
2.13 Extraction, detection and quantification of MTA.....	57
2.13.1 Extraction of MTA.....	57
2.13.2 LC-MS/MS analysis of MTA.....	57
2.14 Detection of AI-2 using <i>V. harveyi</i> bioassay	58

Chapter 3: Analysis of the metabolic implications of the *P. aeruginosa* AHL synthase genes in *E. coli*..... 60

3.1 Introduction	61
3.2 Cloning of <i>lasI_{Pa}</i> and <i>rbII_{Pa}</i>	61
3.3 <i>lasI_{Pa}</i> and <i>rbII_{Pa}</i> synthesize the cognate AHLs in MG1655.....	62
3.4 LC-MS/MS profiling of AHLs reveals that LasI produces several other AHLs in MG1655	65

3.5 LasI and RhII proteins are detected in MG1655	68
3.6 Production of AHL synthases in MG1655 alters the levels of metabolites of the AMC	68
3.7 Production of AI-2 is increased in the MG1655-AHL synthase strains	71
3.8 MTA levels increase upon expression of the PA01 AHL synthases	73
3.9 Production of LasI and RhII affect the growth of MG1655	74
3.10 Exogenous methionine addition improves the growth of MG1655[pME- <i>lasI_{Pa}</i>] in MOPS minimal media	75
3.11 Discussion	79

Chapter 4: Analysis of the metabolic implications of the *P. aeruginosa* AHL synthase genes by site directed mutagenesis . 84

4.1 Introduction	85
4.2 Identification of important residues of LasI and RhII.....	85
4.3 Predicting a model for the structure of RhII.....	87
4.4 Generation of SDMs in LasI and RhII.....	91
4.4.1 Generation of SDMs in LasI and RhII	91
4.4.2 PCR amplification of LasI and RhII with single codon substitutions.....	91
4.4.3 Selection and confirmation of site directed mutagenesis of LasI and RhII	92
4.4.4 Subcloning of mutant AHL synthase genes for overexpression	92
4.5 Analysis of the synthase activity of each SDMs in MG1655	93
4.6 LC-MS/MS profiling of AHLs produced by SDMs of <i>lasI_{Pa}</i> and <i>rhII_{Pa}</i> in MG1655	93
4.7 Stability of synthase proteins from site-directed mutagenesis of <i>lasI_{Pa}</i> and <i>rhII_{Pa}</i>	94
4.8 AMC metabolite profiles of <i>lasI_{Pa}</i> and <i>rhII_{Pa}</i> SDMs.....	99

4.9 Recombinant expression of <i>P. aeruginosa</i> AHL synthase SDMs in <i>E. coli</i> leads to variation in extracellular AI-2 levels.....	101
4.10 Intracellular MTA levels of <i>lasI_{Pa}</i> and <i>rhII_{Pa}</i> SDMs are lower when less AHLs are made.....	101
4.11 Fitness profiles of <i>P. aeruginosa</i> AHL synthase SDMs in <i>E. coli</i>	104
4.12 Discussion	107

Chapter 5: Analysis of the metabolic implications of the *lasI_{Pa}* and *rhII_{Pa}* in *E. coli* MG1655Δ*luxS*, Δ*pfs*, Δ*sdiA* mutants110

5.1 Introduction	111
5.2 Elevated SAH and SRH levels, and reduced HCY levels and AHL profiles characterise the expression of <i>lasI_{Pa}</i> and <i>rhII_{Pa}</i> in the <i>luxS</i> mutant	112
5.3 Expression of <i>lasI_{Pa}</i> and <i>rhII_{Pa}</i> in the <i>pfs</i> mutant leads to growth defects, reduced AHL profiles and altered AMC metabolite levels.....	118
5.4 <i>lasI_{Pa}</i> and <i>rhII_{Pa}</i> create different AMC metabolite and AHL profiles in the <i>sdiA</i> mutant.....	121
5.5 Discussion	123

Chapter 6: Analysis of the metabolic implications of the AHL synthase genes in the native *P. aeruginosa* background..... 128

6.1 Introduction	129
6.2 Production of QSSMs is significantly reduced in the PA01Δ <i>lasI</i> , PA01Δ <i>rhII</i> and PA01Δ <i>lasI</i> Δ <i>rhII</i> mutants and can be restored upon complementation.....	129
6.3 AMC metabolites.....	130
6.4 Intracellular MTA levels decrease with removal of the AHL synthase genes and increase back with complementation.....	133
6.5 Growth defects of <i>P. aeruginosa</i> AHL synthase mutants	135

6.6 Discussion	137
Chapter 7: General discussion	139

List of figures

Figure 1.1: Quorum sensing (QS): Cell to cell communication in a bacterial population .	3
Figure 1.2: QS in Gram-negative bacteria	3
Figure 1.3: AHL and AQ-dependent QS in <i>P. aeruginosa</i>	16
Figure 1.4: The structure of the main QS signal molecules (QSSMs) produced by <i>P. aeruginosa</i>	18
Figure 1.5: Scheme for PQS biosynthesis and degradation	26
Figure 1.6: The activated methyl cycle (AMC).....	28
Figure 1.7: Fatty acid biosynthesis pathway	31
Figure 3.1: Schematic representation of the strategy adopted for cloning the <i>lasI_{Pa}</i> and <i>rhlI_{Pa}</i> genes.....	63
Figure 3.2: Cloned <i>lasI_{Pa}</i> and <i>rhlI_{Pa}</i> genes lead to the production of OC ₁₂ -HSL and C ₄ -HSL respectively in <i>E. coli</i> MG1655	64
Figure 3.3: Relative molar proportions and quantitative profiling of AHLs produced by <i>lasI_{Pa}</i> expression in <i>E. coli</i> in LB growth media.....	66
Figure 3.4: Relative molar proportions and quantitative profiling of AHLs produced by <i>rhlI_{Pa}</i> expression in <i>E. coli</i> in LB growth media	67
Figure 3.5: Protein production confirmed from cloned synthase genes in <i>E. coli</i> MG1655	69
Figure 3.6: Reduced levels of AMC-linked metabolic profile of <i>E. coli</i> MG1655-AHL synthase strains	70
Figure 3.7: Reduced AI-2 production in induced MG1655[pME- <i>lasI_{Pa}</i>] and MG1655[pME- <i>rhlI_{Pa}</i>] cell free-extract	72

Figure 3.8: LC-MS/MS analysis of late exponential phase cultures revealed MTA levels increase with expression of the AHL synthases, which is emphasised by removal of the Pfs enzyme which metabolises MTA in MG1655.....	76
Figure 3.9: Introduction of the AHL synthase genes into MG1655 results in a growth defect that is more apparent in defined media.....	77
Figure 3.10: Exogenous methionine addition improves growth of MG1655[pME- <i>lasI_{Pa}</i>] and has no effect on MG1655[pME- <i>rbII_{Pa}</i>] in MOPS minimal media.....	78
Figure 4.1: <i>P. aeruginosa</i> RhlI AA homology with the crystal structure of LasI	86
Figure 4.2: Predictive modelling of <i>P. aeruginosa</i> RhlI structure.....	89
Figure 4.3: The proposed structure of RhlI gained from predictive modelling.....	90
Figure 4.4: SDMs of <i>lasI_{Pa}</i> and <i>rbII_{Pa}</i> produce differing levels of OC ₁₂ -HSL and C ₄ -HSL...	95
Figure 4.5: Relative molar proportions and cumulative profiling of AHLs produced by SDMs of <i>lasI_{Pa}</i> and <i>rbII_{Pa}</i> in <i>E. coli</i>	96
Figure 4.6: The majority all SDMs of <i>lasI_{Pa}</i> and <i>rbII_{Pa}</i> lead to the production of a stable protein in <i>E. coli</i> MG1655	98
Figure 4.7: AMC metabolite profiles of <i>lasI_{Pa}</i> and <i>rbII_{Pa}</i> SDMs in <i>E. coli</i>	100
Figure 4.8: <i>V. harveyi</i> biosensor-based AI-2 detection for <i>P. aeruginosa</i> AHL synthase SDMs expressed in <i>E. coli</i>	102
Figure 4.9: LC-MS/MS analysis of late exponential phase cultures revealed variable MTA levels of <i>lasI_{Pa}</i> and <i>rbII_{Pa}</i> SDMs in <i>E. coli</i> MG1655Δ <i>pfs</i>	103
Figure 4.10: Fitness profiles of <i>P. aeruginosa</i> AHL synthase SDM in <i>E. coli</i>	105
Figure 5.1: Relative molar proportions and cumulative profiling of AHLs produced by <i>lasI_{Pa}</i> and <i>rbII_{Pa}</i> in <i>E. coli</i> MG1655, MG1655Δ <i>luxS</i> , MG1655Δ <i>pfs</i> and MG1655Δ <i>sdiA</i>	113
Figure 5.2: Recombinant expression of <i>lasI_{Pa}</i> and <i>rbII_{Pa}</i> in the MG1655 <i>luxS</i> mutant leads to the build up of intracellular SRH and SAH and fall of HCY.....	115

Figure 5.3: Expression of the AHL synthase genes in MG1655 Δpfs creates a growth defect, while there are no significant differences between MG1655, MG1655 $\Delta luxS$ and MG1655 $\Delta sdiA$ 117

Figure 5.4: Recombinant expression of the *P. aeruginosa* AHL synthase genes in the MG1655 *pfs* mutant causes SAH accumulation and SRH and HCY levels to subside ..119

Figure 5.5: The expression of *rhII_{Pa}* and *lasI_{Pa}* in the MG1655 *sdiA* mutant causes significant drains AMC metabolites, but the effect of *rhII_{Pa}* is to a greater extent122

Figure 5.6: Schematic representation of the expected AMC metabolite profiles caused by *lasI_{Pa}* and *rhII_{Pa}* expression in the MG1655 *pfs* and *luxS* mutants127

Figure 6.1: *P. aeruginosa* AHL synthase mutants significantly disrupt AHL profiles and also disrupt levels of AQ and PQS, but to a lesser extent131

Figure 6.2: Increased levels of AMC-linked metabolic profile of *P. aeruginosa* PA01-AHL synthase mutants132

Figure 6.3: LC-MS/MS analysis of late exponential phase cultures revealed MTA levels decrease upon removal of the AHL synthases from the native *P. aeruginosa* background134

Figure 6.4: Removal of the AHL synthase genes from *P. aeruginosa* PA01 results in a growth defect that is more apparent when *lasI* is taken out of the system136

List of tables

Table 1.1: Examples of QS mediated gene regulation in bacteria.....	4
Table 1.2: Selected virulence factors of <i>P. aeruginosa</i> and their biological effects	13
Table 1.3: Global QS regulators in <i>P. aeruginosa</i>	21
Table 2.1: Composition of chemically defined media (CDM).....	36
Table 2.2 Bacterial strains used in this study.....	37
Table 2.3 Plasmids used in this study.....	38
Table 2.4: Standard recipes for agarose gel electrophoresis.....	43
Table 2.5 Oligonucleotide primers used in this study.....	44
Table 2.6: Components of a standard PCR.....	47
Table 2.7: Gold lysis buffer.....	50
Table 2.8: Standard recipes for western blotting solutions	51
Table 2.9: AMC metabolites - Selected precursor product ion m/z values, retention times, and collision energies used to identify and quantify analytes using MRM.....	57
Table 2.10: MTA - Selected precursor product ion m/z values, retention times, and collision energies used to identify and quantify analytes using MRM	58
Table 2.11: Recipe for AB media	59
Table 4.1: Nucleotide substitutions for AA chosen for mutagenesis within the <i>P. aeruginosa</i> AHL synthase genes.....	88
Table 8.1: Metabolic enzyme targets for inhibition of QS	147
Table 9.1: Preparation of MOPS minimal media (MMM)	175
Table 9.2: Standard recipes for agarose gel electrophoresis.....	176

Abbreviations

°C	degrees Celsius
% (w/v)	percentage weight per volume
% (v/v)	percentage volume per volume
AA	amino acid
AB	assay for bioluminescence
ACN	acetonitrile
ACP	acyl carrier protein
acyl-ACP	acylated acyl carrier protein
AdoMet	<i>S</i> -adenosyl-L-methionine
ADP	adenosine diphosphate
AI	autoinducer
AI-2	autoinducer-2
AHL	<i>N</i> -acyl-L-homoserine lactone
AQ	2-alkyl-4-quinolone
AMC	activated methyl cycle
AHQ	2-alkyl-4-hydroxyquinoline
APS	ammonium persulphate
ATP	adenosine-5'-triphosphate
bp	base pair
C₄-HSL	<i>N</i> -butanoyl-L-homoserine lactone
C₆-HSL	<i>N</i> -hexanoyl-L-homoserine lactone
C₈-HSL	<i>N</i> -octanoyl-L-homoserine lactone
C₁₀-HSL	<i>N</i> -decanoyl-L-homoserine lactone

C₁₂-HSL	<i>N</i> -dodecanoyl-L-homoserine lactone
C₁₄-HSL	<i>N</i> -tetradecanoyl-L-homoserine lactone
cAMP	cyclic adenosine monophosphate
Cb	carbenicillin
CCS	CRP-binding consensus sequence
CDM	chemically defined media
CF	cystic fibrosis
Cm	chloramphenicol
CoA	coenzyme A
CRP	cAMP receptor protein
d₉ C₅-HSL	deuterated <i>N</i> -pentanoyl-L-homoserine lactone
DCM	dichloromethane
dH₂O	distilled water
DMSO	dimethyl sulphoxide
DNA	deoxyribonucleic acid
dNTP	deoxynucleoside triphosphate
DPD	4,5-dihydroxy 2,3-pentanedione
EDTA	ethylenediaminetetraacetic acid
ESI	electrospray ionization
EtAC	ethyl acetate
EtBr	ethidium bromide
EtOH	ethanol
g	grams
Gm	gentamicin
GTP	guanosine-5'-triphosphate
h	hour

H₂O	water
HC₄-HSL	<i>N</i> -(3-hydroxy- butanoyl)-L-homoserine lactone
HC₁₀-HSL	<i>N</i> -(3-hydroxy-decanoyl)-L-homoserine lactone
HC₁₂-HSL	<i>N</i> -(3-hydroxy-dodecanoyl)-L-homoserine lactone
HC₁₄-HSL	<i>N</i> -(3-hydroxy- tetradecanoyl)-L-homoserine lactone
HCl	hydrochloric acid
HCN	hydrogen cyanide
HCY	homocysteine
HHQ	2-heptyl-4-quinolone
HHQNO	2-heptyl-4-quinolone <i>N</i> -oxide
HPLC	high-performance liquid chromatography
HSL	homoserine lactone
i-BuCF	iso-butylchloroformate
i-BuOH	iso-butanol
IPTG	isopropylthio-β-D-galacto-pyranoside
IS	internal standard
kb	kilobase
kDa	kilodalton
L	litre
LB	Luria Bertani
LC	liquid chromatography
LPS	lipopolysaccharide
M	molar concentration
mA	milliampere
Mbp	mega base pair
MDR	multi-drug resistant

MeOH	methanol
MET	methionine
min	minute
mg	milligram
ml	millilitre
mm	millimetre
mM	millimolar concentration
MMM	MOPS minimal media
MOPS	4-morpholinepropanesulfonic acid
MS/MS	tandem mass spectrometry
MTA	5'-methylthioadenosine
MTR	5'-methylthioribose
μF	microfaraday
μg	microgram
μl	microlitre
μm	micrometre
μM	micromolar concentration
NADPH	nicotinamide adenine dinucleotide phosphate
NCC	negative control condition
NHQ	2-nonyl-4-quinolone
nm	nanometre
OC₆-HSL	<i>N</i> -(3-oxohexanoyl)-L-homoserine lactone
OC₈-HSL	<i>N</i> -(3-oxooctanoyl)-L-homoserine lactone
OC₁₀-HSL	<i>N</i> -(3-oxodecanoyl)-L-homoserine lactone
OC₁₂-HSL	<i>N</i> -(3-oxododecanoyl)-L-homoserine lactone
OC₁₄-HSL	<i>N</i> -(3-oxotetradecanoyl)-L-homoserine lactone

OD	optical density
O/N	overnight
ORF	open reading frame
pBS	pBluescript vector
PBS	phosphate buffered saline
PCR	polymerase chain reaction
PDB	protein data bank
psi	pounds per square inch pressure
PQS	<i>Pseudomonas</i> quinolone signal; 2-heptyl-3-hydroxy-4-quinolone
QS	quorum sensing
QSSM	quorum sensing signal molecule
R	resistance
RE	restriction enzyme
RNA	ribonucleic acid
rpm	revolutions per minute
RT	room temperature
SAH	S-adenosyl-L-homocysteine
SAM	S-adenosyl-L-methionine
SDM	site-directed mutant
SDS	sodium dodecyl sulphate
SDS-PAGE	sodium dodecyl sulphate polyacrylamide gel electrophoresis
SRH	S-ribosyl-L-homocysteine
T3SH	T3 SAM hydrolase
TAE	tris-acetate-EDTA buffer
Tc	tetracycline

TCS	two-component signal transduction system
TEMED	tetramethylethylenediamine $(\text{CH}_3)_2\text{NCH}_2\text{CH}_2\text{N}(\text{CH}_3)_2$
TLC	thin-layer chromatography
Tris	tris hydroxymethyl aminomethane
UV	ultraviolet
V	volts
WT	wildtype
X-gal	5-bromo-4-chloro-3-indoyl β -D-galacto-pyranoside

Chapter 1

Introduction

1.1 Quorum sensing

For many years, bacteria were considered as autonomous unicellular organisms deprived of the cognitive and co-operative capacities that characterise collective behaviour. A statement by Francois Jacob (1973) sums up that long thought view: “It is perfectly possible to imagine a rather boring Universe without sex, without hormones and without nervous systems peopled only by individual cells reproducing *ad infinitum*. This Universe in fact exists. It is the one formed by a culture of bacteria.” Current knowledge opposes those dated opinions; in fact, the strength of co-operative social community offers far greater benefit as can be demonstrated by a plethora of examples outside the microbial world. The discovery of the co-operative regulation of bioluminescence in two marine bacterial species, *Vibrio fischeri* and *Vibrio harveyi* marked this historical transition. These bacteria demonstrated a co-ordinated behavioural phenotype which was governed by the expression and secretion of specific signalling molecules in a cell-density-dependent manner. Accumulation of these small, diffusible, low-molecular weight autoinducer (AI) or quorum sensing signal molecules (QSSMs) to a critical threshold concentration in the immediate environment triggers alterations in the expression of target genes (Figure 1.1). The communicative phenomenon highlights the importance of a sufficient number or ‘quorum’ of bacteria to be present in the population, hence the term “quorum sensing” (QS) was born (Fuqua, Winans & Greenberg 1994). Table 1.1 lists a selection of bacteria which have been shown to utilise QS, the AI molecules exploited and some of the regulated phenotypes. However, it is important to note that quorum sensing does not function in isolation; such a sophisticated mechanism is considered to act in conjunction with several other parameters which a bacterial cell must integrate in order to adapt and survive within a given ecological niche.

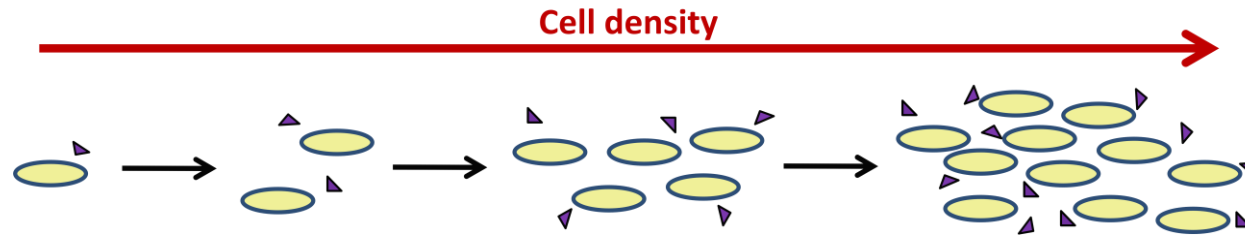


Figure 1.1: Quorum sensing (QS): Cell to cell communication in a bacterial population. Though bacterial cells secrete chemical (purple triangles), the low concentration of signal molecules in the environment does not alter gene expression. Once a specific cell density has been attained and a threshold signal concentration has been exceeded, this triggers signal concentration dependent gene expression.

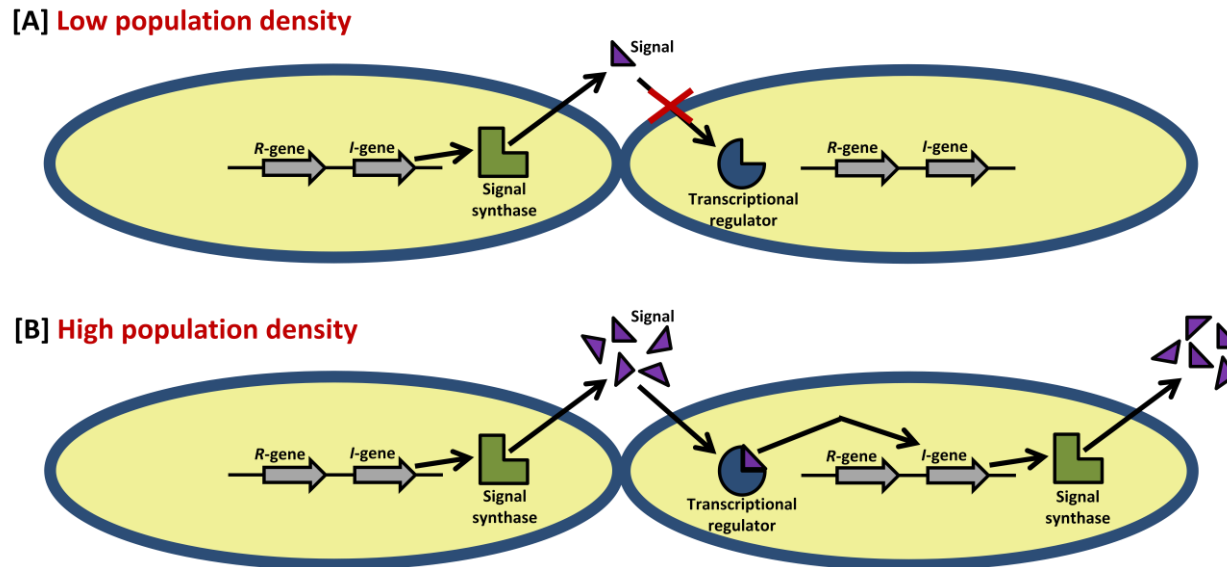


Figure 1.2: QS in Gram-negative bacteria. [A] At low population densities, the concentration of the AI is low and is unable to bind to the corresponding transcriptional regulator protein due to unfavourable binding kinetics. [B] At higher population densities, the concentration of the AI exceeds a threshold level and induces a conformational change in the transcriptional regulator protein, allowing it to bind. The transcriptional regulator-signal complex activates further production of the signal and the expression of various QS dependent phenotypes.

Bacterial Species	QS System	AI Identity	Phenotype
<i>Agrobacterium tumefaciens</i>	TraI/TraR	OC ₈ -HSL	Ti plasmid conjugal transfer (<i>tra</i> , <i>trb</i>)
<i>Bacillus subtilis</i>	ComP/ComA	ComX; CSF (competence and sporulation factor)	Competence; sporulation
<i>Chromobacterium violaceum</i>	CviI/CviR	OC ₆ -HSL	Violacein, HCN, antibiotics; exoproteases
<i>Escherichia coli</i>	?/SdiA	?	Cell division (<i>ftsQAZ</i>); chromosome replication
<i>Erwinia carotovora</i>	(a) ExpI/ExpR; (b) CarI/CarR	OC ₆ -HSL	(a) Exoenzymes; (b) carbapenam antibiotics
<i>Pseudomonas aeruginosa</i>	(a) LasI/LasR; (b) RhlI/RhlR	(a) OC ₁₂ -HSL; (b) C ₄ -HSL	(a) Exoprotease virulence factors (<i>lasA</i> , <i>lasB</i> , <i>toxR</i>); biofilm formation (b) protease (<i>lasB</i>); rhamnolipids (<i>rhlAB</i>); stationary phase
<i>Rhizobium leguminosarum</i>	(a) RhiI/RhiR; (b) CinI/CinR	(a) C ₆ -HSL; (b) HC _{14:1} -HSL	(a) Rhizosphere genes (<i>rhiABC</i>); stationary phase; (b) QS regulatory cascade
<i>Salmonella typhimurium</i>	LuxS	AI-2	Lsr ABC transporter
<i>Serratia liquefaciens</i>	SwrI/?	C ₄ -HSL	Swarming motility; exoprotease
<i>Staphylococcus aureus</i>	AgrC/AgrA	AIP (autoinducing peptide)	Exoenzymes; exotoxins
<i>Streptococcus pneumoniae</i>	ComD/ComE	CSP (competence stimulating peptide)	Competence

<i>Vibrio cholera</i>	LuxS	AI-2	Biofilm formation, cholera toxin, toxin co-regulated pilus, haemagglutinin Protease
<i>Vibrio fischeri</i>	LuxI/LuxR	OC ₆ -HSL; C ₈ -HSL	Bioluminescence (<i>luxICDABE</i>)
<i>Vibrio harveyi</i>	LuxS	AI-2	Bioluminescence, type III secretion, metalloprotease, siderophore, colony morphology
<i>Yersinia pseudotuberculosis</i>	(a) YpsI/YpsR; (b) YtbI/YtbR	(a) OC ₆ -HSL; (b) C ₈ -HSL	Aggregation, motility

Table 1.1: Examples of QS mediated gene regulation in bacteria. Pertinent examples are given of phenotypes as for some, including *P. aeruginosa*, but not all are listed.

1.1.1 Interspecies communication

The QSSM made by the greatest number of bacterial species, a collection that includes both Gram-positives and Gram-negatives, is autoinducer-2 (AI-2). For this reason, it has been proposed that AI-2 may mediate communication between different species. AI-2 was first discovered as a cell-to-cell signal molecule in the marine pathogen *V. harveyi*, where it regulates bioluminescence through a complex independent phosphorelay cascade. The ease in detection of extracellular AI-2 using the *V. harveyi* bioluminescence induction biosensor led to the discovery of functionally equivalent signalling molecules produced by many bacterial species. The LuxS synthase (Surette, Miller & Bassler 1999), responsible for producing the AI-2 precursor, has also been identified in many species and recent figures indicate its presence in approximately half of all sequenced Gram-positive and Gram-negative bacterial genomes (National Centre for Biotechnology Information, NCBI). Despite the identification of the LuxS synthase and confirmation of AI-2 activity as a global regulator of gene expression, the precise chemical nature of the AI-2 molecule secreted with respect to individual species may vary. This may be a consequence of the spontaneous chemical interchange that occurs between the different molecules that constitute the cocktail of AI-2.

The AI-2 precursor molecule, 4,5-dihydroxy-2,3-pentanedione (DPD), is a highly reactive product that can rearrange and undergo further reactions forming various structural derivatizations with similar stereochemistries (Miller *et al.* 2004). In *V. harveyi*, the cyclization pathway leading to AI-2 formation involves hydration of (2*S*, 4*S*)-2,4-dihydroxy-2-methyldihydrofuran-3-one (*S*-DHMF), one of two epimeric furanoses, followed by borate addition, forming (2*S*, 4*S*)-2-methyl-2,3,3,4-tetrahydroxytetrahydrofuran-borate (*S*-THMF-borate) (Chen *et al.* 2002). The structural identification of boron in a QSSM under these circumstances appears to be unusual, but provides a feasible explanation for the biological dependency for the element (Chen *et al.* 2002, Winans 2002). In contrast, *Salmonella typhimurium* recognizes another derivative, proposed to be (2*R*, 4*S*)-2-methyl-2,3,3,4-tetrahydroxytetrahydrofuran (*R*-THMF), formed simply by hydration of the other epimeric furanose (*R*-DHMF) (Miller *et al.*

2004). Therefore, the “AI-2” abbreviation is a collective term used to describe the group of furanone derivatives which form spontaneously from the common DPD precursor.

The primary role of AI-2 as a signal molecule in QS is extremely controversial. The DPD precursor synthesised by the LuxS enzyme is a by-product of the main conversion of substrate *S*-ribosyl-L-homocysteine (SRH) to homocysteine (HYC), which is an essential step in a fundamental recycling pathway referred to as the activated methyl cycle (AMC). Therefore, one potential explanation for the lack of evidence for a role of AI-2 in QS in some species may be due to AI-2 by-production occurring solely as a result of the AMC, rather than for exploitation for QS. Under these circumstances, the activity of LuxS is maintained because the metabolic role of the AMC is important to the cell. Further to this, attempts to restore phenotypes of mutants defective in AI-2 production to those of the parent by the addition of exogenous signal have not all resulted in complementation (DeLisa *et al.* 2001, Sperandio *et al.* 2001; Hardie *et al.* 2003), suggesting a primarily metabolic role for LuxS. In addition, there is a significant lack of evidence for the presence of important functional components including sensors, receptors and response regulators necessary for the corresponding signalling cascade (Sun *et al.* 2004, Rezzonico & Duffy, 2007, Bjarnsholt & Givskov 2008).

1.1.2 Intraspecies communication

Unlike AI-2, most QSSMs are species specific and enable intraspecies communication. In doing so, a species can use the QSSM to monitor its own population density without noise from co-habitants, enabling it to control gene expression accordingly.

1.1.2.1 QS in Gram-positive bacteria

Gram-positive bacteria use peptide-based QS signals and membrane bound sensor histidine kinases in a two-component signal transduction system (TCS); this mechanism allows the modulation of gene expression through a DNA binding protein termed the response regulator (Waters & Bassler 2005). The peptide-based signals are different from other types in that their secretion requires dedicated signal export channels. In the

majority of circumstances, these channels often transport the signal concomitantly with processing and modification such as the addition of thioactone rings (e.g. the autoinducing peptide of *Staphylococcus aureus*), lanthiinines (lantibiotics such as nisin produced by *Lactococcus lactis*) and isoprenyl groups (the comX pheromone of *Bacillus subtilis*) (Waters & Bassler 2005).

1.1.2.2 QS in Gram-negative bacteria

Gram-negative bacteria exploit a variety of small AI molecules for cell-to-cell communication. The best studied signalling systems use a family of molecules referred to as *N*-acyl-L-homoserine lactones (AHLs), which have been found to be produced in at least 70 different bacterial species. AHL-dependent QS circuits are regulated by two component sensory systems, in which a specific synthase 'I' protein generates the signal molecules. After diffusing into the environment, these signals can enter other bacterial cells and bind to the N-terminal AHL binding domain of a cognate transcriptional regulator 'R' protein which acts as the sensor to the system. At low population densities, both proteins are produced at basal levels. When a sufficient concentration of the AI has been attained, its binding to the 'R' protein elicits a conformational change in the protein to allow it to bind via a C-terminal DNA-binding domain and alter the expression of a subset of QS controlled genes. The signal-'R' protein complex can further activate expression of those genes responsible for the production of the signal synthase protein, thus creating a positive feedback loop with increasing concentration of the specific AI (Figure 1.2).

This phenomenon was first reported as a QS system in the regulation of bioluminescence in the marine bacterium *V. fischeri*, a property which allows the organism to live in symbiotic association with a number of eukaryotic hosts. In these circumstances, the regulatory proteins, LuxI and LuxR, regulate production of the luciferase enzyme, *luxCDABE*, which exists as part of a *luxICDABE* operon. LuxI synthesises the signal, *N*-(3-oxohexanoyl)-L-homoserine lactone (OC₆-HSL), whilst LuxR binds this signal, unmasking the LuxR DNA binding domain, allowing it to bind to the *luxICDABE*

promoter and activate its transcription. A positive feedback circuit means that an exponential increase in growth accompanies similar increases in production of OC₆-HSL and thus light emission. Many LuxI/LuxR homologous systems have been now been uncovered in other Gram-negative bacteria, some of which have been listed in Table 1.1; these have diverse biological roles that enable adaptation of a particular bacterial species to its specialized niche.

1.2 The genus *Pseudomonas*

The Pseudomonads are a class of gamma Proteobacteria belonging to the family Pseudomonadaceae. They are aerobic, non-spore forming, oxidase-positive Gram-negative bacilli. These bacteria are extremely versatile, having incredible nutritional versatility which allows adaptability to multiple natural environmental niches, including soil, marches and water reservoirs, as well as vegetation and animal tissues. The most extensively studied member of this genus is *Pseudomonas aeruginosa*, a clinically relevant opportunistic pathogen of the human host, which has been labelled as a “superbug” by the media by virtue of its prevalence in nosocomial environments and resistance to multiple antibiotics. Other members of this genus include the plant pathogen *Pseudomonas syringae*, bioremediation agents *Pseudomonas putida* and *Pseudomonas fluorescens* and several species known for their ability to cause food spoilage, *Pseudomonas fragi*, *Pseudomonas mudicolens* and *Pseudomonas lundensis*. Until 2000, the genus comprised over 100 species; however, the advancement in genotyping methods, primarily use of 16S rRNA sequencing has led to phylogenetic reclassification of many bacterial species to other taxonomic locations including *Burkholderia* spp., *Ralstonia* spp., *Brevundimonas* spp. and *Stenotrophomonas* spp (Anzai *et al.* 2000).

1.2.1 *Pseudomonas aeruginosa*

P. aeruginosa was first described as a unique bacterial species at the end of the 19th century, after the development of sterile culture media by Pasteur. In 1882, the first scientific study on the bacterium was published by a pharmacist named Carle Gessard. *P. aeruginosa*

is a rod-shaped bacterium, with a size of approximately 0.5-1.0 µm in breadth and 1-5 µm in length. The bacterium is monoflagellated and demonstrates unipolar motility. Growth and division of the organism is characterised by the appearance of microscopically-defined clusters of pearlescent spherical colonies. Of particular significance, *P. aeruginosa* secretes aminoacetophenone, giving a distinctive grapelike odour and pyocyanin, a derivative of phenazine which produces a characteristic blue-green pigmentation; these are often valuable in providing viable measures in the definitive identification of the bacterium. The latter characteristic has also been illustrated in old names for the organism: *Bacillus pyocyaneus*, *Bakterium aeruginosa*, *Pseudomonas polycolor*, and *Pseudomonas pyocyaneus*. In terms of its metabolic activity, the bacterium is adaptable to a variety of environmental conditions. *P. aeruginosa* is an obligate aerobe, but due to its capability to synthesize arginine, *P. aeruginosa* can also proliferate in anaerobic conditions. It is able to grow within a reasonably large temperature range, optimally at 37 °C, but notably up to 43 °C (Lyczak *et al.* 2000). Consequently, as well as being found amongst soil, water, humans, animals, plants, sewage, and hospitals, *P. aeruginosa* has the ability to survive in some fairly unusual conditions which include concentrated nitrogenous environments, high mercury concentrations and amongst fuels such as diesel where it utilises the hydrocarbon components. Complete genome sequencing of *P. aeruginosa* PA01 revealed it constitutes 6.3 Mbp and 5,570 predicted open reading frames (ORFs) (Stover *et al.* 2000). This represents one of the largest bacterial genomes to be sequenced to date, having the genetic complexity of a smaller eukaryotic organism, such as *Saccharomyces cerevisiae*.

1.2.1.1 Clinical significance of *P. aeruginosa*

As mentioned, *P. aeruginosa* is an extremely versatile organism, ubiquitous to numerous ecological niches. More significantly, however, *P. aeruginosa* is known for its ability to persist as a dangerous and medically significant human pathogen capable of causing a broad-spectrum of mild to potentially life threatening conditions. The latter is invariably dependent on the organism's predominant opportunistic behaviour. More specifically, *P.*

aeruginosa is associated with a wide variety of community-acquired infections including ulcerative keratitis, otitis externa and skin and soft tissue infections with contact lens solutions, swimming pools and hydrotherapy pools offering possible sources of contamination. Individuals with burns and wounds are also susceptible to infection; upon destruction of the natural skin barrier, *P. aeruginosa* is able to colonise the lower layers of the skin and can release degradative enzymes to cause further destruction whilst simultaneously imposing immune modulatory effects in the host. *P. aeruginosa* infections are often established in patients with primary immunodeficiencies such as those with cancer or AIDS. In addition, the existence of hospital-acquired nosocomial infections such as pneumonia, urinary tract infections (UTIs), and bacteraemia account for an estimated 10,000 cases each year in UK hospitals (Lister, Wolter & Hanson 2009; Mayor 2000; Spencer 1996); often, these are associated with medical interceptive measures such as lumbar punctures, intravenous infusions and intravascular catheters, where *P. aeruginosa* forms complex 'biofilm' bacterial communities that adhere to the surface of biomedical devices. The persistent colonisation of the sinopulmonary tract in cystic fibrosis (CF) patients highlights the bacteria's best known role, with an estimated 80% of adults with CF carrying *P. aeruginosa* in their lungs; chronic and recurrent respiratory infections in these individuals ensures a progressively worsening morbid state, eventually leading to mortality (George, Jones & Middleton 2009; Doring *et al.* 2000). Furthermore, the treatment of conditions caused by *P. aeruginosa* is significantly more problematic due to the continual acquisition of intrinsic antibiotic resistance leading to multi-drug resistant (MDR) strains, which typically exhibit several resistance mechanisms simultaneously (El Solh & Alhajhusain 2009; Lister, Wolter & Hanson 2009; Driscoll, Brody & Kollef 2007). This further highlights the importance of the organism's intrinsic virulence and the need to explore its pathogenic nature.

1.2.1.2 Virulence determinants of *P. aeruginosa*

P. aeruginosa virulence is generally thought to be multifactorial and attributable to several aspects of the organism's variable protein expression profile. Table 1.2 summarises the

function of a selection of virulence determinants displayed by *P. aeruginosa*. These include a wide range of mechanisms encoded chromosomally and/or on plasmids.

Cell surface components include the production of a single flagellum, multiple pili, and the biosurfactant rhamnolipid, all of which confer motility and adherence to host surfaces. *P. aeruginosa* as a pathogen is an interesting organism in that it relies heavily on the secretion of virulence determinants including several exoenzymes; these disrupt host immune defences and mediate damage to target cells whilst simultaneously allowing the provision of nutrients to the bacteria. Specific examples of virulence determinants secreted by *P. aeruginosa* include enzymes (elastase, LasA protease, alkaline protease), toxins, pigments (pyocyanin, pyoverdinin and pyorubin) and other metabolites.

Biofilm formation is another important characteristic of *P. aeruginosa*; distinct from planktonic growth are the bacteria that adhere to a living or non-living surface and/or each other thereby forming a complex community of cells. Development of biofilms is facilitated by an extracellular polymeric matrix or “slime” of secreted polysaccharides, proteins and nucleic acids and water channels that distribute nutrients, oxygen and signalling molecules and remove metabolic waste products (Costerton 1995). Bacterial accumulation through biofilms increases the possibility for horizontal gene transfer and metabolic interactions, conferring resistance to antibiotics and the host immune system, thus the biofilm lifestyle supports survival in hostile environments (Mah *et al.* 2003; Burmolle *et al.* 2006). The development of a biofilm is thought to occur in five distinct stages: (i) initial attachment, (ii) irreversible attachment, (iii) maturation-I, (iv) maturation-II and (v) dispersal (Sauer *et al.* 2002). Most notably the stages involved in biofilm formation highlight the important role of communication within the microbial community. Indeed, communication via QS by *P. aeruginosa* is essential for the collective regulation of gene transcription having subsequent and simultaneous effects on metabolism, protein synthesis and virulence.

Virulence determinant	Biological function	Reference
Alkaline protease	Inactivation of protease inhibitors and complement proteins; hydrolysis of fibrinogen and fibrin.	Howe & Iglewski 1984; Hong & Ghebrehiwet 1992; Gambello, Kaye & Iglewski 1993; Latifi <i>et al.</i> 1995
Alginate	Viscous exopolysaccharide; increases adherence to respiratory epithelia; inhibits phagocytosis; increases resistance to antibiotics and disinfectants	Doig <i>et al.</i> 1987; Leid <i>et al.</i> 2005
Elastase	Degrades elastin leading to breakdown of host tissue.	Blackwood <i>et al.</i> 1983; Elsheikh <i>et al.</i> 1987; Toder <i>et al.</i> 1994
Exoenzyme S	GTPase activating protein; ADP-ribosylation of GTP-binding proteins; inhibits phagocytosis.	Iglewski <i>et al.</i> 1978; Nicas <i>et al.</i> 1985a; Nicas <i>et al.</i> 1985b; Knight <i>et al.</i> 1995
Exoenzyme T	GTPase activating protein; inhibits host-cell division and phagocytosis; induces epithelial cell apoptosis	Krall <i>et al.</i> 2000; Shafikhani & Engel 2006; Shafikhani, Morales & Engel 2008
Exoenzyme U	Phospholipase; induces acute cytotoxicity and epithelial injury	Finck-Barbancon <i>et al.</i> 2007; Sato <i>et al.</i> 2003
Exotoxin A	Catalyses ADP-ribosylation causing inactivation of elongation factor 2; inhibits protein synthesis; induces tissue damage and host immunosuppression.	Iglewski, Liu, & Kabat 1977; Blackwood <i>et al.</i> 1983; Wick, Hamood, & Iglewski 1990; Gambello, Kaye & Iglewski 1993; Armstrong, Yates & Merrill 2002
Flagella	Swimming and swarming motility; adherence to cell surfaces.	Arora <i>et al.</i> 1998;
Hydrogen cyanide (HCN)	Inhibits aerobic respiration in host cells; accumulates in CF lungs.	Pessi & Haas 2000; Gallagher & Manoil 2001; Ryall <i>et al.</i> 2008
LasA protease (staphylolysin)	Serine protease; nicks elastin increasing sensitivity to LasB elastase, alkaline protease, and	Kessler <i>et al.</i> 1993

LasB protease	neutrophil elastase degradation. Zinc metalloprotease; degrades elastin.	
Lectins (LecA/LecB)	Mediate adhesion to host epithelial surfaces; cytotoxins; inhibit human ciliary beating	Glick & Garber 1983; Bajolet-Laudinat <i>et al.</i> 1994; Winzer <i>et al.</i> 2000
Lipase	Cleaves lipids; degrades platelets, granulocytes and monocytes.	Konig <i>et al.</i> 1996
LPS	Outermembrane glycolipid; stimulates host inflammatory responses; impedes diffusion of antibiotics.	Pier 2007; Nakamura <i>et al.</i> 2008
Neuraminidase	Cleaves sialic acid residues on host cell surfaces; enhances pilin-mediated adhesion; contributes to biofilm formation.	Cacalano <i>et al.</i> 1992; Soong <i>et al.</i> 2006
Pili	Swimming and swarming motility; adherence to cell surfaces.	Hazlett <i>et al.</i> 1991; Comolli <i>et al.</i> 1999
Phospholipase C	Heamolysin; induces vascular permeability; mediates tissue invasion.	Meyers & Berk 1990
Pyochelin & Pyoverdine	Siderophores; allow iron acquisition from the host; catalyses the formation of free radicals to cause damage to tissue.	Meyer <i>et al.</i> 1996; Britigan <i>et al.</i> 1997
Pyocyanin	Redox-active phenazine pigment; interferes with ion transport; stimulates inflammatory response.	Brint & Ohman 1995; Latifi <i>et al.</i> 1995; Parsek & Greenberg 2000; Mavrodi <i>et al.</i> 2001
Rhamnolipids	Heamolysin; glycolipid biosurfactant; solubilisation of lung surfactant phospholipids to assist phospholipase C; inhibits mucociliary transport and ciliary function of host respiratory epithelium.	Ochsner <i>et al.</i> 1994; Ochsner & Reiser 1995; Lang & Wullbrandt 1999; Pearson, Pesci & Iglewski 1997

Table 1.2: Selected virulence factors of *P. aeruginosa* and their biological effects.

1.3 QS in *P. aeruginosa*

P. aeruginosa is a species in which cell-to-cell communication systems have been intensely investigated. Microarray studies have suggested that 6% of the *P. aeruginosa* genome is regulated by QS (Schuster *et al.* 2003; Wagner *et al.* 2003). Figure 1.3 summarises the QS system of *P. aeruginosa*, including regulators. Like many Gram-negative bacteria, *P. aeruginosa* possesses two AHL-dependent QS circuits; these LuxRI homologues are recognised as the *las* and *rhl* systems. The *las* system was the first cell-to-cell signalling system to be described in *P. aeruginosa* as a regulator of the expression of the LasB elastase, hence the origin of its name. This system includes the transcriptional activator LasR (Gambello & Iglewski 1991), and the AHL synthase, LasI (Passador *et al.* 1993), which regulates the production of primary *N*-(3-oxododecanoyl)-L-homoserine lactone (OC₁₂-HSL) (Figure 1.4) (Pearson *et al.* 1994). Together, the activated complex of LasR and OC₁₂-HSL are effective regulators of a variety of virulence genes including *aprA*: alkaline protease (Gambello, Kaye & Iglewski 1993; Latifi *et al.* 1995) *lasA/lasB*: elastase A/B (Toder *et al.* 1994), *toxA*: exotoxin (Gambello, Kaye & Iglewski 1993) and also *lasI* itself, therefore creating a positive feedback loop (Seed, Passador & Iglewski 1995). The *rhl* system is secondary and was termed according to its ability to control the production of rhamnolipid; it consists of the transcriptional regulator RhlR, and the AHL synthase, RhlI, which is responsible for the synthesis of *N*-butanoyl-L-homoserine lactone (C₄-HSL) (Figure 1.4) and small amounts of *N*-hexanoyl-L-homoserine lactone (C₆-HSL). Inducing the synthesis of this AHL is known to activate RhlR (Brint & Ohman 1995; Latifi *et al.* 1995), and in turn induce the expression of numerous pathogenicity determinants including *lasB*: elastase A (Pearson, Pesci & Iglewski 1997), *rhlAB*: rhamnolipid surfactant (Ochsner & Reiser 1995; Pearson, Pesci & Iglewski 1997), *rpoS*: stationary phase (Latifi *et al.* 1996), pyocyanin (Brint & Ohman 1995; Latifi *et al.* 1995), *hcnABC*: HCN (Pessi & Haas 2000), *lecA*: cytotoxic lectins (Winzer *et al.* 2000) and *rhlI*.

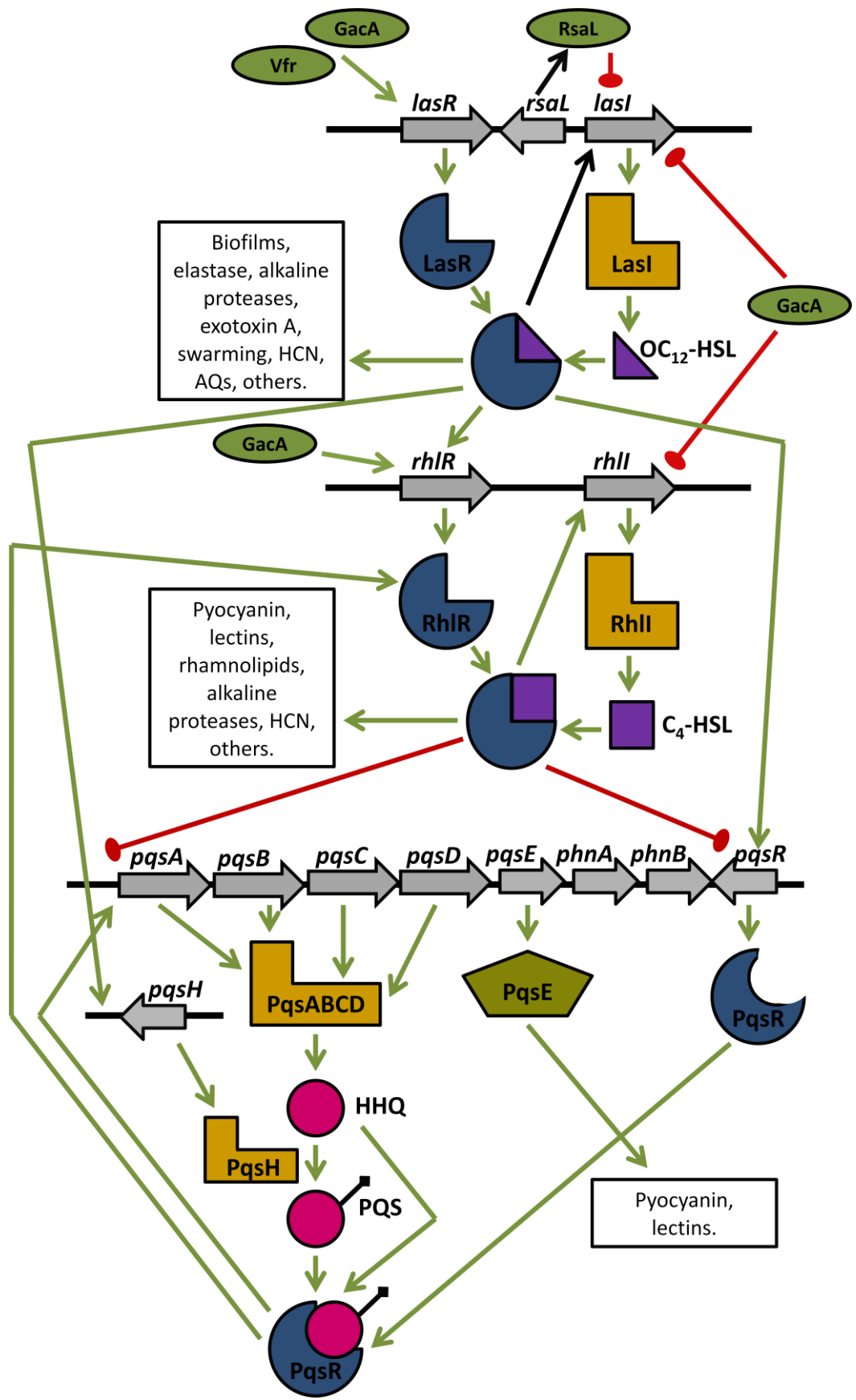


Figure 1.3: AHL and AQ-dependent QS in *P. aeruginosa*. The AHL-based QS cascade is initiated when bacterial cells exceed a critical population density, with the activation of the LasR protein by OC₁₂-HSL. Together, the activated complex of LasR and OC₁₂-HSL in turn activates the *rhl* system. The AHL-dependent system is intimately linked to the AQ system via LasR–OC₁₂-HSL being necessary for *pqsH* expression, *pqsR* being positively regulated by LasR–OC₁₂-HSL and RhlR–C₄-HSL repressing *pqsA* and *pqsR*. The AHL and AQ-dependent systems are responsible for the regulation of numerous, sometime overlapping, phenotypes. The entire system is itself regulated at various points by numerous regulators.

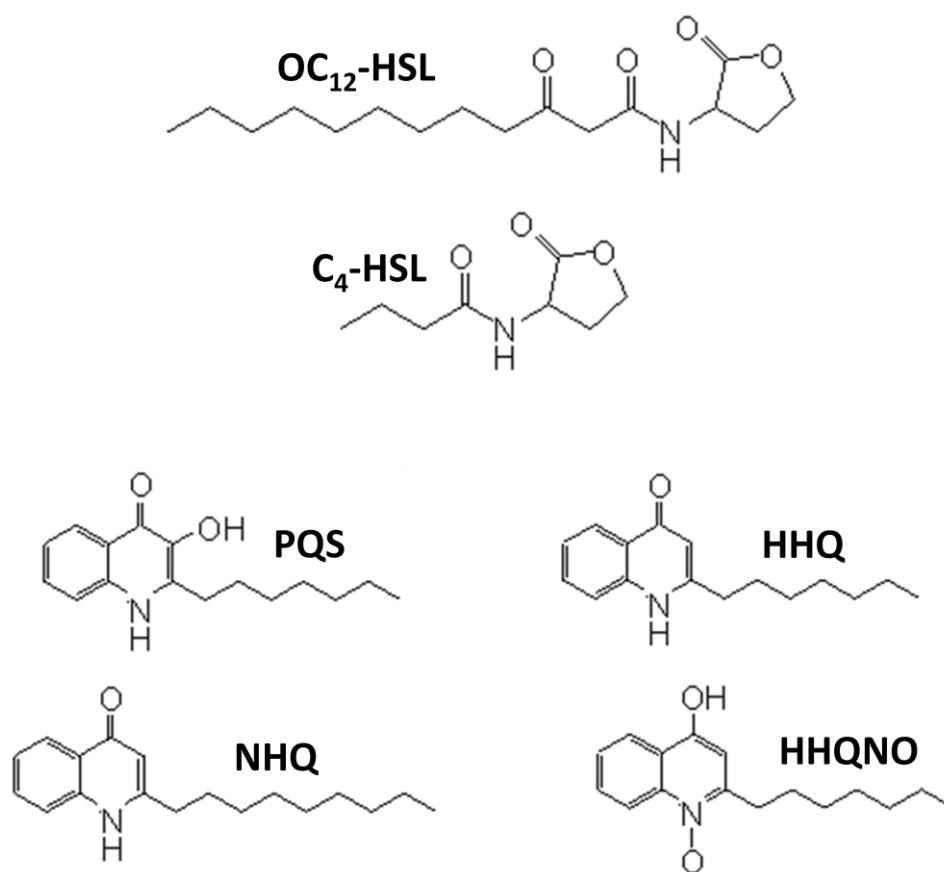


Figure 1.4: The structure of the main QSMMs produced by *P. aeruginosa*. *N*-acyl-L-homoserine lactones (AHLs): *N*-(3-oxododecanoyl)-L-homoserine lactone (OC₁₂-HSL) and *N*-butanoyl-L-homoserine lactone (C₄-HSL), and alkyl-4(1H)-quinolones (AQs): 2-heptyl-3-hydroxy-4-quinolone (PQS), 2-heptyl-4-quinolone (HHQ), 2-nonyl-4-quinolone (NHQ) and 2-heptyl-4-quinolone *N*-oxide (HHQNO).

Expression of some phenotypes such as alkaline protease, elastase and HCN are under the control of both the *las* and *rhl* systems. As well as existing as mutually exclusive circuits, with their respective AIs unable to activate the transcriptional regulator protein of the other system, the two systems interact creating a hierarchical organisation between them. The *las* system exerts positive control over the *rhl* system; in *P. aeruginosa* and *Escherichia coli*, LasR and OC₁₂-HSL have been shown to positively regulate the transcription of *rhlI* and *rhlR*, and in *E. coli* OC₁₂-HSL posttranslationally controls RhlR by blocking the interaction of C₄-HSL with RhlR (Latifi *et al.* 1996; Pesci *et al.* 1997).

In 1999, further investigations by Pesci *et al.* showed that spent culture supernatant of *P. aeruginosa* wildtype (WT) strain PA01 was able to induce *lasB* expression in an AHL-negative PA01 *lasR* mutant. Spent culture media extracted from a double AI *lasI/rhlI* mutant had a similar effect on the *lasR* mutant. This provided strong evidence for the discovery of a novel non-AHL-dependent QS system in *P. aeruginosa*. The chemically distinct molecule was characterised as 2-heptyl-3-hydroxy-4-quinolone, being designated as the *Pseudomonas* quinolone signal (PQS) (Figure 1.4). PQS is a derivative molecule belonging to a family of compounds known as 2-alkyl-4(1H)-quinolones (AQs), which were originally identified by their antibacterial properties, more specifically the preventative development of anthrax in rabbits. PQS represents one of many AQs produced by the species; other major AQs produced by *P. aeruginosa* include 2-heptyl-4-quinolone (HHQ), 2-nonyl-4-quinolone (NHQ) and 2-heptyl-4-quinolone *N*-oxide (HHQNO) (Figure 1.4).

The study by Pesci *et al.* (1999) additionally demonstrated that the signal in culture extracts of WT PA01 and PA01 *lasI/rhlI* mutant failed to induce *lasB* expression in a PA01 *lasR/rhlR* mutant, suggesting that the *rhl* system was required for the bioactivity of PQS. Subsequently, using *lacZ* reporter fusions it was confirmed that PQS regulates *rhlI* at a transcriptional level (McKnight, Iglewski & Pesci 2000), thus illustrating that PQS was significant to the hierarchical QS circuitry, providing another fundamental regulatory link between the *las* and *rhl* systems. In addition to this, Gallagher *et al.* (2002) illustrated that LasR controls PQS production via the transcription of *pqsH* which is required for the

final conversion of HHQ to PQS, Furthermore, the relevance of PQS to *P. aeruginosa* virulence has been demonstrated through the abundance of the molecule in the lungs of *P. aeruginosa*-infected CF patients (Collier *et al.* 2002).

1.4 Global QS regulators in *P. aeruginosa*

As well as the *las*, *rhl* and AQ systems, other global regulators, operating at both the transcriptional and translational level have been identified. These influence the expression of the various QS components and the associated virulence determinants under their control. Table 1.3 lists some of the important global regulators together with the regulated aspects of QS and associated virulence determinants. It also includes the two additional LuxR homologues, QscR and VqsR.

1.5 Biosynthesis of AHLs in *P. aeruginosa*

More than 40 AHL synthases homologous to LuxI have now been characterised (Fuqua, Winans & Greenberg 1994), which collectively generate a considerable repertoire of AHLs, with all conforming to a general structure of a homoserine lactone (HSL) ring linked to an acyl chain. Specificity is attained by variable acyl chain lengths from C₄ to C₁₈, oxidation at the C₃ position and different degrees of unsaturation. In consideration of the above, the nature of the AHL molecule(s) synthesised is determined by the specific LuxI homologue present in an organism's genome (Jiang *et al.* 1998). More specifically, this variability is a function of the synthase acyl chain specificity. In fact, the introduction of RhlI into *E. coli* has demonstrated production of both C₄-HSL and C₆-HSL to levels similar to that observed in *P. aeruginosa*, confirming both the former and the availability of all the necessary substrates in *E. coli*. More specifically, Jiang *et al.* (1998) showed that RhlI catalyses the *in vitro* enzymatic synthesis of C₄-HSL and C₆-HSL from either S-adenosyl-L-methionine (SAM) (also referred to as AdoMet) or HSL and the butanoyl- or hexanoyl-charged coenzyme A (CoA) derivative in an NADPH-dependent manner.

Regulator	Type	Phenotypes Regulated & References
GacA/GacS	Two component regulator system: comprising a membrane bound histidine kinase sensor that relays information on environmental stimuli to a phosphorylated response regulator (Rodrigue <i>et al.</i> 2000)	– Positively activate <i>las</i> and <i>rhl</i> systems: enhances C ₄ -HSL and associated virulence factor production (Reimmann <i>et al.</i> 1997) including biofilm development (Parkins, Ceri & Storey 2001)
MvaT	DNA binding protein of H-NS family	– Global regulator of virulence determinants: suggested QS repressor since <i>mvaT</i> mutants demonstrate reduced swarming behavior and LasA and LasB protease production, and enhanced <i>lecA</i> expression, pyocyanin production and C ₄ -HSL and C ₁₂ -HSL levels (Diggle <i>et al.</i> 2002) – Also microarray analysis has shown approximately 150 genes are differentially expressed in <i>mvaT</i> mutant (Vallet <i>et al.</i> 2004)
QscR (quorum-sensing-control repressor)	Suggested function: transcriptional antagonist which sequesters LasR and RhlR monomers forming inactive heteromultimers thus preventing “false” activation of QS controlled genes (Fuqua 2006); LuxR homologue exhibiting significant homology to	– Repression of <i>lasI</i> since a <i>qscR</i> mutant has premature C ₁₂ -HSL production which leads to premature expression of a number of QS regulated genes including those responsible for the AHL synthesis, HCN, pyocyanin and elastase (Chugani <i>et al.</i> 2001; Ledgham <i>et al.</i> 2003) – Transcription profiles of more than 400 genes also differentially expression in a <i>qscR</i> mutant (Lequette <i>et al.</i> 2006)

RsaL	LasR and RhlR Transcriptional regulator	<ul style="list-style-type: none"> – Represses <i>las</i> system at low population densities by binding to the <i>lasI</i> promoter thereby preventing its expression and preventing LasR–OC₁₂-HSL dependent transcription – Regulated itself: <i>las</i> (LasR–OC₁₂-HSL) regulated <i>rsaL</i> transcription (de Kievit <i>et al.</i> 1999; Rampioni <i>et al.</i> 2006)
RsmA	Post-transcriptional regulator which acts via mRNA binding, promoting decomposition or extending stability of the corresponding transcript (Heeb <i>et al.</i> 2006); <i>E. coli</i> CsrA homologue (Romeo <i>et al.</i> 1993)	<ul style="list-style-type: none"> – RsmA positively regulates rhamnolipid biosynthesis, swarming motility and lipase production (Heurlier <i>et al.</i> 2004) – Represses pyocyanin, PA-IL lectin, C₄-HSL and C₁₂-HSL production (Pessi <i>et al.</i> 2001) [RsmA regulation antagonised by the high-affinity binding of small non-coding regulatory RNAs RsmY and RsmZ that prevent it from binding to mRNA (Babitzke & Romeo 2007)]
Vfr	<i>E. coli</i> cyclic adenosine monophosphate (cAMP) receptor protein (CRP) homologue; regulates many genes which are responsible for catabolite repression by glucose (Botsford & Harman 1992; Kolb <i>et al.</i> 1993)	<ul style="list-style-type: none"> – Activates LasR by binding to CRP-binding consensus sequence (CCS) in <i>lux</i> operon promoter region (Dunlap & Greenberg 1988; Shadel, Devine & Baldwin 1990; Stevens, Dolan & Greenberg 1994) – Important to <i>las</i> dependent exotoxin A and protease production (West <i>et al.</i> 1994) – Additionally modulates <i>rhlI</i>, twitching motility, flagella production and various effector proteins involved in type III secretion
VqsR (virulence and quorum sensing regulator)	LuxR homologue	<ul style="list-style-type: none"> – VqsR lies at the same level as RhlR and QscR in the QS hierarchy with direct regulatory control exerted from the <i>las</i> system (Li, Malone & Iglewski

2007)

– Both activates the expression of genes known to be promoted by QS (including phenazine and rhamnolipid biosynthesis, HCN synthesis, protease secretion and PQS production) and negatively regulates the expression of genes known to be repressed by QS (nitrogen metabolism) (Juhas *et al.* 2004)

Table 1.3: Global QS regulators in *P. aeruginosa*

However, the activity of the RhII preparations observed in this study were significantly lower than previously observed with preparations of other LuxI homologues; it has since been confirmed that the substrates are SAM and the appropriately charged acylated acyl carrier protein (acyl-ACP), providing the HSL moiety and acyl chain donor, respectively (Val & Cronan 1998).

The synthase enzymes are thought to produce AHLs in a “bi-ter” sequentially ordered reaction. In the primary acylation reaction, the acyl chain is presented to the AHL synthase as a thioester of the ACP phosphopantetheine prosthetic group, and results in nucleophilic attack on the carbonyl position of C1 by the amino nitrogen of SAM, generating an amide linkage. The secondary lactonization reaction, subsequent to, or concomitant with, amide bond formation, occurs by nucleophilic attack on the γ carbon of SAM by its own carboxylate oxygen and results in HSL ring formation; this is coupled to the release of by-products holo-acyl carrier protein (holo-ACP) and 5'-methylthioadenosine (MTA) (Parsek *et al.* 1999).

1.6 AQ-dependent QS in *P. aeruginosa*

Synthesis of the PQS is dependent upon anthranilate availability and a functional biosynthetic *pqsABCDE* operon. To date, the enzymatic contribution of many of the individual *pqs* gene products to PQS biosynthesis remains unclear, although sequence comparisons have illustrated putative functions. PqsA demonstrates significant homology to a variety of benzoate coenzyme A ligases (Gallagher *et al.* 2002), and has been confirmed to be required for the activation of the anthranilate precursor; the ligase generates an activated anthraniloxy-CoA thioester which is necessary for priming anthranilate for PQS biosynthesis (Coleman *et al.* 2008). The *pqsB*, *pqsC* and *pqsD* genes are thought to encode for 3-oxo-acyl-(ACP) synthases and may be important in the synthesis of the corresponding fatty acid hydrocarbon chains. Recently, crystal structures of PqsD have revealed its involvement in a condensation reaction between anthraniloxy-PqsD and malonyl-CoA or malonyl-ACP with 2,4-dihydroxyquinoline (DHQ) as the product (Zhang *et al.* 2008; Bera *et al.* 2009); however, though PqsD has relevance to PQS

biosynthesis, DHQ has not been shown to be a possible PQS precursor to date. The last gene in the polycistronic operon, *pqsE*, is either thought to facilitate the cellular response to PQS or be involved in the synthesis of a currently unidentified PQS-derivative signalling molecule. The crystal structure of PqsE indicates a metallo- β -lactamase fold with a Fe(II)Fe(III) centre in the active site and the presence of benzoate indicating the possible substrate may be a chorismate derivative (Yu *et al.* 2009). Nevertheless, it has been determined that AQs are formed via the condensation of anthranilate and a β -keto-fatty acid; the 2-heptyl-4-quinolone (HHQ) intermediate which is released into the extracellular environment is hypothesised to be converted into PQS by the addition of a hydroxyl group by a cytoplasmic FAD-dependent monooxygenase (*pqsH*) in a neighbouring cell.

The anthranilate requirement for PQS synthesis draws on one of several aspects of aromatic amino acid (AA) metabolism (Figure 1.5). The *P. aeruginosa* genome encodes several distinct anthranilate synthase enzymes, notably TrpEG, and PhnAB, which is located downstream from the PQS biosynthetic operon (Essar *et al.* 1990a). Both synthase enzymes are thought to synthesize the anthranilate precursor of PQS from shikimate via chorismate (Essar *et al.* 1990a). In the former, the *trpE* and *trpG* genes have been shown to participate in the tryptophan synthetic pathway (Essar *et al.* 1990b), whilst the *phnA* and *phnB* genes are important for the biosynthesis of phenazine antibiotics, particularly in the production of the pyocyanin pigment (Mavrodi *et al.* 2001). In contrast, a recent paper by Farrow & Pesci (2007) suggests that the degradation of tryptophan through the kynurenine (*kyn*) pathway additionally represents a fundamental source of anthranilate for PQS production. This research has extended an earlier suggestion made by D'Argenio *et al.* (2002) in relation to the involvement of tryptophan 2,3-dioxygenase (*kynA*) in autolysis. Nevertheless, levels of tryptophan are consistent with PQS biosynthesis (Farrow & Pesci 2007).

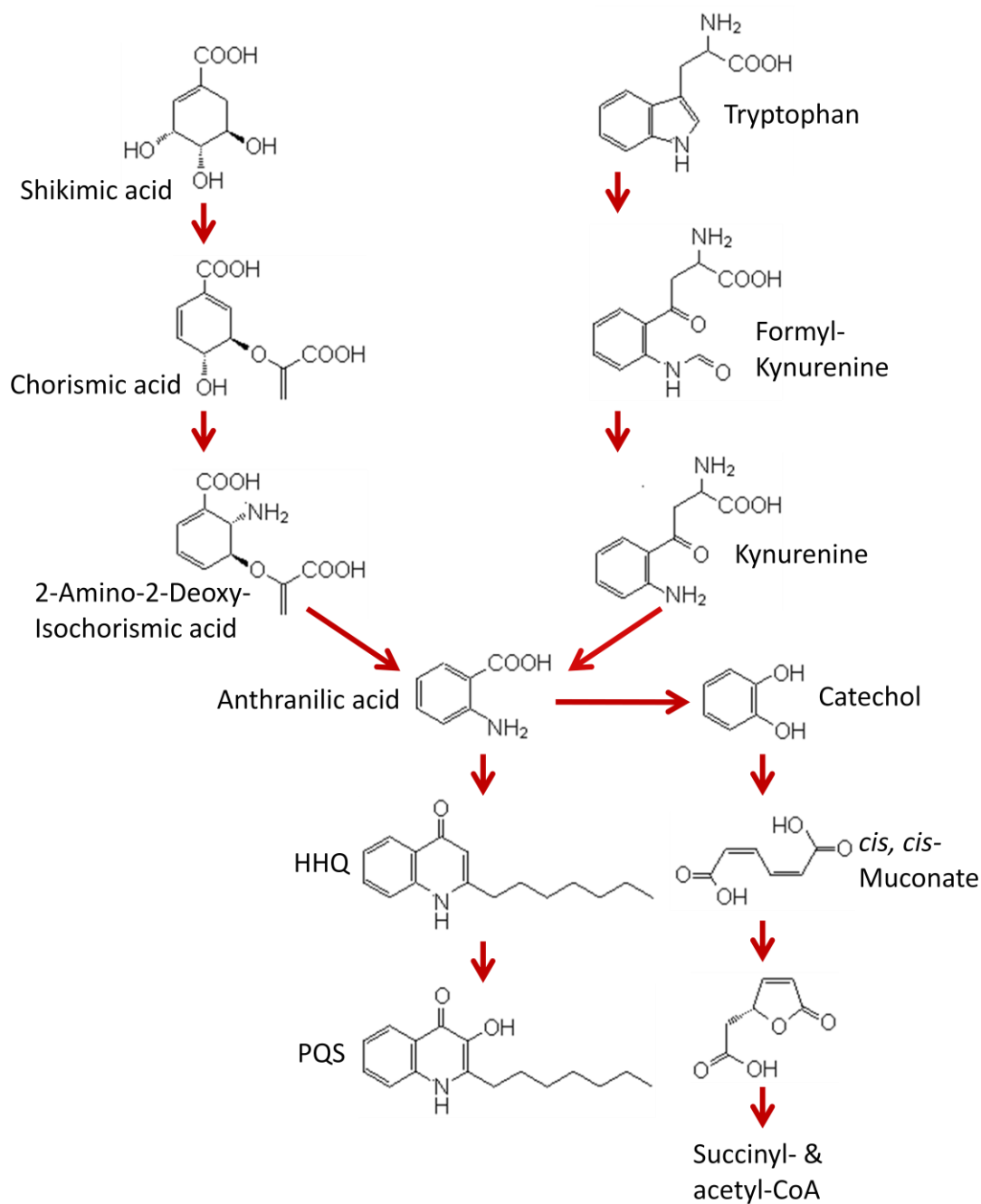


Figure 1.5: Scheme for PQS biosynthesis and degradation. Production of anthranilic acid can occur through two alternative routes, either from shikimic acid via chorismic acid or through tryptophan degradation in the kynurenine pathway. Anthranilic acid condenses with β -ketodecanoic acid to produce the PQS precursor (HHQ) upon decarboxylative cyclisation and this undergoes oxidative hydroxylation at the 3-position thus giving PQS. Anthranilate catabolism produces several aromatic intermediates, notably catechol, *cis,cis* muconate and muconolactone.

Through the development of a synthetic medium that nutritionally mimics CF sputum, Palmer, Aye & Whiteley (2007) have additionally demonstrated the high incidence of aromatic AAs, notably phenylalanine and tyrosine, in CF sputum samples. This occurs in association with elevated production of PQS, and several PQS-regulated factors including pyocyanin. Other aromatic AAs linked to anthranilate metabolism include catechol, the initial product of anthranilate catabolism via the anthranilate dioxygenase (*antABC*), *cis,cis* muconate, the product of catechol degradation by catechol dioxygenase (*catA*), and muconolactone, the result of processing by muconate lactonizing enzyme (*catB*); the latter are involved in the β -ketoacid pathway in *P. aeruginosa* (Kukor, Olsen & Ballou 1988).

1.7 The activated methyl cycle (AMC)

As well as the significance of SAM to the production of AHLs, it is an extremely versatile molecule with several additional functions, one of which is fundamental to the recycling pathway linked to methionine metabolism. The AMC is a pathway dedicated to the metabolism of SAM, the major methyl donor in eubacterial, archaeobacterial and eukaryotic cells (Figure 1.6). However, the metabolic link between the AMC to AHL synthesis via SAM is rarely taken into consideration; it may actually be of greater importance to determine the metabolic consequences of AHL synthesis upon the organism's cell physiology given that alterations to intracellular SAM levels are likely to subsequently impact upon essential methylation reactions within the cell.

Living organisms exploit methionine for the production of SAM. SAM is an essential nucleoside that serves as an activated group donor in various metabolic and biosynthetic reactions, including methylation, propylamine group transfer in polyamine synthesis and SAM radical-mediated vitamin synthesis (Parveen & Cornell 2011). DNA methylation is critical in the regulation of gene expression and the bacterial cell cycle, allows nuclease recognition and performs protective roles against damage from other restriction endonucleases. Methylation additionally represents an important post-transcriptional modification for rRNA and proteins, carbohydrates, lipids and other molecules.

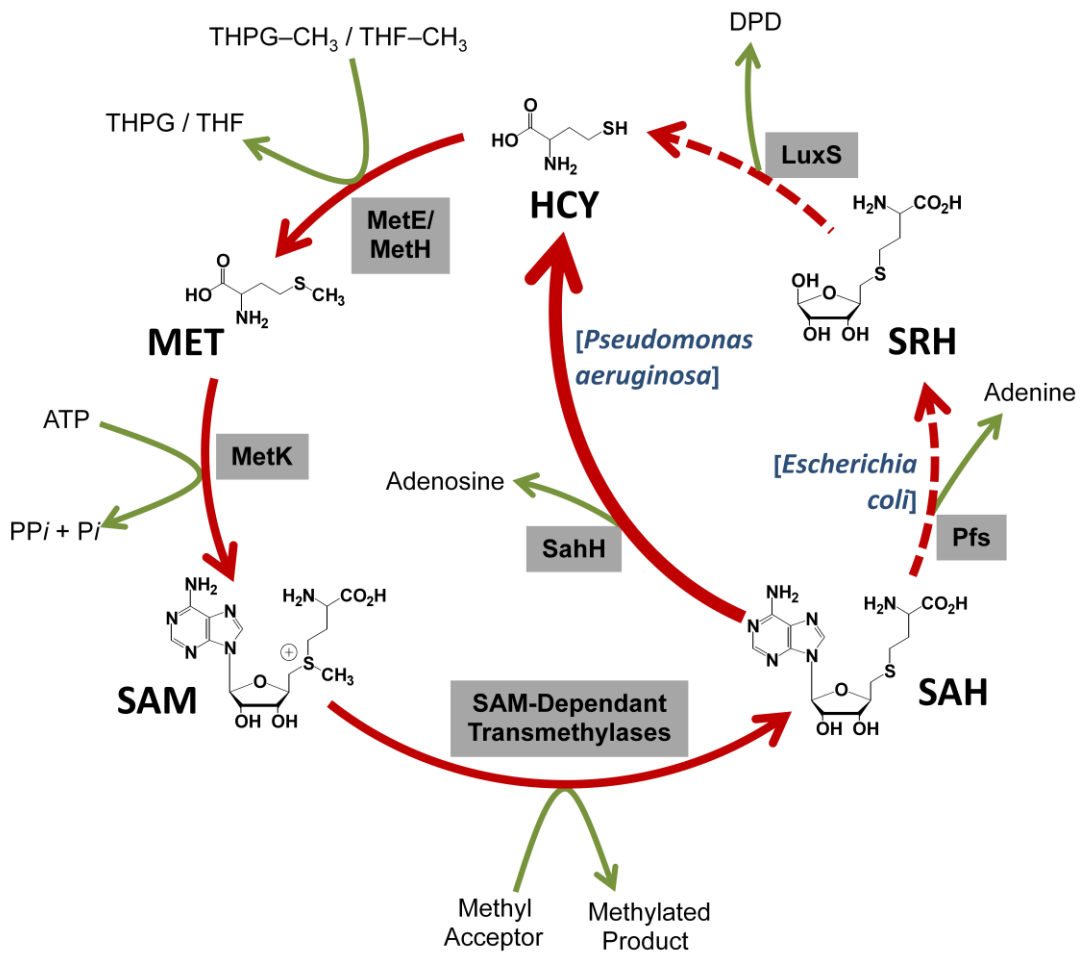


Figure 1.6: The activated methyl cycle (AMC). Methionine is converted to *S*-adenosyl-L-methionine (SAM) in a reaction catalyzed by the SAM synthetase (Met K, methionine adenosyltransferase). Through the action of numerous methyltransferases, SAM is converted to the toxic metabolite *S*-adenosyl-L-homocysteine (SAH). It is acknowledged that two alternative routes exist for processing SAH, but only one of which produces the precursor of AI-2, 4,5-dihydroxy 2,3-pentanedione (DPD). In bacteria generating AI-2, SAH is immediately detoxified to *S*-ribosyl-L-homocysteine (SRH) and adenine by the Pfs enzyme (5'-methylthioadenosine/*S*-adenosyl-L-homocysteine nucleosidase). During the conversion of SRH to homocysteine (HCY), LuxS, originally identified as the SRH cleavage enzyme, then produces DPD and this forms AI-2 via spontaneous cyclization. Eukaryotes, archaebacteria and certain eubacteria replace this two step process with a single enzyme, SAH hydrolase. In these circumstances, the removal of SAH generates adenosine and homocysteine with no production of AI-2. In either case, the cycle is completed via the regeneration of methionine from homocysteine by a homocysteine methyltransferase (MetE, 5-methyltetrahydropteroyltriglutamate-homocysteine methyltransferase or MetH, 5-methyltetrahydrofolate-homocysteine methyltransferase).

For example, in *P. aeruginosa*, PhzM is necessary for production of the pyocyanin pigment (Parsons *et al.* 2007). In SAM-dependent methyltransferase reactions, SAM is converted to *S*-adenosyl-L-homocysteine (SAH).

Analysis of 138 bacterial species by Sun *et al.* (2004) demonstrated 51 possess SAH nucleosidase, 60 possess SAH hydrolase, 20% possess neither, whilst a couple, *Bifidobacterium longum* and *Escherichia blattae* had both; the AMC therefore functions as an important SAH-degradation pathway that reduces feedback inhibition of SAM-dependent methylation (Figure 1.4). The importance of SAM has been illustrated by growth and cell division defects which arise following alterations to normal levels of the metabolite. SAM mediated-activities such as DNA modifications and spermidine biosynthesis from putrescine were shown to be impaired with high levels of expression of T3 SAM hydrolase (T3SH) (Hughes, Brown & Ferro 1987). In a similar manner, Posnick and Samson (1999) have demonstrated an increase in hemimethylated or unmethylated GATC sites of both chromosomal and plasmid DNA with a reduction in SAM pool size. In *E. coli*, reduced SAM synthase activity in *metK* mutants has been associated with a partial cell division defect characterised by the formation of long filaments and even nucleoid distribution intracellularly (Newman *et al.* 1998). In certain circumstances, the altered phenotypes are due to the accumulation of SAH and other thionucleosides including MTA which have been shown to inhibit mammalian and bacterial methyltransferase and polyamine synthesis activities.

In providing the available metabolic pool of SAM, the AMC represents an important pathway, which will be affected by changes in the production of various AHLs since their synthesis consumes SAM, and *vice versa*. Experimentally, this has been demonstrated *in vivo* by Val and Cronan (1998); one of their major findings indicated that comparatively small reductions in levels of intracellular SAM, achieved by expression of bacteriophage T3SH resulted in a significantly marked reduction in AHL production driven via recombinant TraI in *E.coli*. Furthermore, this consequential effect is not confined just to AHL QSSMs; Winzer *et al.* (2002a) showed that expression of bacteriophage T3SH and

rat liver SAM synthetase lead to a significant reduction and moderate increase in AI-2 levels respectively.

1.8 Fatty acid biosynthesis

The fatty acid precursor to AHL synthesis is an important one as it defines each individual AHL molecule with differing specificities; the fatty acyl side may vary in length, backbone saturation and in the nature of the substitutions present (Waters & Bassler 2005). The confusion surrounding the origin of the acyl chains of AHLs has now been resolved; contradictory to the previous notion that they are acquired as CoA intermediates of the fatty acid β -oxidation pathway, it has now been confirmed that the precursors are acyl-ACPs, which are derived from intermediates in the fatty acid biosynthesis pathway (Figure 1.7).

As with SAM and the AMC, the fact that AHL synthesis draws on the activity of the fatty acid biosynthesis pathway means that it is probable that an interlinked relationship can be observed. Several studies have reinforced the relationship between various proteins involved in fatty acid biosynthesis and the subsequent consequences on AHL production. Through the construction of a temperature-sensitive *fabG* mutant, Hoang *et al.* (2002) have demonstrated that the reduction of β -ketoacyl ACP reductase activity correlated with an altered AHL profile, most notably an elevated incidence of short chain 3-oxo-substituted AHLs. In another study of reductases, it was shown that reduction of the enoyl-ACP reductase (FabI) activity, correlated with a 50% decrease in the production of C₄-HSL and 3-oxo-C₁₂-HSL (Hoang & Schweizer 1999). Other components of the Fab system, including FabB (β -ketoacyl-ACP synthase I) and FabZ (β -hydroxyacyl-ACP dehydratase), have additionally been shown to be essential for AHL formation (Hoang *et al.* 2002).

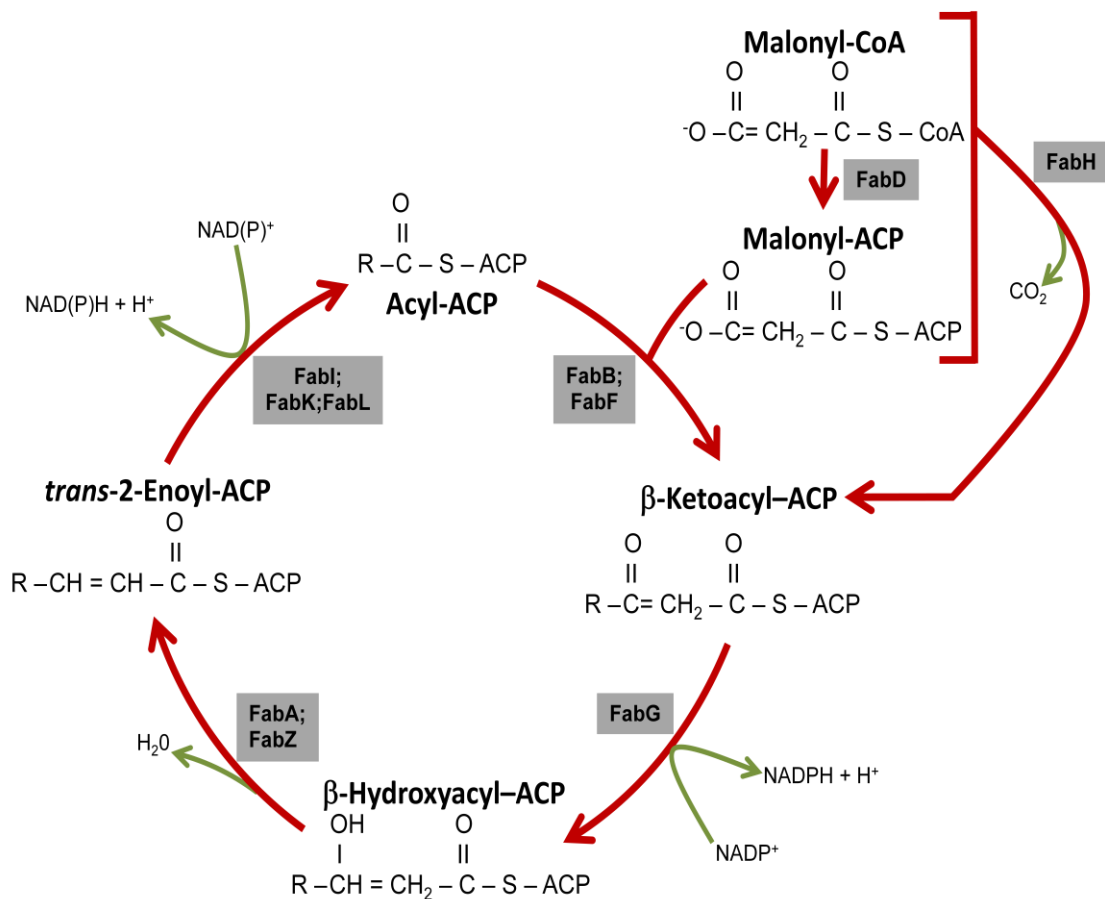


Figure 1.7: Fatty acid biosynthesis pathway. FabD is responsible for transferring malonyl-CoA to ACP, whilst FabH is responsible for performing continuous cyclization reactions resulting in the elongation of fatty acids. The next step of the elongation cycle is carried out by β -ketoacyl-ACP reductase (FabG). The β -hydroxyacyl-ACP intermediate then undergoes dehydration to form *trans*-2-enoyl-ACP (FabA or FabZ) and the final steps of elongation are catalysed by enoyl-ACP reductase (FabI, FabK or FabL) producing acyl ACPs. Subsequent elongation is initiated via the elongation condensing enzymes (FabB and FabF). The acyl ACP end products of fatty acid synthesis provide the precursor for production of AHLs.

1.8 Aims and objectives

In order to further define the specific associations which interlink the QS and metabolic circuits, the main aim of this project is to determine the influence that AHL synthesis has upon the levels of metabolites linked to the AMC and vice versa. This can more specifically be assessed by the objectives described below:

- i. It is hypothesised that QS directed by the production of signal molecules will draw on resources from metabolic pathways which are common to other cellular processes. The precise nature of this was investigated. The potential of the hierarchical organisation of the *P. aeruginosa* QS system to complicate such studies was avoided by using a heterologous host. Here, the AHL synthase genes, *lasI* and *rhII*, were cloned downstream of an inducible promoter and transformed into *Escherichia coli*, which lacks the equivalent QS system but possesses the appropriate metabolic pathways for sourcing of AHL substrates. The consequences of these expression studies was analysed using established mass spectroscopic methods to determine AMC metabolite profiles. Fitness tests were also performed in both rich and chemically defined media to determine whether the associated metabolic disruptions caused cellular growth defects.
- ii. To take this further, and determine the importance of specific AA residues of LasI and RhII, site-directed mutagenesis was combined with metabolic analyses in the heterologous host system described above. It was unknown whether the residues chosen and substitutions made would produce functional synthases with signal producing activity; however, it was hypothesised that the metabolic status and signal production phenotypes of the mutant proteins would determine whether the synthases needed to fully active to influence metabolism.
- iii. With the hypothesis that disrupting the levels of AMC metabolites would impact upon AHL synthesis, mutants of the heterologous host predicted to alter AMC metabolite levels were analysed for their capacity to support AHL synthesis.
- iv. Lastly, the reciprocal of these studies was conducted via analysis of *P. aeruginosa* AHL synthase mutants. It was hypothesised that this would increase the

intracellular availability of metabolites. However, the complexity of the regulatory QS cascade would predict that this approach would generate new avenues of investigation by revealing novel links between cellular metabolism and QS.

Chapter 2

Materials and methods

2.1 Chemical reagents

2.1.1 General chemicals

All general chemicals were obtained from Sigma (UK) unless otherwise stated. High-performance liquid chromatography (HPLC)-grade solvents including acetonitrile (ACN), ethanol (EtOH), ethyl acetate (EtAc), methanol (MeOH) and dichloromethane (DCM) were obtained from Fisher Scientific (Loughborough, UK).

2.1.2 Synthesis of QSSMs

Synthetic AHLs and Aqs were made by A. Truman/ S.R. Chhabra at the School of Molecular Medical Sciences, Centre for Biomolecular Sciences, The University of Nottingham as described in Diggle *et al.* (2006). The compounds were stored as stocks of the appropriate concentration in ACN (AHLs), MeOH or DMSO (Aqs) and stored at -20 °C.

2.2 Growth media and additives

All media were obtained from Oxoid Ltd (UK) and prepared according to the manufacturers' instructions, using distilled H₂O (dH₂O) and autoclaved at 121 °C for 20 min at 15 psi unless otherwise stated (Sambrook *et al.* 1989).

2.2.1 Luria Bertani media

Luria Bertani (LB) broth was prepared as described by Sambrook *et al.* (1989) and consisted of 10 g tryptone, 5 g yeast extract and 10 g NaCl in 1 L of dH₂O. LB agar was prepared by addition of 0.8 % (w/v) Technical Agar No. 3 (Oxoid) to LB broth.

2.2.2 Chemically defined media (CDM)

Chemically defined media (CDM) was prepared as described by Ombaka *et al.* (1983).

Chemical	Final Concentration / mM
D-C ₆ H ₁₂ O ₆	20
KCl	3
NaCl	3
(NH ₄) ₂ SO ₄	12
MgSO ₄ ·7H ₂ O	3.2
K ₂ HPO ₄	0.02
MOPS (pH 7.8)	1.2

Table 2.1: Composition of chemically defined media (CDM).

2.2.3 MOPS minimal media (MMM)

MOPS (4-morpholinepropanesulfonic acid) minimal media (MMM) (Table 9.1) was prepared as described by Neidhardt *et al.* (1974).

2.2.4 Antibiotics/ X-Gal/ IPTG

Antibiotic supplements to the media and their working concentrations were: carbenicillin (Cb) 25 µg/ml (*E. coli*); chloramphenicol (Cm) 25 µg/ml (*E. coli*); gentamicin (Gm) 10 µg/ml (*P. aeruginosa*); tetracycline (Tc) 25 µg/ml (*E. coli*) and 100 µg/ml (*P. aeruginosa*). To perform screening for positive transformants using blue/white colour selection of recombinants on LB plates, 5-bromo-4-chloro-3-indolyl-β-D-galacto-pyranoside (X-Gal) was added to molten agar to a final concentration of 50 µg/ml. To induce expression of genes under the control of a P_{tac} promoter in pME6032, isopropylthio-β-D-galactoside (IPTG) was added at a final concentration of 1 mM. All stock solutions were prepared according to Sambrook *et al.* (1989), filter sterilised before use (0.22 µm- Sartorius Minisart) and stored according to the manufacturers' recommendations.

2.3 Growth conditions

V. harveyi was grown at 30 °C unless otherwise stated. *E. coli* and *P. aeruginosa* were routinely grown at 37 °C. Liquid cultures were grown in LB with agitation at 200 rpm in a shaking incubator. Growth of bacterial cultures was monitored by absorbance readings at a wavelength of 600 nm (optical density, OD₆₀₀) using a Biomate 3 spectrophotometer (Thermo Scientific), or a TECAN Infinite F200 multifunctional, automated luminometer-spectrometer. When performing growth curves, strains were grown in identical 500 ml-Erlenmeyer flasks containing 125 ml LB, CDM or MMM.

2.4 Bacterial strains

The bacterial strains used in this study are listed in Table 2.2.

Strain	Description	Reference/Source
<i>Escherichia coli</i>		
DH5α	F ⁺ /endA1, hsdR17(R- M+), supE44, thi-1, recA1, gyrA, relA1, Δ(lacZYA-argF)U169, deoR[Φ80d lacΔ(lacZ)M15]	Sambrook <i>et al.</i> (1989)
JM109	[F ⁺ traD36, proAB, lacI ^q , lacZΔM15] recA1, endA1, gyrA96, thi, hsdR17, supE44, relA1 Δ(lac-proAB) mcrA	Yanisch-Perron <i>et al.</i> (1985)
MG1655	F ⁺ λ ilvG- rfb-50 rph-1	Jensen <i>et al.</i> (1993)
MG1655::pfs	pfs::Km ^r derivative of MG1655	Tavender <i>et al.</i> (2008)
MG1655::luxS	luxS::Cm ^r derivative of MG1655	Tavender <i>et al.</i> (2008)
MG1655::sdiA	sdiA::Km ^r derivative of MG1655	Van Houdt <i>et al.</i> (2006)
<i>Pseudomonas aeruginosa</i>		
PA01	Wildtype, Nottingham strain	Klockgether <i>et al.</i> (2010); Stover <i>et al.</i> (2000)

PAO1 Δ <i>lasI</i>	PAO1 derivative with a Gm cassette insertion into a unique <i>EcoRI</i> site within the <i>lasI_{Pa}</i> gene, Gm ^r	Beatson <i>et al.</i> (2002)
PAO1 Δ <i>rbII</i>	PAO1 derivative with a Tc cassette insertion into a unique <i>KpnI</i> site within the <i>rbII_{Pa}</i> gene, Tc ^r	Beatson <i>et al.</i> (2002)
PAO1 Δ <i>lasI</i> Δ <i>rbII</i>	PAO1 derivative with chromosomal deletion of <i>lasI_{Pa}</i> and <i>rbII_{Pa}</i> genes	Pustelny (personal communication)
<i>Vibrio harveyi</i> BB170	Biosensor AI-1 ⁻ , biosensor AI-2 ⁺	Bassler <i>et al.</i> (1993)

Table 2.2 Bacterial strains used in this study.

2.5 Plasmids

All plasmids used in this study are listed in Table 2.3.

Plasmids	Description	Reference/ Source
pGEM-T Easy	Cloning vector, Cb ^r , Amp ^r , <i>lacZ</i> , allowing selection via blue-white screening	Promega
pGEM- <i>lasI_{Pa}</i>	pGEM-T Easy derivative carrying the <i>lasI_{Pa}</i> gene, Cb ^r	This study
pGEM- <i>lasI_{Pa}</i> 23: R > W	pGEM- <i>lasI_{Pa}</i> derivative carrying a substitution of Arg for Try at codon 23 of the <i>lasI_{Pa}</i> ORF, Cb ^r	This study
pGEM- <i>lasI_{Pa}</i> 27: F > L	pGEM- <i>lasI_{Pa}</i> derivative carrying a substitution of Phe for Leu at codon 27 of the <i>lasI_{Pa}</i> ORF, Cb ^r	This study
pGEM- <i>lasI_{Pa}</i> 27: F > Y	pGEM- <i>lasI_{Pa}</i> derivative carrying a substitution of Phe for Tyr at codon 27 of the <i>lasI_{Pa}</i> ORF, Cb ^r	This study
pGEM- <i>lasI_{Pa}</i> 33: W > G	pGEM- <i>lasI_{Pa}</i> derivative carrying a substitution of Try for Gly at codon 33 of the <i>lasI_{Pa}</i> ORF, Cb ^r	This study

pGEM- <i>lasI_{Pa}</i> 103: S > A	pGEM- <i>lasI_{Pa}</i> derivative carrying a substitution of Ser for Ala at codon 103 of the <i>lasI_{Pa}</i> ORF, Cb ^r	This study
pGEM- <i>lasI_{Pa}</i> 103: S > E	pGEM- <i>lasI_{Pa}</i> derivative carrying a substitution of Ser for Glu at codon 103 of the <i>lasI_{Pa}</i> ORF, Cb ^r	This study
pGEM- <i>lasI_{Pa}</i> 103: S > V	pGEM- <i>lasI_{Pa}</i> derivative carrying a substitution of Ser for Val at codon 103 of the <i>lasI_{Pa}</i> ORF, Cb ^r	This study
pGEM- <i>rbII_{Pa}</i>	pGEM-T Easy derivative carrying the <i>rbII_{Pa}</i> gene, Cb ^r	This study
pGEM- <i>rbII_{Pa}</i> 28: F > L	pGEM- <i>rbII_{Pa}</i> derivative carrying a substitution of Phe for Leu at codon 28 of the <i>rbII_{Pa}</i> ORF, Cb ^r	This study
pGEM- <i>rbII_{Pa}</i> 28: F > Y	pGEM- <i>rbII_{Pa}</i> derivative carrying a substitution of Phe for Tyr at codon 28 of the <i>rbII_{Pa}</i> ORF, Cb ^r	This study
pGEM- <i>rbII_{Pa}</i> 34: W > G	pGEM- <i>rbII_{Pa}</i> derivative carrying a substitution of Try for Gly at codon 34 of the <i>rbII_{Pa}</i> ORF, Cb ^r	This study
pGEM- <i>rbII_{Pa}</i> 103: S > A	pGEM- <i>rbII_{Pa}</i> derivative carrying a substitution of Ser for Ala at codon 103 of the <i>rbII_{Pa}</i> ORF, Cb ^r	This study
pGEM- <i>rbII_{Pa}</i> 103: S > E	pGEM- <i>rbII_{Pa}</i> derivative carrying a substitution of Ser for Glu at codon 103 of the <i>rbII_{Pa}</i> ORF, Cb ^r	This study
pGEM- <i>rbII_{Pa}</i> 103: S > V	pGEM- <i>rbII_{Pa}</i> derivative carrying a substitution of Ser for Val at codon 103 of the <i>rbII_{Pa}</i> ORF, Cb ^r	This study
pME6032	<i>lacI^Q</i> Ptac expression vector, Tc ^r	Heeb <i>et al.</i> 2002
pME- <i>lasI_{Pa}</i>	pME6032 derivative carrying the <i>lasI_{Pa}</i> gene under Ptac control, Tc ^r	This study
pME- <i>lasI_{Pa}</i> 23: R > W	pME- <i>lasI_{Pa}</i> derivative carrying a substitution of Arg for Try at codon 23 of the <i>lasI_{Pa}</i> ORF, Tc ^r	This study
pME- <i>lasI_{Pa}</i> 27: F > L	pME- <i>lasI_{Pa}</i> derivative carrying a substitution of Phe for Leu at codon 27 of the <i>lasI_{Pa}</i> ORF, Tc ^r	This study

pME- <i>lasI_{Pa}</i> 27: F > Y	pME- <i>lasI_{Pa}</i> derivative carrying a substitution of Phe for Tyr at codon 27 of the <i>lasI_{Pa}</i> ORF, Tc ^r	This study
pME- <i>lasI_{Pa}</i> 33: W > G	pME- <i>lasI_{Pa}</i> derivative carrying a substitution of Try for Gly at codon 33 of the <i>lasI_{Pa}</i> ORF, Tc ^r	This study
pME- <i>lasI_{Pa}</i> 103: S > A	pME- <i>lasI_{Pa}</i> derivative carrying a substitution of Ser for Ala at codon 103 of the <i>lasI_{Pa}</i> ORF, Tc ^r	This study
pME- <i>lasI_{Pa}</i> 103: S > E	pME- <i>lasI_{Pa}</i> derivative carrying a substitution of Ser for Glu at codon 103 of the <i>lasI_{Pa}</i> ORF, Tc ^r	This study
pME- <i>lasI_{Pa}</i> 103: S > V	pME- <i>lasI_{Pa}</i> derivative carrying a substitution of Ser for Val at codon 103 of the <i>lasI_{Pa}</i> ORF, Tc ^r	This study
pME- <i>rbII_{Pa}</i>	pME6032 derivative carrying the <i>rbII_{Pa}</i> gene under <i>P_{tac}</i> control, Tc ^r	This study
pME- <i>rbII_{Pa}</i> 28: F > L	pME- <i>rbII_{Pa}</i> derivative carrying a substitution of Phe for Leu at codon 28 of the <i>rbII_{Pa}</i> ORF, Tc ^r	This study
pME- <i>rbII_{Pa}</i> 28: F > Y	pME- <i>rbII_{Pa}</i> derivative carrying a substitution of Phe for Tyr at codon 28 of the <i>rbII_{Pa}</i> ORF, Tc ^r	This study
pME- <i>rbII_{Pa}</i> 34: W > G	pME- <i>rbII_{Pa}</i> derivative carrying a substitution of Try for Gly at codon 34 of the <i>rbII_{Pa}</i> ORF, Tc ^r	This study
pME- <i>rbII_{Pa}</i> 103: S > A	pME- <i>rbII_{Pa}</i> derivative carrying a substitution of Ser for Ala at codon 103 of the <i>rbII_{Pa}</i> ORF, Tc ^r	This study
pME- <i>rbII_{Pa}</i> 103: S > E	pME- <i>rbII_{Pa}</i> derivative carrying a substitution of Ser for Glu at codon 103 of the <i>rbII_{Pa}</i> ORF, Tc ^r	This study
pME- <i>rbII_{Pa}</i> 103: S > V	pME- <i>rbII_{Pa}</i> derivative carrying a substitution of Ser for Val at codon 103 of the <i>rbII_{Pa}</i> ORF, Tc ^r	This study
pSB1142	<i>lux</i> -based acyl-HSL bioreporter, Tc ^r	Winson <i>et al.</i> 1998
pSB436	<i>lux</i> -based acyl-HSL bioreporter, Amp ^r	Winson <i>et al.</i> 1998

Table 2.3 Plasmids used in this study.

2.6 DNA preparation and manipulation

2.6.1 Preparation of plasmid DNA

Small scale plasmid DNA isolation was performed using the Qiagen Miniprep Kit (QIAGEN, Ltd) according to the manufacturer's instructions. Briefly, cells pelleted from 1-10 ml of an overnight (O/N) bacterial culture was subjected to alkaline lysis, then neutralised and centrifuged at 13,000 rpm for 10 min to remove denatured and precipitated cellular debris. Crude lysates were then loaded onto a silica-gel column, washed and plasmid DNA was eluted into 30-50 μ l HPLC grade H₂O (Fisher Scientific, UK).

Preparation of microgram quantities of low copy number plasmids was performed using the Qiagen Midiprep Kit (QIAGEN, Ltd) according to the manufacturer's protocol. Briefly, cells pelleted from 100 ml of an O/N bacterial culture was subjected to alkaline lysis, then neutralised and centrifuged at 10,000 rpm in a Beckman Avanti 30 centrifuge for 30 min to remove denatured and precipitated cellular debris and then centrifuged for another 15 min. Crude lysates were then loaded onto a pre-equilibrated anion-exchange resin column, washed and plasmid DNA was eluted with 4 ml high-salt buffer. Finally, the DNA was precipitated with isopropanol, desalted by washing with 70% (v/v) EtOH and resuspended in 50-100 μ l HPLC grade H₂O (Fisher Scientific, UK).

2.6.2 Purification of chromosomal DNA

To amplify specific genes or DNA sequences from *E. coli* or *P. aeruginosa*, genomic DNA was used as a template. Genomic DNA was isolated as per the manufacturer's instructions using the Wizard® Genomic DNA Purification Kit (Promega, UK). Bacterial cells pelleted from 1 ml of an O/N culture were lysed by incubation with 600 μ l Nuclei Lysis Solution at 80 °C for 5 min. After cooling to room temperature, 3 μ l of RNase Solution was added and the sample incubated at 37 °C for 15-60 min. Proteins were precipitated by adding 200 μ l of Protein Precipitation Solution, followed by 5 min on ice and centrifugation at 13,000 rpm for 3 min. The supernatant was added to 600 μ l

of isopropanol and centrifuged for 10 min at 13,000 rpm. After removal of the supernatant, 600 µl of 70 % (v/v) EtOH was added and the resulting mix centrifuged at 13,000 rpm for 5 min. The ethanol was aspirated off and the DNA pellet air-dried for 10-15 min. The pellet was rehydrated in 100 µl Rehydration Solution for 1 h at 65 °C.

2.6.3 Precipitation of DNA

DNA precipitation was routinely performed by adding 2.5 volumes of 100% EtOH to the samples and 0.1 volumes of 3 M NaOAc, pH 5.2. This was left at -20 °C for at least 20 min or O/N before centrifugation at 13,000 rpm for 20 min at 4 °C. The pellet was washed with 70% (v/v) EtOH followed by centrifugation at 13,000 rpm for 10 min at 4 °C. The ethanol was carefully removed and the pellet allowed to dry. The DNA was resuspended in an appropriate volume of HPLC grade H₂O.

2.6.4 Quantifying DNA concentrations

The NanoDrap[®] ND-1000 (Nanodrop Technologies) was used to measure DNA concentrations. 1-2 µl of sample was used to determine characteristic absorbance and concentrations. Whole spectra of samples could also be measured to assess purity.

2.6.5 Restriction enzymes

Restriction enzymes (REs) were purchased from Promega (UK) and New England Biolabs (UK) and were used according to the manufacturers' recommendations. Reactions generally contained 0.05-1 µg DNA, 0.5-1 µl restriction endonuclease(s) and 1x appropriate restriction buffer made to a final volume of 20 µl with sterile dH₂O and incubated at the appropriate temperature for a minimum of 1 h or until the digestion was complete.

2.6.6 Analysis and purification of DNA by agarose gel electrophoresis

DNA loading buffer (Table 2.4) was added to DNA samples and analysed on 0.7-1% (w/v) agarose gels using horizontal gel apparatus (Biorad, UK). The gels were prepared using the method described by Sambrook *et al.* (1989), using analytical grade agarose (Promega, UK) in 1x tris-acetate-ethylenediaminetetraacetic acid (TAE) buffer with the addition of ethidium bromide (EtBr) to a final concentration of 10 µg/ml. The gels were run in 1× TAE buffer and electrophoresis was performed at 70-120 V. DNA fragments were visualised on a UV transilluminator with Vision Works software (UVP, USA). DNA fragments were extracted from agarose gel slices using the Qiagen Qiaquick Gel Extraction Kit (QIAGEN, Ltd) in accordance with the manufacturer's instructions. Final elution of the purified product was carried out using 30-50 µl HPLC grade H₂O (Fisher Scientific, UK).

6x DNA loading buffer	
Sucrose	10% (w/v)
Orange G (in 1x TAE)	0.4% (w/v)
1x TAE	
Tris-acetate-EDTA base	40 mM
EDTA pH 8.0	50 mM
Glacial acetic acid	0.1142% (v/v)

Table 2.4: Standard recipes for agarose gel electrophoresis.

DNA loading buffer and 1x TAE were stored at RT.

2.6.7 Molecular weight markers

To establish the size of DNA fragments, 1 µg of 1 kb Plus Ladder (Invitrogen, UK) in DNA loading buffer were loaded on agarose gels.

2.6.8 DNA ligation

DNA ligations were routinely performed using 1:1, 1:3 or 1:10 ratios of vector to insert. Reactions were carried out at 4 °C O/N using 1 µl T4 DNA ligase (Promega, UK) and 2 µl T4 ligation buffer in a final volume of 20 µl. Control ligations containing no insert were also conducted where appropriate.

2.7 Polymerase chain reaction (PCR) amplification

2.7.1 Synthesis of oligonucleotide primers

Oligonucleotide primers were synthesised by Sigma-Genosys Ltd (UK). All primers contained a minimum of 18 bases to ensure accurate hybridization. Where necessary, restriction sites were incorporated into the 5' end of the primer to aid cloning of the PCR product. Primer sequences are listed in Table 2.5.

Oligonucleotides	Sequence (5' → 3')	Function
lasIF	TAT <u>CAATIGAT</u> GATGA TCGTACAAATTTGG TCGG	Forward primer used to amplify the <i>lasI_{Pa}</i> ORF region with an underlined <i>MfeI</i> restriction site directly upstream of the start codon (bold)
lasI R23W F	[Phos]TTG <i>TGG</i> GCT CAAGTGTTTC	Forward primer used to amplify the <i>lasI_{Pa}</i> ORF region with bold italicized codon for substitution of Arg for Trp
lasI F27L F	[Phos]TG <i>CTG</i> AAG GAGCGCAAAG	Forward primer used to amplify the <i>lasI_{Pa}</i> ORF region with bold italicized codon for substitution of Phe for Leu
lasI F27Y F	[Phos]TG <i>TAC</i> AAGG AGCGCAAAG	Forward primer used to amplify the <i>lasI_{Pa}</i> ORF region with bold italicized codon for substitution of Phe for Tyr
lasI W33G F	[Phos]AGGC <i>GGC</i> G ACGTTAGTGT	Forward primer used to amplify the <i>lasI_{Pa}</i> ORF region with bold italicized codon for substitution of Tyr for Gly
lasI S103A F	[Phos]TCG <i>CCC</i> GTT TCGCCATCA	Forward primer used to amplify the <i>lasI_{Pa}</i> ORF region with bold italicized codon for substitution of Ser for Ala

lasI S103E F	[Phos]TG <i>GA</i> ACTCG AGCGTTTC	Forward primer used to amplify the <i>lasI_{Pa}</i> ORF region with bold italicized codon for substitution of Ser for Glu
lasI S103V F	[Phos]TCG <i>TG</i> CGTT TCGCCATCA	Forward primer used to amplify the <i>lasI_{Pa}</i> ORF region with bold italicized codon for substitution of Ser for Val
lasIR	<u>ATAAGGCC</u> <i>T</i> TCAT GAAACCGCCAGTC GCT	Reverse primer used to amplify the <i>lasI_{Pa}</i> ORF region with an underlined <i>StuI</i> restriction site directly downstream of the stop codon (bold)
lasI R23W R	[Phos]CTTGTGCAT CTCGCCCAG	Reverse primer used to amplify the <i>lasI_{Pa}</i> ORF region for substitution of Arg for Trp
lasI F27L R	[Phos]CTTGAGCAC GCAACTTGT	Reverse primer used to amplify the <i>lasI_{Pa}</i> ORF region for substitution of Phe for Leu
lasI F27Y R	[Phos]CTTGAGCAC GCAACTTGT	Reverse primer used to amplify the <i>lasI_{Pa}</i> ORF region for substitution of Phe for Tyr
lasI W33G R	[Phos]TTGCGCTCC TTGAACACT	Reverse primer used to amplify the <i>lasI_{Pa}</i> ORF region for substitution of Tyr for Gly
lasI S103A/V R	[Phos]GTTCCCAGA TGTGCGGCG	Reverse primer used to amplify the <i>lasI_{Pa}</i> ORF region for substitution of Ser for Ala or Val
lasI S103E R	[Phos]GATGTGCG GCGAGCAAGG	Reverse primer used to amplify the <i>lasI_{Pa}</i> ORF region for substitution of Ser for Glu
Ptac	CGGCTCGTATAAT GTGTGGA	Primer to sequence multiple cloning site in pME6032
P6032	CCCTCACTGATCC GCTAGTC	Primer to sequence multiple cloning site in pME6032
rhII F	<u>TATCAAT</u> <i>TG</i> ATGA TCGAATTIGCTCTC TGAAT	Forward primer used to amplify the <i>rhII</i> ORF region with an underlined <i>MfeI</i> restriction site directly upstream of the start codon (bold)
rhII F28L F	[Phos]TC <i>CT</i> GATCG AGAAGCTGG	Forward primer used to amplify the <i>rhII_{Pa}</i> ORF region with bold italicized codon for

rhII F28Y F	[Phos]TC TAC ATCG AGAAGCTGG	substitution of Phe for Leu Forward primer used to amplify the <i>rhII_{Pa}</i> ORF region with italicized codon for substitution of Phe for Tyr
rhII W34G F	[Phos]TGGGC GGC GACGTGGTCT	Forward primer used to amplify the <i>rhII_{Pa}</i> ORF region with italicized codon for substitution of Tyr for Gly
rhII S103A F	[Phos]T TGCC CGCT ACGCCGCCA	Forward primer used to amplify the <i>rhII_{Pa}</i> ORF region with italicized codon for substitution of Ser for Ala
rhII S103E F	[Phos]TGGGAGCT T GAGC GCTAC	Forward primer used to amplify the <i>rhII_{Pa}</i> ORF region with italicized codon for substitution of Ser for Glu
rhII S103V F	[Phos]T TGTG CGCT ACGCCGCCA	Forward primer used to amplify the <i>rhII_{Pa}</i> ORF region with italicized codon for substitution of Ser for Val
rhII R	<u>ATAAGGCCT</u> TCAC ACCGCCATCGACA GC	Reverse primer used to amplify the <i>rhII_{Pa}</i> ORF region with an underlined <i>StuI</i> restriction site directly downstream of the stop codon (bold)
rhII F28L R	[Phos]CCTGATGCC GGTAGCGTC	Reverse primer used to amplify the <i>rhII_{Pa}</i> ORF region with italicized codon for substitution of Phe for Leu
rhII F28Y R	[Phos]CCTGATGCC GGTAGCGTC	Reverse primer used to amplify the <i>rhII_{Pa}</i> ORF region with italicized codon for substitution of Phe for Tyr
rhII W34G R	[Phos]GCT TCT CGA TGAAGACCT	Reverse primer used to amplify the <i>rhII_{Pa}</i> ORF region with italicized codon for substitution of Tyr for Gly
rhII S103A/V R	[Phos]GCTCCCAGA CCGACGGAT	Reverse primer used to amplify the <i>rhII_{Pa}</i> ORF region with italicized codon for substitution of Ser for Ala or Val
rhII S103E R	[Phos]GACCGACG GATCGCTCGG	Reverse primer used to amplify the <i>rhII_{Pa}</i> ORF region with italicized codon for substitution of Ser for Glu

Table 2.5 Oligonucleotide primers used in this study.

2.7.2 PCR amplification

PCR amplification was performed according to methods described by Sakai *et al.* (1988) in a final volume of 50 μ l.

PCR mix	
Template DNA	50-100 ng
Forward primer	1 μ M
Reverse primer	1 μ M
dNTPs	1-2 mM
High Fidelity Polymerase (Roche)	1-2.5 U
PCR buffer including MgCl ₂	1x buffer
dH ₂ O	make up to 50 μ l

Table 2.6: Components of a standard PCR.

Reactions were carried out in a Progene PCR Thermocycler (Techne) for a total of 35 cycles. Briefly, the DNA template was denatured at 96 °C for 5-10 min, followed by 30-35 cycles of extension at 72 °C for 1-3 min depending on the DNA polymerase and length of the DNA to be amplified (1 min per kb), denaturation at 96 °C for 20 s and then annealing at 55-65 °C for 30 s. The last cycle finished with a final extension stage at 72 °C for 10 min to ensure completion of all strands. The annealing temperature was varied depending on the nature of the primers used and the stringency levels required. Reaction mixes were then incubated at 4 °C indefinitely to allow PCR reactions to be carried out O/N.

2.8 DNA sequencing

2.8.1 Obtaining DNA sequence data

Routine DNA sequencing was conducted by the DNA Sequencing Laboratory, Queens Medical Centre, University of Nottingham, using the Applied Biosystems BigDye[®] Terminator v3.1 Cycle Sequencing Kit and 3130x1 Genetic Analyzer.

2.8.2 DNA sequence analysis

All pre-determined DNA and protein sequences were obtained from the NCBI (<http://www.ncbi.nlm.nih.gov/>) 'Gene' and 'Protein' databases respectively. The Pseudomonas Genome Sequence Database (<http://www.pseudomonas.com>) was additionally used to analyse *P. aeruginosa* sequences. Analysis of DNA sequences was performed using the Lasergene DNASTar software package. Comparison of DNA and protein sequences to identify homology was carried out using the NCBI 'BLAST' server.

2.9 Transformation

2.9.1 Preparation of electro-competent *E. coli* cells

To prepare competent *E. coli* cells, a 1% (v/v) inoculum from an O/N *E. coli* culture was added to 100 ml of sterile LB broth in a 500 ml-Erlenmeyer flask and grown at 37 °C with shaking at 200 rpm to an OD₆₀₀ of 0.4-0.8 (reached approximately 6 h after inoculation). Cells were harvested by centrifugation at 6000 rpm (JA-14, Beckman) for 10 min at 4 °C and washed twice in sterile ice-cold 10% (v/v) glycerol containing 1 mM MOPS before being resuspended in 1 ml of the same buffer. Cells were aliquoted into 50 µl samples in microcentrifuge tubes, flash frozen in liquid nitrogen and stored at -80 °C until needed.

2.9.2 Electroporation of electro-competent *E. coli* cells

For electroporation of DNA into *E. coli* cells, salts were firstly removed from the DNA solution by filter dialysis on 0.025 µm Millipore filters (Millipore Corporation, UK) for at least 20 min. Electroporation was then performed in 0.2 cm electrode gap Gene Pulser cuvettes (BioRad, UK) containing 50 µl of competent cells and 2-3 µl dialysed DNA. An electroporation pulse of 2.5 kV (25 µF, 200 Ω) was delivered using the BioRad Gene Pulser connected to a BioRad pulse controller (BioRad, UK). A 0.95 ml volume of pre-warmed (37 °C) LB broth was added to the cells which were then incubated at 37 °C for 1 h in the absence of antibiotics. Aliquots of cells were subsequently plated onto LB agar plates containing appropriate antibiotics to select for transformants and grown O/N at

37 °C. Negative controls of electroporated cells with no plasmid were also similarly prepared.

2.9.3 Preparation of electro-competent *P. aeruginosa* cells

Competent *P. aeruginosa* cells for electroporation were prepared from 1.5 ml of culture, grown O/N in LB at 37 °C, by centrifugation at 13,000 rpm for 5 min. The cells were washed with 1 ml ice-cold 10% (v/v) glycerol with 1 mM MOPS prior to a second centrifugation step. The pellet was then resuspended in 50 µl ice-cold 10% (v/v) glycerol with 1 mM MOPS and the resulting electro-competent cells were immediately used for electroporation. If necessary, the cells were flash frozen in liquid nitrogen and stored at -80 °C.

2.9.4 Electroporation of electro-competent *P. aeruginosa* cells

Transformation of *P. aeruginosa* cells was performed as for *E. coli* using electro-competent cells prepared as described in Section 2.8.2.

2.10 Recombinant protein production, purification and analysis

2.10.1 Whole cell protein preparation

Strains to be investigated were grown in an appropriate volume of LB broth as previously described. At specific time points, the OD₆₀₀ of the culture was determined and 1 ml aliquots removed. The aliquots were pelleted by centrifugation for 2 min at 13,000 rpm and prepared in the following way. Pelleted cells were then resuspended in 50 µl gold lysis buffer (Table 2.7) to which phenylmethanesulphonylfluoride (PMSF) protease inhibitor was then added. Resuspended cell pellets were then incubated on ice for 30 min and sonicated for approximately 30 s. 50 µl sample loading buffer was then added and the samples were boiled for 5 min prior to loading on an SDS-PAGE gel. When necessary, samples were stored at -20 °C.

Gold lysis buffer	
Tris-HCl pH 8.0	20 mM
NaCl	137 mM
EDTA	5 mM
Triton X-100	1% (v/v)
Glycerol	15% (v/v)

Table 2.7: Gold lysis buffer.

Stored at RT.

2.10.2 Sodium dodecyl sulphate-polyacrylamide gel electrophoresis (SDS-PAGE) analysis

For the analysis of proteins, SDS-PAGE (sodium dodecyl sulphate polyacrylamide gel electrophoresis) was performed as described by Laemmli (1970). A 12% resolving gel was used in gels shown in this thesis, which allowed separation of proteins which had first been electrophoresed through a 5% stacking gel. Samples were boiled for 5 min prior to loading and 10 µl aliquots of prepared samples were loaded onto the stacking gel with a disposable gel loading tip (Bio-Rad). 10 µl of the Bio-Rad Precision Plus Dual Colour Protein Standard was also loaded and provided the molecular weight marker. Electrophoresis was performed in electrophoresis running buffer (Table 9.2) using a Bio-Rad mini-protean II gel pouring and electrophoresis rig and separated using a Bio-Rad power pack at 16 mA per gel until the protein entered the resolving gel. Subsequently, 40 mA per gel was used to allow samples to resolve, until the dye had migrated to the bottom of the gel. The gel was stained and destained to visualize the proteins.

2.10.3 Western blotting

To detect proteins of interest, they were transferred from SDS-PAGE gels onto nitrocellulose membranes using a Mini Trans-Blot cell (Biorad, UK). Blotting was performed in blotting buffer at 80 V for 1 h at RT. Once the polyacrylamide gel had been transferred to a nitrocellulose membrane, the membrane was submerged into 5-10 ml Ponceau S (Table 2.8) for 1-2 min or until the bands had become visible. The membrane

was then rinsed with copious dH₂O until the protein bands were no longer visible. The membrane was then blocked shaking for 1 h at RT or O/N at 4 °C in blocking solution (Table 2.8). The blocking solution was discarded and the membrane incubated shaking with the appropriate dilution of the primary antibody in fresh blocking solution for 1 h. The membrane was washed (3 x 20 min) before addition of the secondary antibody at 1:1000 dilution in blocking buffer and incubated at RT shaking for 1 h. The membrane was again thoroughly washed as before. The blot was developed using the ECL Plus Western Blotting Detection System (Amersham Biosciences, UK) for approximately 1 min. Blots were exposed to Hyperfilm™ Chemiluminescence Film (Amersham Biosciences, UK) for 2-60 min. The film was developed and allowed to dry.

Blotting buffer	
Tris base	20 mM
Glycine	150 mM
MeOH	20% (v/v)
Blocking solution	
PBS with:	-
Tween-20	0.05% (v/v)
Dried skimmed milk power	5% (w/v)
Ponceau S	
Ponceau S	0.5% (w/v)
Acetic acid	10% (v/v)
Washing solution	
PBS with:	-
Tween-20	0.05% (v/v)

Table 2.8: Standard recipes for western blotting solutions.

Blotting buffer was stored at 4 °C, ponceau S at RT and blocking and washing solutions freshly prepared for each experiment.

2.11 Extraction, detection and quantification of QSSMs

2.11.1 Extraction of QSSMs

For extraction of AHLs, *E. coli* and *P. aeruginosa* strains were grown in 125 ml LB supplemented with 1 mM IPTG (in 500 ml Erlenmeyer flasks) at 37 °C. Cells were removed by centrifugation and 1 ml supernatant samples were spiked with 5 µl of 10 µM deuterated *N*-pentanoyl-L-homoserine lactone (d_9 C₅-HSL; 1 µM in ACN) as the internal standard (IS). Supernatants were combined with 1 ml acidified ethyl acetate with 0.01% acetic acid, the mixture vortexed for 30 s and the organic phase removed following brief centrifugation at 10,000 rpm. The extraction procedure was performed three times and the combined extracts were evaporated to dryness with a rotary evaporator. The dried extracts were stored at -80 °C until reconstituted in 50 µl of ACN.

A ten point calibration line was established by spiking sterile LB medium with a mixture of analytes with a concentration range from 2 to 500 µM of *N*-butanoyl-L-homoserine lactone (C₄-HSL) and *N*-(3-oxo-dodecanoyl)-L-homoserine lactone (OC₁₂-HSL); a concentration range from 0.2 to 50 µM of *N*-hexanoyl-L-homoserine lactone (C₆-HSL) and *N*-(3-oxodecanoyl)-L-homoserine lactone (OC₁₀-HSL); and a concentration range from 0.08 to 20 µM of *N*-acyl-L-homoserine lactone (C₈-, C₁₀-, C₁₂- and C₁₄-HSLs), *N*-(3-oxo-acyl)-L-homoserine lactone (OC₄-, OC₆-, OC₈- and OC₁₄-HSLs) and *N*-(3-hydroxy-acyl)-L-homoserine lactone (HC₄-, HC₆-, HC₈-, HC₁₀-, HC₁₂- and HC₁₄-HSLs). Stock solutions of 1 mg/ml were prepared in ACN and stored at -20 °C before use.

2.11.2 Analysis of AHLs by TLC-biosensor overlay plates

5 µl samples of extracted culture or cell-free supernatant fractions and 1 µl of 10 mM synthetic AHL standard were spotted individually onto a RP-18 F_{254s} reversed phase silica (Merck). Spots were dried with a hairdryer. Extracts were separated using a MeOH:H₂O (60:40 v/v) mobile phase until the solvent front was approximately 1 inch from the top of the plate. After chromatography, TLC plates were dried and then overlaid with 0.3% (w/v) LB agar seeded with 0.5% (v/v) of an O/N culture of either *E. coli* JM109[pSB536]

for C₄-HSL or JM109[pSB1142] for C₁₂-HSL. Plates were incubated at 37 °C and bioluminescence examined after 4-6 h using a Luminograph LB980 (Berthold, Pforzheim, Germany) photon video camera.

2.11.3 AHL detection by biosensor strain overlay plates

Rapid confirmation of AHL production was performed using a similar method to that described above in section 2.11.2. 5 µl samples of extracted culture or cell-free supernatant fractions and 1µl of 10 mM synthetic AHL standard were applied to wells made in LB agar plates (petri dishes) overlaid with 0.3 % (w/v) LB agar seeded with 0.5% (v/v) of an O/N culture of either *E. coli* JM109[pSB536] for C₄-HSL or JM109[pSB1142] for C₁₂-HSL. Once plates had been prepared, they were placed in a sealed container to prevent evaporation and incubated at 37 °C. Bioluminescence was examined after 2-4h using a Luminograph LB980 (Berthold, Pforzheim, Germany) photon video camera.

2.11.4 LC-MS/MS analysis of QSSMs

LC-MS/MS analysis of QSSMs in extracted supernatants was performed as described by Ortori *et al.* (2011). Briefly, a 5 µl volume of the crude extracts resuspended in ACN was separated at a flow rate of 0.45 ml/min by HPLC equipped with binary pumps, a vacuum degasser, a SIL-HTc autosampler and column oven (Shimadzu, Columbia, MD, USA) using a Phenomenex Gemini Column C18, 150 x 2 mm (5 µm particle size) heated at 50 °C. The HPLC system used a mobile phase A constituted by 0.1 % formic acid and 200 µM EDTA in water and a mobile phase B constituted by 0.1 % formic acid in ACN. The mobile phase A was sonicated for 30 min and all mobile phases were filtered through 0.45 µm nylon Whatman disk filters (Maidstone, UK) prior to use. The HPLC gradient profile was as follows: isocratic for 1 min, a linear gradient from 10% to 50% B over 0.5 min, then a further gradient from 50% to 99% B over 4 min followed by 99% B for 1.5 min, at a flow rate of 0.45 ml/min. The column was re-equilibrated for a total of 2.9 min.

All mass spectrometry (MS) experiments were conducted on a 4000 QTRAP hybrid triple-quadruple linear ion trap mass spectrometer (Applied Biosystems, Foster City, CA,

USA) equipped with a TurboIon source used in positive ion electrospray mode. A Windows XP (Microsoft, Redmond, WA, USA) workstation running Analyst (version 1.4.1) was used for data acquisition and processing. MRM parameters (precursor and product ion pairs, declustering potential, collision cell exit potential and collision energy) were optimized by software automation whilst infusing at 50 $\mu\text{l}/\text{min}$ with the MS peak widths set to 0.7 Th. Source parameters were optimized during infusion experiments at the working flow rate and were as followed: curtain, Gas 1 and 2 were 20, 30 and 10 respectively. The ion source potential was 5000 V and the source was held at 450 °C. Quantification was performed using Analyst 1.4.1.

2.12 Extraction, detection and quantification of AMC metabolites

2.12.1 Sample collection and storage

E. coli and *P. aeruginosa* strains were grown up in 125 ml LB media in 500 ml Erlenmeyer flasks at 37 °C shaking as previously described. At appropriate ODs, samples were harvested by the rapid addition and mixing of 5 ml of the bacterial culture into 15 ml of ice-cold PBS. A volume of the quenched culture, equivalent to 2.5 ml of a culture with $\text{OD}_{600} = 1.0$, was pelleted by centrifugation at -5 °C and 5,000 rpm for 5 min to produce a standard-sized cell pellet. Once the supernatant was discarded, cell pellets were washed by resuspending in a 10 ml aliquot of the ice-cold PBS and pelleted again by centrifugation at -5 °C and 5,000 rpm for 5 min. After discarding the supernatant, the cell pellets were stored at -80 °C until metabolite extraction was carried out.

2.12.2 Extraction of AMC metabolites

Extraction of AMC metabolites in bacterial pellets was facilitated by solvent extraction as described by Halliday *et al.* (2010). Briefly, cell pellets were resuspended in 0.5 ml of 80% (v/v) MeOH spiked with 10 μl of the IS mix ($[^{13}\text{C}_3]\text{MET}$ and SAC were used as ISs at a concentration of 1.0 $\mu\text{g}/\text{ml}$ in dH_2O). Cell lysis was ensured by repeated cycles of freeze–

thaw (cooling to $-80\text{ }^{\circ}\text{C}$), with rapid vortex mixing between cycles. Cellular debris was pelleted by centrifugation (13,000 rpm, $0\text{ }^{\circ}\text{C}$, 10 min), and the methanolic extract was transferred to a clean sample vial. Cell pellets were extracted twice more with 0.5 ml portions of 80% (v/v) MeOH, combining extracts to give a total volume of approximately 1.5 ml of methanolic extract per sample. Extracts were concentrated to approximately 20% of the initial volume under vacuum and then dried by lyophilisation O/N.

2.12.3 Chemical derivatization of AMC metabolites

Following solvent extraction, compounds underwent chemical derivatization as this improves the extraction, ionization, and chromatographic properties of all the AMC metabolites (Halliday *et al.*, 2010). For this, the dried extracted metabolite samples were first redissolved in 80 μl dH_2O . 10 μl of 0.05M tris-(hydroxyl-propyl)phosphine (THP; Novagen, Merck Chemicals, Nottingham, UK) solution was added and the samples were allowed to stand for approximately 30 min at RT. Then 40 μl of iso-butanol (*i*-BuOH)/pyridine mix (3:1, v/v) was added, followed by 10 μl of iso-butylchloroformate (*i*-BuCF). The samples were then vortex-mixed for approximately 30 s, and 200 μl of DCM/*tert*-butylmethyl ether (1:2, v/v) was added. After a further period of vortex mixing, the layers were separated and 150 μl of the upper organic phase containing the derivatized metabolites was removed to an autosampler vial. The aqueous layer was then extracted with a second 200 μl portion of the organic solvent mix and combined with the initial organic extract. The organic solvent was removed under vacuum, and the residue of derivatized metabolites was dissolved in 100 μl of the initial LC mobile phase (55% MeOH in 10 mM aqueous ammonium formate).

2.12.4 LC-MS/MS analysis of AMC metabolites

LC-ESI-MS/MS was performed as described by Halliday *et al.* (2010) using a triple quadrupole Quattro Ultima mass spectrometer (Waters Micromass, Manchester, UK) in conjunction with an Agilent 1100 LC system (Agilent Technologies, Waldbron, Germany) with a cooled autosampler. The LC column was a Luna ODS C18(2) (5 μm , 150 \times 2.0 mm, Phenomenex, Macclesfield, UK) with an appropriate guard column, maintained at 30 $^{\circ}\text{C}$ with a mobile phase flow rate set at 200 $\mu\text{l}/\text{min}$. Gradient elution mobile phases consisted of A (aqueous 10 mM ammonium formate) and B (10 mM ammonium formate in MeOH). The gradient began initially at 55% B, increasing linearly to 100% B over 15 min, maintained at this percentage for a further 5 min and returned to 55% B for reequilibration. The total run time was 30 min for each sample. Sample temperature was maintained at 4 $^{\circ}\text{C}$ in the autosampler prior to analysis with injections of 20 μl per sample. Quantitation of analytes was undertaken using tandem electrospray mass spectrometry in positive mode (+ESI). Cone and desolvation gas flows of 155 and 765 L/h with source and desolvation temperatures of 150 and 350 $^{\circ}\text{C}$, respectively, were used. The dominant product ion for each derivatized metabolite was selected to monitor in multiple reaction monitoring (MRM) mode (Table 2.11). Dwell time was set to 0.1 s. Peaks were integrated, and the software package MassLynx (version 4, Waters) was used to quantify levels of the AMC metabolites.

Analyte	Retention time (min)	Precursor ion (<i>m/z</i>)	Product ion (<i>m/z</i>)	Collision energy (eV)	IS used
HCY	18.6	392.2	292.4	14	[¹³ CD ₃]MET
MET	15.8	306.2	104.2	19	[¹³ CD ₃]MET
SAH	12.1	541.2	136.1	25	SAC
SAM	12.2	655.1	202.3	24	SAC
SRH	11.5	424.2	202.2	20	[¹³ CD ₃]MET
[¹³ CD ₃]MET ^a	15.7	310.2	108.3	19	-
SAC ^a	11.2	527.2	136.2	23	-
(HCY) ₂ ^b	19.3	581.2	290.4	17	-

Table 2.9: AMC metabolites - Selected precursor product ion *m/z* values, retention times, and collision energies used to identify and quantify analytes using MRM.

^a Internal standards. ^b The presence of these oxidized metabolites was monitored for but not quantified.

2.13 Extraction, detection and quantification of MTA

2.13.1 Extraction of MTA

Extraction of MTA in bacterial pellets was facilitated by solvent extraction. Briefly, cell pellets were resuspended in 0.5 ml MeOH spiked with 10 µl 2-chloroadenosine (2-C.ADE) as the IS. Cell lysis was ensured by repeated cycles of freeze–thaw (cooling to -80 °C), with rapid vortex mixing between cycles. Cellular debris was pelleted by centrifugation (10 min, 13,000 rpm, 0 °C), and the methanolic extract was transferred to a clean sample vial. Cell pellets were extracted twice more with 0.5 ml portions of MeOH, combining extracts to give a total volume of approximately 1.5 ml of methanolic extract per sample. Extracts were then evaporated to dryness and reconstituted in 100 µl dH₂O.

2.13.2 LC-MS/MS analysis of MTA

LC–ESI–MS/MS was performed using a triple quadruple Quattro Ultima mass spectrometer (Waters Micromass, Manchester, UK) in conjunction with an Agilent 1100 LC system (Agilent Technologies, Waldbron, Germany) with a cooled autosampler, with

conditions as described by Stevens *et al.* (2008). The LC column was a Synergi 4u Hydro-RP (4 μm , 150 \times 2.0 mm, Phenomenex, Macclesfield, UK) with an appropriate guard column. The column oven was kept at 25 $^{\circ}\text{C}$ with a mobile phase flow rate set at 125 $\mu\text{l}/\text{min}$. LC separation was carried out using a mobile phase consisting of 0.1% acetic acid in H_2O (A) and 0.1% acetic acid in ACN (B). The gradient employed was as follows: 0–10 min linear increase from 0 to 100% solvent B, hold at 100% solvent B for 5 min. The total run time was 25 min for each sample. Sample temperature was maintained at 4 $^{\circ}\text{C}$ in the autosampler prior to analysis with injections of 20 μl per sample. Quantitation of analytes was undertaken using tandem electrospray mass spectrometry in positive mode (+ESI). Cone and desolvation gas flows of 155 and 765 L/h with source and desolvation temperatures of 150 and 350 $^{\circ}\text{C}$, respectively, were used. Peaks were integrated, and the software package MassLynx (version 4, Waters) was used to quantify levels of MTA.

Analyte	Retention time (min)	Precursor ion (m/z)	Product ion (m/z)	Collision energy (eV)	IS used
MTA	4.6	298.2	136.2	15	2-C.ADE
2-C.ADE ^a	4.5	302.2	170.3	16	-

Table 2.10: MTA - Selected precursor product ion m/z values, retention times, and collision energies used to identify and quantify analytes using MRM.

^a Internal standard.

2.14 Detection of AI-2 using *Vibrio harveyi* bioassay

Measurement of AI-2 activity within samples using *V. harveyi* BB170 was based upon methods described by Bassler *et al.* (1997). O/N cultures of *V. harveyi* BB170 were diluted 50-fold in fresh LB medium and grown for 7-8 h. The culture was then diluted 5000-fold in assay for bioluminescence (AB) medium (Table 2.11). 20 μl volumes of each test sample for AI-2 analysis were added to 180 μl aliquots of the *V. harveyi* dilution in AB medium. Changes in bioluminescence were monitored at 30 $^{\circ}\text{C}$ every 30 min using a

multifunctional, automated luminometer-spectrometer (TECAN Infinite F200). This was performed in 96 well clear bottomed, black polystyrene plates (Matrix).

For a single experiment, the *V. harveyi* bioassay was performed in triplicate for each sample. An appropriate negative control sample was also included for each set of test samples. The light emission in response to this control was charted, the time during the assay at which light output in response to this control sample had reached a minimum level was identified. Consequently, all values of bioluminescence determined during this study are depicted in terms of fold-induction of bioluminescence relative to a negative control sample.

AB media	
NaCl	0.3 mM
MgSO ₄	0.05 M
Vitamin-free casamino acids	0.2% (w/v) mM
K ₂ HPO ₄	10 mM
HEPES (pH 7.8 using KOH)	25 mM
L-arginine	1 mM
Glycerol	0.5% (v/v)

Table 2.11: Recipe for AB media.

Stored at RT.

Chapter 3

Analysis of the metabolic
implications of the
P. aeruginosa AHL synthase
genes in *E. coli*

3.1 Introduction

To enable *P. aeruginosa* to cause infection, the QSSMs it produces to control virulence factor production are synthesized from substrates that are derived from central metabolism. In *P. aeruginosa*, QS achieves co-ordinated cell-cell communication through the production of *N*-acyl-L-homoserine lactones (AHLs) and the *Pseudomonas* quinolone signal (PQS). Production of AHLs requires precursors including fatty acids and *S*-adenosyl-L-methionine (SAM). SAM is derived from the activated methyl cycle (AMC) that functions as a metabolic pathway dedicated to the degradation of the toxic metabolite *S*-adenosyl-L-homocysteine (SAH). The AMC is therefore performing a highly important function and this is rarely taken into consideration in the context of QS. However, since metabolites integral to the AMC may be subverted for AHL synthesis, there are likely to be metabolic consequences of AHL synthesis which alter the bacterial cell's physiology, and consequently fitness and this ultimately may impact upon virulence.

To study each QSSM synthase in isolation, each was subcloned into *E. coli* to avoid complicating interactions imposed by the *P. aeruginosa* hierarchical QS system. An IPTG-inducible expression vector was exploited and the constructs transferred to a strain of *E. coli*, a heterologous bacterial host which has the appropriate metabolic systems yet does not itself produce any AHLs thus avoiding any interference issues.

3.2 Cloning of *lasI*_{Pa} and *rhII*_{Pa}

Figure 3.1 shows the strategy adopted for cloning the sequences of the *P. aeruginosa* AHL synthase genes. The ORFs of the *lasI*_{Pa} and *rhII*_{Pa} genes were PCR-amplified using chromosomal DNA isolated from *P. aeruginosa* strain PA01 (Nottingham) using the primer pairs lasIF/lasIR and rhIIF/rhIIR respectively (Table 2.5). The resultant products were separated using agarose gel electrophoresis, which demonstrated the presence of the two expected 0.624 kb fragments (0.606 kb *lasI*_{Pa}/*rhII*_{Pa} and 0.018 kb for additional restriction sites). The amplified sequences were excised from the gel and each sample purified via gel extraction. Directed ligation of the pGEM-T Easy cloning vector

(Promega) and inserts, produced pGEM-*lasI*_{Pa} and pGEM-*rbII*_{Pa}, which were transformed into *E. coli* DH5 α and plated out onto the appropriate selective medium comprising LB agar, Cb and X-gal, to allow selection via blue-white screening. As expected, subjecting the DH5 α competent cells to transformation with water alone generated no transformants, whilst undigested pBS vector generated a lawn of transformants.

The insertional inactivation of the *lacZ* gene with the *lasI*_{Pa} and *rbII*_{Pa} genes to disrupt β -galactosidase production resulted in a significant number of white colonies, some of which were chosen for further analysis. The plasmids extracted from all selected transformants generated the expected DNA fragments when digested with the REs *MfeI* and *StuI* confirming the presence of the AHL synthase encoding genes. An absence of point mutations was confirmed by DNA sequencing.

The *lasI*_{Pa} and *rbII*_{Pa} inserts were released from their respective constructs in the pGEM-T Easy vector in a double digestion reaction with *MfeI* and *StuI*. The same REs were used to digest pME6032 and ligation of the two, produced pME-*lasI*_{Pa} and pME-*rbII*_{Pa}, which were again transformed into *E. coli* DH5 α . Colony PCR of potential Tc resistant clones confirmed the presence of either of the AHL synthase encoding genes. Sequencing was performed to verify that no point mutations had occurred.

3.3 *lasI*_{Pa} and *rbII*_{Pa} synthesize the cognate AHLs in MG1655

Following successful cloning of *lasI*_{Pa} and *rbII*_{Pa} into pME6032, and transformation into *E. coli* MG1655, AHL production was confirmed. This was performed using strain overlay plates in the first instance, and then thin-layer chromatography (TLC) analyses (Figure 3.2). Both methods confirmed that expression of *lasI*_{Pa} and *rbII*_{Pa} in MG1655 leads to the production of OC₁₂-HSL and C₄-HSL, respectively.

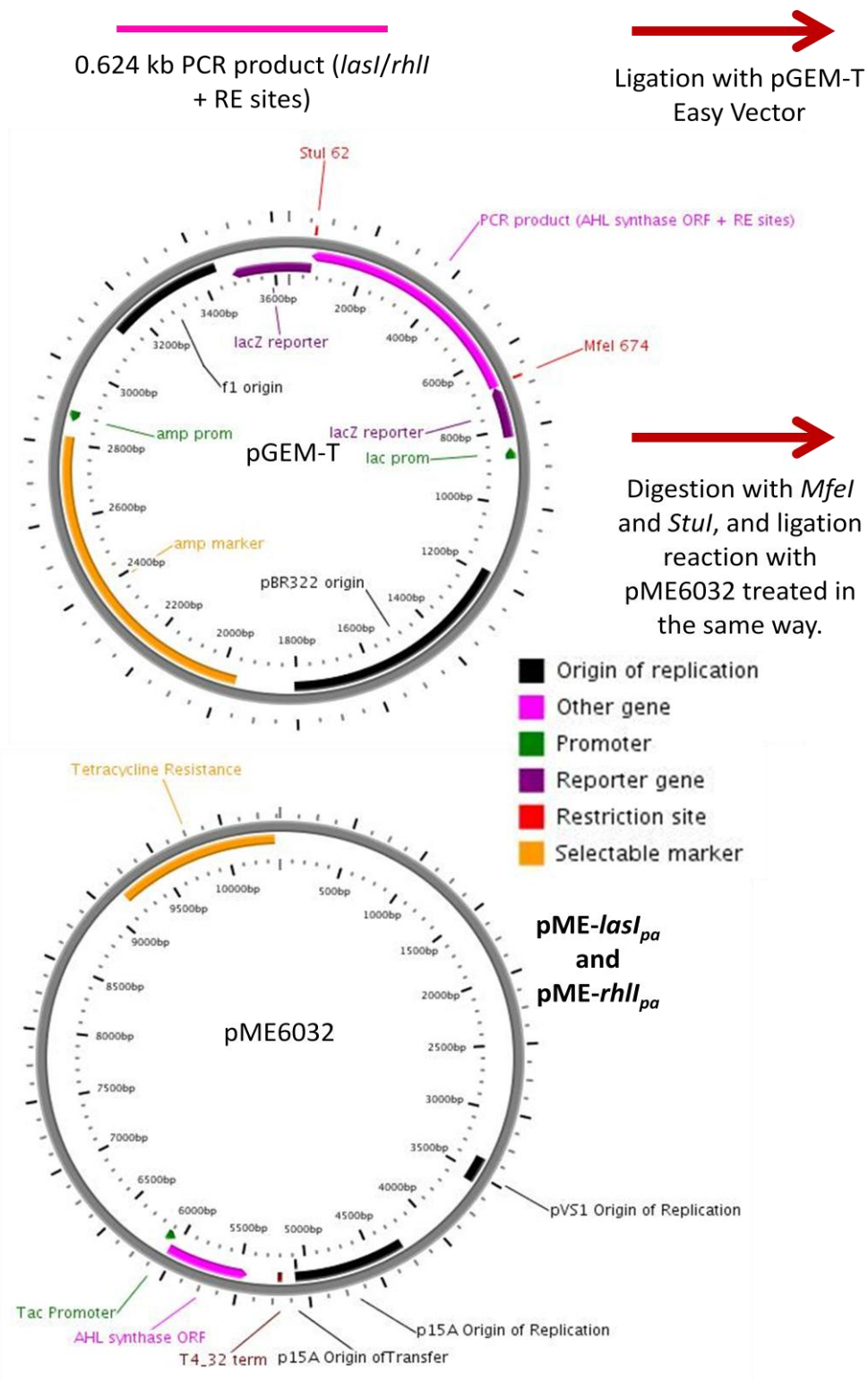


Figure 3.1: Schematic representation of the strategy adopted for cloning the *lasI*_{Pa} and *rhlI*_{Pa} genes. The ORF sequence of each gene was PCR amplified to incorporate *MfeI* and *StuI* RE sites and then cloned into the pGEM-T Easy vector. Once successful, digestion of the recombinant T-clone construct with *MfeI* and *StuI* produces the insert and vector fragments upon electrophoresis. The insert sequences were then cloned into pME6032 digested with the same REs.

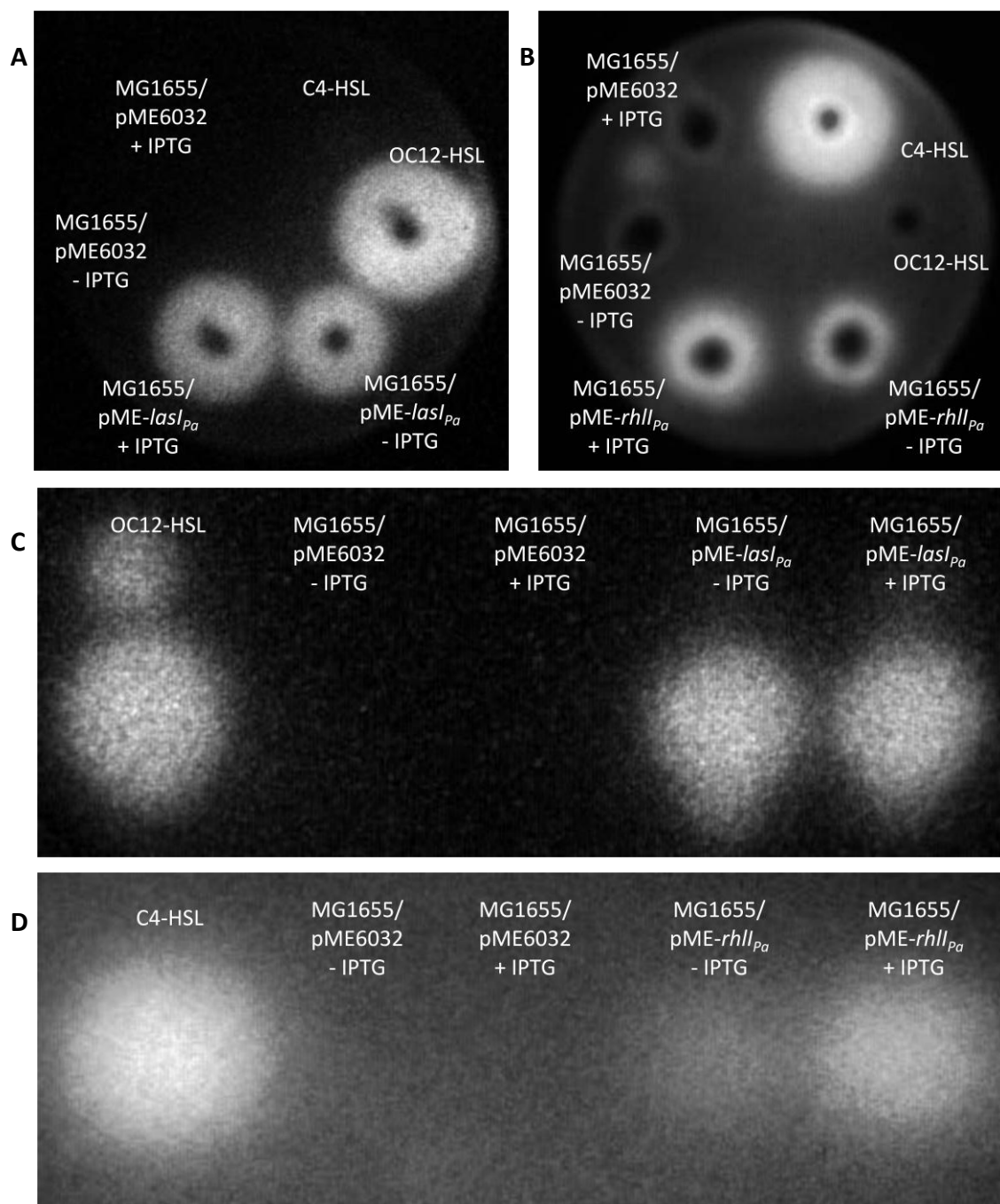


Figure 3.2: Cloned *lasI*_{pa} and *rhII*_{pa} genes lead to the production of OC₁₂-HSL and C₄-HSL respectively in *E. coli* MG1655. Strain overlay plates [A, B] and thin layer chromatography [C, D] of methanol extracts of MG1655[pME6032] and -AHL synthase strains grown with and without IPTG induction in LB to late exponential phase. A and C have been overlaid with JM109[pSB1142], responding to long-chain AHLs, whilst B and D with JM109[pSB536], which luminescence in response to short-chain AHLs. AHL production occurs even without IPTG induction representing leaky vector.

The negative control, *E. coli* MG1655[pME6032], which lacked a cloned AHL synthase was completely devoid of detectable AHL production. However, both MG1655[pME-*lasI_{Pa}*] and MG1655[pME-*rhII_{Pa}*], directed production of their cognate AHL in the absence of the gene expression induced by IPTG, albeit at lower levels.

3.4 LC-MS/MS profiling of AHLs reveals that *LasI* produces several other AHLs in MG1655

As well as OC₁₂-HSL and C₄-HSL, *P. aeruginosa* produces other AHLs including C₆-HSL, as well as an array of AQS. It was therefore interesting to investigate whether the AHL synthase genes would perform exactly the same function and replicate the AHL profile observed in the chosen heterologous organism. As expected, OC₁₂-HSL and C₄-HSL were the overriding signals, being detected above 600 μ M and 800 μ M, respectively, occupying averages of 71% and 95%, respectively of the total AHL profiles for recombinant *lasI_{Pa}* and *rhII_{Pa}* expression (Figure 3.3 and 3.4). The distribution demonstrated by *lasI_{Pa}* was far more interesting, with the observance of 12 other AHLs, with half of them being present at concentrations above 5 μ M (Figure 3.2). Amongst these, the OC-series seemed to dominate, with, as already mentioned, OC₁₂-HSL, occupying the major percentage (71%) followed by, averages of 111.73 μ M OC₁₄-HSL (13%) and 50.07 μ M OC₁₀-HSL (6%). Subsequently, significant concentrations of the C-series were observed, with averages corresponding to 41.87 μ M C₁₂-HSL and 18.8 μ M C₁₄-HSL. Other AHLs, in descending order of concentration, include OC₈-HSL (5.45 μ M), OC₆-HSL (3.54 μ M), HC₁₄-HSL (2.81 μ M), C₁₀-HSL (2.36 μ M), C₈-HSL (2.10 μ M), HC₁₀-HSL (0.45 μ M) and C₆-HSL (0.36 μ M). In contrast, the AHL profile for *rhII_{Pa}* was far narrower and differed from the *lasI_{Pa}*-dependent AHL profile since smaller acyl chains were linked to the lactone ring (Figure 3.4). In addition to C₄-HSL, 3 other AHLs were observed with the average concentrations observed as follows: HC₄-HSL (36.15 μ M), C₆-HSL (6.06 μ M) and C₈-HSL (1.72 μ M).

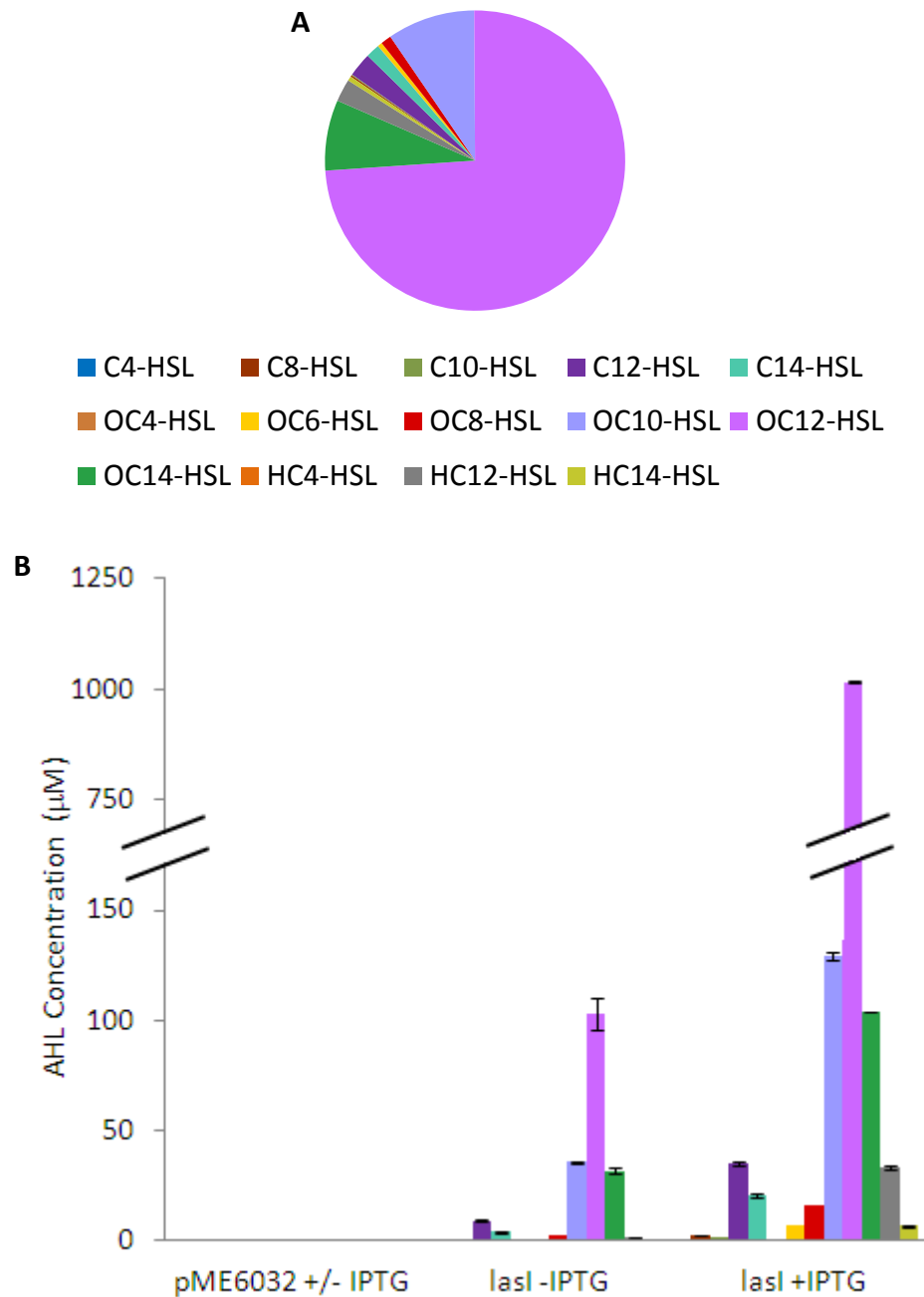


Figure 3.3: Relative molar proportions and quantitative profiling of AHLs produced by $lasI_{Pa}$ expression in *E. coli* in LB growth media. Compounds were extracted from late exponential phase supernatants with acidified ethyl acetate and profiled by LC-MS/MS analysis. (A) The ratio between the different signalling molecules present in supernatants is represented by pie charts. (B) The actual concentration of AHLs.

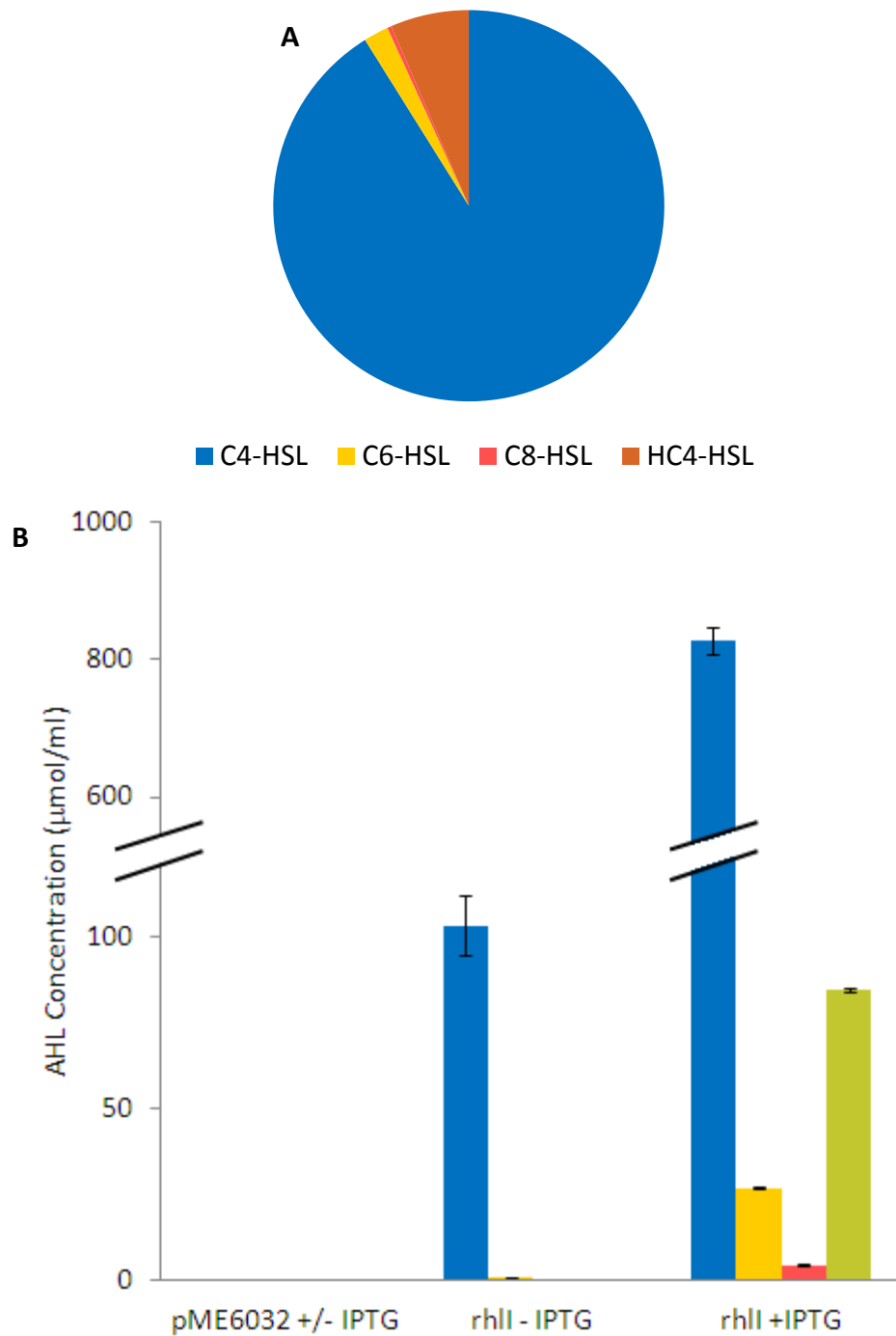


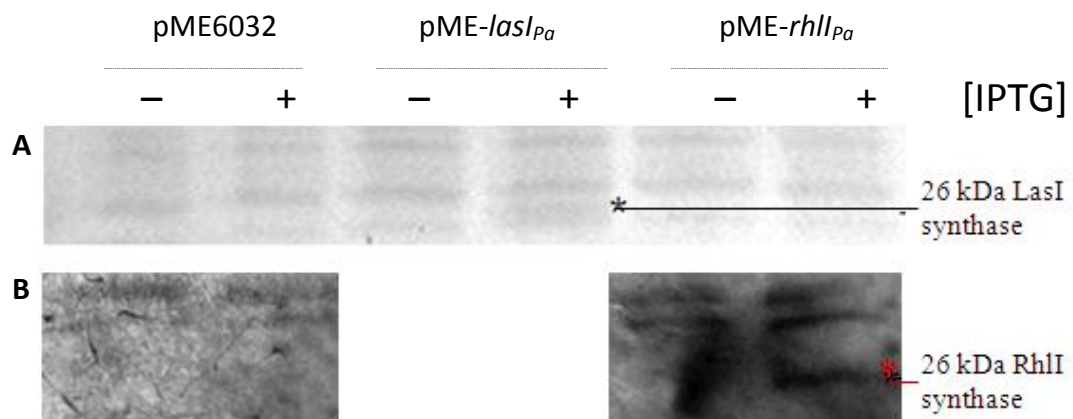
Figure 3.4: Relative molar proportions and quantitative profiling of AHLs produced by $rhII_{Pa}$ expression in *E. coli* in LB growth media. Compounds were extracted from late exponential phase supernatants with acidified ethyl acetate and profiled by LC-MS/MS analysis. (A) The ratio between the different signalling molecules present in supernatants is represented by pie charts. (B) The actual concentration of AHLs.

3.5 LasI and RhII proteins are detected in MG1655

To confirm the production of the synthases themselves, protein profiles of the induced and uninduced *E. coli* expression strains were analysed. With the induced MG1655[pME-*lasI_{pa}*], it was possible to visualize the presence of an additional 26 kDa protein corresponding to the LasI synthase with Coomassie staining of an SDS-PAGE (Figure 3.5A). The absence of this protein from profiles of extracts prepared from the uninduced strain and moreover MG1655 harbouring the empty vector, confirmed that its production was due to *lasI_{pa}*. Furthermore, this protein was sequenced via MALDI fingerprint analysis to confirm its identity (Figure 3.5C). In contrast, with MG1655[pME-*rhII_{pa}*], despite 3 independent rounds of sample collection, preparation and running of SDS-PAGE, detection of the RhII synthase was not possible. However, the availability of a specific antibody meant that it was possible to visualise an additional protein corresponding to the RhII synthase though a Western blot approach (Figure 3.5B).

3.6 Production of AHL synthases in MG1655 alters the levels of metabolites of the AMC

As LasI and RhII synthesize AHLs from metabolite substrates, it was interesting to determine the metabolic repercussions of introducing these enzymes into *E. coli*. The AMC metabolic profile (SAM, SAH, SRH, HCY and MET) was determined in extracts prepared from late exponential phase cultures (125 ml LB in 500 ml-Erlenmeyer flasks at 37°C shaking) of *E. coli* MG1655 with the empty vector or carrying an AHL synthase. The absence of calibration meant that the precise concentrations of each compound cannot be determined, but the presence of an internal standard allowed the comparison of metabolite composition from one extract to the other, the concentrations being expressed in arbitrary units. Introduction of AHL synthases reduced the level of each of the metabolites compared to the non-induced strain and the WT with the empty vector (Figure 3.6).



C

	Accession	Mass	Score	Description
1.	gi 15596629	22848	89	autoinducer synthesis protein LasI [Pseudomonas aeruginosa PAO1]
2.	gi 52695393	22788	89	Chain A, Crystal Structure Of The Ahl Synthase LasI

Figure 3.5: Protein production confirmed from cloned synthase genes in *E. coli* MG1655. *E. coli* MG1655 alone [pME6032] or containing pME-*lasI*_{pa} (LasI) or pME-*rhlI*_{pa} (RhlI) were grown in LB to OD₆₀₀=0.5 and induced with (+) IPTG or not (-). After approximately 1 h, whole cell extracts were prepared and separated through 12% SDS-PAGE gels which were subjected to Coomassie staining (A) or Western blotted using α RhlI (B). SDS-PAGE reveals the presence of the 26 kDa LasI protein (*) in lysates of the IPTG induced MG1655[pME-*lasI*_{pa}] strain, whilst IPTG induction of MG1655[pME-*rhlI*_{pa}] leads to expression of the 26 kDa RhlI synthase (*) as shown by Western blotting. The top matches from the Mascot search of fragments generated from MALDI fingerprint analysis of the suspected LasI band confirm its identity (C).

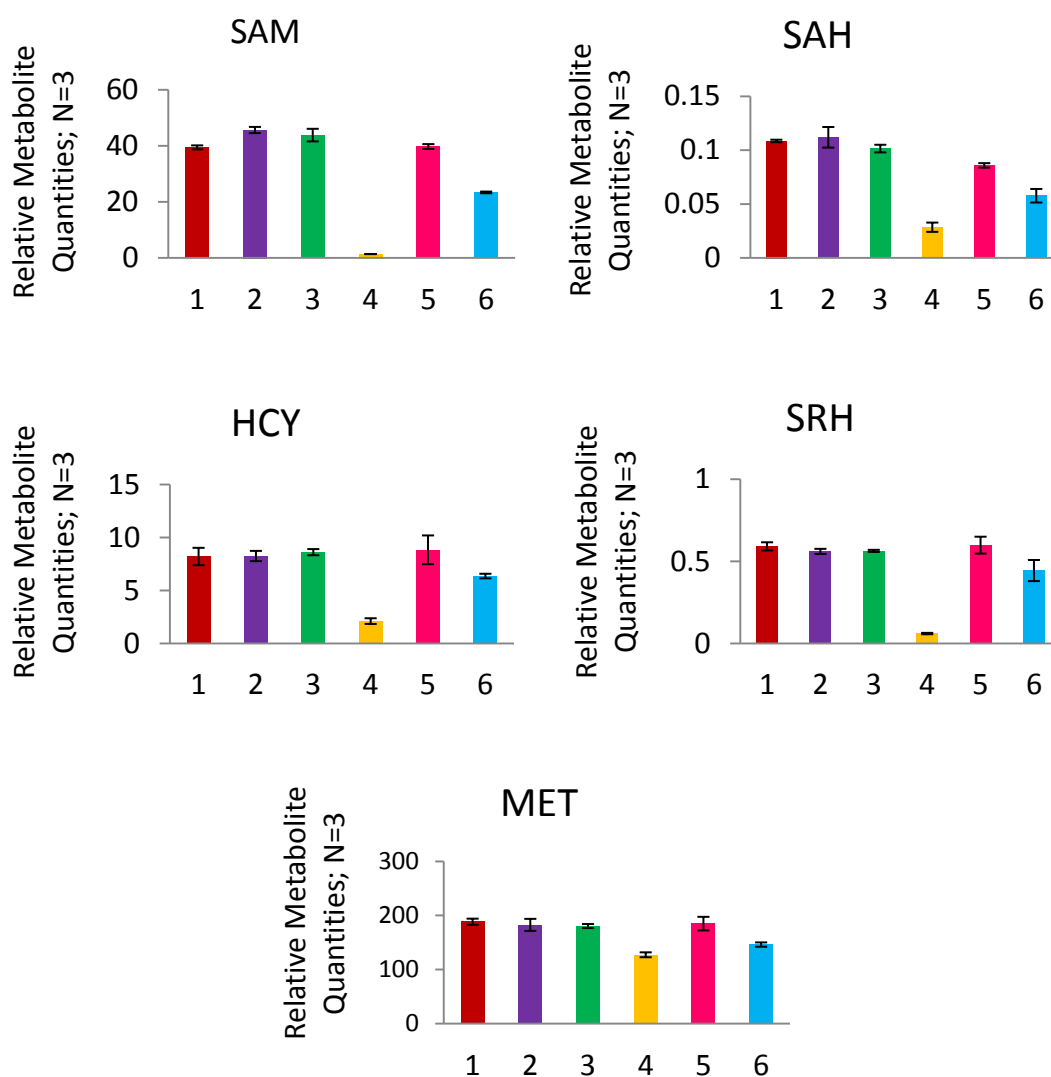


Figure 3.6: Reduced levels of AMC-linked metabolic profile of *E. coli* MG1655-AHL synthase strains. Intracellular accumulation of SAM, SAH, SRH, HCY and MET were determined by LC-MS analysis in three *E. coli* strains MG1655[pME6032] (1, 2), MG1655[pME-*lasI_{Pa}*] (3, 4) and MG1655[pME-*rhII_{Pa}*] (5, 6) grown in LB with (2, 4, 6) and without (1, 3, 5) IPTG induction. Peak area corresponding to each compound was divided by the peak area of the appropriate internal standard for normalisation.

Addition of IPTG to the strain with the empty plasmid (negative control conditions; NCCs) did not alter AMC metabolite levels. Metabolic concentrations were most reduced when *lasI_{pa}* was induced. Intracellular SAM concentrations average 42.19 ± 3.06 in the NCCs and are significantly reduced to 1.39 ± 0.02 with IPTG induction of MG1655[pME-*lasI_{pa}*] and to 23.40 ± 0.30 with induction of MG1655[pME-*rhII_{pa}*]. Similarly, SAH levels decrease to 28% with *lasI* and 57% with *rhII* induction. HCY and SRH concentrations for MG1655[pME-*lasI_{pa}*] are approximately 4-fold and almost 10-fold lower than the corresponding NCC averages. In MG1655[pME-*rhII_{pa}*] +IPTG HCY and SRH levels fall, but less drastically. Changes in intracellular concentrations of MET are also less pronounced, but nevertheless do fall; average metabolite quantities are 127.39 ± 4.53 and 146.28 ± 4.00 for MG1655[pME-*lasI_{pa}*] and MG1655[pME-*rhII_{pa}*] respectively compared to the equivalent mean of the NCC (184.20 ± 3.43).

3.7 Production of AI-2 is reduced in the MG1655-AHL synthase strains

As the *E. coli* AMC includes an enzymatic reaction catalysed by LuxS, it was interesting to look at the effect of *lasI_{pa}* and *rhII_{pa}* on the synthesis of AI-2. As exploited by many others, the detection of extracellular AI-2 was undertaken using the *Vibrio harveyi* biosensor. Late exponential phase culture supernatants of the MG1655-AHL synthase strains were analysed using this bioassay and bioluminescence measured every 30 mins in an automated luminometer-spectrometer (TECAN Infinite F200). The stimulation of light production in the *V. harveyi* reporter over the initial 12-hr period is shown in Figure 3.7.

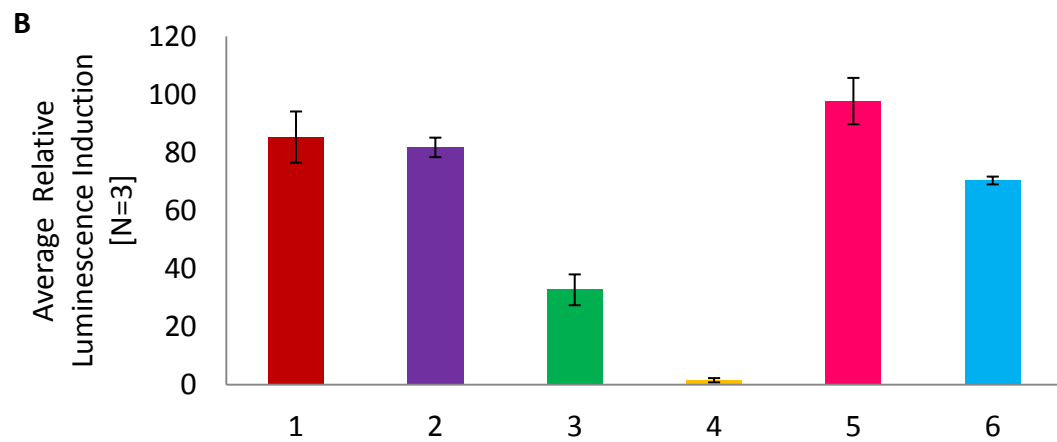
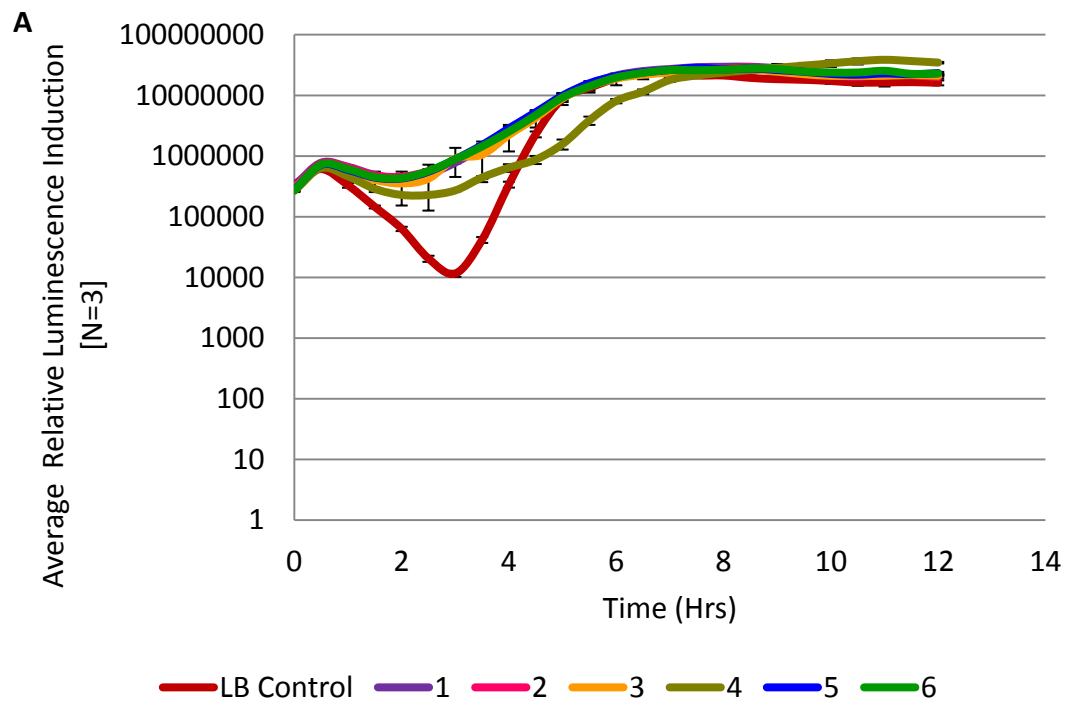


Figure 3.7: Reduced AI-2 production in induced MG1655[pME-*lasI_{pa}*] and MG1655[pME-*rhlI_{pa}*] cell free-extract. (A) Stimulation of light production in *V. harveyi* BB170 over the first 12 hrs of growth. (B) Average induction of bioluminescence at three hours for three *E. coli* strains: MG1655[pME6032] (1, 2), MG1655[pME-*lasI_{pa}*] (3, 4) and MG1655[pME-*rhlI_{pa}*] (5, 6) grown in LB with (2, 4, 6) and without (1, 3, 5) IPTG induction. AI-2 activities for a single experiment are shown, although the experiment has been repeated three times with similar results.

Maximal light production occurred at three hours and demonstrated that introduction of the synthases caused a reduction in the levels of AI-2 detected (Figure 3.7). The uninduced MG1655[pME-*lasI_{pa}*] strain illustrated significantly lower levels of extracellular AI-2 compared to the other NCCs. Despite this reduction in AI-2 which likely indicates weak constitutive expression of *lasI_{pa}* in the pME6032 vector. IPTG induction was associated with further reduction in production of AI-2, giving a massive 20-fold reduction in bioluminescence levels compared to the uninduced strain. Furthermore, if compared to the NCCs (MG1655[pME6032]) this corresponds to an approximate 55-fold decrease. For MG1655[pME-*rhlI_{pa}*], the reduction in AI levels is comparatively less. However, it still corresponds to a 95.33% reduction when considered against conditions of no IPTG induction and a similar 98.17% decrease in comparison with the empty vector strains (Figure 3.7).

3.8 MTA levels increase upon expression of the PA01 AHL synthases

As introduction of LasI and RhlI into the foreign MG1655 system led to the associated production of AHLs which is not normally a characteristic of the *E. coli* system, it was interesting to determine the changes to intracellular levels of MTA since this is a by product of AHL synthesis. The presence of MTA was determined from cell extracts prepared from late exponential phase cultures of MG1655 with the empty vector or carrying a synthase gene. As with profiling of the AMC metabolites, the presence of an internal standard meant that different extracts could be compared. With independent experiments, the levels of intracellular MTA observed were variable and this seemed unusual given that only two compounds were being selected for in one LC-MS/MS method; Figure 3.7A shows only one example. However, in *E. coli*, the Pfs enzyme which catalyses the detoxification of SAH to SRH, also acts as an MTA nucleosidase; this means that any MTA present in the cell will be susceptible to the activity of this enzyme making it difficult to access any alterations to levels of this metabolite caused by introduction of either of the synthase genes. In order to correct for this, the empty vector

and those carrying the AHL synthase genes were transferred to a Δpfs strain and the quantification repeated in exactly the same way (Figure 3.8B). Quantifying intracellular MTA using this strain gave rise to the much tighter standard deviation values as would have been expected. In fact, levels of this metabolite were generally higher in all conditions compared to the numerical scale for the analysis performed in the WT (Figure 3.8A). Nevertheless, MTA levels are significantly higher with introduction of the synthase genes, with recombinant *lasI_{Pa}* expression causing a 32-fold increase and that of *rhII_{Pa}* causing a 13-fold increase.

3.9 Production of LasI and RhII affect the growth of MG1655

The growth of the three strains was initially compared in rich media (Figure 3.9A). In these conditions, the AHL synthase strains, MG1655[pME-*lasI_{Pa}*] and MG1655[pME-*rhII_{Pa}*], growth curves differ from that of the WT with the empty vector, MG1655[pME6032]. The difference only affects the initial growth period; expression of *lasI_{Pa}* in MG1655 results in a slight extension to the length of the lag phase when compared to that of the WT. In contrast, this initial growth period is slightly reduced with introduction of the *rhII_{Pa}* synthase gene. However, in both situations, the remaining growth curve mimics that of the WT.

Since the AHL synthases use SAM as a substrate (Moré *et al.* 1996, Jiang *et al.* 1998), it was predicted that AHL synthesis would draw upon the AMC. To test the hypothesis that cell fitness will be compromised when nutrient availability is limited in the environment and metabolites of the AMC are diverted, the *E. coli* strains were grown in MOPS minimal media (Figure 3.9B).

Again, the lag phase of the MG1655[pME-*lasI_{Pa}*] is significantly extended. Indeed, there appears to be no distinction between ending this initial period and exponential phase growth; the rate of growth over the entire period monitored is extremely slow. In these circumstances, MG1655[pME-*lasI_{Pa}*] is not able to achieve the population size (OD₆₀₀)

that is attainable by MG1655[pME6032] by stationary phase over the period monitored (Figure 3.9B).

Whilst MG1655[pME-*rhII_{Pa}*] did not grow as well as MG1655[pME6032], it grew better than MG1655[pME-*lasI_{Pa}*]. The length of the *rhII_{Pa}* strain's lag phase was 3 hours longer than that of the WT and approximately 5 hours greater than that observed in LB medium. However, once exponential growth is initiated, the growth profile mimicked MG1655[pME6032] (Fig. 3.9B).

3.10 Exogenous methionine addition improves the growth of MG1655[pME-*lasI_{Pa}*] in MOPS minimal media

As LasI and RhlI production impedes the growth of *E. coli* and alters intracellular AMC metabolic pools, the ability of an exogenous compound that is able to feed into the AMC to restore growth was investigated. Methionine was added at various concentrations to 125 ml MOPS minimal media batch cultures grown up in 500 ml-Erlenmeyer flasks at 37°C shaking. MG1655[pME6032] and MG1655[pME-*lasI_{Pa}*] were additionally grown up without further methionine supplementation and respectively provided the appropriate positive and negative controls for the experiment. The cell density (OD₆₀₀) was monitored regularly for an initial 10-hour period during which none of the methionine concentrations tested significantly improved growth of MG1655[pME-*lasI_{Pa}*]. However, the following day, those cultures supplemented with 250 µM and 500 µM methionine had an optical density comparable to the WT. To enable continuous monitoring of cell densities, growth was subsequently monitored in an automated spectrometer (TECAN Infinite F200). Use of the automated spectrometer also meant that a wider concentration range of methionine supplementation could be tested. Despite the approximate 14-hour lag phase, exogenous methionine addition did allow MG1655[pME-*lasI_{Pa}*] to grow. From Figure 3.10A, the higher the concentration of methionine supplementation, the greater the rate of exponential growth measurable over 24-hours.

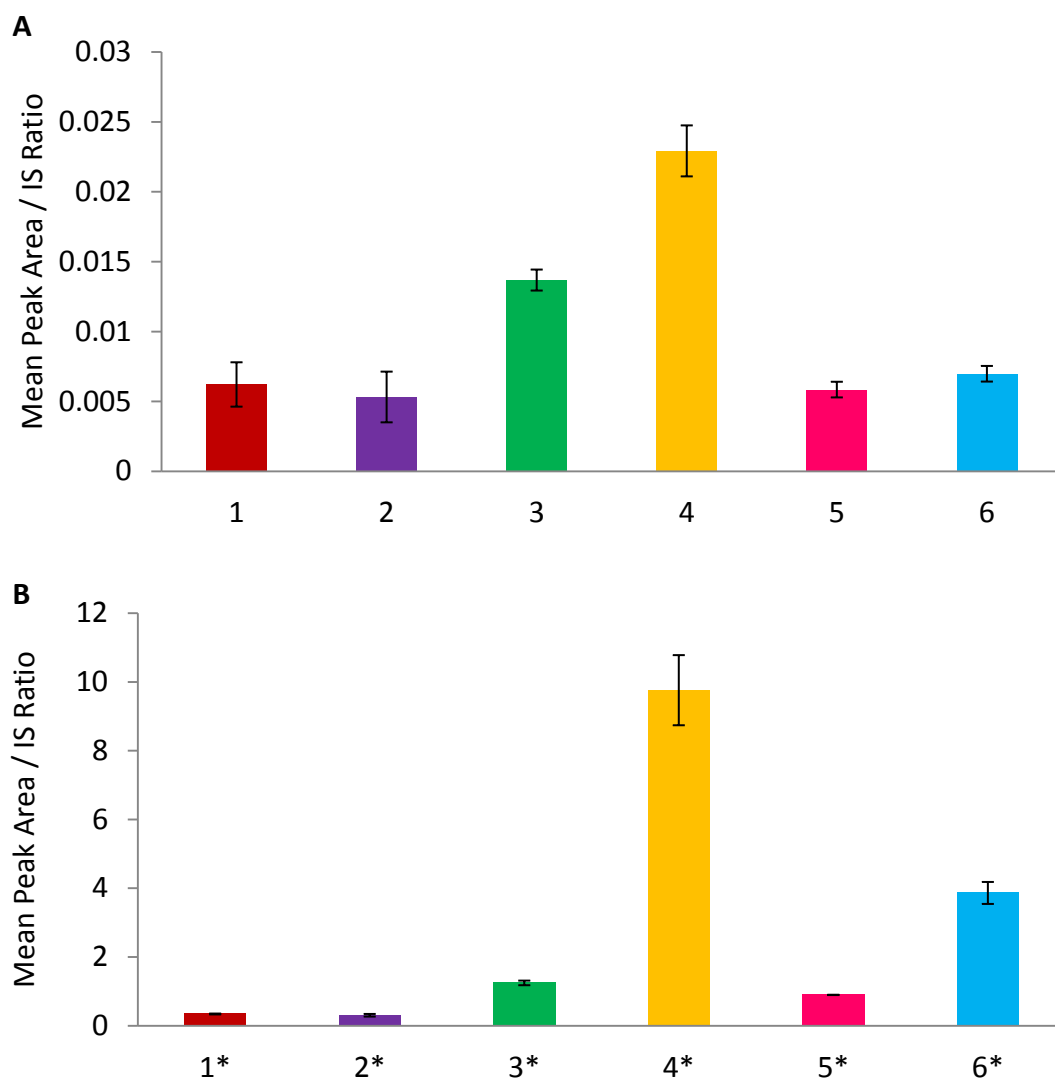


Figure 3.8: LC-MS/MS analysis of late exponential phase cultures revealed MTA levels increase with expression of the AHL synthases, which is emphasised by removal of the Pfs enzyme which metabolises MTA in MG1655. (A) Intracellular accumulation of MTA as determined by LC-MS analysis in three *E. coli* strains MG1655[pME6032] (1, 2), MG1655[pME-*lasI_{Pa}*] (3, 4) and MG1655[pME-*rhlI_{Pa}*] (5, 6) grown in LB with (2, 4, 6) and without (1, 3, 5) IPTG induction. (B) Quantification of MTA levels in MG1655 Δ *pfs* are indicated by asterisks alongside an identical numbering system. Peak area corresponding to MTA was divided by the peak area of the appropriate internal standard for normalisation.

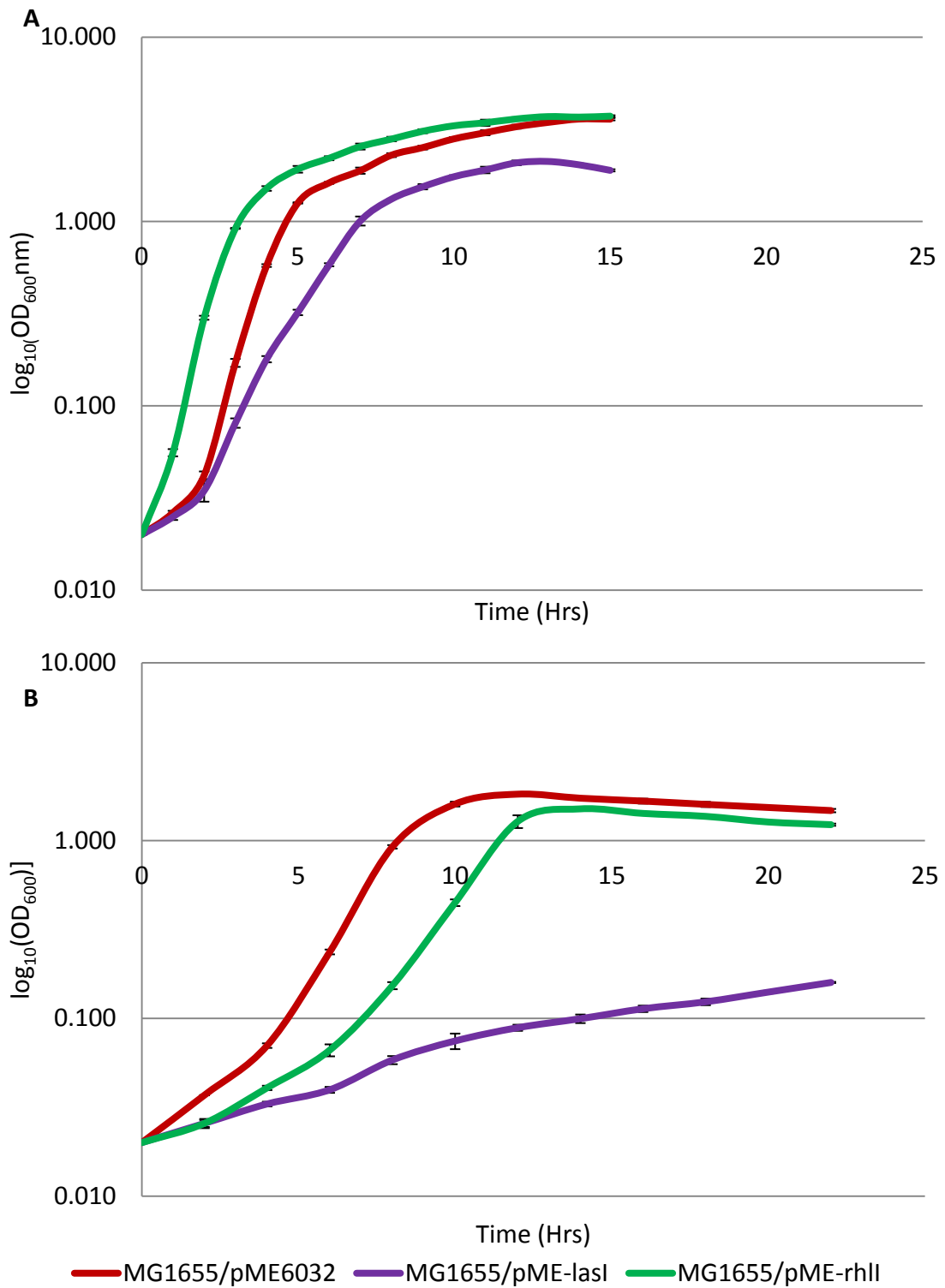


Figure 3.9: Introduction of the AHL synthase genes into MG1655 results in a growth defect that is more apparent in defined media. Three strains MG1655[pME6032], MG1655[pME-*lasI*_{Pa}], and MG1655[pME-*rhlI*_{Pa}] were inoculated into 125 ml LB (A) or MOPS minimal media (B), IPTG induced and grown shaking at 37°C in 500 ml-Erlenmeyer flasks. 1 ml samples were taken at regular intervals and measured with a spectrophotometer. The cell density (OD_{600}) is plotted against time.

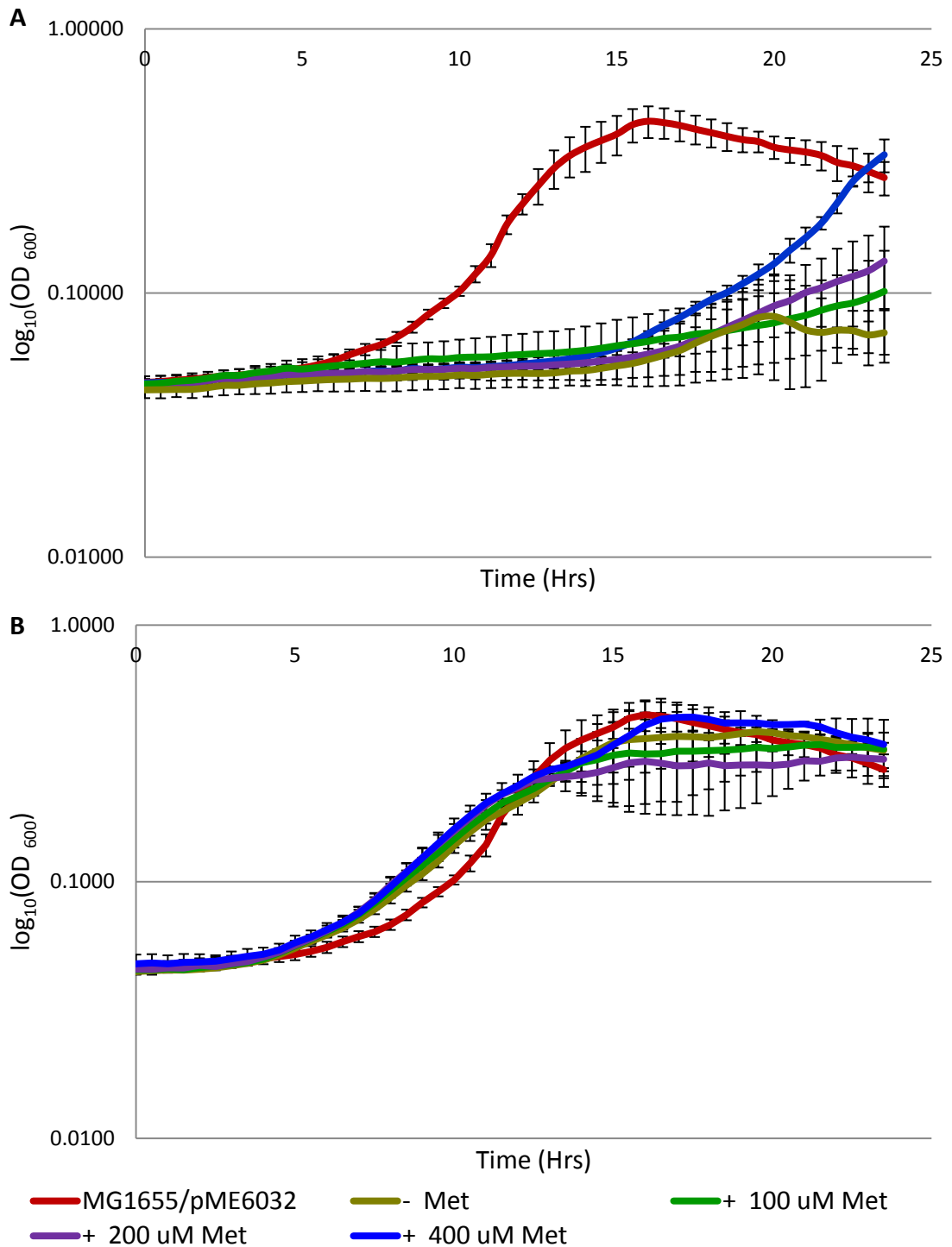


Figure 3.10: Exogenous methionine addition improves growth of MG1655[pME-*lasI_{pa}*] and has no effect on MG1655[pME-*rhlI_{pa}*] in MOPS minimal media. MG1655[pME6032], MG1655[pME-*lasI_{pa}*] (A) and MG1655[pME-*rhlI_{pa}*] (B) were inoculated into MOPS minimal media and methionine was added to those cultures indicated at the point of set up of the experiment. Strains were grown in an automated spectrometer (TECAN Infinite F200) and changes in cell density (OD_{600}) were monitored at 30°C every 30 min. For each single experiment, the strain was grown in triplicate and the average shown.

3.11 Discussion

The AMC plays a fundamental role in all living organisms. It functions as an important SAH-degradation pathway that reduces feedback inhibition of important SAM-dependent methylation reactions. In other words, it ensures the constant availability of SAM, thus allowing the continuation of normal metabolic processes. Simultaneously, this reaction also relieves any inhibitory effects caused by the accumulation of MTA. In *Pseudomonas*, SAM has another role; it additionally functions as a substrate for polyamine spermidine synthesis, providing valuable carbon and nitrogen sources and potential protection of DNA from oxidative stress. Furthermore, SAM radical enzymes have been shown to be important in production of vitamins, metabolites and antibiotics and the effective MTA/SAH nucleosidase ensures removal of inhibitory product 5'-deoxyadenosine (5'dADO). As well as SAM, other components of the AMC have alternative metabolic functions; in particular, methionine is an AA which is needed for protein synthesis. It is inevitable therefore that the repercussions of any AMC-associated alterations will somewhat stimulate compensatory pathways to counterbalance the perturbations. To investigate this, the implications of disrupting the AMC have been studied by assessing the independent effects of the AHL synthase genes upon this cycle in the context of an *E. coli* background.

Introduction of the *P. aeruginosa* PA01 AHL synthase genes into *E. coli* MG1655 led to the intended expression of the proteins and production of the corresponding signal molecules. Actual abundant concentrations of OC₁₂-HSL and C₄-HSL were confirmed upon LC-MS/MS based AHL profiling of the *lasI_{Pa}* and *rhlI_{Pa}* expression systems in *E. coli*, respectively. Furthermore, the identification of OC₁₀-HSL and OC₁₄-HSL in association with *lasI_{Pa}* was no surprise, given that these are additionally characteristic of the *P. aeruginosa* system. The remaining AHLs were novel to the *E. coli* background (Gould *et al.*, 2006). Gould *et al.* (2006) reported remarkable differences between AHL production profiles between *lasI_{Pa}* expression in *P. aeruginosa* and *E. coli*. However, the methods chosen for mass spectrometric analysis were focused on the AHL OC-series

and did not identify the fuller spectrum of AHL production included in the analysis described here, which revealed production of C₁₂-HSL and C₁₄-HSL. The overall differences, however, can be attributed to the allowance of the LasI active site to accommodate a larger repertoire of acyl-ACPs substrates; crystallisation of this enzyme has demonstrated that the shape of the acyl chain binding site is tunnelled, placing no limitation on the length of the acyl chain exploitable for the synthetic reaction. Hence, a variation in the proportion of acyl-ACP substrates and/or the availability of alternatively sized acyl-ACPs pools in the heterologous host allows for recombinant LasI to be able to produce a different AHL distribution. Ultimately, under these environmental circumstances, AHLs from the preferential acyl-ACPs will be produced initially, as they offer the most kinetically efficient choice, then others at sufficiently high concentrations will be utilised, given their favourability to the K_m values for the enzyme; this is evident by signal distribution being skewed by AHLs of the OC-series. Obviously, this will vary in any particular cell throughout the duration of the growth cycle and be heavily dependent on the temporal metabolic status. For example, the importance of FabG, which is central to the fatty acid biosynthesis pathway, in facilitating acyl-ACP elongation, allows for a much larger substrate repertoire (Hoang *et al.*, 2002). In contrast, the observance of a smaller spectrum of AHLs with recombinantly expressed *rhII_{Pa}* indicates the more restrictive nature of the acyl-ACP binding pocket, giving the enzyme a much higher intrinsic specificity.

AHL production was accompanied by a growth defect for MG1655 harbouring the *lasI_{Pa}* gene in rich and defined media. In contrast, *rhII_{Pa}* had a less detrimental effect on fitness causing only a slight extension to the length of the lag phase in MOPS minimal media. One possible explanation for the compromised cell fitness could be the production and accumulation of a foreign protein that may be partly aggregating or imposing a drain on transcriptional and/or translational machineries. Alternatively, the defective growth patterns could be the result of an adverse response to the unusual signalling molecule types synthesised by the expressed synthases. Moreover, and in relation to the latter, the altered growth could be accounted for by the disruption to metabolism, specifically

demonstrated here by the reduction in intracellular concentrations of the metabolites of the AMC. The available pool of SAM is redistributed upon introduction of the AHL synthase genes to accommodate production of AHLs; this equates to a reduced availability for the continuation of normal cellular processes and homeostatic functions such as methylation reactions. Methylation directed by methyltransferases represents a fundamental epigenetic inheritance mechanism that plays an important role in cell survival through the regulation of transcriptional gene expression and the prevention of death (Hartwell *et al.*, 2004); this primarily occurs following DNA replication and could explain the inability to maintain comparative growth rates. Methylation additionally affects RNA and proteins and could therefore affect the availability of methionine for synthesis of proteins. This seems like a feasible explanation given that supplementation with exogenous methionine helps to restore growth although not completely back to the phenotype of that of the WT. Full complementation may only be achievable in circumstances where balanced substitutions are provided for both SAM and the corresponding fatty acyl chains, thus compensating for the substrates directed towards AHL production.

AI bioassays with *Vibrio harveyi* illustrated reduced levels of AI-2 in stationary phase culture supernatants of MG1655[pME-*lasI_{pd}*] and MG1655[pME-*rhII_{pd}*]. This may again relate to the reductions in intracellular concentrations of metabolites across the AMC profile; lower levels of SAM, and in turn SAH translate to a reduced availability of the LuxS substrate, SRH, needed to provide 4,5-dihydroxy 2,3-pentanedione (DPD), the precursor to AI-2. Decreased AI-2 concentrations could additionally be the result of lower metabolite levels and reflect the organism's controlled uptake in association with processing and/or degradation of this 5 carbon compound for catabolism (Winzer *et al.*, 2002). Consistent with early and mid-exponential growth, a prolonged period during which the requirement for SAM is elevated and flux through the activated methyl cycle is maximal, it is necessary to remove the increasing amounts of AI-2 into the extracellular environment (Winzer *et al.*, 2002). This is thought to prevent the build up of the toxic SAH metabolite intracellularly. SAH is structurally and biochemically similar to the MHF

and DMHF compounds, both of which have DNA-damaging and potentially mutagenic properties (Winzer *et al.*, 2002). The toxicity of SAH provides an alternative explanation to signal molecule accumulation beyond a threshold level consistent with a mechanism of monitoring population density (Winzer, Hardie, & Williams 2002). However, during late exponential phase, the transition to stationary phase and stationary phase itself, AI-2 concentrations decrease, reflecting controlled uptake in association with catabolism. The build up of AI-2 activity in stationary phase culture supernatants has been described by the term GRAIL (Glucose Retention of AI-2 Levels) (Surette & Bassler 1998; Surette & Bassler 1999; Hardie *et al.*, 2003). In *E. coli* and *Salmonella typhimurium*, reductions in AI-2 activity appear to be associated with the absence of a preferential carbon source; this effect has primarily been observed with glucose, but is also consistent with other carbohydrate monomers such as glycerol, maltose and galactose, suggestive of a “catabolite repression”-like effect (Hardie *et al.*, 2003). Therefore, in these circumstances, lower levels of AI-2 could correlate with its degradation to maintain normal cellular processes and homeostatic functions. From a metabolic perspective, this can also be viewed as an advantageous mechanism in that the loss of a single ‘ribose equivalent’ per methylation reaction is expensive, and so is minimised effectively via degradation at an alternative, metabolically ‘less stressful’ time (Winzer *et al.*, 2002). Under the circumstances of AHL synthase gene expression, energy demands may be prioritised for signal production and the energy requirement for AI-2 catabolism becomes of secondary importance. It might be interesting to investigate whether there is a difference in ATP utilisation/availability throughout the growth of the three strains. Alternatively, reduced AI-2 activity may be due to the unexpected transcriptional and/or translational effects of the synthase upon the LuxS enzyme in a way which means it functions less effectively. Feasible aspects of posttranscriptional regulation which could be affected include indirect global regulator, CRP and/or the CRP-activated small non-coding regulatory RNA, CyaR, the latter of which has been shown to directly negatively regulate the translation of *luxS* and decrease AI-2 production (Wang *et al.*, 2005; De Lay & Gottesman 2009). In addition, in *Edwardsiella tarda*, disruption of *luxS* expression by antisense RNA interference (constitutive transcription of *luxS* antisense RNA: corresponding to the

region between positions 149 and -65 relative to the translational start) lowered the level of AI-2 activity; this target therefore offers an alternative explanation for the altered AI-2 levels observed with recombinant AHL synthase expression (Zhang, Sun & Sun 2008). The expression of *lasI* and *rhII* may adversely affect the import and processing of AI-2 by its ABC transporter designated the Lsr transporter, the operon of which contains seven genes, *lsrACDBFGE*, and is itself *luxS* regulated (Taga, Semmelhack & Bassler 2001). In association with this *lsrK* and *gfpD*, encoding the AI-2 kinase and the glycerol-3-phosphate dehydrogenase have been shown to regulate AI-2 internalization by affecting transcription of the *lsr* operon (Xavier & Bassler 2005). To discount some of these possibilities, future investigations might involve performing a comparative microarray analysis of MG1655 comprising the empty vector, those comprising the synthase gene constructs and possibly even the constructs transferred to a *luxS* mutant, though this might introduce other complications.

AHL synthesis is accompanied by the production of MTA and levels were determined. Independent experiments to monitor MTA levels produced variable results, often different patterns in the levels observed between strains or larger error bars causing insignificant results. MTA levels were therefore confirmed in a Δpfs strain in which MTA could accumulate. This led to higher overall levels of MTA and this can be accounted for by metabolite production as a result of normal intracellular processes and its accumulation due to an inability to convert it MTR; nonetheless, this increase affects all the conditions being tested equally. MG1655 containing recombinant AHL synthases increased intracellular MTA levels, with *lasI_{Pa}* causing a significantly higher increase compared to *rhII_{Pa}*. This may relate to the larger distribution of AHLs associated with *lasI_{Pa}*.

Overall, it is apparent and interesting that LasI affected AMC profiles, MTA levels and AI-2 production more severely than RhII. This may be due to the larger repertoire of AHLs made by LasI.

Chapter 4

Analysis of the metabolic implications of the *P. aeruginosa* AHL synthase genes by site-directed mutagenesis

4.1 Introduction

The results presented in the previous chapter demonstrate that the *P. aeruginosa* AHL synthases cause significant AMC-related metabolic disturbances and in-turn these cause other aspects of metabolism and fitness to be compromised. To determine the relationship between the extent of metabolic modulation and the specific activity of the AHL synthases, site-directed mutagenesis was performed using existing knowledge of crystal structures and the role of specific residues of these considerably homologous enzymes. By altering the specificity of the active site with the aim of modulating substrate binding and thus creating differing AHL profiles, the consequential metabolic repercussions could be assessed.

4.2 Identification of important residues of LasI and RhlI

LasI and RhlI belong to a larger superfamily of AHL synthase proteins which are homologues of LuxI. To date, more than 40 AHL synthases have now been characterised. These enzymes share four blocks of signature sequence with an average of 37% identity and eight absolutely conserved residues associated with each block. (Fuqua, Winans & Greenberg 1994, Watson *et al.* 2002). Overall, LasI and RhlI demonstrate 30% identity and this has been illustrated using the characterised crystal structure of LasI which was published in 2004 by Gould, Schweizer & Churchill (Figure 4.1). A crystal structure for RhlI remains undetermined.

From the crystal structure of EsaI, an AHL synthase of *Pantoea stewartii*, it was predicted that several essential conserved residues including Arg23, Phe27 and Trp33 were highly mobile and stabilized via a conformational change caused by substrate binding (Watson *et al.* 2002). Through determination of the LasI structure, it has been shown that Phe27 and Trp33 are important for the N-terminal SAM binding pocket (Gould, Schweizer & Churchill 2004).



Figure 4.1: *P. aeruginosa* RhlI AA homology with the crystal structure of LasI. The conserved AA residues shared between LasI and RhlI have been highlighted in yellow in the LasI ribbon model.

In addition, Trp33 contributes structurally to the acyl-chain tunnel and may assist in correctly orientating the acyl-chain for catalysis. Arg23, on the other hand, participates in an N-terminal core electrostatic cluster of residues and is thought to be fundamental to the synthetic reaction (Gould, Schweizer & Churchill 2004). Furthermore, using random and site-directed mutagenesis, Parsek, Schaefer, & Greenberg (1997) demonstrated the importance of several residues in RhII including those mentioned above. The serine at position 103 represents another well conserved residue and may be critical for substrate binding and amide bond formation (Parsek, Schaefer, & Greenberg 1997). Due to the conservation of AA residues between LasI and RhII, these were chosen for the following mutagenesis studies. In a first round of mutagenesis, those RhII site-directed mutants (SDMs) of interest from the study by Parsek, Schaefer, & Greenberg (1997) were replicated and the equivalent SDMs constructed in LasI. A second round of mutagenesis was then undertaken based on the findings from the initial batch. Their locations amongst the protein sequences and the nucleotides substituted in the *lasI_{Pa}* and *rhII_{Pa}* genes have been summarised in Table 4.1.

4.3 Predicting a model for the structure of RhII

The predictive modelling has been performed by Abigail Emtage and was determined as follows. The primary sequence of the RhII protein was retrieved from the NCBI protein sequence database (RHII_PSEAE; <http://www.ncbi.nlm.nih.gov/protein/12230962>) in FASTA format. Modeller version 9v7 was then used according to standard protocols (Sali & Blundell 1993, Sanchez & Sali 2000, Eswar *et al.* 2007) to search the protein data bank for homologues with known atomistic 3D structures. The results were used to produce a list of the best potential templates for constructing the RhII model. The protein data files were downloaded for the top matches from the protein data bank (PDB); these were the *P. aeruginosa* LasI synthase (PDB ID: 1RO5) and *P. stewartii* EsaI synthase (PDB ID: 1KZF), which have 30% and 22% identity with the RhII protein sequence respectively. The 1RO5 and 1KZF template structures were aligned and the template RhII sequence was aligned with the templates to visualise the resulting output alignment.

AA Position	AA Encoded	WT DNA Seq	Mutant AA	Mutant DNA Seq
A <i>lasI_{Pa}</i>				
23	R	CGT	W ^b	TGG
27	F	TTC	L ^a	CTG
		TTC	Y ^b	TAC
33	W	TGG	G ^a	GGC
103	S	AGC	A ^b	GCC
		AGC	E ^a	GAA
		AGC	V ^b	TGC
B <i>rhlI_{Pa}</i>				
28	F	TTC	L ^a	CTG
		TTC	Y ^b	TAC
34	W	TGG	G ^a	GGC
103	S	TCG	A ^b	GCC
		TTC	E ^a	GAG
		TTC	V ^b	GTG

Table 4.1: Nucleotide substitutions for AA chosen for mutagenesis within the *P. aeruginosa* AHL synthase genes. Nucleotides substitutions leading to mutagenesis in *lasI_{Pa}* (A) and *rhlI_{Pa}* (B) have been highlighted in red.

^a Based on structural knowledge and previous studies.

^b Refined choices following findings from ^a.

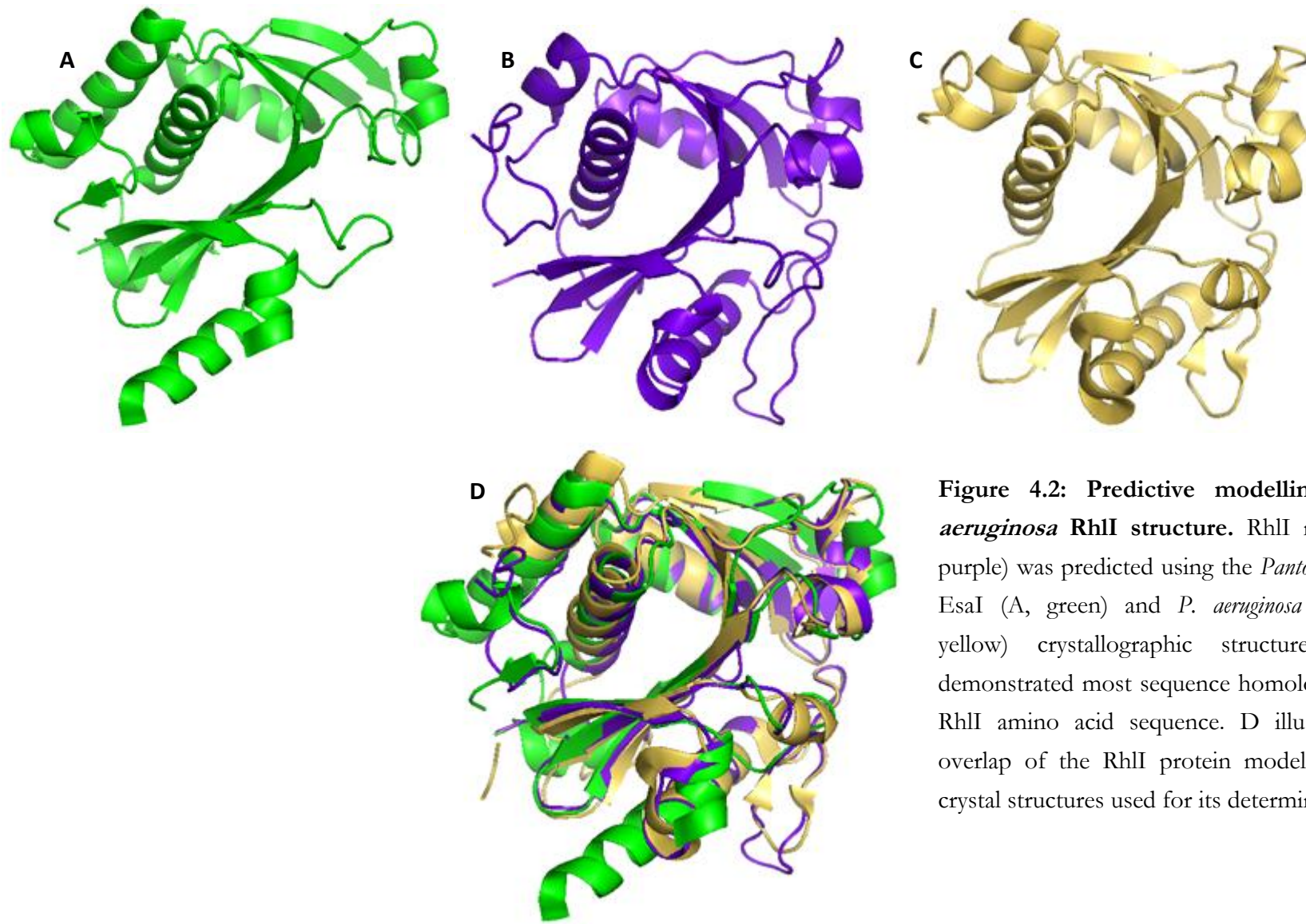


Figure 4.2: Predictive modelling of *P. aeruginosa* RhlI structure. RhlI model (B, purple) was predicted using the *Pantoea stewartii* EsaI (A, green) and *P. aeruginosa* LasI (C, yellow) crystallographic structures which demonstrated most sequence homology to the RhlI amino acid sequence. D illustrates an overlap of the RhlI protein model with the crystal structures used for its determination.

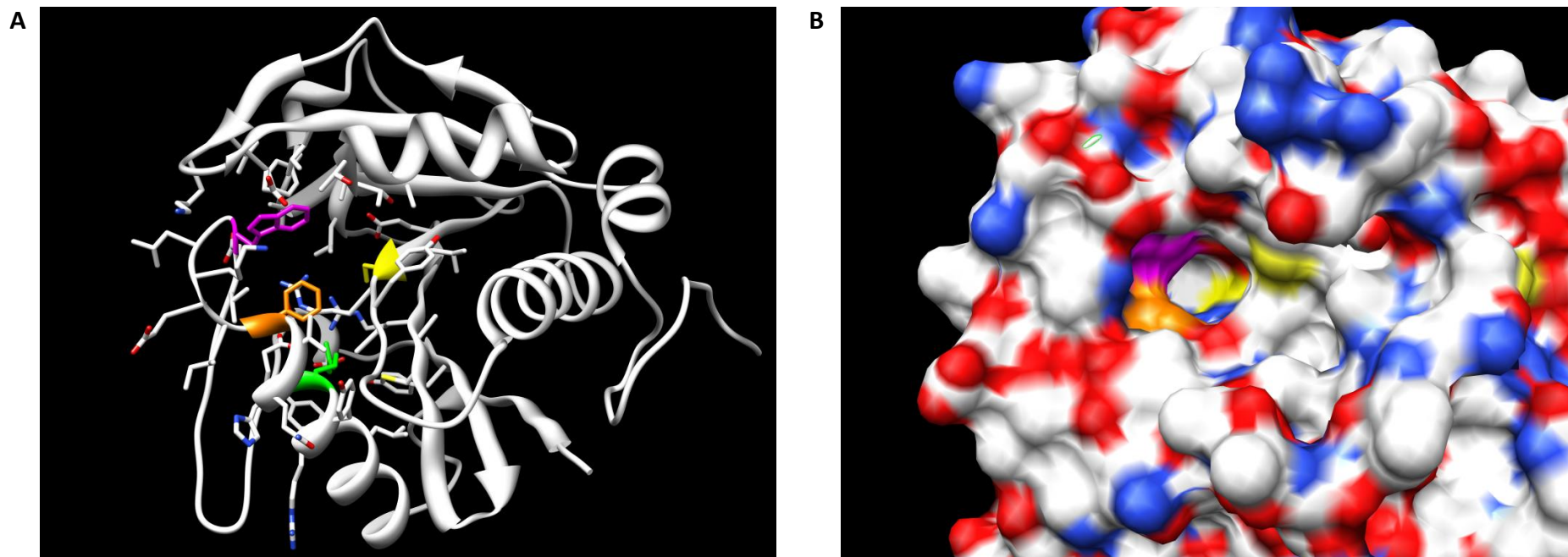


Figure 4.3: The proposed structure of RhlI gained from predictive modelling. Ribbon (A) and hydrophobicity (B) models of one of 5 of the predicted models for RhlI. The location of the conserved residues selected for mutagenesis are indicated in various colours and are as follows: R23: green, F28: orange, W34: magenta and S103: yellow.

This was used to create five output models, the average of which has been shown in Figure 4.2 alongside the AHL synthase crystal structures upon which the model has been based. Chimera was used for visualisation of the models, looking particularly at the location of the residues chosen for mutation within the suspected substrate binding pocket (Figure 4.3).

4.4 Generation of SDMs in *LasI* and *RhlI*

Having chosen some important residues involved in the catalysis of AHL synthesis by *LasI* and *RhlI*, a variation of a commercially available method of site directed mutagenesis developed by Finnzyme (Finland) was exploited.

4.4.1 Design of mutagenic primers

Mutagenic primers were designed to replace specific residues with alternative ones. To incorporate the desired AA substitutions, single, double or triple base mutations were incorporated into the mutagenic primers, creating mismatches which would create the alternative residue following transcription and translation. This primer was designed to allow at least 10 bp flanking the mutagenic site for the PCR amplification. The strategy employed additionally required an alternate primer which was non-mutagenic for each site. The non-mutagenic primer was designed to flank the mutagenic one on the opposite strand resulting in the correct sequence for the remaining template to be amplified. For each single AA substitution, both sets of primers were phosphorylated at the 5' ends to eliminate the need for a separate phosphorylation step following PCR amplification prior to the ligation process.

4.4.2 PCR amplification of *LasI* and *RhlI* with single codon substitutions

The reverse PCR reactions for site directed mutagenesis exploited previously prepared cloned constructs of the *lasI* and *rhlI* genes in the pGEM-T Easy vector (pGEM-*lasI*_{pa} and pGEM-*rhlI*_{pa}) to provide the template. For each mutation, a PCR product was purified

corresponding to a linear fragment comprising the mutant AHL synthase gene and the pGEM-T Easy cloning vector.

4.4.3 Selection and confirmation of site directed mutagenesis of LasI and RhII

The linear PCR fragments generated from the reverse PCR were ligated to form a circularised vector product and immediately transformed into the transient host strain *E. coli* DH5 α . Screening was initially performed via PCR, and subsequently DNA sequencing to confirm the presence of the desired base substitutions for each of the mutant *lasI* (pGEM-*lasI*_{pa}: R23W; pGEM-*lasI*_{pa}: F27L; pGEM-*lasI*_{pa}: F27Y; pGEM-*lasI*_{pa}: W33G; pGEM-*lasI*_{pa}: S103A; pGEM-*lasI*_{pa}: S103E and pGEM-*lasI*_{pa}: S103V) and *rhII* (pGEM-*rhII*_{pa}: F28L; pGEM-*rhII*_{pa}: F28Y; pGEM-*rhII*_{pa}: W34G; pGEM-*rhII*_{pa}: S103A; pGEM-*rhII*_{pa}: S103E and pGEM-*rhII*_{pa}: S103V) genes in pGEM-T Easy.

4.4.4 Subcloning of mutant AHL synthase genes for overexpression

As previously with the cloning of *lasI*_{pa} and *rhII*_{pa}, the inserts were released from their respective constructs in the pGEM-T Easy vector in a double digestion reaction with *MfeI* and *StuI*, as was the multiple cloning site of pME6032. Directed ligation of the two, produced the corresponding constructs in pME6032 comprising the *lasI* (pME-*lasI*_{pa}: R23W; pME-*lasI*_{pa}: F27L; pME-*lasI*_{pa}: F27Y; pME-*lasI*_{pa}: W33G; pME-*lasI*_{pa}: S103A; pME-*lasI*_{pa}: S103E and pME-*lasI*_{pa}: S103V) and *rhII* (pME-*rhII*_{pa}: F28L; pME-*rhII*_{pa}: F28Y; pME-*rhII*_{pa}: W34G; pME-*rhII*_{pa}: S103A; pME-*rhII*_{pa}: S103E and pME-*rhII*_{pa}: S103V) mutant genes. PCR of potential Tc resistant clones confirmed the presence of either of the gene sequences and hence successful constructs. Sequencing was repeated for final confirmation. The successful clones were subsequently used for transformation into electrocompetent *E. coli* MG1655.

4.5 Analysis of the synthase activity of each SDMs in MG1655

As with the WT AHL synthase genes, AHL production was tested in the first instance using strain overlay plates to identify whether any of the SDMs of *lasI_{Pa}* and *rhlI_{Pa}* gave rise to functional proteins with enzymatic activity (Figure 4.4). Using the corresponding synthetic AHL standard and WT AHL synthase constructs as positive controls and the empty vector construct as the appropriate negative control, it was possible to identify those SDM still capable of producing AHLs and those null of any identifiable synthase activity. For SDM of *lasI_{Pa}*, the bioassay demonstrated MG1655 harbouring constructs pME-*lasI_{Pa}*: F27L; F27Y and S103A to be positive for AHL production whilst those carrying pME-*lasI_{Pa}*: R23W; W33G; S103A and S103V were devoid of detectable AHL production. In contrast, two SDMs of *rhlI_{Pa}*, pME-*rhlI_{Pa}*: S103A and S103V screened positive for production of short-chained AHLs whilst the others did not (pME-*rhlI_{Pa}*: F28L; F28Y; W34G and S103E).

4.6 LC-MS/MS profiling of AHLs produced by SDMs of *lasI_{Pa}* and *rhlI_{Pa}* in MG1655

A full spectrum AHL profiling was performed to identify whether the AHL repertoire and absolute levels produced by the SDMs were similar to those demonstrated by expression of *lasI_{Pa}* and *rhlI_{Pa}* in MG1655. LC-MS/MS confirmed the lack of AHL production with MG1655 strains harbouring the SDM *lasI_{Pa}* constructs: pME-*lasI_{Pa}*: R23W; W33G; S103A; S103V (Figure 4.5B) and *rhlI_{Pa}* constructs: pME-*rhlI_{Pa}*: F28L; F28Y; W34G and S103E (Figure 4.5D). Interestingly, the remaining AHL producing SDMs of *lasI_{Pa}* each demonstrated differing QSSM profiles. The overall QSSM profile resulting from the *lasI_{Pa}*: F27L was severely reduced compared to *lasI_{Pa}*; there was a significant 93% decrease in the cumulative AHL concentration (Figure 4.5B) and amongst the six AHLs profiled, OC₁₂-HSL and OC₁₄-HSL were observed as the dominant signals, accounting for 62% and 29% respectively (Figure 4.5A), hence

changing the proportions of the AHLs observed compared to *lasI_{Pa}*. In contrast, the *lasI_{Pa}*:F27Y mutation did not have much effect on the resulting AHL profile; the overall QSSM concentration and individual AHL proportions were similar to those demonstrated by the unaffected *lasI_{Pa}* gene. The *lasI_{Pa}* S103A mutation additionally illustrated an AHL profile similar to *lasI_{Pa}* and the *lasI_{Pa}*:F27Y mutation with one significant difference. Under these circumstances, C₄-HSL is heavily produced and represents the second dominant signal in the entire profile after OC₁₂-HSL, accounting for 20% of the total profile. With the QSSM producing SDM of *rhII_{Pa}* (pME-*rhII_{Pa}*: S103A and S103V), the overall AHL profile is similar to *rhII_{Pa}* (Figure 4.5C), with the S103V mutation causing a reduction in AHL production by approximately 200 μM.

4.7 Variable stability of synthase proteins from site-directed mutagenesis of *lasI_{Pa}* and *rhII_{Pa}*

The production of a stable synthase protein was imperative to its functional activity especially in the heterologous host and the subsequent metabolic repercussions as shown in the previous chapter. It was therefore an important step to determine whether the substituting residues chosen for mutagenesis gave rise to stable protein products. As previously, detection of *lasI_{Pa}* SDM was performed via SDS-PAGE and *rhII_{Pa}* SDM via Western blotting. In most cases, the detection method confirmed production of a protein approximately corresponding to 26 kDa (Figure 4.6). These were present only in lanes correlating to IPTG induced cultures. In the majority of these instances, the abundant protein of interest was accompanied by a less abundant protein migrating slightly above. In order to clarify the secondary protein was unrelated to the synthase, MALDI fingerprint analysis was exploited for sequencing of the two closely migrating proteins in one randomly chosen mutant: MG1655[pME-*lasI_{Pa}*: F27L]. The slower migrating protein gave rise to some overall non-confident matches of hypothetical proteins, whilst the slightly faster, lower band was confirmed to match the “autoinducer synthesis protein LasI (*P. aeruginosa* PA01)”.

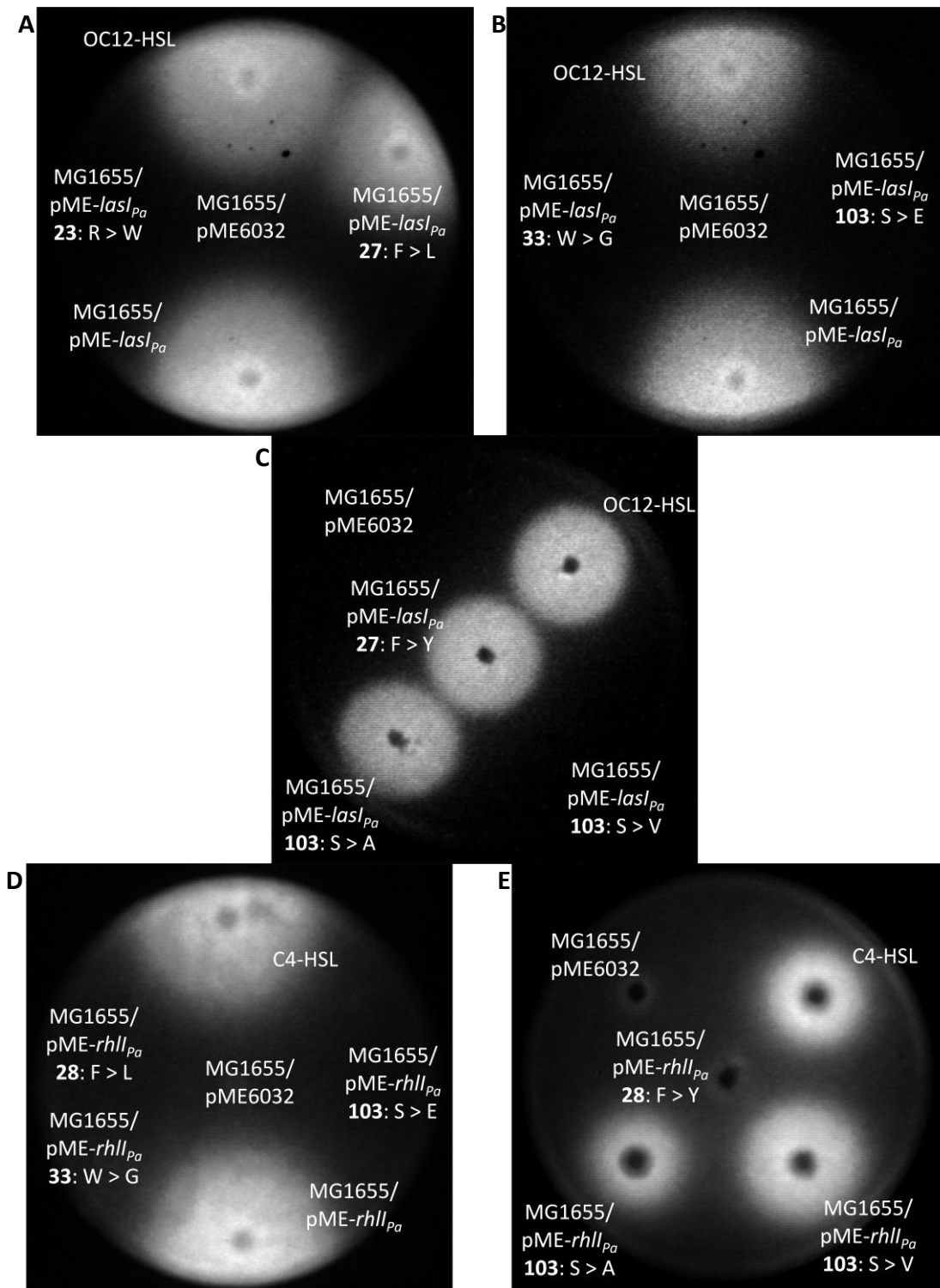
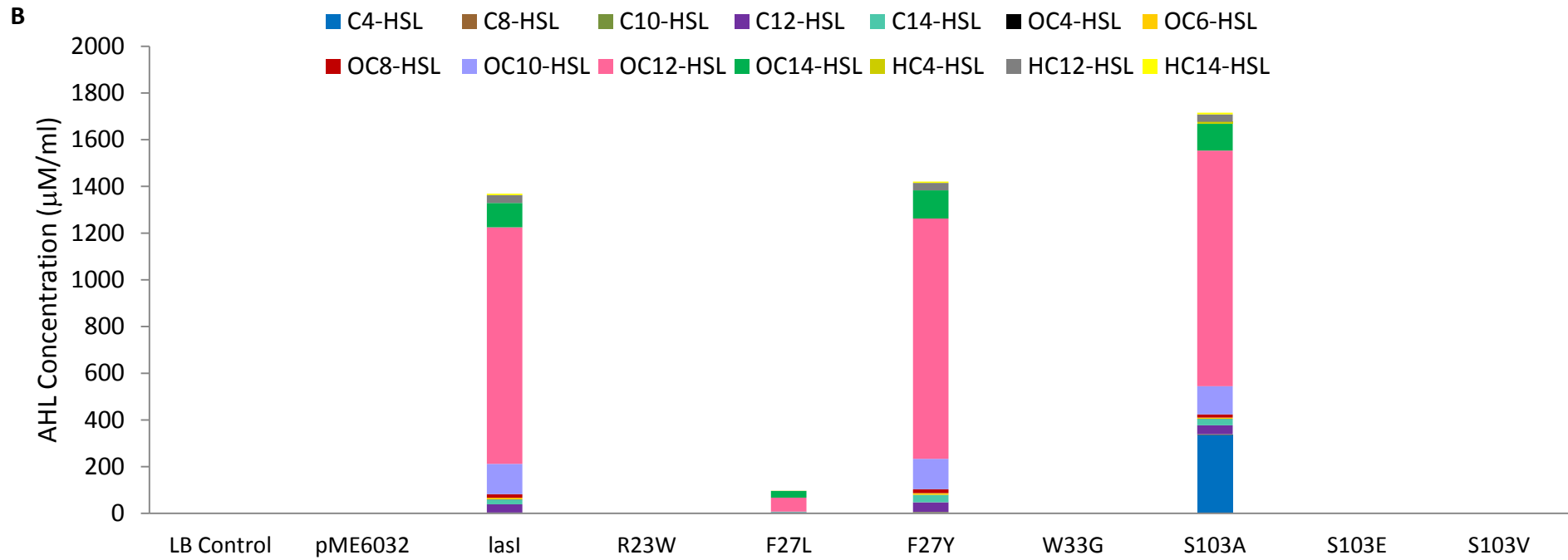
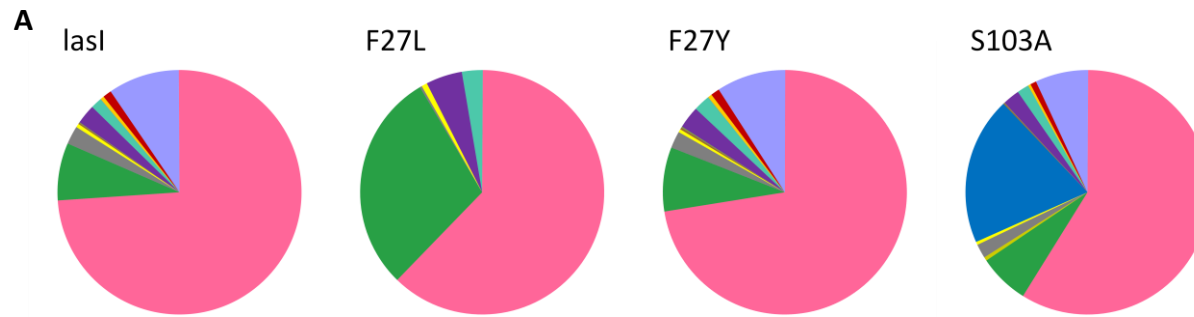


Figure 4.4: SDMs of *lasI*_{pa} and *rhII*_{pa} produce differing levels of OC₁₂-HSL and C₄-HSL. Strain overlay plates of MeOH extracts of MG1655[pME6032], WT and SDM AHL synthase genes grown with IPTG induction in LB to late exponential phase. A, B and C have been overlaid with JM109[pSB1142], responding to long-chain AHLs, whilst D and E with JM109[pSB536], which luminescence in response to short-chain AHLs. AHL production occurs with *lasI* (pME-*lasI*_{pa} **27: F > L**; **27: F > Y** and **103: S > A**) and *rhII* (pME-*rhII*_{pa} **103: S > A** and **103: S > V**) mutants.



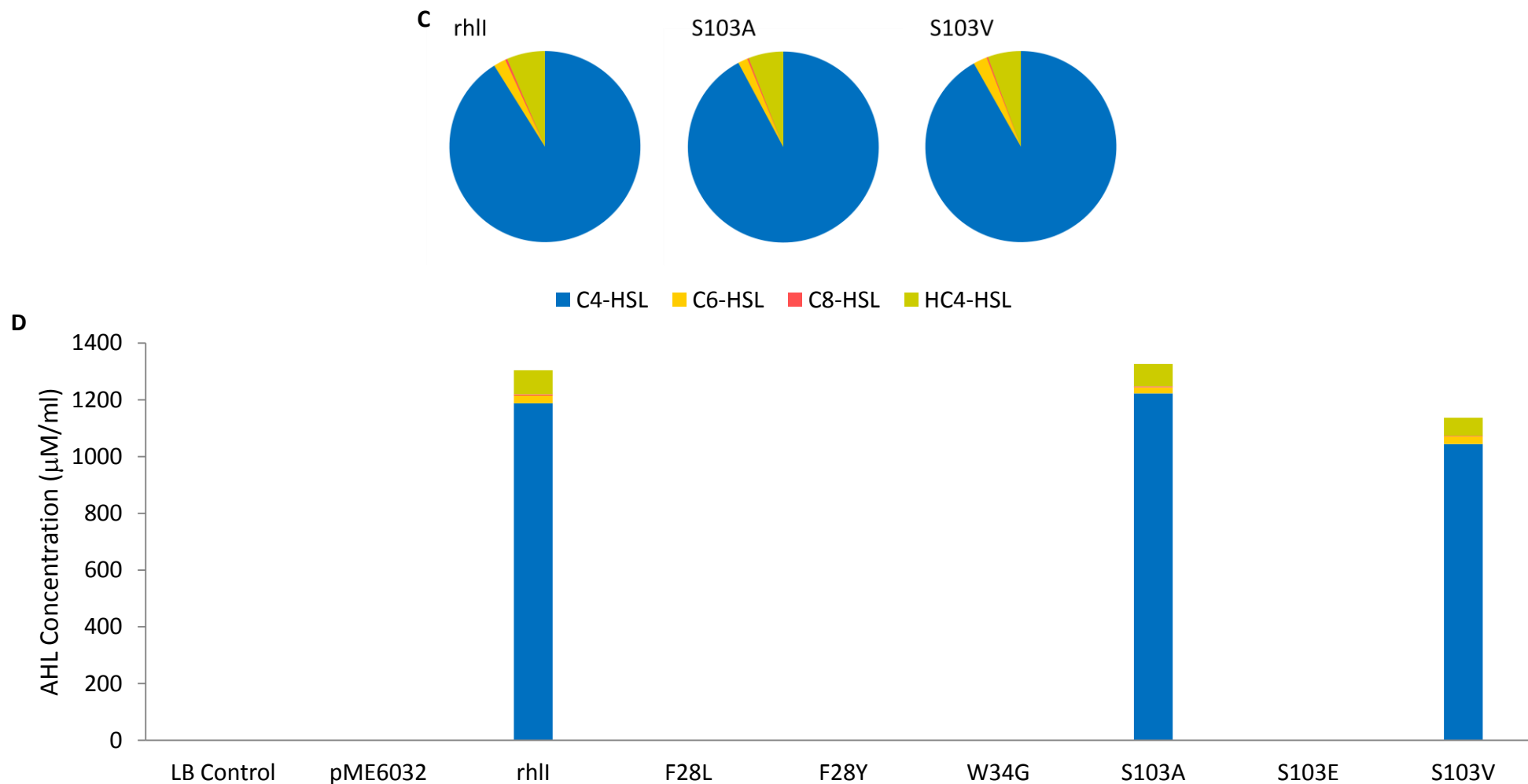


Figure 4.5: Relative molar proportions and cumulative profiling of AHLs produced by SDMs of *lasI_{pa}* and *rhII_{pa}* in *E. coli*. Compounds were extracted from late exponential phase supernatants with acidified ethyl acetate and profiled by LC-MS/MS analysis. (A) and (C) The ratio between the different signalling molecules present in supernatants is represented by pie charts for *lasI_{pa}* (A) and *rhII_{pa}* (C) SDM producing AHLs. (B) and (D) The actual concentration of AHLs for *lasI_{pa}* (B) and *rhII_{pa}* (D) SDMs.

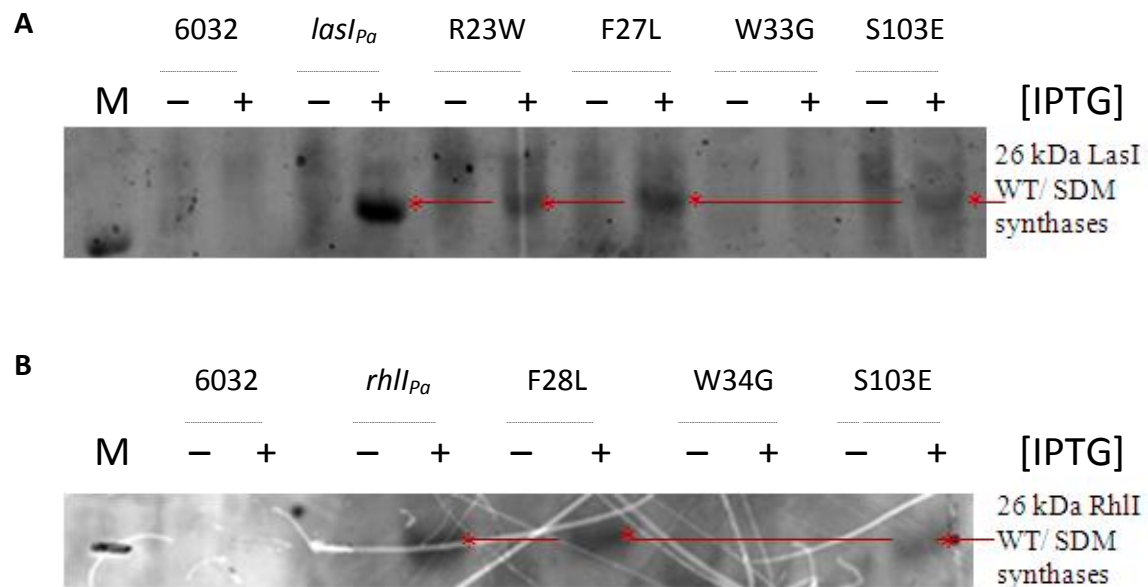


Figure 4.6: The majority SDMs of *lasI_{pa}* and *rhlI_{pa}* lead to the production of a stable protein in *E. coli* MG1655. *E. coli* MG1655 alone [pME6032] or containing pME-*lasI_{pa}* (LasI), pME-*rhlI_{pa}* (RhlI) or pME6032 harboring a SDMs of either gene were grown in LB to OD₆₀₀=0.5 and induced with (+) IPTG or not (-). After approximately 1 h, whole cell extracts were prepared and separated through 12% SDS-PAGE gels which were subjected to Coomassie staining (A) or Western blotted using α RhlI (B). SDS-PAGE reveals the presence of the 26 kDa protein (*) in lysates of the IPTG induced *lasI_{pa}* WT and SDMs except for the substitution of W33G. Similarly, IPTG induction of *rhlI_{pa}* SDMs leads to the expression of stable synthase proteins (26 kDa) (*) except for the W34G mutation. M indicates the lane of the size marker.

There was however, one exception. With both *lasI_{P_a}* and *rhII_{P_a}*, it was not possible to visualise a recombinant protein associated with the mutation at residue 33/34: W > G.

4.8 AMC metabolite profiles of *lasI_{P_a}* and *rhII_{P_a}* SDMs

In section 3.6, we confirmed that the AHL synthases cause significant disturbances to the homeostatic maintenance of metabolites of the AMC. It was therefore interesting to determine whether the production of AHLs from the mutant versions of the AHL synthase genes had any different effects on the metabolites through the AMC. Figure 4.7 shows the metabolic change expressed as a percentage for each mutant relative to the WT *E. coli* strain possessing the empty vector. Two mutants of each of the AHL synthases demonstrate similar metabolic derivations to the unmutated genes: *lasI_{P_a}*: F27Y, *lasI_{P_a}*: S103A, *rhII_{P_a}*: S103A and *rhII_{P_a}*: S103V (For numerical figures on AMC metabolite levels of recombinantly expressed *lasI_{P_a}* and *rhII_{P_a}* see Section 3.6). For each AMC metabolite detected, there appears to be no difference between levels demonstrated by the specific SDMs and the corresponding unmutated AHL synthase gene. The *lasI_{P_a}*: F27L mutant also has intracellular AMC metabolite levels which differ from that of *lasI_{P_a}* expressed alone but the reductions are much less than any of the SDMs mentioned above (SAM -22.0%, SAH -25.0%, SRH -15.2%, HCY -14.7% and MET -7.3%). The remaining SDMs (*lasI_{P_a}*: R23W, *lasI_{P_a}*: W33G, *lasI_{P_a}*: S103E, *lasI_{P_a}*: S103V, *rhII_{P_a}*: F28L, *rhII_{P_a}*: 28: F > Y, *rhII_{P_a}*: W34G and *rhII_{P_a}*: S103E) did not trigger any severe metabolic disruptions. For these mutants, the lack of a significant percentage change as shown in Figure 4.7 indicates that the metabolic status of the cell in terms of the AMC is similar to the MG1655 control harbouring the pME6032 construct.

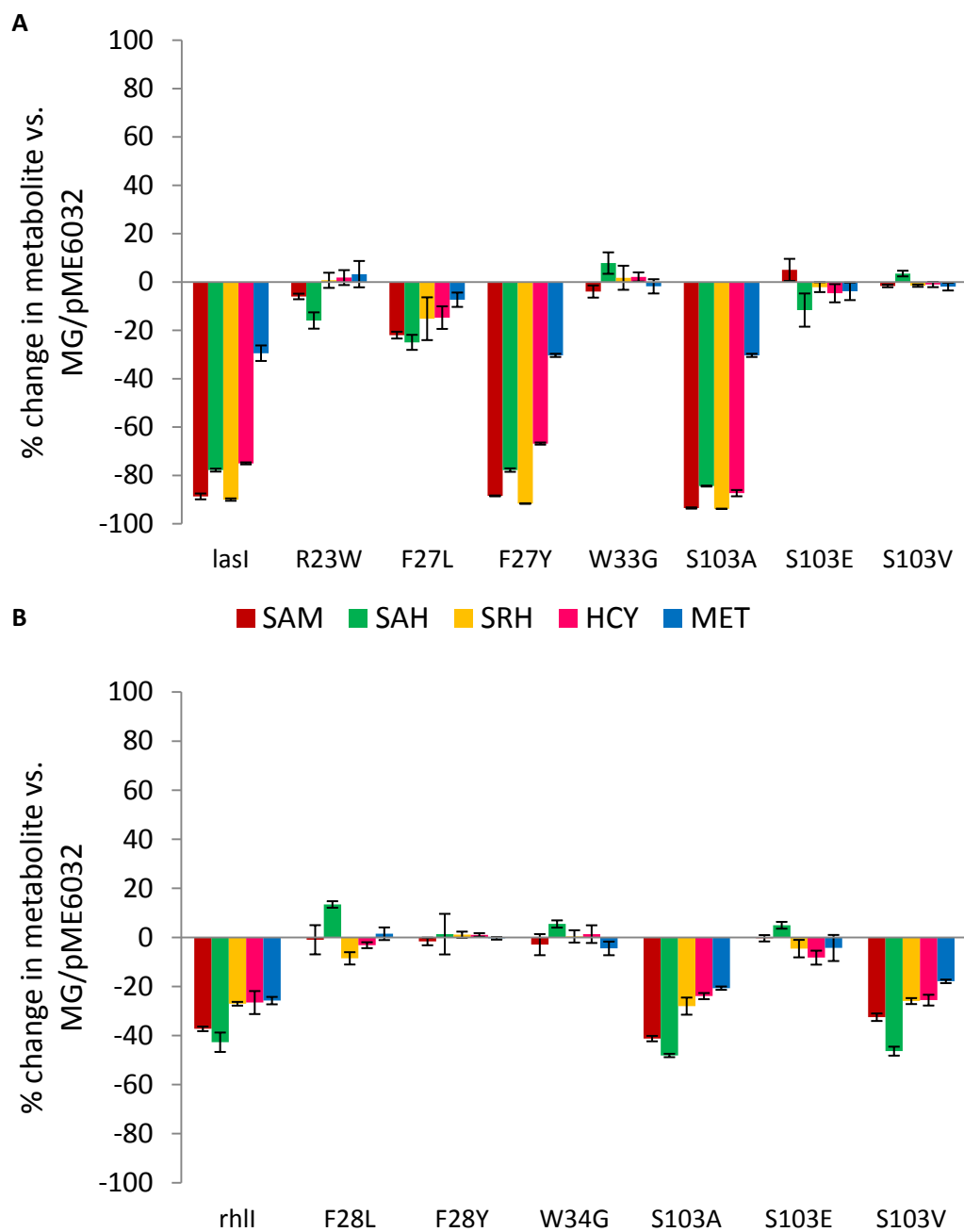


Figure 4.7: AMC metabolite profiles of *lasI_{pa}* and *rhII_{pa}* SDMs in *E. coli*. Metabolite levels were determined in *E. coli* AHL synthase SDMs grown in LB with IPTG induction. Intracellular accumulation of SAM, SAH, SRH, HCY and MET were determined by LC-MS analysis. Peak area corresponding to each compound was divided by the peak area of the appropriate internal standard for normalisation.

4.9 Recombinant expression of *P. aeruginosa* AHL synthase SDMs in *E. coli* leads to variation in extracellular AI-2 levels.

Since the SDMs generated a range of altered AMC metabolite profiles, the impact of these changes was assessed upon the levels of the byproduct of the AMC, AI-2. Supernatants collected from late exponential phase cultures of all the SDMs were applied to the *V. fischeri* biosensor assay and comparisons made at 3 h which corresponded to maximal light production in the positive control, as described previously. As can be seen in Figure 4.8, the SDMs with lower AMC metabolite levels also made less AI-2.

4.10 Intracellular MTA levels of *lasI*_{Pa} and *rhlI*_{Pa} SDMs are lower when less AHLs are made

In Section 3.8, heterologous expression of the AHL synthase genes in MG1655 was associated with large increases in concentrations of intracellular MTA which correlated with the AHL production in this host. This was confirmed within an MG1655 Δ *pf3* strain in which the conversion of MTA to MTR is not feasible. In order to detect MTA without any interference, the constructs for all SDMs within pME6032 were therefore also transferred to this Pfs inactive strain, the quantification was performed as previously described and it can be clearly seen in Figure 4.9 that higher levels of MTA were detected with SDMs that produced higher levels of AHLs.

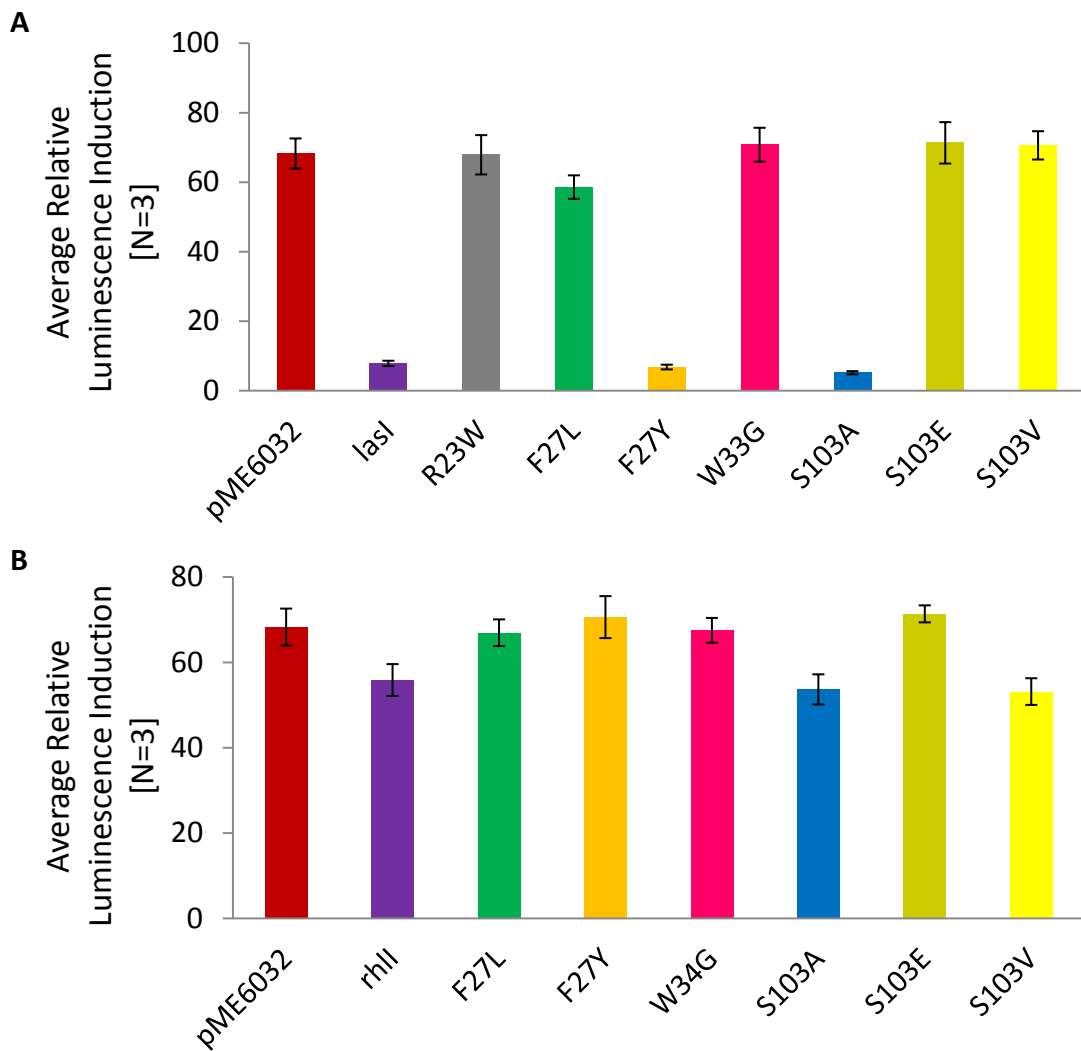


Figure 4.8: *V. harveyi* biosensor-based AI-2 detection for *P. aeruginosa* AHL synthase SDMs expressed in *E. coli*. Average induction of bioluminescence at three hours for MG1655 strains expressing AHL synthase SDMs of *lasI*_{Pa} (A) and *rhII*_{Pa} (B) alongside empty vector control, MG1655[pME6032], and the corresponding non mutated gene, MG1655[pME-*lasI*_{Pa}] or MG1655[pME-*rhII*_{Pa}], respectively. AI-2 activities for a single experiment are shown, although the experiment has been repeated three times with similar results.

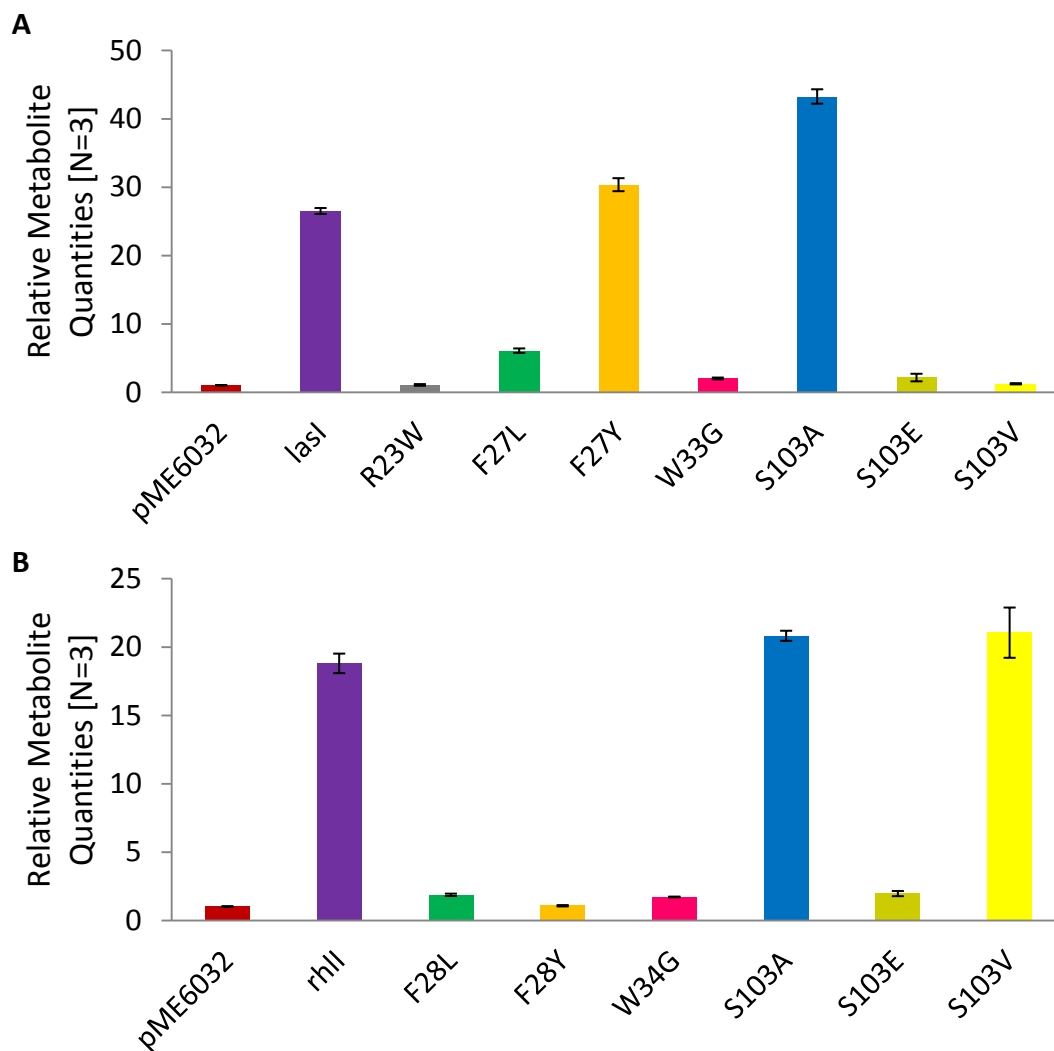
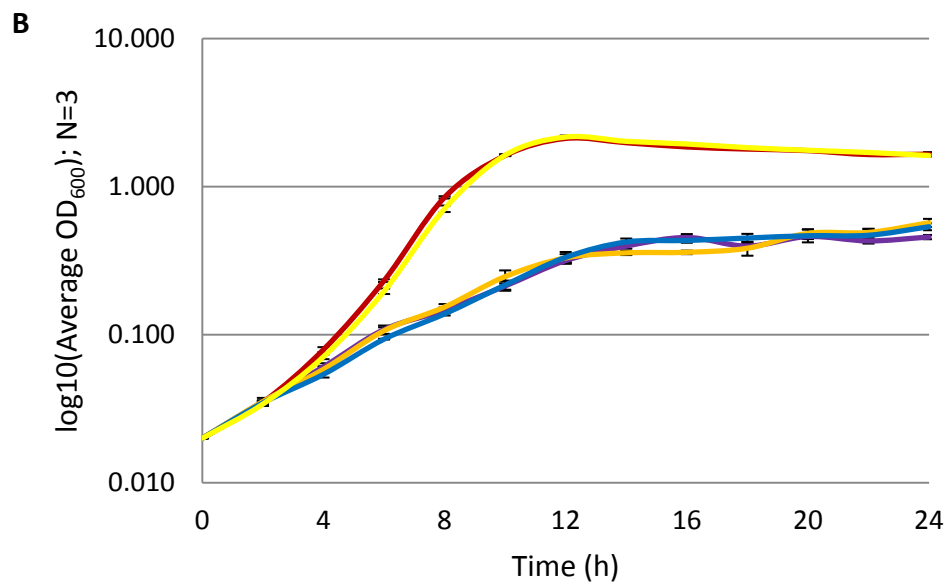
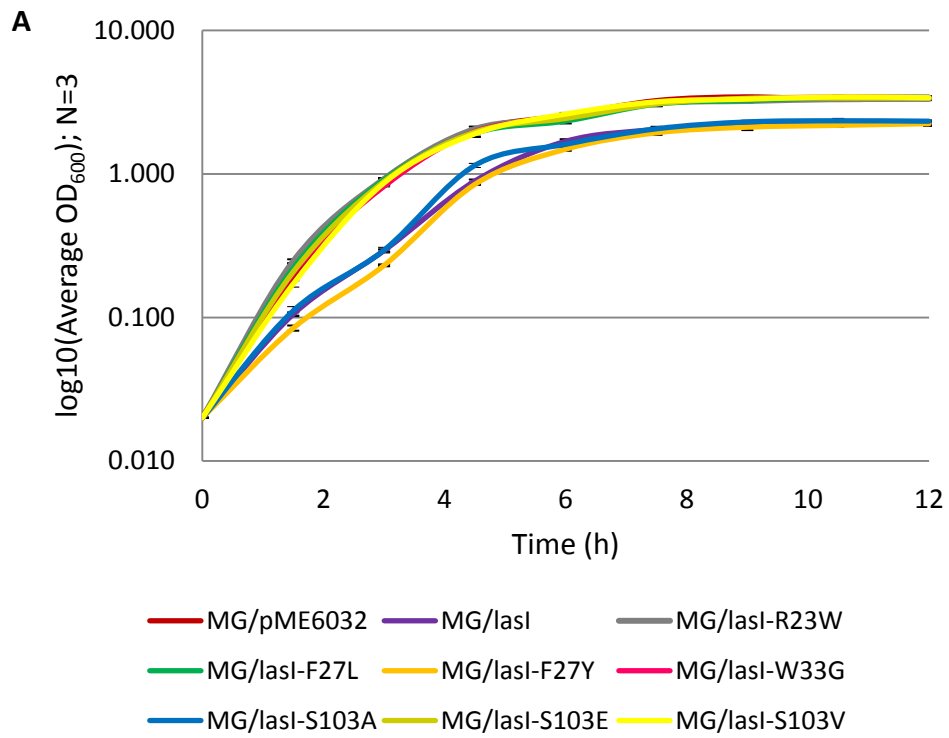


Figure 4.9: LC-MS/MS analysis of late exponential phase cultures revealed variable MTA levels of *lasI_{pa}* and *rhII_{pa}* SDMs in *E. coli* MG1655 Δ *pfs*. Intracellular accumulation of MTA as determined by LC-MS analysis in several *E. coli* strains including 13 *lasI_{pa}* (A) and *rhII_{pa}* (B) SDMs grown in LB with IPTG induction. Peak area corresponding to MTA was divided by the peak area of the appropriate internal standard for normalisation.

4.11 Fitness profiles of *P. aeruginosa* AHL synthase SDMs in *E. coli*.

To establish whether the mutagenesis of *lasI_{Pa}* and *rhlI_{Pa}* had any additional pleiotropic effects on the heterologous host, the growth rates and profiles of the SDMs and the WT AHL synthase genes were initially compared when grown in rich media (Figure 4.10A and C). The growth profiles of the *rhlI_{Pa}* SDMs were indistinguishable from *rhlI_{Pa}* and the empty vector control (Figure 4.10C). This was additionally true for the majority of the SDMs of *lasI_{Pa}*, which demonstrated no significant growth differences from MG1655[pME6032] strain (Figure 4.10A). As mentioned in Section 3.9, the expression of *lasI_{Pa}* in MG1655 has minor effects on the growth profile causing slight extensions to the length of the initial lag phase. As expected from the AHL and metabolite level analysis, the F27Y and S103A SDMs of *lasI_{Pa}* grew in a similar manner, displaying an overall slower exponential growth rate and a marginally reduced optical density at stationary phase.

The growth of the strains in CDM was then compared (Figure 4.10B and D). Again, all SDMs of *rhlI_{Pa}* grew at a similar rate to the *rhlI_{Pa}* construct in MG1655 (Figure 4.10D). In contrast, growth in minimal media highlighted that some of the SDMs of *lasI_{Pa}* were suffering from poorer overall fitness levels (Figure 4.10B). This appeared to influence the growth of the F27Y and S103A SDMs of *lasI_{Pa}* which demonstrate identical growth curves to the unmutated *lasI_{Pa}* in *E. coli*, achieving a maximal OD₆₀₀ at stationary phase of just above 0.500 following 24 hr. The remaining SDMs of *lasI_{Pa}* grow at a similar rate to MG1655[pME6032] in CDM, reaching a population size which is approximately half of that achievable under nutrient rich conditions.



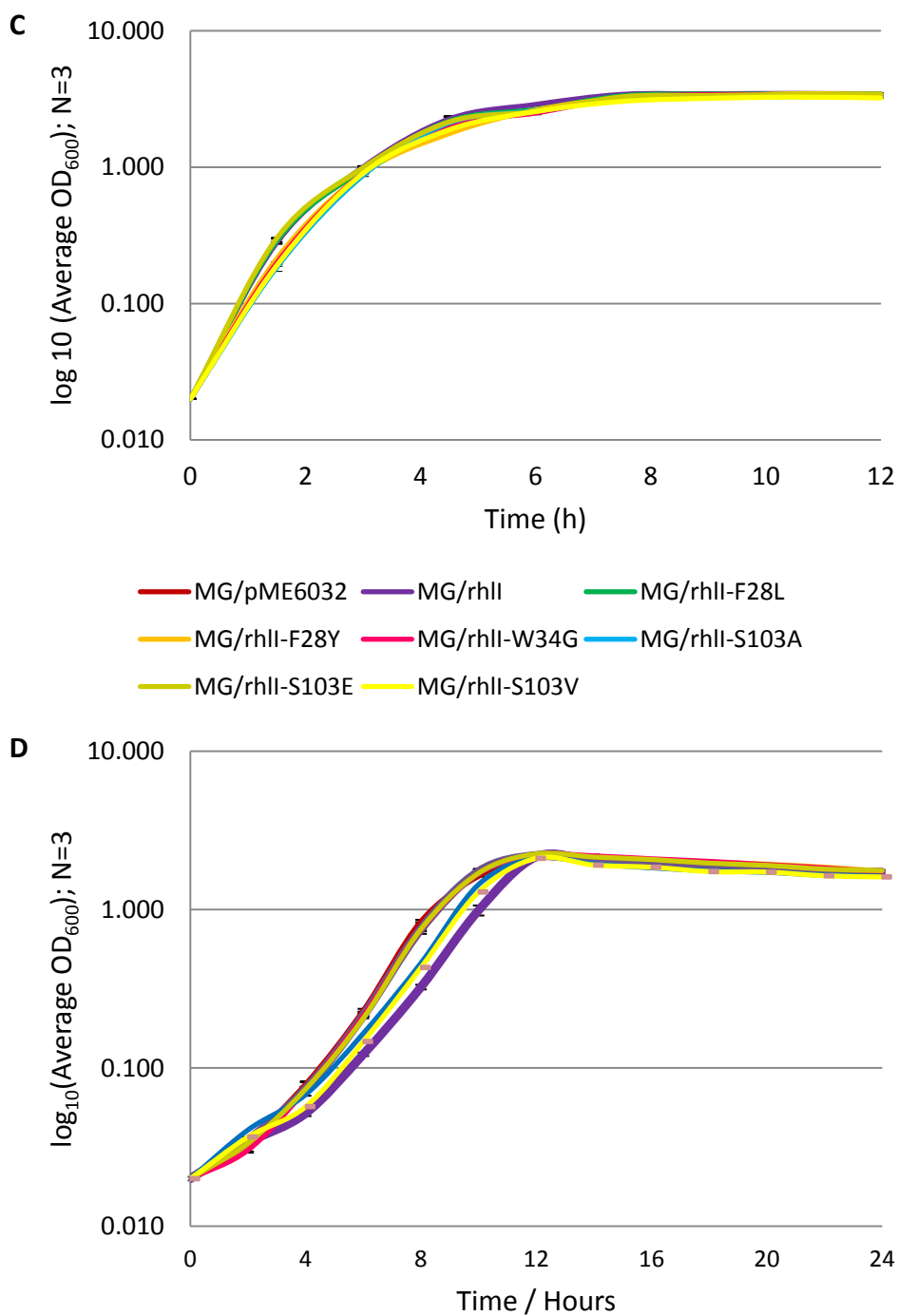


Figure 4.10: Fitness profiles of *P. aeruginosa* AHL synthase SDM in *E. coli*. *E. coli* SDM strains were inoculated into 125 ml LB media (A, C) or MMM (B, D) and grown shaking at 37°C in 500 ml-Erlenmeyer flasks. Aliquots (1ml) were taken at regular intervals and the mean OD_{600nm} values of triplicate culture samples are shown. Error bars indicate standard deviations from the means. Fitness is compromised for *lasI_{pa}* F27Y and S103A strains in MMM.

4.12 Discussion

Following on from the recombinant expression of *lasI_{Pa}* and *rhlI_{Pa}* in *E. coli*, the next strategic step involved using site-directed mutagenesis to target specific synthase residues. Combined with metabolic profiling, this was an interesting approach to unravel the biosynthetic activities of LasI and RhlI.

Given that our initial batch of SDMs was based on a similar analysis performed with RhlI by Parsek *et al.* (1997), it was interesting to compare the findings observed here with what had been previously reported. Between the two studies, the common *rhlI_{Pa}* SDMs were F28L, W34G and S103E. Here, no significant differences in the AHL profiles, AMC metabolite profiles, intracellular MTA levels and AI-2 production between the three SDMs were observed; all mimicked a WT profile, as if no synthase gene had been expressed. In contrast, Parsek *et al.* (1997) reported differences in the C₄-HSL producing activity of the SDMs as compared to the protein expressed from the unmutated *rhlI_{Pa}* gene. In order of F28L, W34G and S103E, a 500-, 1000- and 18-fold decrease in activity was observed. Though these figures vary considerably, they all indicate highly significant reductions in activity compared to the fully functional version of RhlI, therefore creating virtually inactive proteins or enzymes with very low levels of activity. However, the methods exploited to characterise such activities involved several rigorous steps which may have contributed to discrepancies between the two investigations. Nevertheless, the first batch of mutants were drastic ones and led to the construction of a second batch constituting milder substitutions and the potential for more variable metabolic alterations. The findings from all of the SDMs are discussed below.

Targeted site directed mutagenesis of identical residues in the *P. aeruginosa* AHL synthases has highlighted key functional differences in the catalytic roles played in each case. Whilst substitution of serine for valine at position 103 in *rhlI_{Pa}* allows for the synthesis of a fully functional enzyme still capable of producing AHLs associated with severe metabolic consequences, this is not true for an identical substitution amongst *lasI_{Pa}*. With the latter, the active site structure of the protein appears to be somewhat altered, changing the

activity of the synthase such that no detectable AHLs are produced. This is perhaps due to hindering substrate access and/or catalysis of the enzymatic reaction.

Abolition of AHL synthesis also occurred when phenylalanine substitutions were performed at positions 27/28 (*lasI_{Pa}*/*rhII_{Pa}*). Whilst exchange for slightly more hydrophilic tyrosine does not appear to affect the activity of LasI, it created a null mutation in the resulting RhII protein, illustrated in the drastic outcome of a relatively subtle mutation of this particular residue in this protein. The substitution of phenylalanine (F) for leucine (L) at the same position exchanges one hydrophobic side chain for another, allowing for the production of stable proteins in both instances. Whilst the resultant synthase exhibited a significantly reduced activity, there remained a residual activity in LasI, whilst a similar substitution in RhII was again unable to produce any detectable AHLs. In RhII, the phenylalanine residue at position 28 resides close to a salt bridge structure but more importantly appears to be close to the edge of a pocket, possibly altering active site structure when mutated. Where other substitutions have been performed mutating identical residues in *lasI_{Pa}* and *rhII_{Pa}*, there is a similar outcome. The substitution of tryptophan at position 34 for glycine gives rise to unstable proteins that are not detectable for either LasI or RhII by SDS PAGE. The predictive modelling for RhII indicates that this tryptophan residue lies in a completely different position in the same binding pocket mentioned previously and the substitution of tryptophan (W) for glycine (G) constitutes loss of indole aromatic compound which creates a very different environment within the binding pocket; an ineffective protein is therefore expected.

The serine residue at position 103 chosen for mutagenesis appears to occupy a deeper position within the same pocket. Its exchange for glutamic acid (E) results in the gain of a negatively charged side chain which causes significant disruption to the structure and is sufficient to inactivate the protein in AHL production. On the other hand, the substitution this serine for alanine (A) constitutes only the loss of a hydroxyl group and does not appear to affect the activity of the resulting mutant LasI and RhII proteins and their associated metabolic profiles. The remaining mutation has substituted the arginine (R) residue at position 23 of LasI. Arginine is normally localised to the outside of

proteins where it can interact with the polar environment; however, in this case it appears to reside within the synthase's structure participating in the formation of a salt bridge which is essential for holding the structure together. As a result, the tryptophan substitution is drastic and does not give rise to a stable protein; the destruction of the salt bridge correlates with a non-feasible structure incapable of performing the catalytic reaction.

All mutagenesis resulting in detectable AHL produced profiles of a similar constitution, and the AHLs expressed were present at similar concentrations to each other and the recombinantly expressed AHL synthase genes from *P. aeruginosa*. However, the substitution of serine for alanine at position 103 in *lasI_{Pa}* gives rise to an AHL profile additionally constituting significant concentrations of C₄-HSL, which accounts for 20% of the overall spectrum. In Section 3.4, recombinant expression of *lasI_{Pa}* in *E. coli* leads to the identification of specific AHLs which are not observed in the *P. aeruginosa* background.

Overall, it is clear that the strategy of site-directed mutagenesis combined with metabolic profiling can reveal a breadth of information about the importance of specific residues within a protein. Unquestionably, this approach could be exploited further, and all findings collated to enable the development of new therapeutic approaches based on the enzymes' unique specificity.

Chapter 5

Analysis of the metabolic
implications of *lasI*_{P_q} and
*rhlI*_{P_q} in *E. coli*

MG1655Δ*luxS*, Δ*pfs* and
Δ*sdiA* mutants

5.1 Introduction

From the findings in Chapter 3, it has been indicated that *lasI_{Pa}* and *rhII_{Pa}* rely heavily on the AMC. In order to determine the extent of this relationship and identify novel players, the AHL synthase constructs were transferred into several MG1655 mutants (*luxS*, *pfs* and *sdiA*) and the associated consequences determined.

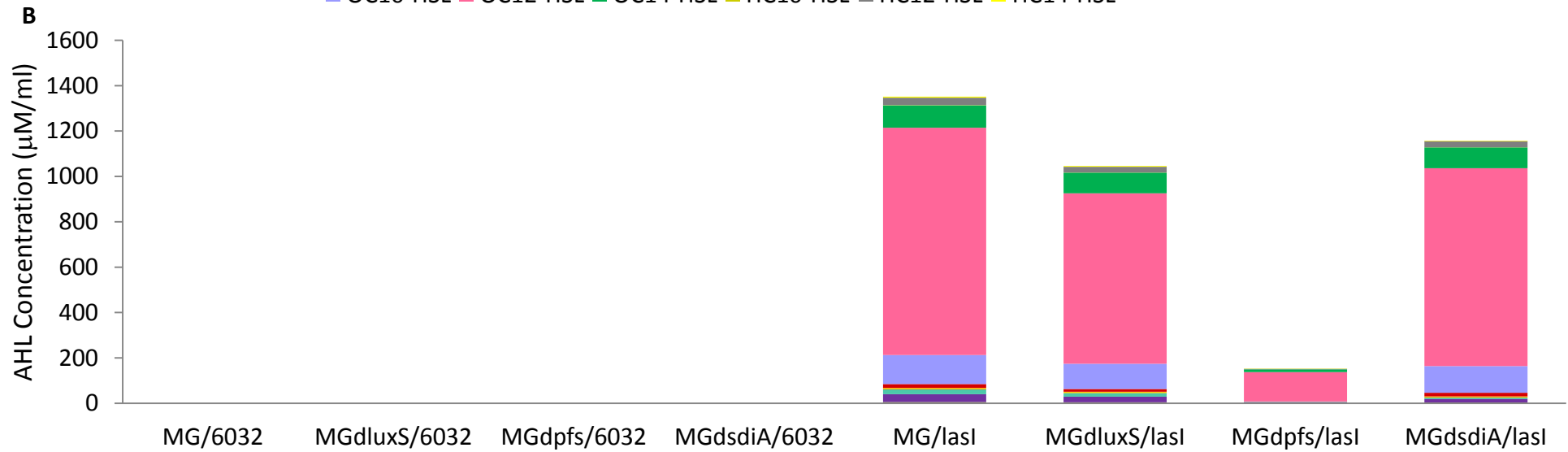
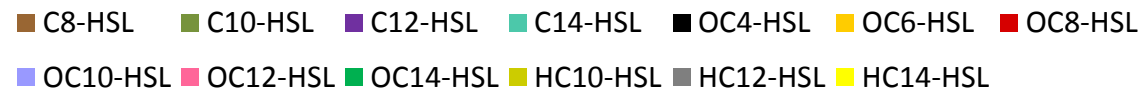
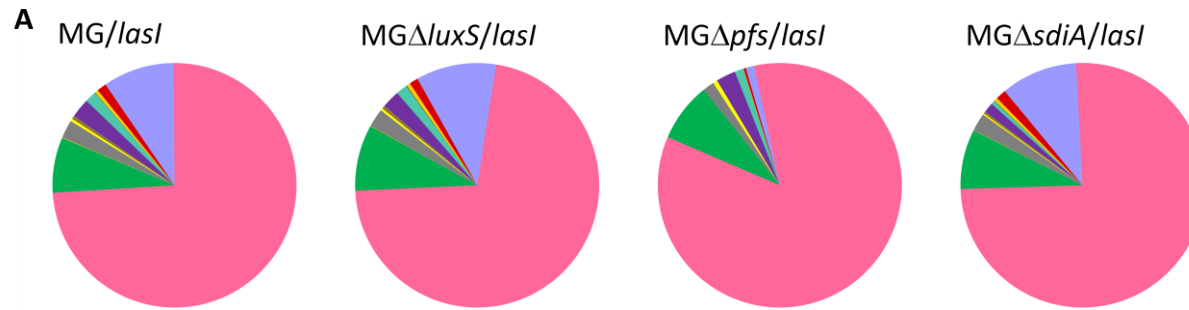
Pfs and LuxS are integral components of methionine metabolism since they contribute to the AMC directly. Together they recycle SAH by converting it to homocysteine in one version of the two alternative AMCs. Pfs first catalyses the bioconversion of substrate SAH into SRH and adenine (Miller & Duerre 1968; Della Ragione *et al.* 1985), then LuxS (*S*-ribosylhomocysteinase) catalyses the cleavage of the thioether bond in SRH to produce HCY and DPD. DPD is the precursor of AI-2 (Schauder *et al.* 2001). Pfs has a dual function in that it additionally converts MTA to MTR, which is a preliminary step in the methionine salvage pathway for regeneration of SAM in certain bacterial species (Della Ragione *et al.* 1985; Sekowska *et al.* 2004).

The suppressor of cell division, SdiA, is a homologue of the QS regulator LuxR. Since AHL production by *E. coli* has not been detected and a LuxI homologue has not been found, it is proposed that SdiA enables detection of exogenous AHL molecules and it appears to exert transcriptional control over a number of genes (Kanamaru *et al.* 2000; Rudd 2000). There remains considerable uncertainty over the precise role of *sdiA* in *E. coli*. However, in *Salmonella enterica* serovar Typhimurium, SdiA has been shown to detect AHLs produced by other bacterial genera (Michael *et al.* 2001; Smith & Ahmer 2003).

5.2 Elevated SAH and SRH levels, and reduced HCY levels and AHL profiles characterise the expression of *lasI_{Pa}* and *rhlI_{Pa}* in the *luxS* mutant

The inactivation of *luxS* in MG1655 led to significant differences in the QSSM profiles detected with recombinant expression of the AHL synthase genes (Figure 5.1). In contrast to the levels of QS signals observed with the WT, expression of AHL synthase genes in the *luxS* mutant led to much lower levels of total AHL production. For *lasI_{Pa}*, the overall QSSM profile was lowered by 22.6% compared to MG1655[pME-*lasI_{Pa}*]. Each of the 13 AHLs in the profile was affected, with the largest reductions influencing C₁₀-HSL (-25.1%), C₁₂-HSL (-28.6%), OC₁₂-HSL (-25.0%), HC₁₀-HSL (-44.1%) and HC₁₄-HSL (-31.9%) production. In addition, Figure 5.1D illustrates how the cumulative AHL profile in the *luxS* mutant decreases by approximately 30.4% compared to the equivalent expression of [pME-*rhlI_{Pa}*] in the WT strain. Again, the associated relative molecular proportions remain reasonably similar. (Figure 5.1C) More specifically, the individual percentage reductions indicate the extent to which each AHL in the profile was affected; the figures are reported as follows: C₄-HSL (28.5%), C₆-HSL (39.6%), C₈-HSL (38.4%) and HC₄-HSL (54.6%).

Having already determined that the AHL synthases considerably draw from the AMC for acquisition of one of their common substrates, SAM (Section 3.6), it was an interesting next step to establish the effect of AHL synthesis upon AMC metabolites in a mutant of the AMC, here one with an inactivation of the *luxS* gene. The vector control and constructs harbouring *lasI_{Pa}* and *rhlI_{Pa}* were transferred into MG1655Δ*luxS*, grown, and extraction, derivatisation, and LC-MS/MS conditions used as described previously. As expected, profiling of the *luxS* mutant harbouring the pME6032 vector revealed several key differences in AMC metabolites in comparison to the equivalent WT strain (Figure 3.2). The inactivation of *luxS* in MG1655 led to significant differences in the QSSM profiles detected with recombinant expression of the AHL synthase genes.



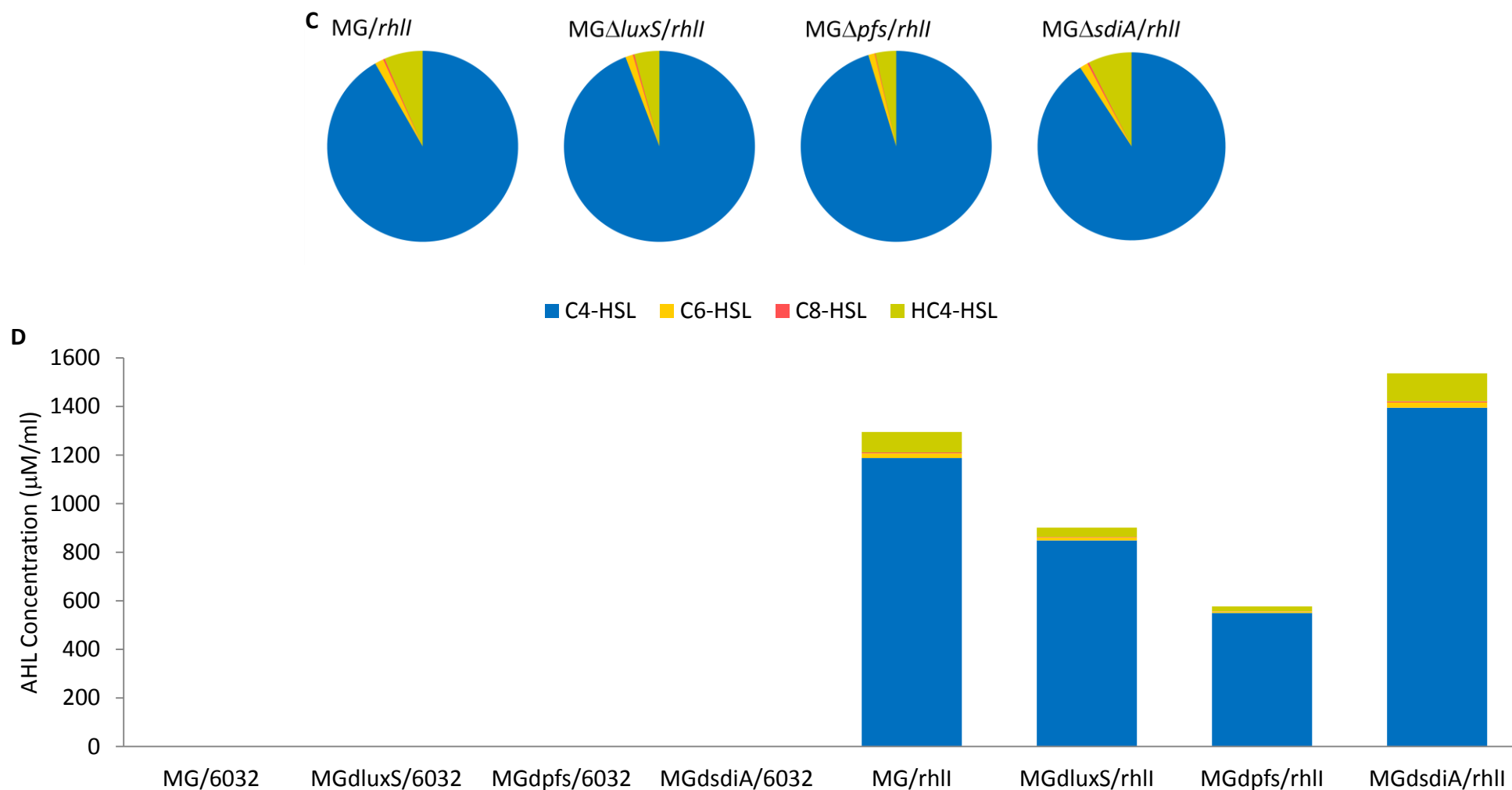


Figure 5.1: Relative molar proportions and cumulative profiling of AHLs produced by $lasI_{Pa}$ and $rhlI_{Pa}$ in *E. coli* MG1655, MG1655 $\Delta luxS$, MG1655 Δpfs and MG1655 $\Delta sdiA$. Compounds were extracted from late exponential phase supernatants with acidified ethyl acetate and profiled by LC-MS/MS analysis. The ratio between the different signalling molecules present in supernatants is represented by pie charts for recombinant $lasI_{Pa}$ (A) and $rhlI_{Pa}$ (C) constructs in the various MG1655 strains. The actual concentration of AHLs for recombinant $lasI_{Pa}$ (B) and $rhlI_{Pa}$ (D) constructs in the various MG1655 strains.

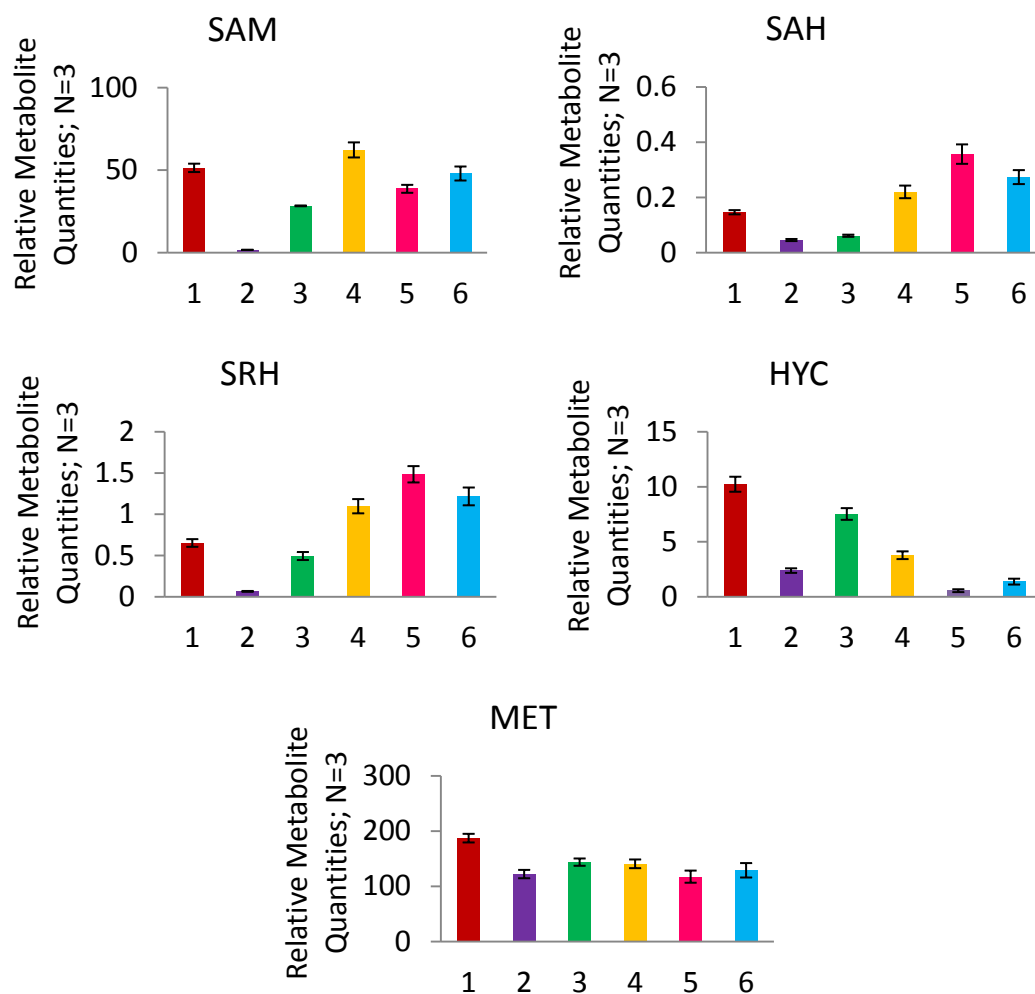


Figure 5.2: Recombinant expression of $lasI_{Pa}$ and $rhlI_{Pa}$ in the MG1655 $luxS$ mutant leads to the build up of intracellular SRH and SAH and fall of HCY. Intracellular accumulation of SAM, SAH, SRH, HCY and MET were determined by LC-MS analysis in six *E. coli* strains MG1655[pME6032] (1), MG1655[pME- $lasI_{Pa}$] (2), MG1655[pME- $rhlI_{Pa}$] (3), MG1655 $\Delta luxS$ [pME6032] (4), MG1655 $\Delta luxS$ [pME- $lasI_{Pa}$] (5) and MG1655 $\Delta luxS$ [pME- $rhlI_{Pa}$] (6) grown in LB with IPTG induction. Peak area corresponding to each compound was divided by the peak area of the appropriate internal standard for normalisation.

In contrast to the levels of QS signals observed with the WT, expression of AHL synthase genes in the *luxS* mutant led to much lower levels of total AHL production. The largest metabolic fluctuations affect intracellular SRH and HCY levels. As expected, the *luxS* mutation alone causes SRH levels (its substrate) to increase by 68.5% and HCY (its product) to decrease by 63.1%. However, on expression of *lasI_{Pa}* and *rhlI_{Pa}*, SRH is further elevated by 59.4% and 18.2%, respectively, and HCY reduced even more so, by 31.6% and 23.5%, respectively. This is in contrast to the effect of these genes in a WT background, where as previously seen in Chapter 3, SRH levels fell when the AHL synthases were present. Additional quantification of SAM and SAH levels has demonstrated that they also undergo significant changes in the $\Delta luxS$ cell with levels shown to increase by 21.2% and 50.5%, respectively. The presence of the synthases causes the levels of the two metabolites to encounter opposing patterns of change. SAH further accumulates whilst intracellular SAM levels decrease, the latter of which is similar to what was observed in the WT background (Section 3.9); the corresponding changes for SAH and SAM are 63.3% and 37.9%, respectively for *lasI_{Pa}* and 24.4% and 23.0% for *rhlI_{Pa}* (SAH increase and SAM decrease cf. MG1655 $\Delta luxS$ [pME6032]). In contrast, levels of intracellular MET experienced more subtle alterations; with reference to MG1655[pME6032], the *luxS* mutation causes levels to decrease by 24.8%. With *lasI_{Pa}* and *rhlI_{Pa}*, this is lowered by another 12.4% and 6.3%.

Figure 5.3A shows the fitness profiles for MG1655 and the *luxS* mutant independently expressing [pME6032], [pME-*lasI_{Pa}*] and [pME-*rhlI_{Pa}*]. However, there does not appear to be any noticeable differences between the growth curves of the two strains expressing each construct.

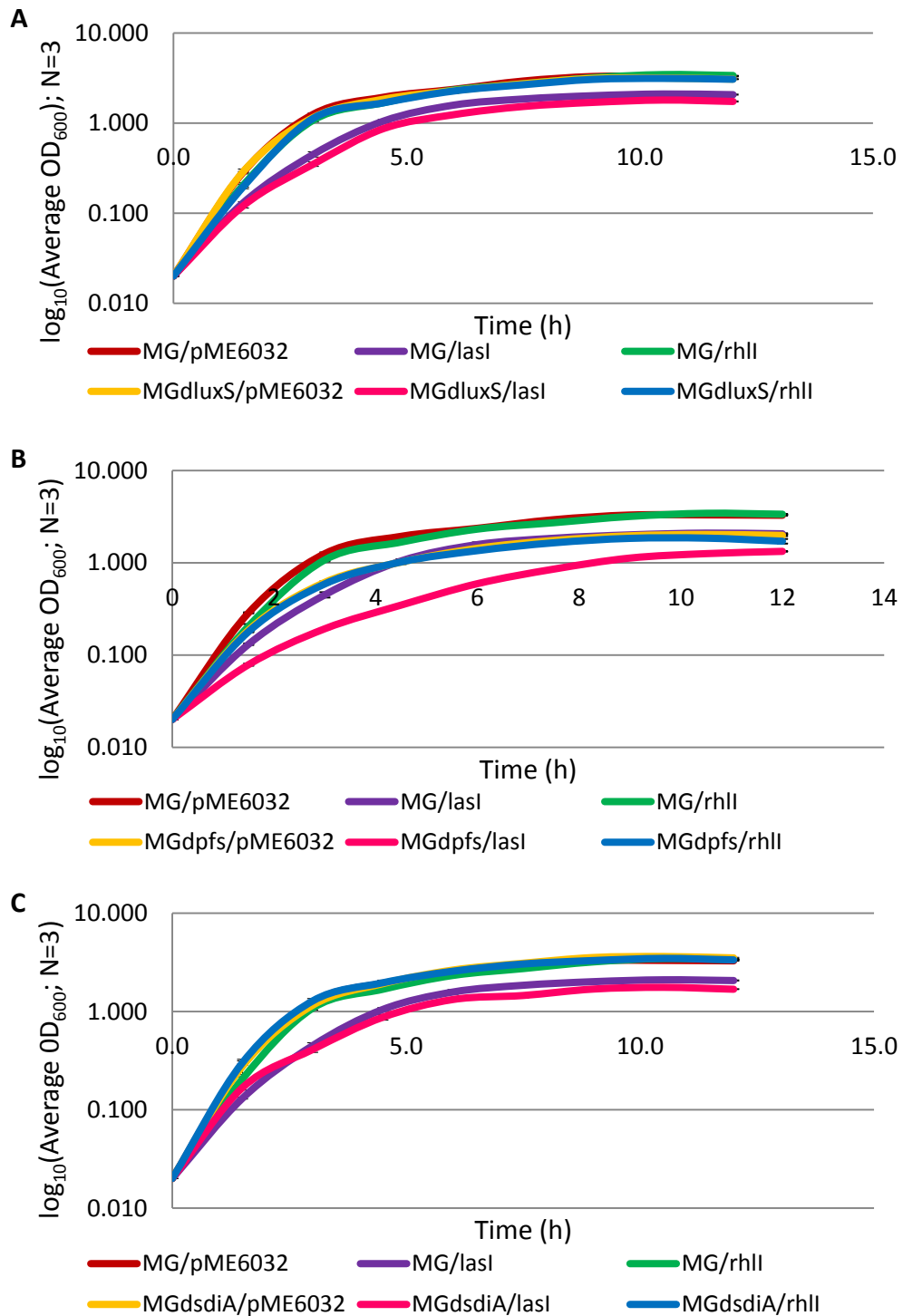


Figure 5.3: Expression of the AHL synthase genes in *MG1655Δpfs* creates a growth defect, while there are no significant differences between *MG1655*, *MG1655ΔluxS* and *MG1655ΔsdiA*. *MG1655*, *MG1655ΔluxS*, *MG1655Δpfs* and *MG1655ΔsdiA*, each expressing *pME6032*, *pME-luxI_{Pa}* and *[pME-rhlI_{Pa}]* were inoculated into 125 ml LB, IPTG induced and grown shaking at 37°C in 500 ml-Erlenmeyer flasks. 1 ml samples were taken at regular intervals and measured with a spectrophotometer. The cell density (OD_{600}) is plotted against time.

5.3 Expression of $lasI_{Pa}$ and $rhII_{Pa}$ in the pfS mutant leads to growth defects, reduced AHL profiles and altered AMC metabolite levels

Expression of the AHL synthase genes in MG1655 ΔpfS led to the most significant differences in QSSM profiling compared to the WT and other mutants used for comparative analysis in this chapter. Recombinant expression of both $lasI_{Pa}$ and $rhII_{Pa}$ in this strain caused a considerable reduction in the levels of each AHL present in each individual profile and therefore the overall cumulative total compared to that of MG1655 (Figure 5.1B and D). These were considerably more significant than the alterations observed in the $luxS$ mutant described above. With $lasI_{Pa}$, the majority of AHLs present below 5 μ M in MG1655 were absent in MG1655 ΔpfS (C_8 -HSL, C_{10} -HSL and OC_4 -HSL), whilst those which were present at reasonable concentrations were reduced by at least 90% (C_{12} -HSL, C_{14} -HSL, OC_6 -HSL, OC_8 -HSL and HC_{12} -HSL) (Figure 5.1B). Production of predominant AHLs OC_{12} -HSL and OC_{10} -HSL were additionally reduced by 87.0% and 87.9%, respectively. Furthermore, with $rhII_{Pa}$, detection of C_4 -HSL, C_6 -HSL, C_8 -HSL and HC_4 -HSL were reduced by 53.7%, 68.0%, 78.4% and 77.1%, respectively, compared to levels observed with MG1655, resulting in an extensive 55.4% decrease in the overall QSSM profile (Figure 5.1D).

Constructs were transformed into MG1655 ΔpfS and treated in exactly the same way as for the $luxS$ mutant for determination of metabolites of the AMC (Figure 5.4). The major metabolic disturbances in this background affected SAH, which accumulates in the mutant, a massive increase in intracellular levels of approximately 157.7%, and builds up even further with expression of $lasI_{Pa}$ and $rhII_{Pa}$, by an additional 93.3% and 69.8%, respectively. Furthermore, levels of the AHL substrate SAM are enhanced upon introduction of the pfS mutation (16.0%), but as with the MG1655 strain and $luxS$ mutant, intracellular concentrations subside when hosting $lasI_{Pa}$ and $rhII_{Pa}$, a decrease of 21.6% and 11.7% when values are calculated against MG1655 ΔpfS [pME6032].

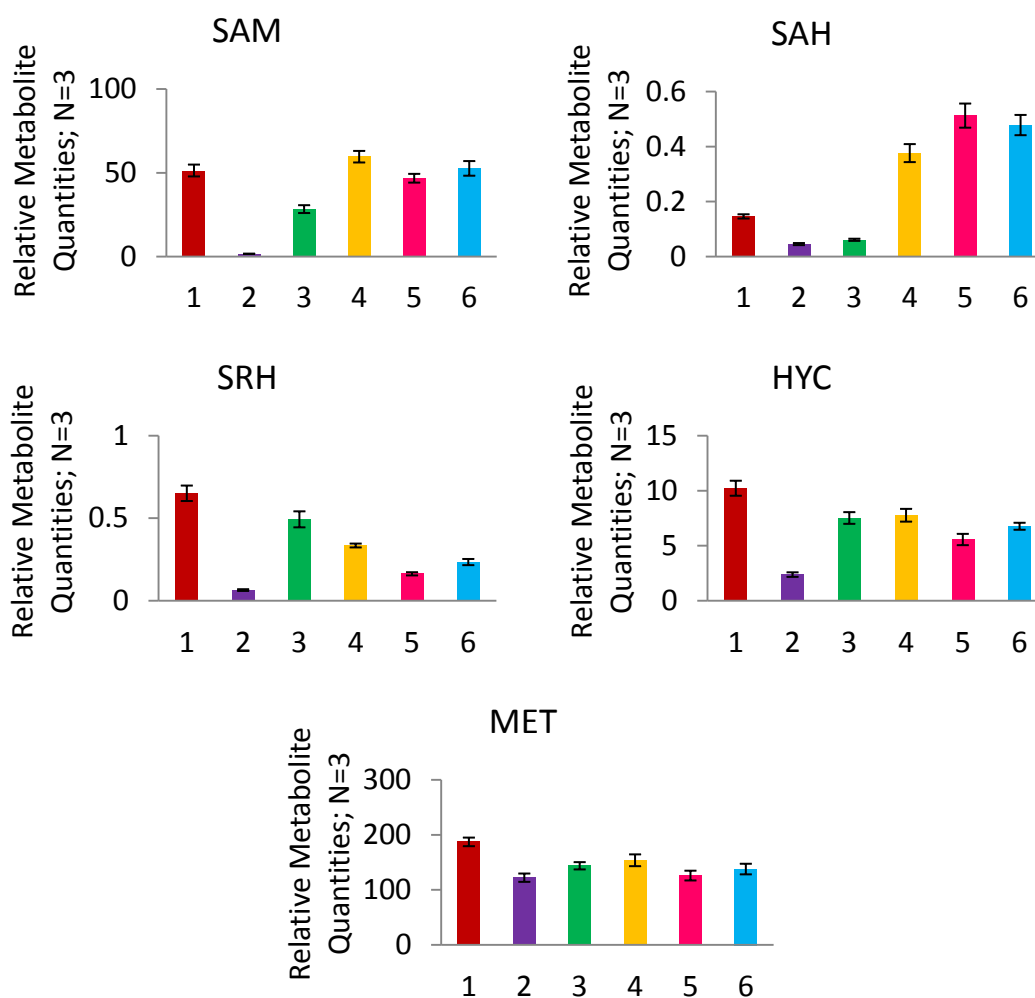


Figure 5.4: Recombinant expression of the *P. aeruginosa* AHL synthase genes in the MG1655 *pfs* mutant causes SAH accumulation and SRH and HCY levels to subside. Intracellular accumulation of SAM, SAH, SRH, HCY and MET were determined by LC-MS analysis in six *E. coli* strains MG1655[pME6032] (1), MG1655[pME-*lasI*_{Pa}] (2), MG1655[pME-*rhII*_{Pa}] (3), MG1655Δ*pfs*[pME6032] (4), MG1655Δ*pfs*[pME-*lasI*_{Pa}] (5) and MG1655Δ*pfs*[pME-*rhII*_{Pa}] (6) grown in LB with IPTG induction. Peak area corresponding to each compound was divided by the peak area of the appropriate internal standard for normalisation.

Another distinguishing feature of the metabolic profiling in the *pfS* mutant is the significant differences in intracellular SRH levels. The mutation itself results in a considerable drop in background levels compared to the WT, which equates to a decrease of roughly 48.6%. The disruption to levels of this metabolite are further impaired with *lasI_{Pa}* (26.3%) and *rhII_{Pa}* (15.4%). HCY are substantially reduced (24.0%) in MG1655 Δ *pfS* compared to the WT. As with SRH, the intracellular quantities of this metabolite subside further with the presence of each AHL synthase, and approximately correspond to another 21.6% with *lasI_{Pa}* and 9.8% with *rhII_{Pa}* when compared to MG1655[pME6032]. Similar to what has been observed previously with mutation of *luxS*, MET levels do not experience the major alterations encountered by the other AMC metabolites in the AMC. There is a small (17.8%) background reduction in MET, caused by mutation of the *pfS* gene, which is lowered slightly more when *lasI_{Pa}* (14.9%) and *rhII_{Pa}* (8.5%) are expressed.

Fitness profiles of the MG1655 Δ *pfS* strain expressing *lasI_{Pa}* and *rhII_{Pa}* determined in nutrient rich media illustrated a growth defect compared to the equivalent MG1655 strains (Figure 5.5B). The growth profiles of MG1655 Δ *pfS*[pME6032] and MG1655 Δ *pfS*[pME-*rhII_{Pa}*] were similar to that of MG1655[pME-*lasI_{Pa}*] with a slightly slower rate of exponential phase growth and incapability of achieving the maximal stationary phase cell density as possible by the WT[empty vector] strain. In comparison, the fitness of MG1655 Δ *pfS*[pME-*lasI_{Pa}*] in the same media type was further compromised, with a significant decrease in growth exhibited throughout the growth curve demonstrated over 12 h.

5.4 *lasI_{Pa}* and *rbII_{Pa}* create different AMC metabolite and AHL profiles in the *sdiA* mutant

Given the suspected regulatory links of the *sdiA* gene to QS, the profiles of AHLs and AMC metabolites were characterised in the *sdiA* mutant of MG1655.

Interestingly, the QSSM profiles created by *lasI_{Pa}* and *rbII_{Pa}* in the *sdiA* mutant were different (Figure 5.1). Whilst *lasI_{Pa}* led to a decrease in the overall AHL profile in comparison to what has been observed in the WT, *rbII_{Pa}* demonstrated a comparative increase. For *lasI_{Pa}*, the majority of AHLs detected within the C- and HC-series series were reduced by at least 36.1%, whilst those of the OC-series were reduced to a lesser extent (OC₄-HSL: -4.1%, OC₆-HSL: -11.1%, OC₈-HSL: -6.6%, C₁₀-HSL: -8.2%, C₁₂-HSL: -12.9% and C₁₄-HSL: -7.6%) (Figure 5.1B). In contrast, the expression of *rbII_{Pa}* in the MG1655Δ*sdiA* led to a substantial increase in the levels detected of all its associated AHLs. Absolute concentrations of C₄-HSL, C₆-HSL, C₈-HSL and HC₄-HSL rose by 17.4%, 13.2%, 27.3% and 36.3, respectively when compared to profiles obtained from MG1655. Overall, this corresponds to an increase of approximately 18.6% (Figure 5.1D).

The impact of the AHL synthase genes on AMC metabolite profiles in this strain was coordinately affected (Figure 5.5). With both synthases, and all metabolites profiled, a definitive decrease was apparent. The drain of all five metabolites upon *lasI_{Pa}* expression was significantly less than that observed in the WT. The percentage decrease in the WT followed by that in the *sdiA* mutant as compared to the corresponding empty vector control are as follows: SAM (-96.8%, -32.7%), SAH (-68.9%, -43.6%), SRH (-90.1%, -13.0%), HCY (-76.8%, -21.9%) and MET (-34.8%, -20.0%). In contrast, the equivalent values for *rbII_{Pa}* are: SAM (-44.9%, -83.1%), SAH (-58.3%, -74.9%), SRH (-24.3%, -84.4%), HCY (-26.5%, -63.7%) and MET (-23.2%, -40.3%).

The fitness profiles demonstrated by recombinant expression of *lasI_{Pa}* and *rbII_{Pa}* in the *sdiA* mutant were similar to those observed with the WT, as described in Section 3.9 (Figure 5.3C).

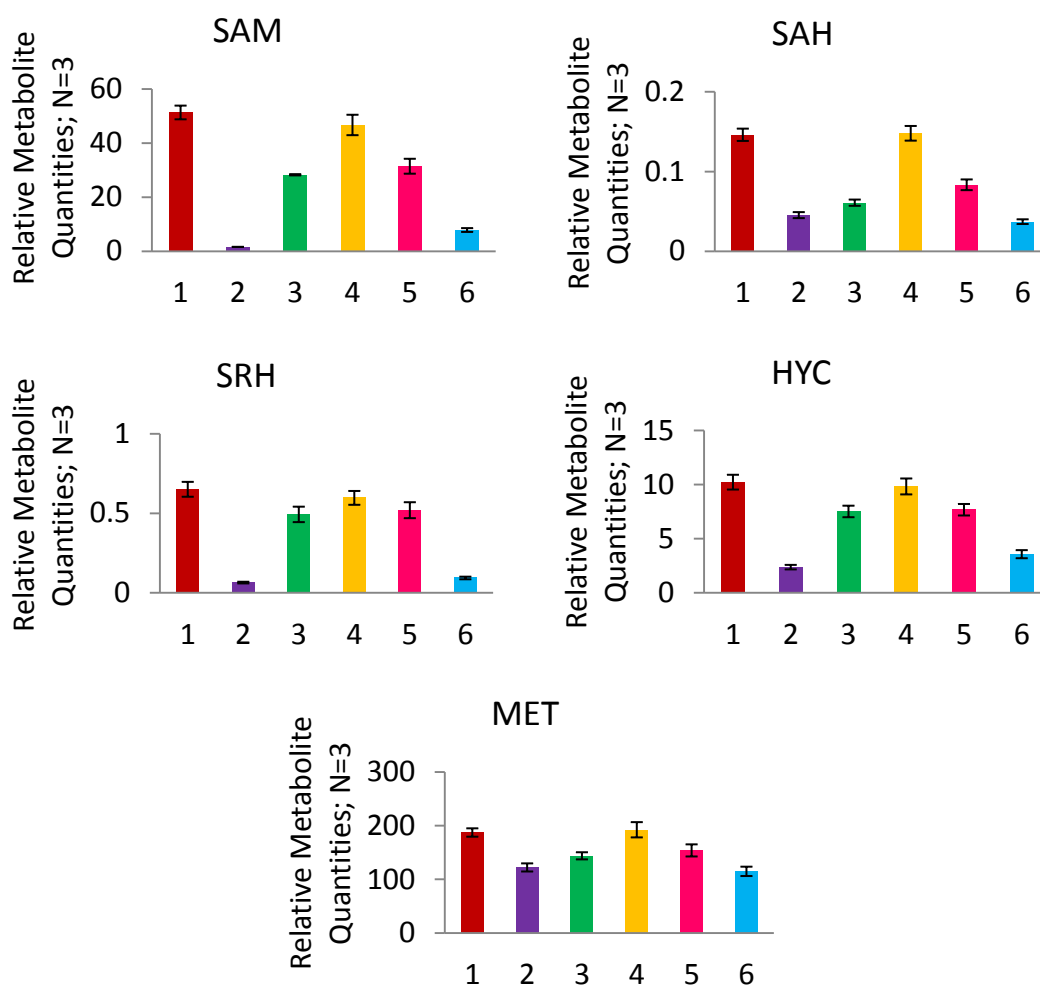


Figure 5.5: The expression of *rhII_{Pa}* and *lasI_{Pa}* in the MG1655 *sdiA* mutant causes significant drains AMC metabolites, but the effect of *rhII_{Pa}* is to a greater extent. Intracellular accumulation of SAM, SAH, SRH, HCY and MET were determined by LC-MS analysis in six *E. coli* strains MG1655[pME6032] (1), MG1655[pME-*lasI_{Pa}*] (2), MG1655[pME-*rhII_{Pa}*] (3), MG1655Δ*sdiA*[pME6032] (4), MG1655Δ*sdiA*[pME-*lasI_{Pa}*] (5) and MG1655Δ*sdiA*[pME-*rhII_{Pa}*] (6) grown in LB with IPTG induction. Peak area corresponding to each compound was divided by the peak area of the appropriate internal standard for normalisation.

5.5 Discussion

Metabolic profiling of the consequences of the heterologous expression of the *P. aeruginosa* AHL synthase genes in MG1655 *luxS*, *pfs* and *sdiA* mutants has provided further information as to the greater metabolic complications caused when other aspects of metabolism are compromised..

Both LuxS and Pfs are important components of the AMC, the recycling pathway central to methionine metabolism. The absence of either constitutes significant metabolic disruptions, preventing the normal rate of channelling of metabolites through the cycle. This is clearly demonstrated here through direct comparisons of each mutant containing the empty plasmid vector to the corresponding WT. Introducing *lasI_{Pa}* and *rhlI_{Pa}* into these systems exacerbates the metabolic disruptions further and is illustrated by the substantial reductions in the cumulative AHL production profiles, which are significantly more drastic in the MG1655 *pfs* mutant than the *luxS* mutant. This may seem strange given that there is an increase in availability of SAM in both mutants. However, both also lead to elevated SAH concentrations, which are much higher upon removal of Pfs, its sole recycling route. In terms of other metabolites, there are similar trends for HCY and MET in both mutants. The absence of LuxS also leads to the build up of SRH; this makes sense as it can no longer be removed. The *pfs* mutant, on the other hand, is able to degrade SRH, so the trends observed are similar to the WT, although the basal level is lower to begin with so expression of the synthase genes leads to less dramatic changes. Removal of Pfs is associated with further complications; not only does it lead to accumulation of the toxic SAH by-product, but additionally MTA. As mentioned previously, the build up of the latter results from the recombinant production of AHLs and the inability to recycle the metabolite produced from the cell's other processes. Both SAH and MTA are potent inhibitors of SAM-dependent reactions including methyltransferase and polyamine biosynthesis activities. Furthermore, both have been shown to directly inhibit the LuxI synthase family (Parsek *et al.* 1999). Moreover, given the toxicity of SAH and MTA, there may be further consequences; for example, there

may be transcriptional or post-translational effects on the cell response that could shut down another metabolic pathway, leading to reduced secondary substrates and therefore reduced provisions for AHL synthesis. A precedent for this would be the information given in the paragraph below.

In Gram-positive bacterium, *Listeria monocytogenes*, extracellular accumulation of SRH has been shown to modulate biofilm formation, with both SAH and SRH found in culture supernatants via a mechanism which remains unknown (Challan Belval *et al.* 2006). It has been suggested that the export of these metabolites may provide an appropriate system to eliminate SAH when the detoxification pathway is overwhelmed or down regulated (Challan Belval *et al.* 2006). This might also provide a feasible explanation for the reduced AHLs detected with the associated mutants. As mentioned in Section 3.11, a similar removal mechanism has been suggested for SAH via increasing extracellular AI-2 concentrations during exponential growth until stationary phase when AI-2 is brought back into the cell to overcome catabolite repression (Surette & Bassler 1998; Surette & Bassler 1999; Winzer *et al.*, 2002; Hardie *et al.*, 2003). A study investigating the effect of a *luxS* mutation on biofilm formation in another Gram-negative bacterium, *Shewanella oneidensis*, has demonstrated the upregulation of three metabolic enzymes, cysteine synthase, malate dehydrogenase and transketolase using a secretome analysis (Bodor *et al.* 2011). The authors hypothesise that these changes are either due to the need to compensate for the lack of HCY or the channelling of the accumulating SRH into carbon metabolism. It might be interesting to investigate whether the equivalent or functionally related proteins are affected in the MG1655 *luxS* mutant used for this study and more importantly whether there are any further changes in response to the functioning of the *lasI_{Pa}* and *rbII_{Pa}* genes via a similar secretome analysis or simpler SDS-PAGE or western blotting methods.

To date, there have been several studies which have investigated the consequences of *luxS* and *pfs* mutations in other bacteria. In *Neisseria meningitidis*, both mutants have been shown to suffer growth defects in a sulphur limited medium (a commercial Dulbecco modified Eagle medium: c-DMEM); the fitness of the *pfs* mutant in rich medium, like

here, was additionally compromised (Heurlier *et al.* 2009). In terms of AMC metabolite profiling, the *pfs* mutant experienced no significant differences with levels of SAM and MET, whilst SRH was absent, SAH increased and HCY was found to be reduced under some conditions (c-DMEM). The *luxS* mutant was associated with increased SRH and HCY levels (Heurlier *et al.* 2009). In contrast, HCY was significantly lower in an *E. coli luxS* mutant when compared to the equivalent WT. Similarly, however, the accumulation of SRH also characterized a metabolite analysis of *Helicobacter pylori* and *E. coli luxS* mutants (Doherty *et al.* 2010, Halliday *et al.* 2010). Overall, it appears that the findings reported in this study complement the major metabolic disturbances caused by the two AMC mutations in the profiled bacterial strains; there is even further opposition for the findings reported with regards to HCY in *N. meningitidis* (Heurlier *et al.* 2009).

Another important consideration relates to how the AHL profile connects to the metabolite levels observed. SAM is directly exploited for AHL biosynthesis (Moré *et al.* 1996, Jiang *et al.* 1998). In the *luxS* and *pfs* mutants, there is an increase in intracellular SAM levels, whilst overall AHL production decreases when compared to the WT. In contrast, levels of SAM decrease and AHL production increases with the expression of *rhII_{Pa}* in the *sdiA* mutant. In a general sense, a feasible explanation can be offered to both of the trends observed in the different mutants. In the former, the accumulation of toxic by-products that can directly inhibit the synthase enzymes leads to an exhaustive reaction; as a result, despite the increased availability of the substrate, the amount of enzyme capable of performing a feasible reaction is limited and is therefore not able to produce as much product as is possible in the WT situation. In contrast, the expression of *rhII_{Pa}* in the *sdiA* mutant; given the reaction, increased substrate availability allows increased product formation, reducing substrate levels as a result. In terms of the specific alterations in AMC metabolites, Figure 5.6 illustrates a model for the expected trends in each of the AMC mutants.

The difference in QSSM expression profiles caused by *lasI_{Pa}* and *rhII_{Pa}* in the *sdiA* mutant are difficult to interpret given the lack of information concerning the role of this regulator in *E. coli*. The absence of the SdiA protein appears to remove regulatory links

on other aspects of the cells which somehow affect the *lasI_{Pa}* and *rhlI_{Pa}* gene, their proteins expressed and/or the resulting AHLs differently.

A *pfs*

B *luxS*

Figure 5.6: Schematic representation of the expected AMC metabolite profiles caused by *lasI_{Pa}* and *rhlI_{Pa}* expression in the MG1655 *pfs* and *luxS* mutants. In a *pfs* mutant, the enzyme's substrate SAH accumulates, as does SAM, whilst levels of SAH and HCY decrease. The expression of the synthases in this mutant directly reduces levels of SAM, and consequently MET, HCY and SRH, whilst intracellular SAH builds up even further. In contrast, the *luxS* mutant's inability to recycle SRH means it accumulates, and so does the substrate of the upstream reaction, SAH. Simultaneously, intracellular HCY and MET levels decrease due to the continuation of downstream reactions. In these circumstances, recombinant AHL synthesis draws SAM from the AMC causing SAH and SRH to accumulate and HCY and MET to further decrease.

Chapter 6

Analysis of the metabolic
implications of the AHL
synthase genes in the native
P. aeruginosa background

6.1 Introduction

The metabolic costs of communication through signal production investigated in the context of *E. coli* have suggested that the AHL synthase genes constitute major substrate drainage systems in *P. aeruginosa*. The heterologous host was exploited to avoid complications imposed by various regulatory components and interlinks between the various systems that could cause difficulties with interpretation of the level of dependency on the associated metabolic systems. In order to provide a more complete overview, the metabolic profiling of the *P. aeruginosa* PA01 AHL synthase mutants was undertaken.

6.2 Production of QSSMs is significantly reduced in the PA01 Δ *lasI*, PA01 Δ *rbII* and PA01 Δ *lasI* Δ *rbII* mutants and can be restored upon complementation

LasI expression in the context of *E. coli* revealed the production of an interesting array of AHLs; it was therefore of interest to determine how comparable this was to the native host. *P. aeruginosa* PA01 produces a variety of AHLs, the majority of which are synthesised at very low concentrations. The major AHLs of the profile are C₄-HSL and OC₁₂-HSL. The mutation of *lasI* alone does not prevent *rbII* activity as the production of the majority of shorter chain AHLs was found to still occur under these circumstances and shown to be only slightly reduced compared to the WT. In contrast, the majority of longer chains AHLs are absent or concentrations are significantly reduced. In comparison with PA01[pME6032], PA01 Δ *rbII*[pME6032] was associated with a higher prevalence of longer chain AHLs. In contrast, the dual *lasI/rbII* mutations abolished AHL production completely or to very low AHL concentrations. However, complementation of the single gene mutants is sufficient to re-establish AHL synthesis back to approximate WT concentrations with both of the synthase mutants.

Studying within the context of *P. aeruginosa* means it's possible to determine the consequences of these AHL disturbances on AQ production since there are multiple regulatory links between the two types of QS systems. The inactivation of either of the *lasI* or *rhII* genes and/or both together was sufficient to completely knock out production of the entire repertoire of AQ that are observed with PA01 and PA01[pME6032] (Figure 6.1b). LC-MS/MS demonstrated the absence of the entire AQ series with the three mutants tested. These phenotypes were restored upon complementation of the single gene mutants with the corresponding pME-*lasI*_{Pa} and pME-*rhII*_{Pa} constructs.

6.3 AMC metabolites

In Chapter 3, the *P. aeruginosa* AHL synthases were shown to drain levels of several intracellular metabolites including those of the AMC in *E. coli*. The subsequent and logical next step was therefore to determine the metabolic repercussions of removing the activity of these enzymes from *P. aeruginosa*. The AMC metabolite profiles (SAM, SAH, HCY and MET) were again determined from late exponential phase cultures (125 ml LB in 500 ml-Erlenmeyer flasks at 37°C) of the PA01 WT, mutant and complemented strains. Mutating the AHL synthase genes independently and/or together amplified the concentrations of each of the metabolites compared to the WT with empty vector with the exception of SAH (Figure 6.2). The most significant and maximal level of change coordinated with the dual *lasI/rhII* mutant (SAM: +128.5%, SAH: -29.1%, HCY: 109.6% and MET: 139.7%) with percentage reductions of each metabolite reported comparable to PA01[pME6032], but this was only marginally greater than the levels observed with the single gene mutants. Of the four metabolites constituting the *P. aeruginosa* AMC, MET increased the most.

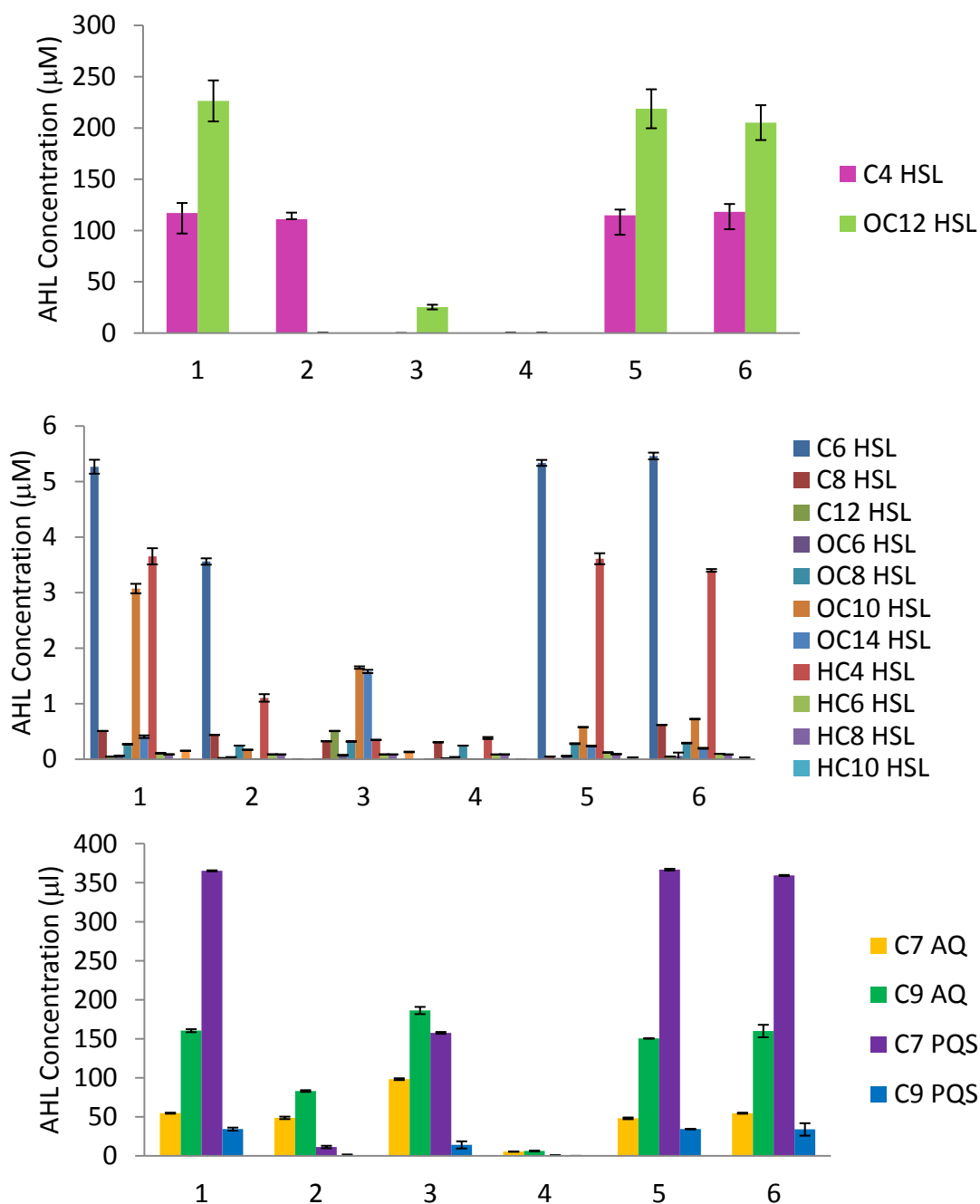


Figure 6.1: *P. aeruginosa* AHL synthase mutants significantly disrupt AHL profiles and also disrupt levels of AQ and PQS, but to a lesser extent. Compounds were extracted from late exponential phase supernatants of six *P. aeruginosa* strains PA01[pME6032] (1), PA01 Δ lasI[pME6032] (2), PA01 Δ rbII[pME6032] (3), PA01 Δ lasI Δ rbII[pME6032] (4), PA01 Δ lasI[pME-*lasI_{pa}*] (5) and PA01 Δ rbII[pME-*rbII_{pa}*] (6) grown in LB with IPTG induction. Supernatants were extracted with acidified ethyl acetate and profiled by LC-MS/MS analysis. The actual concentration of AHLs is shown.

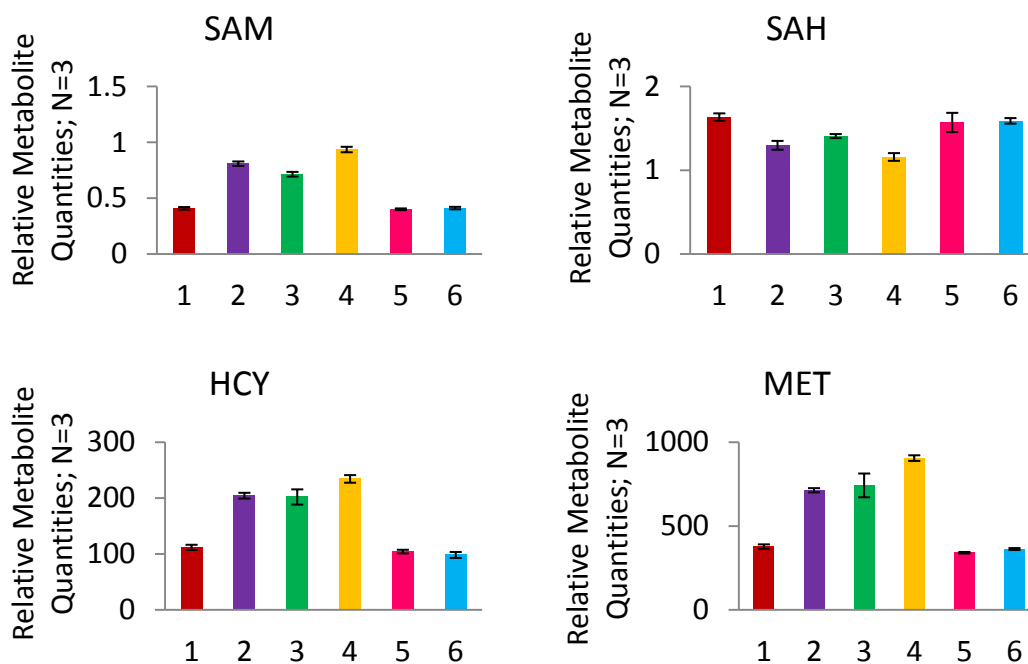


Figure 6.2: Increased levels of AMC-linked metabolic profile of *P. aeruginosa* PA01-AHL synthase mutants. Intracellular accumulation of SAM, SAH, HCY and MET were determined by LC-MS analysis in six *P. aeruginosa* strains PA01[pME6032] (1), PA01 Δ *lasI*[pME6032] (2), PA01 Δ *rbII*[pME6032] (3), PA01 Δ *lasI* Δ *rbII*[pME6032] (4), PA01 Δ *lasI*[pME-*lasI*_{Pa}] (5) and PA01 Δ *rbII*[pME-*rbII*_{Pa}] (6) grown in LB with IPTG induction. Peak area corresponding to each compound was divided by the peak area of the appropriate internal standard for normalisation.

On the other hand, compared to the other metabolites and the levels of the PA01[pME6032] strain, SAH demonstrated opposing levels of change. Similarly, however, the maximum percentage change, which in this case was the decrease of SAH (29.1%) was observed with PA01 Δ *lasI* Δ *rhII*[pME6032], followed closely by the *lasI* (20.5%) and *rhII* (13.8%) mutants. Complementation of the single gene mutants with the corresponding vector construct brought metabolite levels approximately back to those measured in the WT/empty vector control.

6.4 Intracellular MTA levels decrease with removal of the AHL synthase genes and increase back with complementation

Since expression of *lasI* and *rhII* increased intracellular MTA concentrations in *E. coli* (Chapter 3), it was of interest to determine the consequences of their mutation in *P. aeruginosa*. Unlike *E. coli*, the AMC of *P. aeruginosa* constitutes a single step SAH detoxification reaction to HCY carried out by the SAH hydrolase enzyme and lacks the alternative Pfs enzyme which also catalyses the conversion of MTA to MTR. The levels of MTA observed in *P. aeruginosa* are therefore not affected by the activity of this latter enzyme and any differences that may be observed will be due to the inactivation of the corresponding AHL synthases. For control purposes, the detection of comparable levels of MTA in PA01 and PA01[pME6032] confirmed that the presence of the chosen expression vector did not affect intracellular levels of this metabolite (Figure 6.3). Interrupting the expression of the *las* system by mutating *lasI* drastically reduces MTA levels in the cell (93.9%). The *rhII* mutant similarly demonstrates lower levels, but the reduction (41.1%) is significantly less than that seen with PA01[pME-*lasI*_{pd}]. In addition, levels of MTA detected with the double AHL synthase mutant, PA01 Δ *lasI* Δ *rhII*[pME6032] are significantly less than the WT carrying the empty vector (92.5%) and mimic the level observed with the *lasI* mutant alone.

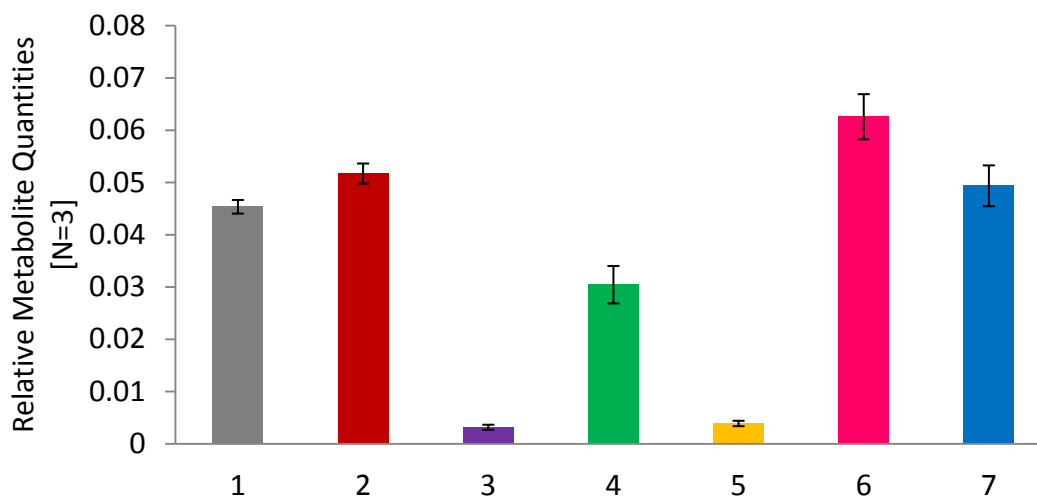


Figure 6.3: LC-MS/MS analysis of late exponential phase cultures revealed MTA levels decrease upon removal of the AHL synthases from the native *P. aeruginosa* background. Intracellular accumulation of MTA as determined by LC-MS analysis in seven *P. aeruginosa* strains PA01 (1), PA01[pME6032] (2), PA01 Δ lasI[pME6032] (3), PA01 Δ rbII[pME6032] (4), PA01 Δ lasI Δ rbII[pME6032] (5), PA01 Δ lasI[pME-*lasI_{pd}*] (6) and PA01 Δ rbII[pME-*rbII_{pd}*] (7) grown in LB with (2, 3, 4, 5, 6, 7) and without (1) IPTG induction. Peak area corresponding to MTA was divided by the peak area of the appropriate internal standard for normalisation.

Furthermore, complementation of the *P. aeruginosa lasI* and *rhlI* single gene mutants with the individual AHL synthase constructs pME-*lasI*_{Pa} and pME-*rhlI*_{Pa} (Chapter 3) causes intracellular MTA to be restored approximately back to WT levels.

6.5 Growth defects of *P. aeruginosa* AHL synthase mutants

Given the fitness implications of heterologous expression of *lasI* and *rhlI* mentioned in Chapter 3, it seemed appropriate to investigate whether the mutation of these genes in the native host would additionally impact upon the growth of the organism. The growth profiles were determined by growing the PA01 WT, mutant and complemented strains in nutrient rich LB media and measuring OD₆₀₀ values every 2 h over 12 h. The PA01Δ*rhlI*[pME6032] grows similarly to PA01[pME6032] with an approximate 1 h delay in doubling time that is most apparent during the exponential phase of growth. In contrast, the growth profiles of the *lasI* and *lasI/rhlI* mutants illustrate most deviation from the WT/empty vector strain; both mutants take 6-7 h before exponential growth is initiated leading to a more detrimental 3 h lag in comparison to PA01[pME6032]. Complementation of the *lasI* mutant with pME-*lasI*_{Pa} almost completely restores the growth defect, whilst complementation of the *rhlI* mutant with pME-*rhlI*_{Pa} re-establishes the defective growth profile and improves fitness even better than the WT.

Under more challenging conditions, when nutritional resources in the environment are limited, the compromised growth of the various mutants is highlighted further. In comparison to growth in LB media, it takes approximately 3 h longer for the WT control to attain stationary phase status, totalling 10 h from set up of the experiment. In contrast, the *lasI* and *rhlI* mutants appear to experience fitness difficulties; the length of the lag phase is prolonged to approximately 6 h for both, but the *rhlI* mutant demonstrates exponential growth at a higher OD₆₀₀ value leading to an hour's difference between the two strains.

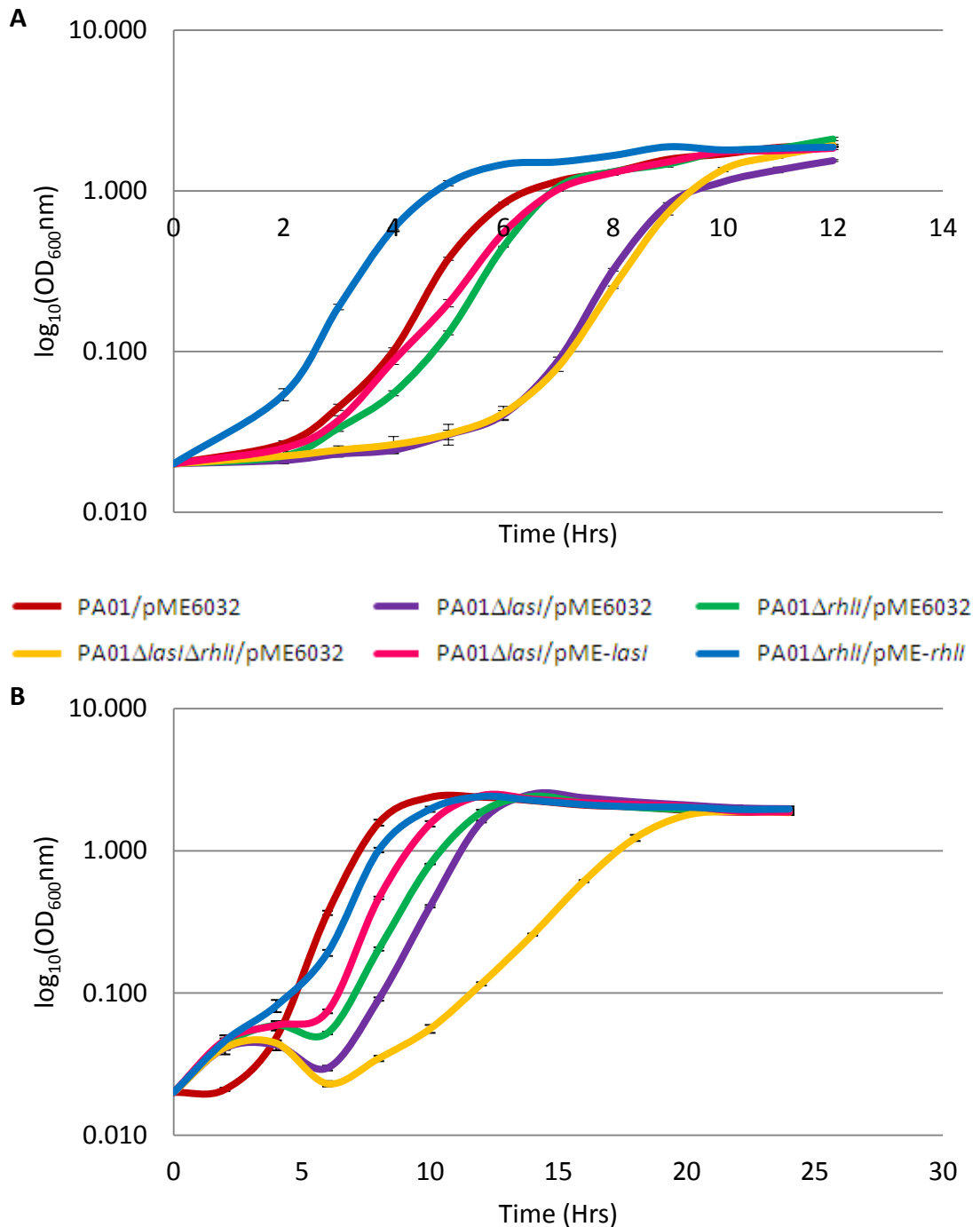


Figure 6.4: Removal of the AHL synthase genes from *P. aeruginosa* PA01 results in a growth defect that is more apparent when *lasI* is taken out of the system. Six strains PA01[pME6032], PA01Δ*lasI*[pME6032], PA01Δ*rhII*[pME6032], PA01Δ*lasI*Δ*rhII*[pME6032], PA01Δ*lasI*[pME-*lasI*_{pd}] and PA01Δ*rhII*[pME-*rhII*_{pd}] were inoculated into 125 ml LB (A) or CDM (B), IPTG induced and grown shaking at 37°C in 500 ml-Erlenmeyer flasks. 1 ml samples were taken at regular intervals and measured with a spectrophotometer. The cell density (OD₆₀₀) is plotted against time.

In comparison to the other strains tested, PA01 possessing the dual *lasI/rhlI* mutations suffers the greatest fitness difficulties; the OD₆₀₀ fluctuates below 0.050 for 10 h, taking approximately 12 h for exponential growth to be initiated. Furthermore, the rate of exponential growth is significantly slower, with OD₆₀₀ values doubling every 2 h in comparison to 1 h with the WT and other mutants.

6.6 Discussion

The previous chapters have focused on the metabolic complications of the *P. aeruginosa* AHL synthase genes in the context of *E. coli*. A parallel investigation into the implications of removing these genes from the native host has revealed the reciprocal accumulation of specific intracellular metabolites. However, the reasons behind the compromised fitness of corresponding mutants remain unclear. The inactivation of the *rhl* system by mutating *rhlI* led to increased production of AHLs with longer acyl side chains and correlates with the heterologous production of AHLs mentioned in Chapter 3. In these environmental circumstances, the supply of metabolic substrates and energy resource is no longer shared between two AHL synthase enzymes; instead LasI has a plentiful supply of SAM and increases synthesis of its repertoire of products. This includes the generation of AHLs not normally observed under WT conditions because the absence of RhlI alters the availability of substrates for LasI. As mentioned previously, the active site of LasI is likely to be less obstructive than that of RhlI and can accommodate a wider range of acyl-ACPs (Gould *et al.* 2006). In contrast, the mutation of *lasI* is associated with considerably reduced RhlI activity; AHL production is limited to C₄-HSL production and to significantly lower levels than in the WT. In these circumstances, the absence of the LasI means that OC₁₂-HSL cannot be synthesised. As a result, the activated transcriptional regulator protein-AHL complex (LasR-OC₁₂-HSL) is not formed leading to the absence of the positive regulation of the *rhlR* gene; in turn this reduces the amount of RhlI-C₄-HSL in the cell and overall this negatively impacts upon the positive regulatory feedback loop existing within the *rhl* system. Furthermore, the absence of both of the AHL synthase genes of *P. aeruginosa* not only completely abolishes production of AHLs, but

additionally the entire repertoire of AQS; the latter makes sense considering the loss of the upper hierarchy of the entire QS circuit.

The quantification of relevant intracellular metabolites revealed increased levels in all cases and with all mutations of the *P. aeruginosa* AHL synthase genes. The exception was SAH, levels of which remained reasonably reduced amongst all the mutant strains tested. Since mutation of an AHL synthase disrupts the QS system reducing the production of AHLs there is an accumulation of the HSL substrate (SAM). It is possible that this triggers an intracellular response leading to a reduction in the flux through the AMC and a channelling of metabolites through alternative pathways. Such a response may be mediated through changes in enzyme kinetics or expression of genes encoding the enzymes required for the pathway. The disruption to QS negatively impacts upon AHL production and leads to reduced synthesis of the associated MTA by-product. The lowest levels of MTA are observed with the *lasI* and *lasI/rhlI* mutants given that they cause production of their associated AHLs to be abolished to the greatest extent.

The compromised fitness levels of the *P. aeruginosa* AHL synthase mutants illustrate the dependency and consequences of QS. Despite the increase in availability of intracellular metabolic resources and overall saving on the expense of not producing the associated signal molecules, the mutants all demonstrate independent growth defects that are most detrimental upon mutation of the *lasI* gene in the native host. In these circumstances, fitness determines growth ability by measuring the rate of multiplication. It therefore remains uncertain as to whether the growth defect stems directly or indirectly from the interruption to the QS hierarchical system. Reduced fitness could be a combinatorial and subsequent consequence of the varying effects on virulence factor production or attributed directly to the QS regulation of specific genes which are essential for growth.

Overall the metabolic repercussions associated with the *P. aeruginosa* AHL synthase mutants support what has been observed with their heterologous expression in the *E. coli* background in the previous chapters.

Chapter 7

General discussion

The principal objective of this study was to investigate the metabolic consequences of the *P. aeruginosa* AHL synthase genes. In order to fulfill their independent, yet integral biological roles amongst the complex, hierarchical QS cascade, they heavily depend on sourcing the appropriate substrates from the AMC and fatty acid biosynthesis pathway. However, the metabolic sources and specific substrates for QSSMs do not only serve the synthases making signaling molecules for cell-cell communication, but have numerous roles which are important to other processes necessary for the maintenance of cellular homeostasis. Given that QS is fundamental to the organism's expression of a multitude of virulence traits and ultimate pathogenicity, investigation into the preliminary biosynthetic mechanisms could offer more feasible routes in the development of novel therapeutic strategies for combating this persistent "superbug".

Through expression of *lasI_{Pa}* and *rhlI_{Pa}* in the chosen heterologous host, a strain of *E. coli* (MG1655), it was possible to determine the metabolic impact caused by the biosynthetic activity of each gene. As hypothesised, within this background, both proteins led to significant reductions in the intracellular pool of metabolites of the AMC. Interestingly, *lasI_{Pa}* was associated with metabolite disturbances of a greater severity compared to *rhlI_{Pa}*; this was observed in conjunction with an unexpected phenotype for LasI, which generated a larger repertoire of AHLs than detected in the natural *P. aeruginosa* host. Although this had been reported previously, some of the AHLs observed here were novel to this study (C₁₂-HSL and C₁₄-HSL). As mentioned in section 3.11, this is likely to be due to the difference in availability of acyl-ACP precursors and the need to maintain the most kinetically favourable reaction mechanism. Future work in this area could investigate the pool of fatty acid precursors posing as feasible substrates for the synthases in *E. coli* alongside their relative abundance in this host. Further manipulation of the substrate pool to investigate whether the resulting AHL repertoire is altered could also reveal new information on the range of potential substrates, which has the possibility to assist improved design of inhibitory compounds.

Both synthases drew significantly from the metabolic pathway investigated as levels of all metabolites of the AMC were found to be significantly reduced when the synthases were

active. Intracellular SAM levels experienced the most drastic alterations. As emphasised throughout, SAM is fundamentally important to the cell, with diverse biological roles in polyamine biosynthesis, bacterial chemotaxis and methylation. In addition, more recently, the significance of SAM to QS has been illustrated through its contribution to the synthesis of a relatively newly discovered class of signals in *Vibrio cholera*, referred to as *cholerae* autoinducer-1 (CAI-1) (Miller *et al.* 2002; Higgins *et al.* 2007; Winans 2011). SAM is the source of an amine group to the synthase of CAI-1 (CqsA, *cholerae* quorum-sensing autoinducer), reacting with decanoyl-CoA to yield a variation of CAI-1 referred to as 3-aminotridec-2-en-4-one or Ea-CAI-1 (Wei *et al.* 2011; Winans 2011). This is intriguing given that SAM provides the HSL moiety for synthesis of AHLs and the related AMC metabolite SRH, the substrate for AI-2 (Moré *et al.* 1996, Jiang *et al.* 1998, Schauder *et al.* 2001).

The metabolic profiling performed here in the *E. coli* background has enabled the metabolic consequences of AHL synthesis to be determined in a system lacking complications due to hierarchical QS control. However, one of the uncertainties with the chosen strategy concerns the unknown mechanism for export of the “foreign” signals since there is no known equivalent to the *P. aeruginosa* MexGHI system in *E. coli*. Under these circumstances, the observance of AHLs in culture supernatants could be due to their potentially toxic nature leading to cell death, lysis, and the release of intracellular contents into the surrounding environment. This could be clarified by performing viability assays such as live/dead staining and/or a colony forming units (CFU) count, both of which should be compared to the WT strain.

More specifically, the chosen expression system could potentially be criticised for variability, given the difference in synthase production as determined by protein levels assessed via different methods (SDS-PAGE and Western blotting). However, both were expressed from constructs created using the same strategy and with the same expression conditions. Nevertheless, one alternative approach would involve integrating the genes of interest into a non-essential region of the host’s genome thereby ensuring comparable expression levels and subsequent conclusions.

Another important consideration is the difference between the steps required to detoxify SAH that exist in the AMC of *E. coli* and *P. aeruginosa*. The conversion of SAH to HCY in *E. coli* requires two enzymatic steps which are replaced by a single one in *P. aeruginosa*. Therefore, the production and profiling of the additional AMC metabolite (SRH) and reaction by-products (AI-2) has been monitored. Changes in these molecules may have had effects on bacterial physiology which would have been restricted to the experiments performed in *E. coli*. Despite these differences, the data presented here clearly shows that the overarching influence that AHL synthesis has on the AMC is mirrored in the two bacterial species.

It is interesting to speculate why there is an absence of LuxS from *P. aeruginosa* with SAH hydrolase performing an analogous role. With the exception of *Bifidobacterium longum* and *Escherichia blattae*, which possess both variants of the AMC, organisms possess either LuxS or SAH hydrolase. As mentioned previously, the exchange of enzymes cannot simply be explained by the need to have LuxS to generate AI-2 to act solely as a QSSM because many organisms including *Campylobacter jejuni*, *Helicobacter pylori* and *Neisseria meningitidis*, primarily rely on the metabolic function of LuxS (Holmes *et al.* 2009; Doherty *et al.* 2010; Heurlier *et al.* 2009). Indeed, the absence of AI-2 from some bacteria casts doubt on its use as a universal language for interspecies communication. If AI-2 is the universal QSSM, why do some bacteria produce the signal and others not? The success of a bacterial population is governed by its ability to progress in an infection and as with all environments, populations are constantly trying to outcompete each other; it makes no sense to communicate in an identical manner between all of them!

Further evidence for the metabolic costs of QSSM production in the associated host has come from the use of MG1655 mutants, in which genes have been removed that encode enzymes of the AMC or *sdhA*, another gene thought to be involved in QS (Chapter 5). Those mutants (*pfs* and *luxS*) harboring disruptions of the AMC limited the cumulative AHL concentrations observed compared to those reported in the WT strain. As expected, this was due to the inability to complete the recycling process and the consequential impact on the levels of linked metabolites. An equivalent study within *P.*

aeruginosa would involve using mutants where the SAH hydrolyse enzyme has been inactivated. Preliminary findings indicate that an *abcY* mutation has little impact on the resulting QSSM profile (Heurlier *et al.* unpublished). However, the associated growth defect has led to difficulties with characterizing aspects of virulence factor production and further investigations are necessary for a definitive conclusion (Heurlier *et al.* unpublished). On the other hand, the expression of *lasI_{Pa}* and *rhII_{Pa}* had opposing effects in the *sdzA* mutant. Currently, not enough is known about the role of *sdzA* in *E. coli* to provide a feasible explanation for the observations described here. Light could be shed on the underlying molecular mechanisms by performing global metabolite profiling (including flux analysis), transcriptomic and post-translational proteomics. Such investigations would identify changes occurring within the cells in the different conditions, thereby highlighting likely players in the modulations.

By constructing single synthase gene complementations, it was possible to gain the first unequivocal evidence for an impact on metabolism in the native *P. aeruginosa* background. Further insight might be possible by creating a double *lasI_{Pa}/rhII_{Pa}* expression vector that would enable future metabolic studies and complementation of those findings reported in Chapter 3. In addition, a double *lasI_{Pa}/rhII_{Pa}* expression vector could be used to restore the *P. aeruginosa* dual mutant strain used in Chapter 6, which would again have provided further supporting evidence for the metabolic complications caused by both AHL based systems together.

Studies incorporating a metabolomic approach often integrated with proteomic and transcriptomic analyses have become popular over the past few years due to the move towards an integrated, systems approach to understand biological phenomena. What these have lacked is focus on quantifying the metabolome which is often directly or indirectly affected by many of the processes under investigation. This study has heavily exploited LC-MS/MS based separation/detection methods for profiling metabolites specific to the AMC alongside the AHL biosynthesis by-product, MTA. A parallel study for characterizing the consequences of PQS biosynthesis offers an interesting area with potential for future research. As it would be hypothesized that this QS system would also

cause a drain on the metabolic pool and would generate new hypotheses concerning the integration of the parallel PQS and AHL QS circuits within *P. aeruginosa*. Such studies would allow reflection on the metabolic influence of AHL production upon PQS biosynthesis and therefore enable complete profiling of a wider repertoire of compounds affected by the synthesis of all the QSSMs observed in *P. aeruginosa*. Interestingly, recent investigation into this area has revealed a growth phase-differential regulation of anthranilate metabolism; this involves an antagonistic interplay of LasR, RhlR, and QscR that is mediated by two intermediate regulators, AntR, involved in anthranilate degradation, and PqsR, and their cofactors, anthranilate and PQS (Choi *et al.* 2011). Further insight might come from the development of a novel LC-MS/MS analytical method for simultaneous detection of several associated compounds involved in this synthetic pathway, including catechol, kynurenine and tryptophan; this was in fact initiated during the early phases of this study. The preliminary phases of method development were successful in being able to simultaneously detect most of the compounds. Further work is required to overcome some of the challenges encountered and progress it into a fully functional detection method. This primarily involves testing various extraction methods to determine which is most suitable for the array of compounds under selection to optimize their detection in biological samples.

As with all biomedical research, final thoughts lead to potential therapeutic applications. The ultimate question is whether there are any targets for novel anti-pseudomonas agents? To date, anti-QS strategies have been clustered into three main categories according to their mode of attack: blockage of QSSM biosynthesis, inactivation of QSSMs and interference with the signal receptor (Rasmussen & Givskov 2006). However, there are multiple enzymes contributing to the various aspects of metabolism which offer alternative targets for bacterial anti-infective drug design via interference with the associated AHL-based QS system. Table 8.1 lists a selection of targets coupled with feasible inhibitors which have been developed to date. Although, not all can be applied to *P. aeruginosa*, they highlight the plethora of examples relevant to the metabolic systems mentioned within this study. Many approaches use transition state analogue inhibitors

that mimic the enzyme's high-affinity for the intermediate, which is stronger than the equivalent substrate or product analogues, and lacks the accompanying chemical reaction. Several are interesting in that they elicit target inhibition without a direct bactericidal effect. This means that as well as blocking the target enzyme's active site, the inhibitors lead to the accumulation of specific metabolites which affect other aspects of the cell. For example, 5'-methylthioadenosine/*S*-adenosylhomocysteine nucleosidases (MTANs) have a multitude of functions, and as well as those mentioned previously, they are involved in processing 5'-deoxyadenosine (5'-dADO) produced by SAM radical enzymes. In these circumstances, inactivation of MTANs prevents degradation of 5'-dADO leading to alterations in vitamin synthesis with knock-on effects on central carbon metabolism. The similarity in enzyme transition states between the bacterial nucleoside and mammalian phosphorylase is worth mentioning. However, there are distinct structural differences, relating to the size of the 5'-alkylthio binding pocket and the distribution of electrostatic regions, which enable specificity for targeted drug design (Lee *et al.* 2004).

The site-directed mutagenesis strategy adopted in this study offers vast potential for future investigation and therapeutics. It is hypothesised that the targeted approach to mutagenesis will enable an in depth understanding of the specificity of AHL synthases and the underlying catalytic mechanism for AHL synthesis. Despite indications of the importance of particular synthase residues, it was impossible to anticipate the outcome of these investigations. An interesting finding came from the substitution of a phenylalanine residue from LasI (F27L) with the initial round of mutagenesis, creating a functional protein with partial activity, which led to the construction of further mutants. Overall, this has direct implication on the possibilities for future work; the residues chosen here could be mutated differently or alternative critical residues subjected to mutagenesis to allow a greater interrogation of substrate binding and prediction of interactions with current drugs. Ultimately, this could lead to the improved design of inhibitors undergoing current development and the design of new inhibitors which directly affect LasI and RhII signal producing ability.

Throughout the course of this study, little has been published on the interrelationship between QS and metabolism. Our understanding of regulatory aspects within the QS hierarchical cascade, however, has been extended. In terms of the additional *P. aeruginosa* LuxR homologues mentioned in Table 1.3, a crystal structure for the QscR signal receptor has been determined and as anticipated, it is consistent with an allosteric mechanism of signal transmission in the regulation of DNA binding and thus virulence gene expression (Lintz *et al.* 2011). In addition, Croda-García *et al.* (2011) have shown that the virulence factor regulator, Vfr (Table 1.3), directly regulates the transcription of *rbfR* by binding to several Vfr-binding sites present in the *rbfR* promoter region. On another note, given the history of research into QS, it is astonishing that until recently, the mechanism for determining the signal threshold has remained unknown. Interestingly, however, Seet and Zhanga (2011) have identified and characterised a novel anti-activator, QslA, which influences the threshold concentration of QS signal needed for QS activation and has been shown to directly regulate LasR.

The metabolic approach to studying *P. aeruginosa* QS offers an alternative strategy to the exhaustive characterisation of the organism's virulence factor production. As a comparison, it can give a multitude of information, often simultaneously that is similar to other modern day techniques such as microarray analysis. Integrated together, however, this can offer more promising routes to the development of novel therapeutics to combating *P. aeruginosa* in the current climate where its infection rates are increasing exponentially.

Enzyme Target	Function	Inhibitory Mode of Action	References
5'-methylthioadenosine/ S-adenosylhomocysteine nucleosidase (MTAN)	Dual function; catalyses the bioconversion of substrate SAH into SRH and adenine. Also the conversion of MTA to MTR.	Immucillin-based transition state analogue inhibitors of <i>E. coli</i> and <i>V. cholera</i> MTAN; slow-onset and tight-binding properties allowing persistence over several generations. Disrupt AI-2 production and biofilm formation, rather than antimicrobial activity	Schramm <i>et al.</i> (2008); Gutierrez <i>et al.</i> (2009)
5'-methylthioadenosine/ S-adenosylhomocysteine nucleosidase (MTAN)	Dual function; catalyses the bioconversion of substrate SAH into SRH and adenine. Also the conversion of MTA to MTR.	High potency purine and deaza purine-based inhibitors. High potency indazole-based inhibitors. Antimicrobial activities reported for <i>Neisseria meningitides</i> , <i>Streptococcus pneumonia</i> and <i>Streptococcus pyogenes</i> in both studies.	Tedder <i>et al.</i> (2004) Li <i>et al.</i> (2003)
5'-methylthioinosine phosphorylase (MTIP)	Processes MTI as part of MTA catabolism; MTA is hypothesised to be converted to MTI via a MTA deaminase, and MTI is then converted to 5'-methylthioribose α -D-1-phosphate (MTR-1-P) and hypoxanthine.	Transition state analogue inhibitors based on immucillins (developed for N-ribosyl transferases) which block MTIP activity; induce slow-onset inhibition and do not interfere with human 5'-methylthioadenosine phosphorylase (MTAP).	Guan <i>et al.</i> (2011)
S-adenosylhomocysteine (SAH) hydrolase	Reversibly hydrolyses SAH to HCY and adenosine as part of the AMC.	Structural analogues based on ilimaquinone, which functions as a nucleoside analogue, hybridised to adenosine.	Byung Gyu <i>et al.</i> (2009)
S-adenosylhomocysteine (SAH) hydrolase	Reversibly hydrolyses SAH to HCY and adenosine as part of the AMC.	Metal coordination compounds: cis and trans isomers of platinum diammine dichloride (DDP); tested with <i>Acinetobacter calcoaceticus</i>	Impagnateiello <i>et al.</i> (1996)

S-adenosylmethionine (SAM) synthetase	Involved in the only known biosynthetic to SAM from L-methionine and ATP substrates	enzyme Most potent known inhibitor is diimidotriphosphate ($O_3PNH-PO_2-NH-PO_3$; PNPNP), which is a non-hydrolyzable slow, tight binding intermediate analogue	Markham & Reczkowski (2003); Reczkowski & Markham (1999)
--	---	--	--

Table 8.1: Metabolic enzyme targets for inhibition of QS. Targets indicated in bold have applications in *P. aeruginosa*.

Bibliography

Anzai, Y., Kim, H., Park, J.Y., Wakabayashi, H. & Oyaizu, H. 2000, "Phylogenetic affiliation of the pseudomonads based on 16S rRNA sequence", *International Journal of Systematic and Evolutionary Microbiology*, vol. 50 Pt 4, pp. 1563-1589.

Armstrong, S., Yates, S.P. & Merrill, A.R. 2002, "Insight into the catalytic mechanism of *Pseudomonas aeruginosa* exotoxin A. Studies of toxin interaction with eukaryotic elongation factor-2", *The Journal of Biological Chemistry*, vol. 277, no. 48, pp. 46669-46675.

Arora, S.K., Ritchings, B.W., Almira, E.C., Lory, S. & Ramphal, R. 1998, "The *Pseudomonas aeruginosa* flagellar cap protein, FliD, is responsible for mucin adhesion", *Infection and Immunity*, vol. 66, no. 3, pp. 1000-1007.

Babitzke, P. & Romeo, T. 2007, "CsrB sRNA family: sequestration of RNA-binding regulatory proteins", *Current Opinion in Microbiology*, vol. 10, no. 2, pp. 156-163.

Bajolet-Laudinat, O., Girod-de Bentzmann, S., Tournier, J.M., Madoulet, C., Plotkowski, M.C., Chippaux, C. & Puchelle, E. 1994, "Cytotoxicity of *Pseudomonas aeruginosa* internal lectin PA-I to respiratory epithelial cells in primary culture", *Infection and Immunity*, vol. 62, no. 10, pp. 4481-4487.

Bassler, B.L., Greenberg, E.P. & Stevens, A.M. 1997, "Cross-species induction of luminescence in the quorum-sensing bacterium *Vibrio harveyi*", *Journal of Bacteriology*, vol. 179, no. 12, pp. 4043-4045.

Bassler, B.L., Wright, M., Showalter, R.E. & Silverman, M.R. 1993, "Intercellular signalling in *Vibrio harveyi*: sequence and function of genes regulating expression of luminescence", *Molecular Microbiology*, vol. 9, no. 4, pp. 773-786.

Beatson, S.A., Whitchurch, C.B., Semmler, A.B. & Mattick, J.S. 2002, "Quorum sensing is not required for twitching motility in *Pseudomonas aeruginosa*", *Journal of Bacteriology*, vol. 184, no. 13, pp. 3598-3604.

Bera, A.K., Atanasova, V., Robinson, H., Eisenstein, E., Coleman, J.P., Pesci, E.C. & Parsons, J.F. 2009, "Structure of PqsD, a *Pseudomonas* quinolone signal biosynthetic enzyme, in complex with anthranilate", *Biochemistry*, vol. 48, no. 36, pp. 8644-8655.

Bjarnsholt, T. & Givskov, M. 2008, "Quorum sensing inhibitory drugs as next generation antimicrobials: worth the effort?", *Current Infectious Disease Reports*, vol. 10, no. 1, pp. 22-28.

Blackwood, L.L., Stone, R.M., Iglewski, B.H. & Pennington, J.E. 1983, "Evaluation of *Pseudomonas aeruginosa* exotoxin A and elastase as virulence factors in acute lung infection", *Infection and Immunity*, vol. 39, no. 1, pp. 198-201.

Bodor, A.M., Jansch, L., Wissing, J. & Wagner-Dobler, I. 2011, "The luxS mutation causes loosely-bound biofilms in *Shewanella oneidensis*", *BMC Research Notes*, vol. 4, pp. 180.

Botsford, J.L. & Harman, J.G. 1992, "Cyclic AMP in prokaryotes", *Microbiological Reviews*, vol. 56, no. 1, pp. 100-122.

Brint, J.M. & Ohman, D.E. 1995, "Synthesis of multiple exoproducts in *Pseudomonas aeruginosa* is under the control of RhIR-RhII, another set of regulators in strain PAO1 with homology to the autoinducer-responsive LuxR-LuxI family", *Journal of Bacteriology*, vol. 177, no. 24, pp. 7155-7163.

Britigan, B.E., Rasmussen, G.T. & Cox, C.D. 1997, "Augmentation of oxidant injury to human pulmonary epithelial cells by the *Pseudomonas aeruginosa* siderophore pyochelin", *Infection and Immunity*, vol. 65, no. 3, pp. 1071-1076.

Burmolle, M., Webb, J.S., Rao, D., Hansen, L.H., Sorensen, S.J. & Kjelleberg, S. 2006, "Enhanced biofilm formation and increased resistance to antimicrobial agents and

bacterial invasion are caused by synergistic interactions in multispecies biofilms", *Applied and Environmental Microbiology*, vol. 72, no. 6, pp. 3916-3923.

Cacalano, G., Kays, M., Saiman, L. & Prince, A. 1992, "Production of the *Pseudomonas aeruginosa* neuraminidase is increased under hyperosmolar conditions and is regulated by genes involved in alginate expression", *The Journal of Clinical Investigation*, vol. 89, no. 6, pp. 1866-1874.

Challan Belval, S., Gal, L., Margiewes, S., Garmyn, D., Piveteau, P. & Guzzo, J. 2006, "Assessment of the roles of LuxS, S-ribosyl homocysteine, and autoinducer 2 in cell attachment during biofilm formation by *Listeria monocytogenes* EGD-e", *Applied and Environmental Microbiology*, vol. 72, no. 4, pp. 2644-2650.

Chen, X., Schauder, S., Potier, N., Van Dorsselaer, A., Pelczer, I., Bassler, B.L. & Hughson, F.M. 2002, "Structural identification of a bacterial quorum-sensing signal containing boron", *Nature*, vol. 415, no. 6871, pp. 545-549.

Choi, Y., Park, H.Y., Park S.J., Park, S.J., Kim, S.K., Ha, C., Im, S.J. & Lee, J.H. 2011, "Growth phase-differential quorum sensing regulation of anthranilate metabolism in *Pseudomonas aeruginosa*", *Molecular Cells*, vol. 32, no. 1, pp. 57-65.

Chugani, S.A., Whiteley, M., Lee, K.M., D'Argenio, D., Manoil, C. & Greenberg, E.P. 2001, "QscR, a modulator of quorum-sensing signal synthesis and virulence in *Pseudomonas aeruginosa*", *Proceedings of the National Academy of Sciences of the United States of America*, vol. 98, no. 5, pp. 2752-2757.

Coleman, J.P., Hudson, L.L., McKnight, S.L., Farrow, J.M., 3rd, Calfee, M.W., Lindsey, C.A. & Pesci, E.C. 2008, "*Pseudomonas aeruginosa* PqsA is an anthranilate-coenzyme A ligase", *Journal of Bacteriology*, vol. 190, no. 4, pp. 1247-1255.

Collier, D.N., Anderson, L., McKnight, S.L., Noah, T.L., Knowles, M., Boucher, R., Schwab, U., Gilligan, P. & Pesci, E.C. 2002, "A bacterial cell to cell signal in the lungs of cystic fibrosis patients", *FEMS Microbiology Letters*, vol. 215, no. 1, pp. 41-46.

Comolli, J.C., Waite, L.L., Mostov, K.E. & Engel, J.N. 1999, "Pili binding to asialo-GM1 on epithelial cells can mediate cytotoxicity or bacterial internalization by *Pseudomonas aeruginosa*", *Infection and Immunity*, vol. 67, no. 7, pp. 3207-3214.

Costerton, J.W. 1995, "Overview of microbial biofilms", *Journal of Industrial Microbiology*, vol. 15, no. 3, pp. 137-140.

Croda-García, G., Grosso-Becerra, V., Gonzalez-Valdez, A., Servín-González, L. & Soberón-Chávez, G., 2011, "Transcriptional regulation of *Pseudomonas aeruginosa* *rhIR*: role of the CRP orthologue Vfr (virulence factor regulator) and quorum-sensing regulators LasR and RhIR", *Microbiology*, vol. 157, no. 9, pp. 2545-2555.

D'Argenio, D.A., Calfee, M.W., Rainey, P.B. & Pesci, E.C. 2002, "Autolysis and autoaggregation in *Pseudomonas aeruginosa* colony morphology mutants", *Journal of Bacteriology*, vol. 184, no. 23, pp. 6481-6489.

de Kievit, T., Seed, P.C., Nezezon, J., Passador, L. & Iglewski, B.H. 1999, "RsaL, a novel repressor of virulence gene expression in *Pseudomonas aeruginosa*", *Journal of Bacteriology*, vol. 181, no. 7, pp. 2175-2184.

De Lay, N. & Gottesman, S. 2009, "The Crp-activated small noncoding regulatory RNA CyaR (RyeE) links nutritional status to group behavior", *Journal of Bacteriology*, vol. 191, no. 2, pp. 461-476.

DeLisa, M.P., Wu, C.F., Wang, L., Valdes, J.J. & Bentley, W.E. 2001, "DNA microarray-based identification of genes controlled by autoinducer 2-stimulated quorum sensing in *Escherichia coli*", *Journal of Bacteriology*, vol. 183, no. 18, pp. 5239-5247.

Della Ragione, F., Porcelli, M., Carteni-Farina, M., Zappia, V. & Pegg, A.E. 1985, "*Escherichia coli* S-adenosylhomocysteine/5'-methylthioadenosine nucleosidase. Purification, substrate specificity and mechanism of action", *The Biochemical Journal*, vol. 232, no. 2, pp. 335-341.

- Diggle, S.P., Cornelis, P., Williams, P. & Camara, M. 2006, "4-quinolone signalling in *Pseudomonas aeruginosa*: old molecules, new perspectives", *International Journal of Medical Microbiology : IJMM*, vol. 296, no. 2-3, pp. 83-91.
- Diggle, S.P., Winzer, K., Lazdunski, A., Williams, P. & Camara, M. 2002, "Advancing the quorum in *Pseudomonas aeruginosa*: MvaT and the regulation of *N*-acylhomoserine lactone production and virulence gene expression", *Journal of Bacteriology*, vol. 184, no. 10, pp. 2576-2586.
- Doherty, N.C., Shen, F., Halliday, N.M., Barrett, D.A., Hardie, K.R., Winzer, K. & Atherton, J.C. 2010, "In *Helicobacter pylori*, LuxS is a key enzyme in cysteine provision through a reverse transsulfuration pathway", *Journal of Bacteriology*, vol. 192, no. 5, pp. 1184-1192.
- Doig, P., Smith, N.R., Todd, T. & Irvin, R.T. 1987, "Characterization of the binding of *Pseudomonas aeruginosa* alginate to human epithelial cells", *Infection and Immunity*, vol. 55, no. 6, pp. 1517-1522.
- Doring, G., Conway, S.P., Heijerman, H.G., Hodson, M.E., Hoiby, N., Smyth, A. & Touw, D.J. 2000, "Antibiotic therapy against *Pseudomonas aeruginosa* in cystic fibrosis: a European consensus", *The European respiratory journal : Official Journal of the European Society for Clinical Respiratory Physiology*, vol. 16, no. 4, pp. 749-767.
- Driscoll, J.A., Brody, S.L. & Kollef, M.H. 2007, "The epidemiology, pathogenesis and treatment of *Pseudomonas aeruginosa* infections", *Drugs*, vol. 67, no. 3, pp. 351-368.
- Dunlap, P.V. & Greenberg, E.P. 1988, "Control of *Vibrio fischeri lux* gene transcription by a cyclic AMP receptor protein-luxR protein regulatory circuit", *Journal of Bacteriology*, vol. 170, no. 9, pp. 4040-4046.
- El Solh, A.A. & Alhajhusain, A. 2009, "Update on the treatment of *Pseudomonas aeruginosa* pneumonia", *The Journal of Antimicrobial Chemotherapy*, vol. 64, no. 2, pp. 229-238.

Elsheikh, L.E., Kronevi, T., Wretling, B., Abaas, S. & Iglewski, B.H. 1987, "Assessment of elastase as a *Pseudomonas aeruginosa* virulence factor in experimental lung infection in mink", *Veterinary Microbiology*, vol. 13, no. 3, pp. 281-289.

Essar, D.W., Eberly, L., Hadero, A. & Crawford, I.P. 1990a, "Identification and characterization of genes for a second anthranilate synthase in *Pseudomonas aeruginosa*: interchangeability of the two anthranilate synthases and evolutionary implications", *Journal of Bacteriology*, vol. 172, no. 2, pp. 884-900.

Essar, D.W., Eberly, L., Han, C.Y. & Crawford, I.P. 1990b, "DNA sequences and characterization of four early genes of the tryptophan pathway in *Pseudomonas aeruginosa*", *Journal of Bacteriology*, vol. 172, no. 2, pp. 853-866.

Eswar, N., Webb, B., Marti-Renom, M.A., Madhusudhan, M.S., Eramian, D., Shen, M.Y., Pieper, U. & Sali, A. 2007, "Comparative protein structure modeling using MODELLER", *Current Protocols in Protein Science*, vol. Chapter 2, pp. Unit 2.9.

Farrow, J.M., 3rd & Pesci, E.C. 2007, "Two distinct pathways supply anthranilate as a precursor of the *Pseudomonas* quinolone signal", *Journal of Bacteriology*, vol. 189, no. 9, pp. 3425-3433.

Finck-Barbancon, V., Goranson, J., Zhu, L., Sawa, T., Wiener-Kronish, J.P., Fleiszig, S.M., Wu, C., Mende-Mueller, L. & Frank, D.W. 1997, "ExoU expression by *Pseudomonas aeruginosa* correlates with acute cytotoxicity and epithelial injury", *Molecular Microbiology*, vol. 25, no. 3, pp. 547-557.

Fuqua, C. 2006, "The QscR quorum-sensing regulon of *Pseudomonas aeruginosa*: an orphan claims its identity", *Journal of Bacteriology*, vol. 188, no. 9, pp. 3169-3171.

Fuqua, W.C., Winans, S.C. & Greenberg, E.P. 1994, "Quorum sensing in bacteria: the LuxR-LuxI family of cell density-responsive transcriptional regulators", *Journal of Bacteriology*, vol. 176, no. 2, pp. 269-275.

- Gallagher, L.A. & Manoil, C. 2001, "*Pseudomonas aeruginosa* PAO1 kills *Caenorhabditis elegans* by cyanide poisoning", *Journal of Bacteriology*, vol. 183, no. 21, pp. 6207-6214.
- Gallagher, L.A., McKnight, S.L., Kuznetsova, M.S., Pesci, E.C. & Manoil, C. 2002, "Functions required for extracellular quinolone signaling by *Pseudomonas aeruginosa*", *Journal of Bacteriology*, vol. 184, no. 23, pp. 6472-6480.
- Gambello, M.J. & Iglewski, B.H. 1991, "Cloning and characterization of the *Pseudomonas aeruginosa lasR* gene, a transcriptional activator of elastase expression", *Journal of Bacteriology*, vol. 173, no. 9, pp. 3000-3009.
- Gambello, M.J., Kaye, S. & Iglewski, B.H. 1993, "LasR of *Pseudomonas aeruginosa* is a transcriptional activator of the alkaline protease gene (*apr*) and an enhancer of exotoxin A expression", *Infection and Immunity*, vol. 61, no. 4, pp. 1180-1184.
- George, A.M., Jones, P.M. & Middleton, P.G. 2009, "Cystic fibrosis infections: treatment strategies and prospects", *FEMS Microbiology Letters*, vol. 300, no. 2, pp. 153-164.
- Glick, J. & Garber, N. 1983, "The intracellular localization of *Pseudomonas aeruginosa* lectins", *Journal of General Microbiology*, vol. 129, no. 10, pp. 3085-3090.
- Gessard, C. 1882, "Sur les colorations bleue et verte des lignes a pansements", *Comptes rendus de l'Académie des Sciences Série D*, vol. 94, pp. 536-538.
- Gould, T.A., Herman, J., Krank, J., Murphy, R.C. & Churchill, M.E. 2006, "Specificity of acyl-homoserine lactone synthases examined by mass spectrometry", *Journal of Bacteriology*, vol. 188, no. 2, pp. 773-783.
- Gould, T.A., Schweizer, H.P. & Churchill, M.E. 2004, "Structure of the *Pseudomonas aeruginosa* acyl-homoserinelactone synthase LasI", *Molecular Microbiology*, vol. 53, no. 4, pp. 1135-1146.

Guan, R., Ho, M.C., Almo, S.C. & Schramm, V.L. 2011, "Methylthioinosine phosphorylase from *Pseudomonas aeruginosa*. Structure and annotation of a novel enzyme in quorum sensing", *Biochemistry*, vol. 50, no. 7, pp. 1247-1254.

Gutierrez, J.A., Crowder, T., Rinaldo-Matthis, A., Ho, M.C., Almo, S.C. & Schramm, V.L. 2009, "Transition state analogs of 5'-methylthioadenosine nucleosidase disrupt quorum sensing", *Nature Chemical Biology*, vol. 5, no. 4, pp. 251-257.

Halliday, N.M., Hardie, K.R., Williams, P., Winzer, K. & Barrett, D.A. 2010, "Quantitative liquid chromatography-tandem mass spectrometry profiling of activated methyl cycle metabolites involved in LuxS-dependent quorum sensing in *Escherichia coli*", *Analytical Biochemistry*, vol. 403, no. 1-2, pp. 20-29.

Hardie, K.R., Cooksley, C., Green, A.D. & Winzer, K. 2003, "Autoinducer 2 activity in *Escherichia coli* culture supernatants can be actively reduced despite maintenance of an active synthase, LuxS", *Microbiology (Reading, England)*, vol. 149, no. Pt 3, pp. 715-728.

Hartwell, L.H., Hood, L., Goldberg, M.L., Reynolds, A.E., Silver, L.M. & Veres, R.C. 2004, *Genetics: From Genes to Genomes*, 2nd edn, McGraw-Hill.

Hazlett, L.D., Moon, M.M., Singh, A., Berk, R.S. & Rudner, X.L. 1991, "Analysis of adhesion, piliation, protease production and ocular infectivity of several *P. aeruginosa* strains", *Current Eye Research*, vol. 10, no. 4, pp. 351-362.

Heeb, S., Blumer, C. & Haas, D. 2002, "Regulatory RNA as mediator in GacA/RsmA-dependent global control of exoproduct formation in *Pseudomonas fluorescens* CHA0", *Journal of Bacteriology*, vol. 184, no. 4, pp. 1046-1056.

Heeb, S., Kuehne, S.A., Bycroft, M., Crivii, S., Allen, M.D., Haas, D., Camara, M. & Williams, P. 2006, "Functional analysis of the post-transcriptional regulator RsmA reveals a novel RNA-binding site", *Journal of Molecular Biology*, vol. 355, no. 5, pp. 1026-1036.

Heurlier, K., Halliday, N., Ruparell, A., Matthijs, S., Cornelis, P., Hardie, K.R. & Winzer, K., " Role of the putative S-Adenosyl Homocysteine hydrolase AhcY of *Pseudomonas aeruginosa* PAO1", *in preparation*.

Heurlier, K., Vendeville, A., Halliday, N., Green, A., Winzer, K., Tang, C.M. & Hardie, K.R. 2009, "Growth deficiencies of *Neisseria meningitidis* *pfs* and *luxS* mutants are not due to inactivation of quorum sensing", *Journal of Bacteriology*, vol. 191, no. 4, pp. 1293-1302.

Heurlier, K., Williams, F., Heeb, S., Dormond, C., Pessi, G., Singer, D., Camara, M., Williams, P. & Haas, D. 2004, "Positive control of swarming, rhamnolipid synthesis, and lipase production by the posttranscriptional RsmA/RsmZ system in *Pseudomonas aeruginosa* PAO1", *Journal of Bacteriology*, vol. 186, no. 10, pp. 2936-2945.

Higgins, D.A., Pomianek, M.E., Kraml, C.M., Taylor, R.K., Semmelhack, M.F. & Bassler, B.L. 2007, "The major *Vibrio cholerae* autoinducer and its role in virulence factor production", *Nature*, vol. 450, no. 7171, pp. 883-886.

Hoang, T.T. & Schweizer, H.P. 1999, "Characterization of *Pseudomonas aeruginosa* enoyl-acyl carrier protein reductase (FabI): a target for the antimicrobial triclosan and its role in acylated homoserine lactone synthesis", *Journal of Bacteriology*, vol. 181, no. 17, pp. 5489-5497.

Hoang, T.T., Sullivan, S.A., Cusick, J.K. & Schweizer, H.P. 2002, "Beta-ketoacyl acyl carrier protein reductase (FabG) activity of the fatty acid biosynthetic pathway is a determining factor of 3-oxo-homoserine lactone acyl chain lengths", *Microbiology (Reading, England)*, vol. 148, no. Pt 12, pp. 3849-3856.

Holmes, K., Tavender, T.J., Winzer, K., Wells, J.M. & Hardie, K.R. 2009, "AI-2 does not function as a quorum sensing molecule in *Campylobacter jejuni* during exponential growth in vitro", *BMC Microbiology*, vol. 9, pp. 214.

- Hong, Y.Q. & Ghebrehiwet, B. 1992, "Effect of *Pseudomonas aeruginosa* elastase and alkaline protease on serum complement and isolated components C1q and C3", *Clinical Immunology and Immunopathology*, vol. 62, no. 2, pp. 133-138.
- Howe, T.R. & Iglewski, B.H. 1984, "Isolation and characterization of alkaline protease-deficient mutants of *Pseudomonas aeruginosa* in vitro and in a mouse eye model", *Infection and Immunity*, vol. 43, no. 3, pp. 1058-1063.
- Hughes, J.A., Brown, L.R. & Ferro, A.J. 1987, "Expression of the cloned coliphage T3 S-adenosylmethionine hydrolase gene inhibits DNA methylation and polyamine biosynthesis in *Escherichia coli*", *Journal of Bacteriology*, vol. 169, no. 8, pp. 3625-3632.
- Iglewski, B.H., Liu, P.V. & Kabat, D. 1977, "Mechanism of action of *Pseudomonas aeruginosa* exotoxin A: adenosine diphosphate-ribosylation of mammalian elongation factor 2 in vitro and in vivo", *Infection and Immunity*, vol. 15, no. 1, pp. 138-144.
- Iglewski, B.H., Sadoff, J., Bjorn, M.J. & Maxwell, E.S. 1978, "*Pseudomonas aeruginosa* exoenzyme S: an adenosine diphosphate ribosyltransferase distinct from toxin A", *Proceedings of the National Academy of Sciences of the United States of America*, vol. 75, no. 7, pp. 3211-3215.
- Impagnatiello, A., Franceschini, N., Oratore, A. & Bozzi, A. 1996, "Inhibition studies of S-adenosylhomocysteine hydrolase purified from *Acinetobacter calcoaceticus* ULA-501", *Biochimie*, vol. 78, no. 4, pp. 267-272.
- Jacob, F. 1973, *The logic of living systems: a history of heredity*. Alan Lane (Division of Penguin Books, Ltd), English translation by Betty E. Spillman, London, UK.
- Jensen, K.F. 1993, "The *Escherichia coli* K-12 "wild types" W3110 and MG1655 have an rph frameshift mutation that leads to pyrimidine starvation due to low *pyrE* expression levels", *Journal of Bacteriology*, vol. 175, no. 11, pp. 3401-3407.

- Jiang, Y., Camara, M., Chhabra, S.R., Hardie, K.R., Bycroft, B.W., Lazdunski, A., Salmond, G.P., Stewart, G.S. & Williams, P. 1998, "In vitro biosynthesis of the *Pseudomonas aeruginosa* quorum-sensing signal molecule *N*-butanoyl-L-homoserine lactone", *Molecular Microbiology*, vol. 28, no. 1, pp. 193-203.
- Juhas, M., Wiehlmann, L., Huber, B., Jordan, D., Lauber, J., Salunkhe, P., Limpert, A.S., von Gotz, F., Steinmetz, I., Eberl, L. & Tummeler, B. 2004, "Global regulation of quorum sensing and virulence by VqsR in *Pseudomonas aeruginosa*", *Microbiology (Reading, England)*, vol. 150, no. Pt 4, pp. 831-841.
- Kanamaru, K., Kanamaru, K., Tatsuno, I., Tobe, T. & Sasakawa, C. 2000, "SdiA, an *Escherichia coli* homologue of quorum-sensing regulators, controls the expression of virulence factors in enterohaemorrhagic *Escherichia coli* O157:H7", *Molecular Microbiology*, vol. 38, no. 4, pp. 805-816.
- Kessler, E., Safrin, M., Olson, J.C. & Ohman, D.E. 1993, "Secreted LasA of *Pseudomonas aeruginosa* is a staphylolytic protease", *The Journal of Biological Chemistry*, vol. 268, no. 10, pp. 7503-7508.
- Kim, B.G., Chun, T.G., Lee, H.Y. & Snapper, M.L. 2009, "A new structural class of *S*-adenosylhomocysteine hydrolase inhibitors", *Bioorganic and Medicinal Chemistry*, vol. 17, no. 18, pp. 6707-6714.
- Klockgether, J., Munder, A., Neugebauer, J., Davenport, C.F., Stanke, F., Larbig, K.D., Heeb, S., Schock, U., Pohl, T.M., Wiehlmann, L. & Tummeler, B. 2010, "Genome diversity of *Pseudomonas aeruginosa* PAO1 laboratory strains", *Journal of Bacteriology*, vol. 192, no. 4, pp. 1113-1121.
- Knight, D.A., Finck-Barbancon, V., Kulich, S.M. & Barbieri, J.T. 1995, "Functional domains of *Pseudomonas aeruginosa* exoenzyme S", *Infection and Immunity*, vol. 63, no. 8, pp. 3182-3186.

Kolb, A., Busby, S., Buc, H., Garges, S. & Adhya, S. 1993, "Transcriptional regulation by cAMP and its receptor protein", *Annual Review of Biochemistry*, vol. 62, pp. 749-795.

Konig, B., Jaeger, K.E., Sage, A.E., Vasil, M.L. & Konig, W. 1996, "Role of *Pseudomonas aeruginosa* lipase in inflammatory mediator release from human inflammatory effector cells (platelets, granulocytes, and monocytes)", *Infection and Immunity*, vol. 64, no. 8, pp. 3252-3258.

Krall, R., Schmidt, G., Aktories, K. & Barbieri, J.T. 2000, "*Pseudomonas aeruginosa* ExoT is a Rho GTPase-activating protein", *Infection and Immunity*, vol. 68, no. 10, pp. 6066-6068.

Kukor, J.J., Olsen, R.H. & Ballou, D.P. 1988, "Cloning and expression of the catA and catBC gene clusters from *Pseudomonas aeruginosa* PAO", *Journal of Bacteriology*, vol. 170, no. 10, pp. 4458-4465.

Lang, S. & Wullbrandt, D. 1999, "Rhamnose lipids--biosynthesis, microbial production and application potential", *Applied Microbiology and Biotechnology*, vol. 51, no. 1, pp. 22-32.

Latifi, A., Foglino, M., Tanaka, K., Williams, P. & Lazdunski, A. 1996, "A hierarchical quorum-sensing cascade in *Pseudomonas aeruginosa* links the transcriptional activators LasR and RhIR (VsmR) to expression of the stationary-phase sigma factor RpoS", *Molecular Microbiology*, vol. 21, no. 6, pp. 1137-1146.

Latifi, A., Winson, M.K., Foglino, M., Bycroft, B.W., Stewart, G.S., Lazdunski, A. & Williams, P. 1995, "Multiple homologues of LuxR and LuxI control expression of virulence determinants and secondary metabolites through quorum sensing in *Pseudomonas aeruginosa* PAO1", *Molecular Microbiology*, vol. 17, no. 2, pp. 333-343.

Ledgham, F., Ventre, I., Soscia, C., Foglino, M., Sturgis, J.N. & Lazdunski, A. 2003, "Interactions of the quorum sensing regulator QscR: interaction with itself and the other regulators of *Pseudomonas aeruginosa* LasR and RhIR", *Molecular Microbiology*, vol. 48, no. 1, pp. 199-210.

Lee, J.E., Settembre, E.C., Cornell, K.A., Riscoe, M.K., Sufrin, J.R., Ealick, S.E. & Howell, P.L. 2004, "Structural comparison of MTA phosphorylase and MTA/AdoHcy nucleosidase explains substrate preferences and identifies regions exploitable for inhibitor design", *Biochemistry*, vol. 43, no. 18, pp. 5159-5169.

Leid, J.G., Willson, C.J., Shirliff, M.E., Hassett, D.J., Parsek, M.R. & Jeffers, A.K. 2005, "The exopolysaccharide alginate protects *Pseudomonas aeruginosa* biofilm bacteria from IFN-gamma-mediated macrophage killing", *Journal of Immunology (Baltimore, Md.: 1950)*, vol. 175, no. 11, pp. 7512-7518.

Lequette, Y., Lee, J.H., Ledgham, F., Lazdunski, A. & Greenberg, E.P. 2006, "A distinct QscR regulon in the *Pseudomonas aeruginosa* quorum-sensing circuit", *Journal of Bacteriology*, vol. 188, no. 9, pp. 3365-3370.

Li, L.L., Malone, J.E. & Iglewski, B.H. 2007, "Regulation of the *Pseudomonas aeruginosa* quorum-sensing regulator VqsR", *Journal of Bacteriology*, vol. 189, no. 12, pp. 4367-4374.

Li, X., Chu, S., Feher, V.A., Khalili, M., Nie, Z., Margosiak, S., Nikulin, V., Levin, J., Sprankle, K.G., Tedder, M.E., Almasy, R., Appelt, K. & Yager, K.M. 2003, "Structure-based design, synthesis, and antimicrobial activity of indazole-derived SAH/MTA nucleosidase inhibitors", *Journal of Medicinal Chemistry*, vol. 46, no. 26, pp. 5663-5673.

Lintz, M.J., Oinuma, K., Wysoczynski, C.L., Greenberg, E.P. & Churchill M.E. 2011, "Crystal structure of QscR, a *Pseudomonas aeruginosa* quorum sensing signal receptor", *Proceedings of the National Academy of Sciences of the United States of America*, vol. 108, no. 38, pp. 15763-15768.

Lister, P.D., Wolter, D.J. & Hanson, N.D. 2009, "Antibacterial-resistant *Pseudomonas aeruginosa*: clinical impact and complex regulation of chromosomally encoded resistance mechanisms", *Clinical Microbiology Reviews*, vol. 22, no. 4, pp. 582-610.

- Lyczak, J.B., Cannon, C.L. & Pier, G.B. 2000, "Establishment of *Pseudomonas aeruginosa* infection: lessons from a versatile opportunist", *Microbes and Infection / Institut Pasteur*, vol. 2, no. 9, pp. 1051-1060.
- Mah, T.F., Pitts, B., Pellock, B., Walker, G.C., Stewart, P.S. & O'Toole, G.A. 2003, "A genetic basis for *Pseudomonas aeruginosa* biofilm antibiotic resistance", *Nature*, vol. 426, no. 6964, pp. 306-310.
- Markham, G.D. & Reczkowski, R.S. 2004, "Structural studies of inhibition of S-adenosylmethionine synthetase by slow, tight-binding intermediate and product analogues", *Biochemistry*, vol. 43, no. 12, pp. 3415-3425.
- Mavrodi, D.V., Bonsall, R.F., Delaney, S.M., Soule, M.J., Phillips, G. & Thomashow, L.S. 2001, "Functional analysis of genes for biosynthesis of pyocyanin and phenazine-1-carboxamide from *Pseudomonas aeruginosa* PAO1", *Journal of Bacteriology*, vol. 183, no. 21, pp. 6454-6465.
- Mayor, S. 2000, "Hospital acquired infections kill 5000 patients a year in England", *BMJ (Clinical research ed.)*, vol. 321, no. 7273, pp. 1370.
- McKnight, S.L., Iglewski, B.H. & Pesci, E.C. 2000, "The *Pseudomonas* quinolone signal regulates *rhl* quorum sensing in *Pseudomonas aeruginosa*", *Journal of Bacteriology*, vol. 182, no. 10, pp. 2702-2708.
- Meyer, J.M., Neely, A., Stintzi, A., Georges, C. & Holder, I.A. 1996, "Pyoverdinin is essential for virulence of *Pseudomonas aeruginosa*", *Infection and Immunity*, vol. 64, no. 2, pp. 518-523.
- Meyers, D.J. & Berk, R.S. 1990, "Characterization of phospholipase C from *Pseudomonas aeruginosa* as a potent inflammatory agent", *Infection and Immunity*, vol. 58, no. 3, pp. 659-666.

- Michael, B., Smith, J.N., Swift, S., Heffron, F. & Ahmer, B.M. 2001, "SdiA of *Salmonella enterica* is a LuxR homolog that detects mixed microbial communities", *Journal of Bacteriology*, vol. 183, no. 19, pp. 5733-5742.
- Miller, C.H. & Duerre, J.A. 1968, "S-ribosylhomocysteine cleavage enzyme from *Escherichia coli*", *The Journal of Biological Chemistry*, vol. 243, no. 1, pp. 92-97.
- Miller, M.B., Skorupski, K., Lenz, D.H., Taylor, R.K. & Bassler, B.L. 2002, "Parallel quorum sensing systems converge to regulate virulence in *Vibrio cholerae*", *Cell*, vol. 110, no. 3, pp. 303-314.
- Miller, S.T., Xavier, K.B., Campagna, S.R., Taga, M.E., Semmelhack, M.F., Bassler, B.L. & Hughson, F.M. 2004, "*Salmonella typhimurium* recognizes a chemically distinct form of the bacterial quorum-sensing signal AI-2", *Molecular Cell*, vol. 15, no. 5, pp. 677-687.
- Moré, M.I., Finger, L.D., Stryker, J.L., Fuqua, C., Eberhard, A. & Winans, S.C. 1996, "Enzymatic synthesis of a quorum-sensing autoinducer through use of defined substrates", *Science (New York, N.Y.)*, vol. 272, no. 5268, pp. 1655-1658.
- Nakamura, S., Higashiyama, Y., Izumikawa, K., Seki, M., Kakeya, H., Yamamoto, Y., Yanagihara, K., Miyazaki, Y., Mizuta, Y. & Kohno, S. 2008, "The roles of the quorum-sensing system in the release of extracellular DNA, lipopolysaccharide, and membrane vesicles from *Pseudomonas aeruginosa*", *Japanese Journal of Infectious Diseases*, vol. 61, no. 5, pp. 375-378.
- Neidhardt, F.C., Bloch, P.L. & Smith, D.F. 1974, "Culture medium for enterobacteria", *Journal of Bacteriology*, vol. 119, no. 3, pp. 736-747.
- Newman, E.B., Budman, L.I., Chan, E.C., Greene, R.C., Lin, R.T., Woldringh, C.L. & D'Ari, R. 1998, "Lack of S-adenosylmethionine results in a cell division defect in *Escherichia coli*", *Journal of Bacteriology*, vol. 180, no. 14, pp. 3614-3619.

- Nicas, T.I., Bradley, J., Lochner, J.E. & Iglewski, B.H. 1985a, "The role of exoenzyme S in infections with *Pseudomonas aeruginosa*", *The Journal of Infectious Diseases*, vol. 152, no. 4, pp. 716-721.
- Nicas, T.I., Frank, D.W., Stenzel, P., Lile, J.D. & Iglewski, B.H. 1985b, "Role of exoenzyme S in chronic *Pseudomonas aeruginosa* lung infections", *European Journal of Clinical Microbiology*, vol. 4, no. 2, pp. 175-179.
- Ombaka, E.A., Cozens, R.M. & Brown, M.R. 1983, "Influence of nutrient limitation of growth on stability and production of virulence factors of mucoid and nonmucoid strains of *Pseudomonas aeruginosa*", *Reviews of Infectious Diseases*, vol. 5 Suppl 5, pp. S880-8.
- Ochsner, U.A., Koch, A.K., Fiechter, A. & Reiser, J. 1994, "Isolation and characterization of a regulatory gene affecting rhamnolipid biosurfactant synthesis in *Pseudomonas aeruginosa*", *Journal of Bacteriology*, vol. 176, no. 7, pp. 2044-2054.
- Ochsner, U.A. & Reiser, J. 1995, "Autoinducer-mediated regulation of rhamnolipid biosurfactant synthesis in *Pseudomonas aeruginosa*", *Proceedings of the National Academy of Sciences of the United States of America*, vol. 92, no. 14, pp. 6424-6428.
- Ortori, C.A., Dubern, J.F., Chhabra, S.R., Camara, M., Hardie, K., Williams, P. & Barrett, D.A. 2011, "Simultaneous quantitative profiling of *N*-acyl-L-homoserine lactone and 2-alkyl-4(1H)-quinolone families of quorum-sensing signaling molecules using LC-MS/MS", *Analytical and bioanalytical chemistry*, vol. 399, no. 2, pp. 839-850.
- Palmer, K.L., Aye, L.M. & Whiteley, M. 2007, "Nutritional cues control *Pseudomonas aeruginosa* multicellular behavior in cystic fibrosis sputum", *Journal of Bacteriology*, vol. 189, no. 22, pp. 8079-8087.
- Parkins, M.D., Ceri, H. & Storey, D.G. 2001, "*Pseudomonas aeruginosa* GacA, a factor in multihost virulence, is also essential for biofilm formation", *Molecular Microbiology*, vol. 40, no. 5, pp. 1215-1226.

- Parsek, M.R. & Greenberg, E.P. 2000, "Acyl-homoserine lactone quorum sensing in gram-negative bacteria: a signaling mechanism involved in associations with higher organisms", *Proceedings of the National Academy of Sciences of the United States of America*, vol. 97, no. 16, pp. 8789-8793.
- Parsek, M.R., Schaefer, A.L. & Greenberg, E.P. 1997, "Analysis of random and site-directed mutations in *rhII*, a *Pseudomonas aeruginosa* gene encoding an acylhomoserine lactone synthase", *Molecular Microbiology*, vol. 26, no. 2, pp. 301-310.
- Parsek, M.R., Val, D.L., Hanzelka, B.L., Cronan, J.E., Jr & Greenberg, E.P. 1999, "Acyl homoserine-lactone quorum-sensing signal generation", *Proceedings of the National Academy of Sciences of the United States of America*, vol. 96, no. 8, pp. 4360-4365.
- Parsons, J.F., Greenhagen, B.T., Shi, K., Calabrese, K., Robinson, H. & Ladner, J.E. 2007, "Structural and functional analysis of the pyocyanin biosynthetic protein PhzM from *Pseudomonas aeruginosa*", *Biochemistry*, vol. 46, no. 7, pp. 1821-1828.
- Parveen, N. & Cornell, K.A. 2011, "Methylthioadenosine/*S*-adenosylhomocysteine nucleosidase, a critical enzyme for bacterial metabolism", *Molecular Microbiology*, vol. 79, no. 1, pp. 7-20.
- Passador, L., Cook, J.M., Gambello, M.J., Rust, L. & Iglewski, B.H. 1993, "Expression of *Pseudomonas aeruginosa* virulence genes requires cell-to-cell communication", *Science (New York, N.Y.)*, vol. 260, no. 5111, pp. 1127-1130.
- Pearson, J.P., Gray, K.M., Passador, L., Tucker, K.D., Eberhard, A., Iglewski, B.H. & Greenberg, E.P. 1994, "Structure of the autoinducer required for expression of *Pseudomonas aeruginosa* virulence genes", *Proceedings of the National Academy of Sciences of the United States of America*, vol. 91, no. 1, pp. 197-201.
- Pearson, J.P., Pesci, E.C. & Iglewski, B.H. 1997, "Roles of *Pseudomonas aeruginosa las* and *rhl* quorum-sensing systems in control of elastase and rhamnolipid biosynthesis genes", *Journal of Bacteriology*, vol. 179, no. 18, pp. 5756-5767.

- Pesci, E.C., Milbank, J.B., Pearson, J.P., McKnight, S., Kende, A.S., Greenberg, E.P. & Iglewski, B.H. 1999, "Quinolone signaling in the cell-to-cell communication system of *Pseudomonas aeruginosa*", *Proceedings of the National Academy of Sciences of the United States of America*, vol. 96, no. 20, pp. 11229-11234.
- Pesci, E.C., Pearson, J.P., Seed, P.C. & Iglewski, B.H. 1997, "Regulation of *las* and *rhl* quorum sensing in *Pseudomonas aeruginosa*", *Journal of Bacteriology*, vol. 179, no. 10, pp. 3127-3132.
- Pessi, G. & Haas, D. 2000, "Transcriptional control of the hydrogen cyanide biosynthetic genes *hcnABC* by the anaerobic regulator ANR and the quorum-sensing regulators LasR and RhlR in *Pseudomonas aeruginosa*", *Journal of Bacteriology*, vol. 182, no. 24, pp. 6940-6949.
- Pessi, G., Williams, F., Hindle, Z., Heurlier, K., Holden, M.T., Camara, M., Haas, D. & Williams, P. 2001, "The global posttranscriptional regulator RsmA modulates production of virulence determinants and N-acylhomoserine lactones in *Pseudomonas aeruginosa*", *Journal of Bacteriology*, vol. 183, no. 22, pp. 6676-6683.
- Pier, G.B. 2007, "*Pseudomonas aeruginosa* lipopolysaccharide: a major virulence factor, initiator of inflammation and target for effective immunity", *International Journal of Medical Microbiology : IJMM*, vol. 297, no. 5, pp. 277-295.
- Posnick, L.M. & Samson, L.D. 1999, "Influence of S-adenosylmethionine pool size on spontaneous mutation, *dam* methylation, and cell growth of *Escherichia coli*", *Journal of Bacteriology*, vol. 181, no. 21, pp. 6756-6762.
- Rampioni, G., Bertani, I., Zennaro, E., Polticelli, F., Venturi, V. & Leoni, L. 2006, "The quorum-sensing negative regulator RsaL of *Pseudomonas aeruginosa* binds to the *lasI* promoter", *Journal of Bacteriology*, vol. 188, no. 2, pp. 815-819.
- Rasmussen, T.B. & Givskov, M. 2006, "Quorum sensing inhibitors: a bargain of effects", *Microbiology (Reading, England)*, vol. 152, no. Pt 4, pp. 895-904.

- Reczkowski, R.S. & Markham, G.D. 1999, "Slow binding inhibition of S-adenosylmethionine synthetase by imidophosphate analogues of an intermediate and product", *Biochemistry*, vol. 38, no. 28, pp. 9063-9068.
- Reimann, C., Beyeler, M., Latifi, A., Winteler, H., Foglino, M., Lazdunski, A. & Haas, D. 1997, "The global activator GacA of *Pseudomonas aeruginosa* PAO positively controls the production of the autoinducer N-butyryl-homoserine lactone and the formation of the virulence factors pyocyanin, cyanide, and lipase", *Molecular Microbiology*, vol. 24, no. 2, pp. 309-319.
- Rezzonico, F. & Duffy, B. 2007, "The role of *luxS* in the fire blight pathogen *Erwinia amylovora* is limited to metabolism and does not involve quorum sensing", *Molecular Plant-Microbe Interactions : MPMI*, vol. 20, no. 10, pp. 1284-1297.
- Rodrigue, A., Quentin, Y., Lazdunski, A., Mejean, V. & Foglino, M. 2000, "Two-component systems in *Pseudomonas aeruginosa*: why so many?", *Trends in microbiology*, vol. 8, no. 11, pp. 498-504.
- Romeo, T., Gong, M., Liu, M.Y. & Brun-Zinkernagel, A.M. 1993, "Identification and molecular characterization of *csrA*, a pleiotropic gene from *Escherichia coli* that affects glycogen biosynthesis, gluconeogenesis, cell size, and surface properties", *Journal of Bacteriology*, vol. 175, no. 15, pp. 4744-4755.
- Rudd, K.E. 2000, "EcoGene: a genome sequence database for *Escherichia coli* K-12", *Nucleic Acids Research*, vol. 28, no. 1, pp. 60-64.
- Ryall, B., Davies, J.C., Wilson, R., Shoemark, A. & Williams, H.D. 2008, "*Pseudomonas aeruginosa*, cyanide accumulation and lung function in CF and non-CF bronchiectasis patients", *The European respiratory journal : official journal of the European Society for Clinical Respiratory Physiology*, vol. 32, no. 3, pp. 740-747.

- Saiki, R.K., Gelfand, D.H., Stoffel, S., Scharf, S.J., Higuchi, R., Horn, G.T., Mullis, K.B. & Erlich, H.A. 1988. "Primer-directed enzymatic amplification of DNA with a thermostable DNA polymerase", *Science* vol. 239, pp. 487-491.
- Sali, A. & Blundell, T.L. 1993, "Comparative protein modelling by satisfaction of spatial restraints", *Journal of Molecular Biology*, vol. 234, no. 3, pp. 779-815.
- Sanchez, R. & Sali, A. 2000, "Comparative protein structure modeling. Introduction and practical examples with modeller", *Methods in Molecular Biology (Clifton, N.J.)*, vol. 143, pp. 97-129.
- Sato, H., Frank, D.W., Hillard, C.J., Feix, J.B., Pankhaniya, R.R., Moriyama, K., Finck-Barbancon, V., Buchaklian, A., Lei, M., Long, R.M., Wiener-Kronish, J. & Sawa, T. 2003, "The mechanism of action of the *Pseudomonas aeruginosa*-encoded type III cytotoxin, ExoU", *The EMBO Journal*, vol. 22, no. 12, pp. 2959-2969.
- Sauer, K., Camper, A.K., Ehrlich, G.D., Costerton, J.W. & Davies, D.G. 2002, "*Pseudomonas aeruginosa* displays multiple phenotypes during development as a biofilm", *Journal of Bacteriology*, vol. 184, no. 4, pp. 1140-1154.
- Schauder, S., Shokat, K., Surette, M.G. & Bassler, B.L. 2001, "The LuxS family of bacterial autoinducers: biosynthesis of a novel quorum-sensing signal molecule", *Molecular Microbiology*, vol. 41, no. 2, pp. 463-476.
- Schramm, V.L., Gutierrez, J.A., Cordovano, G., Basu, I., Guha, C., Belbin, T.J., Evans, G.B., Tyler, P.C. & Furneaux, R.H. 2008, "Transition state analogues in quorum sensing and SAM recycling", *Nucleic Acids Symposium Series (2004)*, vol. (52), no. 52, pp. 75-76.
- Schuster, M., Lostroh, C.P., Ogi, T. & Greenberg, E.P. 2003, "Identification, timing, and signal specificity of *Pseudomonas aeruginosa* quorum-controlled genes: a transcriptome analysis", *Journal of Bacteriology*, vol. 185, no. 7, pp. 2066-2079.

- Seed, P.C., Passador, L. & Iglewski, B.H. 1995, "Activation of the *Pseudomonas aeruginosa lasI* gene by LasR and the *Pseudomonas autoinducer* PAI: an autoinduction regulatory hierarchy", *Journal of Bacteriology*, vol. 177, no. 3, pp. 654-659.
- Seet, Q. & Zhang, L.H. 2011, "Anti-activator QslA defines the quorum sensing threshold and response in *Pseudomonas aeruginosa*", *Molecular Microbiology*, vol. 80, no. 4, pp. 951-965.
- Sekowska, A., Denervaud, V., Ashida, H., Michoud, K., Haas, D., Yokota, A. & Danchin, A. 2004, "Bacterial variations on the methionine salvage pathway", *BMC Microbiology*, vol. 4, pp. 9.
- Shadel, G.S., Devine, J.H. & Baldwin, T.O. 1990, "Control of the *lux* regulon of *Vibrio fischeri*", *Journal of Bioluminescence and Chemiluminescence*, vol. 5, no. 2, pp. 99-106.
- Shafikhani, S.H. & Engel, J. 2006, "*Pseudomonas aeruginosa* type III-secreted toxin ExoT inhibits host-cell division by targeting cytokinesis at multiple steps", *Proceedings of the National Academy of Sciences of the United States of America*, vol. 103, no. 42, pp. 15605-15610.
- Shafikhani, S.H., Morales, C. & Engel, J. 2008, "The *Pseudomonas aeruginosa* type III secreted toxin ExoT is necessary and sufficient to induce apoptosis in epithelial cells", *Cellular Microbiology*, vol. 10, no. 4, pp. 994-1007.
- Smith, J.N. & Ahmer, B.M. 2003, "Detection of other microbial species by *Salmonella*: expression of the SdiA regulon", *Journal of Bacteriology*, vol. 185, no. 4, pp. 1357-1366.
- Soong, G., Muir, A., Gomez, M.I., Waks, J., Reddy, B., Planet, P., Singh, P.K., Kaneko, Y., Wolfgang, M.C., Hsiao, Y.S., Tong, L. & Prince, A. 2006, "Bacterial neuraminidase facilitates mucosal infection by participating in biofilm production", *The Journal of Clinical Investigation*, vol. 116, no. 8, pp. 2297-2305.
- Spencer, R.C. 1996, "Predominant pathogens found in the European Prevalence of Infection in Intensive Care Study", *European Journal of Clinical Microbiology and Infectious*

Diseases : Official Publication of the European Society of Clinical Microbiology, vol. 15, no. 4, pp. 281-285.

Sperandio, V., Torres, A.G., Giron, J.A. & Kaper, J.B. 2001, "Quorum sensing is a global regulatory mechanism in enterohemorrhagic *Escherichia coli* O157:H7", *Journal of Bacteriology*, vol. 183, no. 17, pp. 5187-5197.

Stevens, A.M., Dolan, K.M. & Greenberg, E.P. 1994, "Synergistic binding of the *Vibrio fischeri* LuxR transcriptional activator domain and RNA polymerase to the *lux* promoter region", *Proceedings of the National Academy of Sciences of the United States of America*, vol. 91, no. 26, pp. 12619-12623.

Stevens, A.P., Dettmer, K., Wallner, S., Bosserhoff, A.K. & Oefner, P.J. 2008, "Quantitative analysis of 5'-deoxy-5'-methylthioadenosine in melanoma cells by liquid chromatography-stable isotope ratio tandem mass spectrometry", *Journal of Chromatography.B, Analytical Technologies in the Biomedical and Life Sciences*, vol. 876, no. 1, pp. 123-128.

Stover, C.K., Pham, X.Q., Erwin, A.L., Mizoguchi, S.D., Warrener, P., Hickey, M.J., Brinkman, F.S., Hufnagle, W.O., Kowalik, D.J., Lagrou, M., Garber, R.L., Goltry, L., Tolentino, E., Westbrook-Wadman, S., Yuan, Y., Brody, L.L., Coulter, S.N., Folger, K.R., Kas, A., Larbig, K., Lim, R., Smith, K., Spencer, D., Wong, G.K., Wu, Z., Paulsen, I.T., Reizer, J., Saier, M.H., Hancock, R.E., Lory, S. & Olson, M.V. 2000, "Complete genome sequence of *Pseudomonas aeruginosa* PAO1, an opportunistic pathogen", *Nature*, vol. 406, no. 6799, pp. 959-964.

Sun, J., Daniel, R., Wagner-Dobler, I. & Zeng, A.P. 2004, "Is autoinducer-2 a universal signal for interspecies communication: a comparative genomic and phylogenetic analysis of the synthesis and signal transduction pathways", *BMC Evolutionary Biology*, vol. 4, pp. 36.

- Surette, M.G. & Bassler, B.L. 1998, "Quorum sensing in *Escherichia coli* and *Salmonella typhimurium*", *Proceedings of the National Academy of Sciences of the United States of America*, vol. 95, no. 12, pp. 7046-7050.
- Surette, M.G. & Bassler, B.L. 1999, "Regulation of autoinducer production in *Salmonella typhimurium*", *Molecular Microbiology*, vol. 31, no. 2, pp. 585-595.
- Surette, M.G., Miller, M.B. & Bassler, B.L. 1999, "Quorum sensing in *Escherichia coli*, *Salmonella typhimurium*, and *Vibrio harveyi*: a new family of genes responsible for autoinducer production", *Proceedings of the National Academy of Sciences of the United States of America*, vol. 96, no. 4, pp. 1639-1644.
- Taga, M.E., Semmelhack, J.L. & Bassler, B.L. 2001, "The LuxS-dependent autoinducer AI-2 controls the expression of an ABC transporter that functions in AI-2 uptake in *Salmonella typhimurium*", *Molecular Microbiology*, vol. 42, no. 3, pp. 777-793.
- Tavender, T.J., Halliday, N.M., Hardie, K.R. & Winzer, K. 2008, "LuxS-independent formation of AI-2 from ribulose-5-phosphate", *BMC Microbiology*, vol. 8, pp. 98.
- Tedder, M.E., Nie, Z., Margosiak, S., Chu, S., Feher, V.A., Almassy, R., Appelt, K. & Yager, K.M. 2004, "Structure-based design, synthesis, and antimicrobial activity of purine derived SAH/MTA nucleosidase inhibitors", *Bioorganic and Medicinal Chemistry Letters*, vol. 14, no. 12, pp. 3165-3168.
- Toder, D.S., Ferrell, S.J., Nezezon, J.L., Rust, L. & Iglewski, B.H. 1994, "*lasA* and *lasB* genes of *Pseudomonas aeruginosa*: analysis of transcription and gene product activity", *Infection and Immunity*, vol. 62, no. 4, pp. 1320-1327.
- Val, D.L. & Cronan, J.E., Jr 1998, "In vivo evidence that S-adenosylmethionine and fatty acid synthesis intermediates are the substrates for the LuxI family of autoinducer synthases", *Journal of Bacteriology*, vol. 180, no. 10, pp. 2644-2651.

- Vallet, I., Diggle, S.P., Stacey, R.E., Camara, M., Ventre, I., Lory, S., Lazdunski, A., Williams, P. & Filloux, A. 2004, "Biofilm formation in *Pseudomonas aeruginosa*: fimbrial cup gene clusters are controlled by the transcriptional regulator MvaT", *Journal of Bacteriology*, vol. 186, no. 9, pp. 2880-2890.
- Van Houdt, R., Aertsen, A., Moons, P., Vanoirbeek, K. & Michiels, C.W. 2006, "N-acyl-L-homoserine lactone signal interception by *Escherichia coli*", *FEMS Microbiology Letters*, vol. 256, no. 1, pp. 83-89.
- Wagner, V.E., Bushnell, D., Passador, L., Brooks, A.I. & Iglewski, B.H. 2003, "Microarray analysis of *Pseudomonas aeruginosa* quorum-sensing regulons: effects of growth phase and environment", *Journal of Bacteriology*, vol. 185, no. 7, pp. 2080-2095.
- Wang, L., Hashimoto, Y., Tsao, C.Y., Valdes, J.J. & Bentley, W.E. 2005, "Cyclic AMP (cAMP) and cAMP receptor protein influence both synthesis and uptake of extracellular autoinducer 2 in *Escherichia coli*", *Journal of Bacteriology*, vol. 187, no. 6, pp. 2066-2076.
- Waters, C.M. & Bassler, B.L. 2005, "Quorum sensing: cell-to-cell communication in bacteria", *Annual Review of Cell and Developmental Biology*, vol. 21, pp. 319-346.
- Watson, W.T., Minogue, T.D., Val, D.L., von Bodman, S.B. & Churchill, M.E. 2002, "Structural basis and specificity of acyl-homoserine lactone signal production in bacterial quorum sensing", *Molecular Cell*, vol. 9, no. 3, pp. 685-694.
- Wei, Y., Perez, L.J., Ng, W.L., Semmelhack, M.F. & Bassler, B.L. 2011, "Mechanism of *Vibrio cholerae* autoinducer-1 biosynthesis", *ACS Chemical Biology*, vol. 6, no. 4, pp. 356-365.
- West, S.E., Sample, A.K. & Runyen-Janecky, L.J. 1994, "The *vfr* gene product, required for *Pseudomonas aeruginosa* exotoxin A and protease production, belongs to the cyclic AMP receptor protein family", *Journal of Bacteriology*, vol. 176, no. 24, pp. 7532-7542.

- Wick, M.J., Hamood, A.N. & Iglewski, B.H. 1990, "Analysis of the structure-function relationship of *Pseudomonas aeruginosa* exotoxin A", *Molecular Microbiology*, vol. 4, no. 4, pp. 527-535.
- Winans, S.C. 2002, "Bacterial esperanto", *Nature Structural Biology*, vol. 9, no. 2, pp. 83-84.
- Winans, S.C. 2011, "A new family of quorum sensing pheromones synthesized using S-adenosylmethionine and Acyl-CoAs", *Molecular Microbiology*, vol. 79, no. 6, pp. 1403-1406.
- Winson, M.K., Swift, S., Fish, L., Throup, J.P., Jorgensen, F., Chhabra, S.R., Bycroft, B.W., Williams, P. & Stewart, G.S. 1998, "Construction and analysis of *luxCDABE*-based plasmid sensors for investigating *N*-acyl homoserine lactone-mediated quorum sensing", *FEMS Microbiology Letters*, vol. 163, no. 2, pp. 185-192.
- Winzer, K., Falconer, C., Garber, N.C., Diggle, S.P., Camara, M. & Williams, P. 2000, "The *Pseudomonas aeruginosa* lectins PA-IL and PA-III are controlled by quorum sensing and by RpoS", *Journal of Bacteriology*, vol. 182, no. 22, pp. 6401-6411.
- Winzer, K., Hardie, K.R., Burgess, N., Doherty, N., Kirke, D., Holden, M.T., Linforth, R., Cornell, K.A., Taylor, A.J., Hill, P.J. & Williams, P. 2002, "LuxS: its role in central metabolism and the in vitro synthesis of 4-hydroxy-5-methyl-3(2H)-furanone", *Microbiology (Reading, England)*, vol. 148, no. Pt 4, pp. 909-922.
- Winzer, K., Hardie, K.R. & Williams, P. 2002, "Bacterial cell-to-cell communication: sorry, can't talk now - gone to lunch!", *Current Opinion in Microbiology*, vol. 5, no. 2, pp. 216-222.
- Xavier, K.B. & Bassler, B.L. 2005, "Regulation of uptake and processing of the quorum-sensing autoinducer AI-2 in *Escherichia coli*", *Journal of Bacteriology*, vol. 187, no. 1, pp. 238-248.
- Yu, S., Jensen, V., Seeliger, J., Feldmann, I., Weber, S., Schleicher, E., Haussler, S. & Blankenfeldt, W. 2009, "Structure elucidation and preliminary assessment of hydrolase

activity of PqsE, the *Pseudomonas* quinolone signal (PQS) response protein", *Biochemistry*, vol. 48, no. 43, pp. 10298-10307.

Zhang, Y.M., Frank, M.W., Zhu, K., Mayasundari, A. & Rock, C.O. 2008, "PqsD is responsible for the synthesis of 2,4-dihydroxyquinoline, an extracellular metabolite produced by *Pseudomonas aeruginosa*", *The Journal of Biological Chemistry*, vol. 283, no. 43, pp. 28788-28794.

Zhang, M., Sun, K. & Sun, L. 2008, "Regulation of autoinducer 2 production and *luxS* expression in a pathogenic *Edwardsiella tarda* strain", *Microbiology (Reading, England)*, vol. 154, no. Pt 7, pp. 2060-2069.

Appendix

MOPS minimal media (MMM)

Chemical	Stock Concentration	Volume added / ml
MOPS mixture	10x	100
K ₂ HPO ₄	0.132 M	10
Glucose*	0.1%	10
dH ₂ O		880
TOTAL		1000

1. Mix ingredients above and adjust the pH to 7.2 with approximately 300 µl 10 M NaOH.
2. Autoclave or filter sterilise. Can be stored at 4 °C for up to 1 month.
3. Add carbon source before use*.

10x MOPS mixture

1. In a 1 L beaker with a stir bar, add the following to ~300 ml dH₂O:

Chemical	Weight / g
MOPS	83.72
Tricine	7.17

2. Add 10 M KOH to a final pH of 7.4 (10 to 20 ml).
3. Bring total volume to approximately 440 ml.
4. Add 10ml 0.01 M FeSO₄·7H₂O to the MOPS/Tricine mixture.
5. Add the following solutions to the MOPS/tricine/FeSO₄ mixture in the order shown:

Chemical	Stock Concentration / M	Volume added / ml
NH ₄ Cl	1.9	50
K ₂ SO ₄	0.276	10
CaCl ₂ ·2H ₂ O	0.02	0.25
MgCl ₂	2.5	2.1
NaCl	5	100
Micronutrient stock	-	0.2
dH ₂ O		387
TOTAL		1000

6. Filter sterilise. Can be aliquoted and stored at -20 °C.

Micronutrient stock

Chemical	Formula	Weight / g
Ammonium molybdate	$(\text{NH}_4)_6\text{Mo}_7\text{O}_{24}\cdot 4\text{H}_2\text{O}$	0.009
Boric acid	H_3BO_3	0.062
Cobalt chloride	CoCl_2	0.018
Cupric sulphate	CuSO_4	0.006
Manganese chloride	MnCl_2	0.040
Zinc sulphate	ZnSO_4	0.007

Mix everything together in 50 ml dH₂O. Store at RT.

Table 9.1: Preparation of MOPS minimal media (MMM).

1x Sample loading buffer	
Tris-HCl pH 6.8	50mM
DTT	100 mM
SDS	2% (w/v)
Bromophenol blue	0.1% (w/v)
Glycerol	10% (v/v)
Destaining solution	
Isopropanol	10% (v/v)
Electrophoresis running buffer pH 8.8	
Tris-HCl	25 mM
Glycine	190 mM
SDS	0.1% (w/v)
Resolving buffer	
Tris-HCl pH 8.8	1.5 M
SDS	0.4% (w/v)
Resolving gel (12%)	
Acrylamide	2.5 ml
Resolving buffer	1.25 ml
10 % APS (w/v)	25 µl
TEMED	2.5 µl
dH ₂ O	1.22 ml
Staining solution	
Acetic acid	10% (v/v)

MeOH	25% (v/v)
Coomassie brilliant blue R250	0.2% (v/v)
Stacking buffer	
Tris-HCl pH 6.8	0.5M
SDS	0.4% (w/v)
Stacking gel (3%)	
Acrylamide	200 μ l
Stacking buffer	1 ml
10% APS (w/v)	25 μ l
TEMED	2.5 μ l
dH ₂ O	723 μ l

Table 9.2: Standard recipes for SDS-PAGE electrophoresis.

Blotting buffer was stored at 4 °C, ponceau S at RT and blocking and washing solutions freshly prepared for each experiment.